Investigation of the phospholipid peripheral region of lactose permease in model membranes

Carme Suárez Germà

UNIVERSITAT DE BARCELONA

FACULTAT DE FARMÀCIA

DEPARTAMENT DE FISICOQUÍMICA

Investigation of the phospholipid peripheral region of lactose permease in model membranes

Carme Suárez Germà,
Barcelona, September 2013

Doctoral thesis

UNIVERSITAT DE BARCELONA

FACULTAT DE FARMÀCIA

DEPARTAMENT DE FISICOQUÍMICA

PROGRAMA DE DOCTORAT
Recerca, Control i Desenvolupament de Medicaments

Investigation of the phospholipid peripheral region of lactose permease in model membranes

Memòria presentada per Carme Suárez Germà per optar al títol de doctor per la Universitat de Barcelona

Realitzada sota la codirecció de:

Jordi Borrell Hernández

Òscar Domènech Cabrera

Tutora:

Maria Teresa Montero Barrientos

Carme Suárez Germà,
Barcelona, September 2013

ABSTRACT

The interaction between a membrane protein and its surrounding phospholipids is thought to be crucial for the correct folding and function of the protein. This thesis is focused on the investigation of the interplay between Lactose permease (LacY), a paradigm for secondary transporters present in the inner membrane of *Escherichia coli* and model systems mimicking its natural lipid environment. Since the role of phospholipids in LacY's activity is currently being refined, this work represents a contribution to the field by studying the interaction at two different levels: (i) the LacY interplay with the phospholipids present at the annular region in the vicinity of the protein was studied through FRET measurements between a single-tryptophan LacY mutant and diverse pyrene-marked phospholipids, and (ii) the LacY interaction with the more distanced bulk phospholipids was studied through supported proteo-lipid sheets that were analysed using topography, force-spectroscopy and force-volume Atomic Force Microscopy modes. First, after validating LacY preference for phospholipid fluid (L_α) phases in the studied two-component model systems, a different composition between bulk and annular regions was confirmed. Hence, bulk lipids, which were assimilated to the phospholipids in L_α phase, were mainly formed by PG, while PE was the main component of the annular region. This points to a direct annular phospholipid-LacY selectivity because it discards a random phospholipid distribution near the protein. Second, the LacY selectivity for precise phospholipid species at the annular region was found to be related to: (i) a neutral charged phosholipid (PE or PC, with preference for the former), and (ii) phospholipids with large negative spontaneous curvature (C_0) (DOPE > POPE). In addition, D68 was revealed as an important amino acid for the protein annular lipid selectivity. Third, the interaction between LacY and the bulk lipids was described as reciprocal. Accordingly, the presence of the protein largely modified the topography and the nanomechanics of the lipid system, especially for the L_α phase, whilst the nanomechanics of LacY itself were different depending on the surrounding lipid matrix: more force was needed to pull LacY form the DPPE:POPG (3:1, mol/mol) system than from the POPE:POPG (3:1, mol/mol) one. Therefore, the bilayer lipid composition seems to determine the forces governing the

LacY tight interaction with the membrane and can be thus decisive for the protein correct insertion and activity.

RESUM

La interacció entre una proteïna de membrana i els fosfolípids que l'envolten és considerada crucial pel bon plegament i la correcta funció de la proteïna. Aquesta tesi està centrada en la investigació de la interacció entre la Lactosa permeasa (LacY), un paradigma dels transportadors secundaris que es troba a la membrana interna d'*Escherichia coli,* i sistemes models que mimetitzen el seu entorn lipídic. Tenint en compte que el rol dels fosfolípids en l'activitat de LacY està sent actualment refinat, aquest treball representa una contribució al camp a través de l'estudi de la interacció a dos nivells diferents: (i) la interacció entre LacY i els fosfolípids presents a la regió anular propera a la proteïna ha estat estudiada a través de mesures de FRET entre un mutant de LacY amb un únic triptòfan i diversos fosfolípids marcats amb pirè i (ii) la interacció entre LacY amb els fosfolípids més llunyans o *bulk* fosfolípids s'ha investigat a través de làmines de lípid i proteïna sobre un suport, les quals s'han analitzat a partir de diferents modes de microscòpia de força atòmica (topografia, espectroscòpia de força i *force-volume*). En primer lloc, s'ha validat la preferència de LacY pels fosfolípids en fases fluïdes (L_α) en els sistemes models de dos components estudiats. A més, s'ha confirmat una composició lipídica diferent entre la regió anular i el *bulk*. Així, els lípids *bulk*, considerats com a fosfolípids en fase L_α, tenen PG com a principal component, mentre que PE és el major component de la regió anular. Això sembla indicar una selectivitat directa entre LacY i els fosfolípids anulars, ja que descarta un posicionament aleatori dels fosfolípids a les proximitats de la proteïna. En segon lloc, s'ha descrit que la selectivitat de LacY per una espècie precisa de fosfolípid a la regió anular està relacionada amb (i) la càrrega neutra del fosfolípid (PE o PC, amb preferència pel primer) i (ii) fosfolípids amb curvatura espontània (C_0) negativa (DOPE > POPE). A més, D68 s'ha assenyalat com un aminoàcid important per la selectivitat de la proteïna envers els lípids anulars. En tercer lloc, s'ha descrit una interacció recíproca entre LacY

i els lípids *bulk*. D'aquesta manera, la presencia de la proteïna modifica la topografia i la nanomecànica del sistema lipídic, especialment de la fase L_α, i, alhora, la nanomecànica de la pròpia LacY varia segons la matriu lipídica que l'envolta: cal més força per estirar LacY d'una matriu de DPPE:POPG (3:1, mol/mol) que d'una matriu de POPE:POPG (3:1, mol/mol). Així doncs, la composició lipídica de la bicapa sembla determinar les forces que governen l'estreta interacció de LacY amb la membrana i, per tant, aquesta composició és decisiva per la correcta inserció i activitat de la proteïna.

RESUMEN

La interacción entre una proteína de membrana y los fosfolípidos que la rodean es considerada crucial para el buen plegamiento y la correcta función de la proteína. Esta tesis está centrada en la investigación de la interacción entre la Lactosa permeasa (LacY), un paradigma de los transportadores secundarios que se encuentra en la membrana interna de *Escherichia coli*, y sistemas modelos que mimetizan su entorno lipídico. Teniendo en cuenta que el rol de los fosfolípidos en la actividad de LacY está siendo actualmente refinado, este trabajo representa una contribución en el campo a través del estudio de la interacción a dos niveles diferentes: (i) la interacción entre LacY y los fosfolípidos presentes en la región anular próxima a la proteína ha sido estudiada a través de medidas de FRET entre un mutante de LacY con un único triptófano y varios fosfolípidos marcados con pireno y (ii) la interacción entre LacY y los fosfolípidos más alejados o *bulk* fosfolípidos ha sido investigada a través de láminas de lípido y proteïna sobre un soporte, las cuales se han analizado a partir de diferentes modos de microscopía de fuerza atómica (topografía, espectroscopia de fuerzas y *force-volume*). En primer lugar, se ha validado la preferencia de LacY por los fosfolípidos en fases fluidas (L_α) en los sistemas modelos con dos componentes estudiados. Además, se ha confirmado una composición lipídica diferente entre la región anular y el *bulk*. Así, los lípidos *bulk*, considerados como fosfolípidos en fase L_α, presentan PG como componente principal, mientras que PE es el mayor componente de la región anular. Eso parece indicar una selectividad directa entre LacY y los fosfolípidos anulares, ya

que descarta un posicionamiento aleatorio de los fosfolípidos en las proximidades de la proteína. En segundo lugar, se ha descrito que la selectividad de LacY por una especie precisa de fosfolípido en la región anular está relacionada con (i) la carga neutra del fosfolípido (PE o PC, con preferencia por el primero) y (ii) fosfolípidos con una curvatura espontanea (C_0) negativa (DOPE > POPE). Además, D68 ha sido señalado como un aminoácido importante para la selectividad de la proteína hacia los lípidos anulares. En tercer lugar, se ha descrito una interacción recíproca entre LacY y los lípidos *bulk.* De esta manera, la presencia de la proteína modifica la topografía y la nanomecánica del sistema lipídico, especialmente de la fase L_α, y, al mismo tiempo, la nanomecánica de la propia LacY cambia según la matriz lipídica que la rodea: se necesita más fuerza para estirar LacY de una matriz de DPPE:POPG (3:1, mol/mol) que de una matriz de POPE:POPG (3:1, mol/mol). Así pues, la composición lipídica de la bicapa parece determinar las fuerzas que gobiernan la estrecha interacción entre LacY y la membrana, y, por lo tanto, esta composición es decisiva para la correcta inserción y actividad de la proteína.

RESUMÉ

L'interaction entre une protéine membranaire et les phospholipides qui l'entourent est considérée cruciale pour le repliement et la fonction de la protéine. Cette thèse est centrée sur l'investigation de l'interaction entre la Lactose permease (LacY), un paradigme des transporteurs secondaires qui est placée dans la membrane interne d'*Escherichia coli,* et des systèmes modèles qui miment son entourage lipidique. En prenant compte que le rôle des phospholipides dans l'activité de LacY est en train de s'affiner, ce travail représente une contribution dans le domaine à travers l'étude de cette interaction à deux niveaux différents: (i) l'interaction entre LacY et les phospholipides présents dans la région annulaire a été étudiée grâce à des mesures de FRET entre un mutant de LacY, avec un seul tryptophane, et différents phospholipides marqués à l'aide d'un pyrène, et (ii) l'étude de l'interaction entre LacY et des phospholipides plus éloignés (phospholipides *bulk*) a été effectué à travers l'analyse de lames de lipides et protéines sur un support, qui ont été analysées à l'aide de différents

modes de microscopie de force atomique (topographie, spectroscopie de force et *force-volume*). D'abord, nous avons validé la préférence de LacY pour les phospholipides en phase fluide (L_α) dans les systèmes modèles à deux composants étudiés. En outre, nous avons confirmé une composition lipidique différente entre la région annulaire et le *bulk*. Ainsi, les lipides *bulk*, considérés comme des phospholipides en phase L_α, ont présenté PG comme élément principal, tandis que PE est le composant majeur dans la région annulaire. Cela semble indiquer une sélectivité directe entre LacY et les phospholipides annulaires, puisque ceci exclut un positionnement aléatoire des phospholipides dans les environs de la protéine. Deuxièmement, nous avons démontré que la sélectivité de LacY vers une espèce précise de phospholipide dans la région annulaire est liée à (i) la charge neutre des phospholipides (PE or PC, avec de la préférence pour PE) et (ii) également une préférence pour les phospholipides avec une courbure spontanée (C_0) négative (DOPE > POPE). De plus, D68 s'est avéré être un aminoacide important dans la sélectivité de la protéine vers les lipides annulaires. Troisièmement, nous avons décrit l'interaction réciproque entre LacY et les lipides dis *bulk*. Ainsi, la présence de la protéine modifie la topographie et la nanomécanique du système lipidique, et, parallèlement, la nanomécanique de LacY varie selon la matrice lipidique qui l'entoure : nous avons besoin de plus de force pour étirer LacY d'une matrice de DPPE :POPG (3:1, mol/mol) que d'une matrice de POPE :POPG (3:1, mol/mol). Par conséquent, la composition lipidique de la bicouche semble déterminer les forces qui gouvernent l'étroite interaction entre LacY et la membrane et, de ce fait, cette composition est décisive pour l'insertion et l'activité correcte de la protéine.

CONTENTS

Chapter 1. A physical insight into the cell membrane

1.1 The cell membrane

The cell membrane was originally defined as a structure that permits the compartmentalization of cells and organelles. Certainly, compartmentalization, i.e. separation from the environment, is essential for an organism to enclose an aqueous solution of cellular material as the first requirement to create a complete independent entity [1]. However, the cell membrane is more than that. It is in charge of the relationship between the cell or organelle with the exterior, since although a barrier is needed, controls to surmount it are crucial. This may primarily correspond to basic needs as the uptake of nutrients and disposal of waste. More complicated functions respond to the use of the barrier for energy-storage properties and to the creation of pathways to exchange information between a cell and its environment [2].

The cell membrane as a biological structure is highly universal when considering that it is present in all cells, eukaryotic and prokaryotic, as well as all internal organelles. However, although there are similarities, each biological membrane is highly specialized and has its own particularities. Two main components form all cell membranes, lipids and proteins. About 10% of carbohydrates are also present in biomembranes, but they are not considered as key elements because they are always linked to lipids or proteins conferring them some singularities [3]. More than 550 different types of lipids can be combined in a particular biological membrane [4]. The

reason for such diversity is currently not clear, but since lipids do not form polymers and do not have catalytic activity, it is thought that their diverse functions might likely result from the properties and structures of individual lipids [5,6]. Regarding proteins, a vast array of different proteins are directly embedded or interact in some way with the membrane and are involved in diverse and essential cellular processes.

Lipids present amphipathic nature that provokes their self-assembling into structures that minimize the exposure of the apolar regions to water. In cells, the most common assembly is the lipid bilayer which has the necessary characteristics to act as a permeability barrier [7]. However, its structure and composition is far from being simple. First, due to the great diversity of different lipid species that can be found in the lipid matrix, but also due to their capacity of being organized in compositions other than bilayers. Second, because a large amount of proteins are interacting with the lipids and their inter-play can vary greatly the structural properties of the bilayer. Furthermore, the assembly of all membrane components is generally not determined by covalent bonds but by other weaker interactions [4] which result in higher mobility and variability of the system. This facilitates the participation of membrane lipids in dynamic interactions while permitting changes in membrane thickness, surface packing, lateral or rotational mobility; which are necessary in turn to allow the conformational remodelling needed for protein function. Finally, interactions of the membrane with the cytoskeleton play also an important role in cell membrane functionality [8,9]. And, overall, all these characteristics are finely tuned by the cell in order to response to a high number of external situation (e.g. the cell can regulate protein expression or membrane lipid levels to respond to changes in environmental situations) [10]. This entire picture illustrates how difficult the understanding of the cell membrane system is. Indeed, due to this great compositional complexity the structural and functional aspects of biological membranes are currently a matter of intense debate [4].

Historically, the model that has been traditionally accepted to explain the membrane cell organization was the one proposed by Singer and Nicolson (S-N) in 1972 of the “fluid mosaic model” (Figure 1) [11], which agglutinated at that time all the findings in one single model. It proposed the idea of lipid membranes formed by a fluid bilayer with some proteins dispersed at a low concentration and matching the hydrophobic side chains. Also, the fluidity accounted for freely movement of proteins and lipids inside this “sea of lipids”. Conversely, the extended fluid mosaic model contemplates protein

crowded lipid membranes where structural and functional restraints appear (asymmetry of the bilayers laterally and in cross-section, great variations in bilayer thickness...) [12]. In fact, the principle governing nowadays is that of the patchiness of membranes where lipid-lipid and lipid-protein interaction organize the system in large functional complexes [12]. Moreover, the emerging evidence on supramolecular lipid-protein complexes forming different types of domains and thus non-random distribution of proteins in the membrane at different hierarchical levels modifies de S-N model too [13]. Accordingly, although the S-N model is still valid to some extent, a large number of recent reviews summarize the state of the art of biomembranes research and demand on the development of new models which take clearly into account the ensemble of these new findings [4,5,9,14–16].

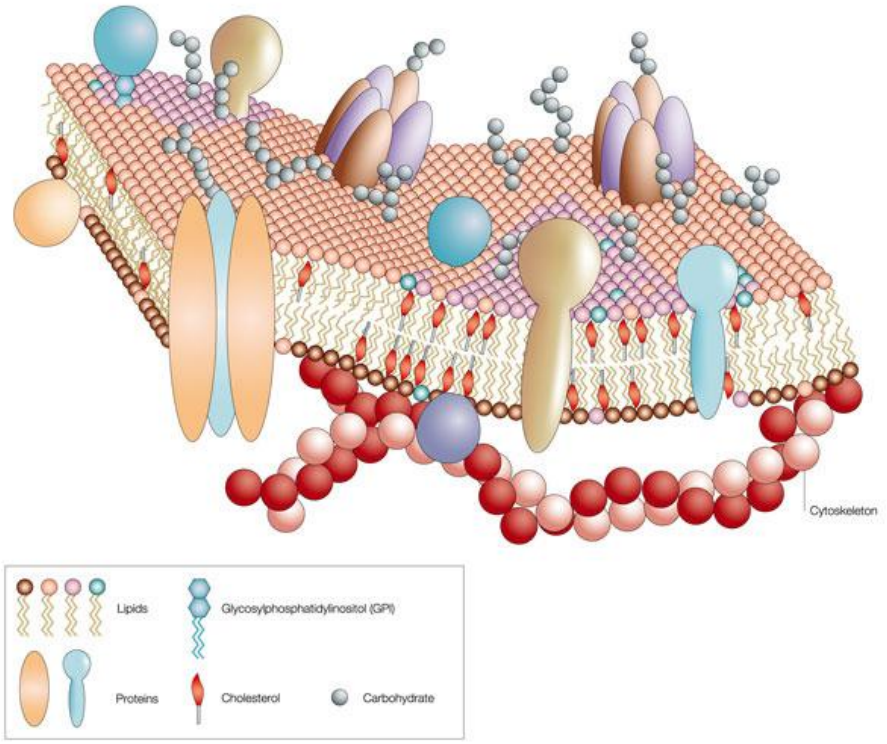

Figure 1. Cartoon of a eukaryotic cell membrane based on the fluid-mosaic model proposed by Singer and Nicolson in 1972 *(http://www.nature.com/scitable).*

1.2 Phospholipids

Lipids are the main component of the cell membrane. Different kinds of lipids are found in this structure, among them phospholipids, glycolipids, sphingolipids or sterols. Other minority phospholipids are also important in some specific cases, such as diphosphatidylglycerols, characteristics of the inner membrane of gram-negative bacteria; although they also play an important role in the mitochondrial inner membrane of eukaryotic cells [3]. However, phospholipids are the most common membrane lipids.

Phospholipids are amphipathic molecules due to the presence in their molecular structure of two distinctive moieties: one hydrophilic and another hydrophobic (see structure in Figure 2). This special disposition is crucial in terms of molecular organization. Chemically, phospholipids are fatty acid esters of glycerol. On the one hand, they have a glycerol skeleton where one of its hydroxyls is bound to a polar phosphate-containing headgroup. This headgroup defines the hydrophilic part of the molecule and can present several structures. On the other hand, the two remaining hydroxyls from the glycerol structure are linked to fatty acids, which define the hydrophobic portion of the structure, named hydrocarbonated or acyl chain. The fatty acids can display different number of carbons in its hydrocarbonated chain as well as different number of unsaturations which confer singularities to the final molecule. Hence, a particular headgroup defines a phospholipid family, whilst different hydrocarbonated chains form diverse phospholipid structures within each family with well-defined characteristics [17]. For example, an increasing level of odd unsaturations in phospholipid acyl chains leads to higher area per lipid and conformationally less ordered chains [18]. Likewise, the global charge of a phospholipid is also an important characteristic to take into account. Phosphoryl group is ionisable and presents a negative charge at physiological pH. The global charge will then be determined by the chemical structure of the polar headgroup. In nature we find most commonly negative phospholipids or zwitterionic ones, this last presenting a total neutral charge coming from the compensation of the negative charge by the presence of a positive charge in the headgroup.

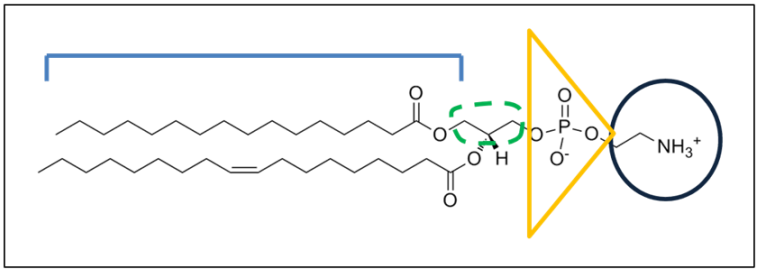

Figure 2. General structure of a phospholipid molecule based in a POPE structure. The polar head is formed by an ethanolamine group (continuous line circle) and a phosphate group (triangle). This headgroup is connected to a glycerol (discontinuous line circle) with two hydrophobic acyl chains (continuous line).

To summarize, the amphiphilicity of phospholipids is defined by the two types of glycerol substituents: fatty acids and polar headgroups. Since the apolar moiety shows a very limited solubility in water, the molecule tends to spontaneously organize in different structures in order to avoid the contact to the hydrophilic environment. This organizing ¨force¨ is known as hydrophobic effect [7,19] and is the major thermodynamic driving effect for stabilizing hydrated lipids aggregates, although other minor stabilizing factors can be present (van der Waals forces or hydrogen bonding) [3]. The hydrophobic effect is entropically leaded and results from the unfavourable constraints appearing when water is packed around a non-polar hydrocarbon [3,20].

1.2.1 Lipid organization in water

Lipids are polymorphic when mixed with water. The particular form that they may adopt is related to several conditions being the more important the phospholipid structure (volume ratio between polar and apolar parts), but also lipid concentration, temperature, pressure, ionic strength and pH [21]. Depending on all these factors, phospholipids can assimilate a variety of structures, called mesophases, which are more ordered than a liquid but less so than a solid. One convenient way to describe lipid phase behaviour is through temperature-composition (*T*-c) phase diagrams. Figure 3 shows a phase diagram of a single lipid system in function of the temperature and water content. We can observe that upon temperature rising, the phospholipid system organizes in two types of mesophases: lamellar (bilayer-forming) and non-lamellar (non-bilayer forming) phases. Particularly, in excess of water phospholipids may coordinate in the following structures [3,22,23]:

I. Lamellar gel phase (L_β): it appears at low temperatures in lipids that form lamellar structures. Activation energy is low and thus molecules are tightly packed. Acyl chains are quite ordered and phospholipids present limited freedom of movement.

II. Lamellar liquid crystalline phase or fluid phase (L_α): it appears upon increasing temperature. Although displaying two-dimensional order, high fluidity and a considerable disorder in the acyl chain level is found. The lattice order is lost.

III. Non-lamellar phases: further increase of the temperature leads to lipid organization in non-bilayer systems. They can form either hexagonal or cubic phases, depending on temperature and phospholipid morphology.

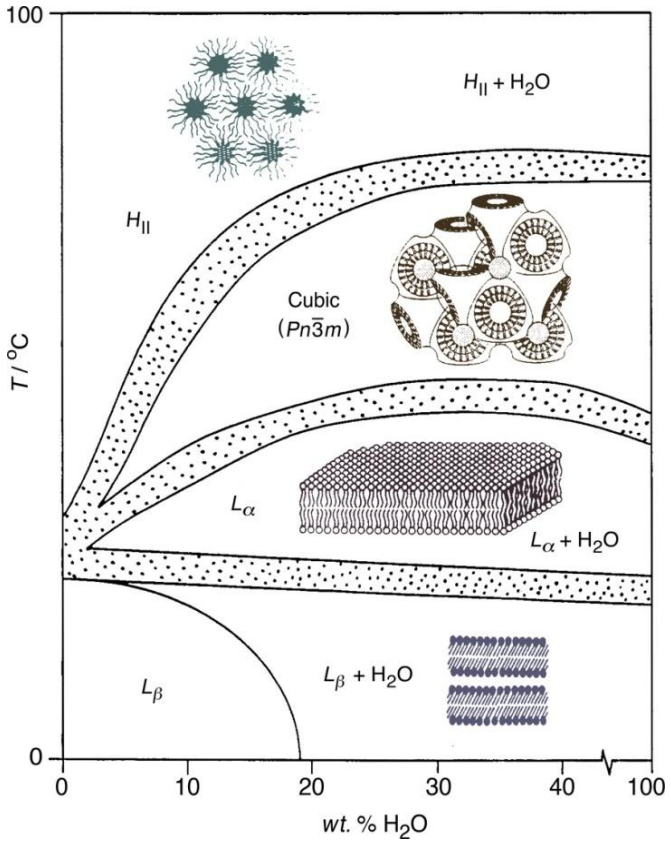

Figure 3. Schematic temperature-water content phase diagram of a pure phospholipid system. The phase diagram represents the polymorphic phospholipid organization upon temperature rising and the increasing of water content in the system *(Figure from Brown, 2012* [22]*)*.

The temperature at which half of the phospholipids in a pure or a mixed system experiences the gel to fluid phase transition is identified as the melting temperature (T_m). Saturated acyl chain phospholipids which present a high degree of order and tight

packing are characterized by high T_m, whilst unsaturated lipids with a *cis* double bond kink present low T_m due to its organization in a more expanded and less ordered system. Headgroup composition influences also the T_m value through hydrogen bonding and size, which affects packing by steric hindrance [24].

It is thought that phospholipids in cell membranes present almost exclusively lamellar fluid phases. Still, it is well-described that membrane topological remodelling (in the cases of fission and fusion for example) is related to the formation of localized non-bilayer intermediates [19,25]. This non-bilayer intermediates would create connections between two or more bilayers (e.g. between a cell membrane and a vesicle) by creating stalks, which are hemifusion intermediates favoured by the presence of phospholipids with negative curvature [26]. In accordance to this idea, significant studies on the growth of microorganisms such as *Acholeplasma laidlawii* [27] and *Escherichia coli* (*E. coli*) [10] have revealed a balance between lamellar and non-lamellar lipids in the bacterial cell membrane which is crucial for its correct function.

1.2.2 The bilayer structure

The cell membrane bilayer structure corresponds to a fluid lamellar phase of $\simeq$ 5 nm thick [4] which presents both short-range and long-range order, as well as anisotropy. The chemical and physical description of this complex structure is vast and extend, although some important generalities are summarized in Figure 4.

I. Transverse lipid asymmetry: the lipid bilayer can present transverse bilayer asymmetry, which corresponds to a different distribution of phospholipids in each bilayer leaflet. To maintain this asymmetry, phospholipids can undergo the so-called flip-flop movement which translocates them from one leaflet to another. Since this movement is unfavourable, cells can accelerate it by a number of different enzymes, which create and support the structural asymmetry of membranes [28,29]. Membrane composition asymmetry is a requirement for the emergence of bilayer curvature. Indeed, bilayers are extremely bendable and this softness, combined with high structural stability is crucial for its biological functionality [30].

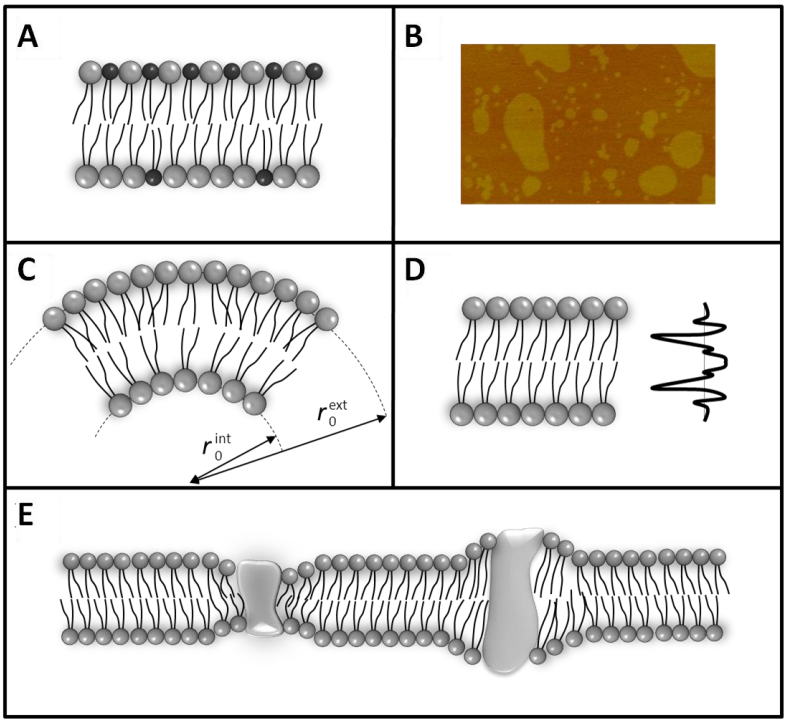

Figure 4. Membrane features involved in the cell membrane formation and organization: transverse lipid asymmetry (**A**), with different phospholipid composition in each bilayer leaflet; lateral bilayer heterogeneity (**B**), exemplified by an AFM image of a supported lipid bilayer that displays two different lipid domains of different step height; membrane curvature (**C**); membrane lateral pressure (**D**); and hydrophobic match (**E**), i.e. adaptation of the phospholipid bilayer thickness to the size of a membrane protein hydrophobic domain.

II. Lateral bilayer asymmetry: the presence of lateral heterogeneity in bilayer structures has recently received increasing attention. Since the early view of lipids homogeneously distributed in most membranes as a consequence of their high mobility, research has evolved with the discovery of superlattice distribution of lipids in fluid-mixed bilayers (e.g. rafts, caveolae) [31,32]. Hence, in artificial [33–36] and natural membranes [37,38] there has been found a rich presence of non-ideal mixing systems of finite size and formed by two or more elements. These structures are called domains. A domain can be briefly described as a short-range ordered structure that differs in lipid and/or protein composition from the surrounding membrane [39]. However, many details of these structures such as their molecular characteristics, function and size distribution, remain to be clarified [40]. The distribution of phospholipids in domains is determined by factors related to lipid-lipid interaction, as well as lipid relationship with surrounding proteins or cytoskeleton [41]. Domains do not cover the whole membrane. Instead, they are small, transient and present a dynamic equilibrium with areas in which

lipids are distributed randomly [13]. In effect, one widely discussed topic is the absolute size of domains: from micro- to nanodomains have been found in membrane cells, and hypothesis for this large size diversity are still being discussed [42,43].

An important physical magnitude related to the presence of lateral heterogeneity in membranes is the line tension (Γ). In this regard, the boundary between domains presents a special lipid packing which mainly results from differences in height between different domains. Consequently, the line tension is described as the energy per length boundary accounted for the deformation of molecules at the domain border in order to prevent the exposure of apolar regions to the aqueous media. Size and stability of a domain are closely related to this line tension parameter [44].

III. Membrane curvature and lateral pressure: As mentioned, most membranes are not completely flat. Instead, the spontaneous curvature of a membrane depends directly on the structure of its lipid components (e.g. their shape, which results from the ratio between the head and the acyl chains volume). Hence, phospholipid structure is determinant for the correct local lipid packing, but also for the bending, since all the molecules collaborate to the total curvature of the membrane. In this regard, each phospholipid presents an intrinsic curvature (or C_0) which corresponds to the shape of relaxed phospholipids with zero bending stress [45–47]. Furthermore, the forced situation of non-lamellar phospholipids placed in a lamellar cell bilayer may cause compression of the acyl tails and thus lead to membrane stress and curvature frustration. This stored stress, which can augment with temperature as it increases the repulsive pressure in the acyl chain region, is the responsible of the apparition in certain cases of the above-mentioned local non-bilayer structures [30].

This bending elasticity can also be described in terms of inhomogeneous profile of lateral pressure across the lipid membrane [48]. The lateral pressure measures the profile distribution of local pressures inside a bilayer and depends on macroscopic and measurable quantities such as surface tension, surface Gibbs energy, C_0 and phospholipid composition [18]. The pressure gradients present along a cell membrane play important roles in the conformational states of transmembrane proteins by modulating their activity or interactions [49,50].

IV. Hydrophobic match: the hydrophobic match occurs at the protein-lipid boundary and corresponds to the adaptation of the lipid curvature to the hydrophobic

transmembrane domains of membrane proteins in order to minimize the energetically unfavourable exposure of the hydrophobic amino acid chains to the aqueous environment. Lipids can physically adapt to match transmembrane domains of various lengths, which results in local variations in membrane thickness [51,52]. Hydrophobic match is further addressed in section 1.4.2.

1.2.3 Artificial or model membranes

Biological membranes have been widely studied in *ex-vivo* approximations by using different types of structures mimicking the cell lipid bilayer, which are named artificial or model membranes. As a result, physical and chemical properties of individual lipids and lipid mixtures have been extensively studied; though the correlation of these researches with the *in vivo* state is still under discussion [6].

The applicability of model membranes as good models of cellular membranes is limited in several ways. One of the most important differences is that, while cellular membranes are out of the equilibrium, most of the experiments with model membranes are performed under equilibrium conditions [53]. Thus, model systems are not affected by cellular dynamic processes such as vesicle trafficking or lipid synthesis and hydrolysis [54]. In addition, absence of cytoskeleton results in considerably different molecular interactions. Lastly, the lack of three-dimensionality brings studies in model membranes to the analysis of processes only into the membrane plane [28]. Nevertheless, direct studies on cellular membranes are still complicated. For example, the study of domains *in vivo* is greatly challenging due to its small size and ephemeral nature within the complexity of the cell membrane. That is why the simplification of the system through the use of model membranes can largely facilitate this study [24]. Other advantages of model membranes are the fine-tuning of the lipid composition and the precise control of environmental conditions (such as ion concentrations) [55].

In summary, extrapolation of the results in lipid model systems to real membranes has to be carefully performed. It is a good preliminary approach in the understanding of organization, polymorphism and phase states of phospholipid sample mixtures, but, as mentioned, it does not consider complex membrane surface structure and completely biomimetic environment [56].

Model membranes can be classified in closed bilayers or liposomes and planar mono- or bilayers (Figure 5).

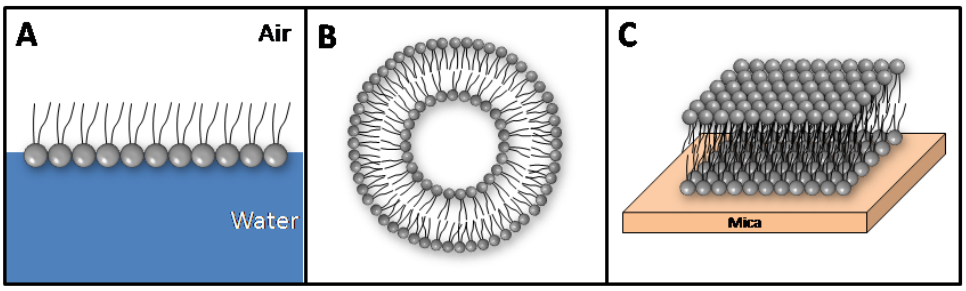

Figure 5. Different model membrane systems: planar monolayers (**A**), liposomes (**B**), and supported lipid bilayers (**C**).

I. Planar monolayers at the air-water interface: planar monolayers are formed by phospholipids adsorbed in the air-water interface in the form of a layer of only one molecule thick, where phospholipids are oriented with the polar heads in contact with the aqueous phase and with the hydrocarbon chains extended facing air. Besides, the monolayer can be supplemented with proteins or membrane-active molecules that may intercalate within the lipid structure. The advantage of this model is that monolayers can be easily studied and manipulated in a Langmuir through which allows the measurements of thermodynamic relationships between surface tension and surface molecular area (for further information see section 3.2.1) [3]. What is more, the in-plane and lateral structure of the monolayer film can be investigated by various methods, such as fluorescence microscopy or Brewster-angle microscopy. Scanning probe microscopies can also be used, provided the monolayer is transferred to a solid support [15].

II. Closed bilayers, liposomes: liposomes are freestanding vesicles consisting of phospholipid bilayers that enclose an aqueous compartment. Liposomes are bilayers closed onto themselves forming spherical structures, which minimize unfavourable contact between hydrophobic moieties of phospholipids and the aqueous solution. The vesicles are generally quite stable and impermeable to many substances [17]. The primary uses of liposomes are (i) as model membranes, and (ii) to encapsulate solutes as drug delivery systems [3]. Liposomes can be prepared in order to obtain structures containing multiple bilayers (multilamellar vesicles or MLVs) or single-walled

structures (unilamellar vesicles). Moreover, as membrane models liposomes present the advantage that they can be formed in different sizes, SUVs (small unilamellar vesicles, <100 nm in diameter), LUVs (large unilamellar vesicles, <1000 nm in diameter), and GUVs (giant unilamellar vesicles, >1000 nm in diameter). Consequently, liposomes allow to study the effect of membrane permeability and curvature, and the dispersion of vesicles can elucidate bulk properties (e.g. thermodynamic and structural properties) [3,15].

III. Planar bilayers onto solid supports, supported lipid bilayers (SLBs): SLBs are planar bilayers formed onto a solid support developed as a model system by McConnell et al. [57]. Like liposomes, this model membrane conserves the lateral and rotational mobility of individual phospholipids. This is possible due to the presence of a thin layer of water (in the order of 1-2 nm) between the distal layer of the membrane and the support [58–60], which acts as a lubricant and permits diffusion of lipids, although in a lower velocity rate as compared to cells. The clearer advantages in contrast to liposomes are related to its facility to be analysed with current, powerful surface analysing techniques: atomic force microscopy (AFM), total internal reflection fluorescence (TIRF) microscopy, or surface plasmon resonance (SPR) spectroscopy. These techniques allow a good visualization of the dynamics and the organization of lipids and proteins even on a single molecule level in real time [61]. Additionally, the presence of the support stabilizes the bilayer and allows its interaction with different scanning probes. For example, the precise puncture of a SLB with an AFM tip permits sensing interaction forces and thus gives light on the nanomechanical characteristics of the system [62].

Drawbacks of this model membrane are, as stated above, that the lipids in SLBs move more than two times slower than in free-floating bilayers [63]. Also, the hydration layer is often not thick enough to accommodate large extramembraneous domains of transmembrane proteins, which may result in restricted motion or even denaturation. Some approaches have been developed to overcome these problems, although caution must be taken when applying them, since they largely complicate the system. One example could be the use of hydrated polymer cushions separating the SLBs and the support [58]. Furthermore, although it has been indicated that the solid support underlying the SLB plays in some way the role of cytoskeleton (Le Grimellec, personal communication), the only clear thing is that the presence of this support may induce an

asymmetric inter-leaflet lipid distribution in SLBs which, at the moment, is still not totally understood [64].

SLBs can be prepared by layer by layer deposition as it is done when using Langmuir-Blodgett or Langmuir-Schaeffer deposition [65], by spin-coating [66] or by the fusion of lipid vesicles on solid supports [64,67]. This latter technique, first described by Brian and McConnell [68], is a very easy way to form bilayer systems onto planar or non-planar surfaces. SUVs adsorb to the surface, rupture and fuse to form a flat bilayer, more likely by the strain in the bilayer due to the small radius of curvature [24]. The main parameters governing this bilayer formation are related to the nature of the support (surface charge, chemical composition and roughness), the lipid vesicles (composition, charge and geometry of the lipids), buffer used (composition, pH and ionic strength), as well as temperature, concentration, and duration of deposition. Moreover, the presence of divalent cations such as calcium or magnesium strongly support vesicle rupture and are important in vesicles with a negative absolute charge because they can screen electrostatic repulsive interactions [64].

1.3 Membrane proteins

Apart from the already exposed importance of phospholipids building blocks in cell membranes, biological membranes are also highly crowded in proteins. All proteins assembled with the cell membrane are called membrane proteins and are structurally and functionally extremely diverse. They can achieve lipid-to-protein (LPR) ratios on weight basis ranging from ~ 0.35 (inner mitochondrial membrane) to ~ 1 (plasma membrane) to > 1 (secretory vesicles) [69], which represent between 20% and 80% (w/w) of the membrane. As a matter of fact membrane proteins are the biochemically active components of the bilayer and provide the diversity of enzymes, transporters, receptors, pores, etc., which distinguishes each particular membrane [3]. Besides, it is estimated that 20-30% [70,71] or even 50% [72] of all the predicted genes in a typical genome encode for membrane proteins.

1.3.1 Classification of membrane proteins

Membrane proteins can be divided into three classes based on their mode of association with the lipid bilayer [1,17]:

I. Integral membrane proteins or transmembrane proteins (TMPs): they are characterised by the presence of hydrophobic regions embedded in the hydrophobic core of the lipid bilayer which establish non-covalent permanent interactions with the fatty acid groups of the membrane phospholipids. Integral membrane proteins span completely through the membrane and, as a consequence, parts of the protein are exposed on both the outer and the inner surface of the bilayer. When more than one transmembrane segment (TM) is present, they are connected by cytoplasmic and exoplasmic loops. Despite most of the integral membrane proteins show TMs in α-helix organizations of hydrophobic residues, less commonly they can also display the polypeptide backbones arranged in an anti-parallel β-sheet.

II. Peripheral membrane proteins: this type of membrane proteins do not interact with the hydrophobic core of the phospholipid membrane and do not traverse completely the bilayer. Consequently, they are present only in one face of the membrane where they are usually associated either to polar headgroups of membrane lipids or to integral membrane proteins by charge-charge interactions, hydrogen bonding and other non-covalent interactions.

III. Lipid-anchored membrane proteins: they are membrane proteins linked to a fatty acyl group, often myristate or palmitate, by a covalent bond. The fatty acid is in turn embedded in the bilayer, anchoring in this way the protein to the membrane.

Membrane proteins are very relevant drug targets due to their involvement in many cellular activities, such as cell growth and division, solute and ion transport, energy production, or sensory stimuli transduction and information processing [73,74]. According to their functions, membrane proteins can also be divided in different subgroups (e.g. membrane receptors, enzymes, adhesion molecules). One of these subgroups is composed by the TMPs in charge of the transport across the membrane, which is formed by the following membrane protein types (Figure 6) [1,17]:

I. Ion channels and pores: they are specialized TMPs which provide a pathway through the membrane barrier to polar and charged small molecules and ions. They facilitate passive diffusion of ions down their concentration gradient by forming a protein-lined passageway across the membrane where multiple ions and molecules can move simultaneously.

II. Passive Transporters: they are also specialized TMPs that permit the circulation of molecules and ions from the intramembranous space to the exterior. As the formers, they transport by moving the solute down its concentration gradient in a favourable membrane potential. The difference lies in their higher specificity due to their possibility to bind and transport one by one larger molecules such as proteins. Passive transporters can be uniporters (they carry only one ion/molecule at a time), symporters (they transport two ions/molecules in the same direction) or antiporters (they transport two ions/molecules in opposite directions).

III. Active transporters: they resemble to passive transporters in the overall mechanism, kinetic properties and uniport/symport/antiport classification, but they require an energy source to transport. **Primary active transporters** are powered by a direct source of energy such as ATP or light. By contrast, **secondary active transporters** are driven by an ion concentration gradient ($\Delta\tilde{\mu}_i$).

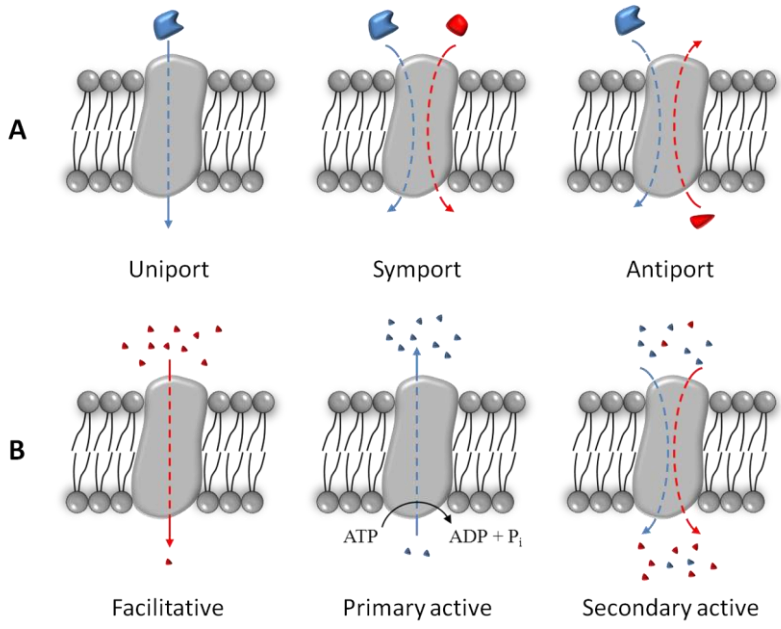

Figure 6. Classification of the membrane transporters according to the direction of the transported molecules (**A**), and according to the energy requirement (**B**).

In order to move substrates across the membrane, transporters must cycle through several conformations. Since they are in thigh relationship with the surrounding phospholipids in order to maintain the diffusion barrier and the electrochemical equilibrium, the lipid-protein interaction might have effects on protein conformational plasticity and thus modulate transport [75,76]. Indeed, it has been demonstrated that protein function can be either regulated (e.g. transport can be disabled if a particular lipid species is not present) or modulated (transport activity can be shifted) by lipids [76]. Although the molecular basis of these effects has not been conclusively explained, a brief resume on this subject will be found in the following section.

1.4 Lipid-protein interaction

Considering the cell membrane as a matrix were lipids and proteins interact, it is clear that the study of this interaction is of high interest in order to better understand how the system operates. In fact, despite the extensive information gathered on the importance of the surrounding lipid composition for many membrane proteins [77–79], there are still controversies about the mechanisms by which membrane proteins and phospholipids affect their functions reciprocally. In this sense, there are currently two complementary points of views to address this subject: the biophysical and the chemical based visions.

In the **biophysical approach** the membrane is considered as a continuum liquid-crystalline material where its physical non-specific lipid properties affect the membrane proteins in a mean field manner [22]. This means that there exist lipid-associated parameters defining physical attributes of the biological membrane which are known to modulate membrane proteins. Hence, factors described in 1.2.2 such as lateral pressure [49,80], spontaneous curvature C_0 and hydrophobic matching, membrane fluidity, surface charge distribution or membrane domains segregation can affect membrane protein structure and function [22,77,81]. All these effects are non-stoichiometric in nature, that is, they do not depend on specific lipid-to-protein ratio [76]. Remodelling of the bilayer due to lipid-protein interactions is a source of work for protein

conformational changes. Alternatively, a membrane protein can also alter the physical properties of its lipid surroundings [72].

The **chemical approach** considers that the important features governing cell membrane are the molecular-molecular interactions or site-specific interactions (lipid-lipid, protein-lipid) [72,77–79]. These interactions are very case specific and respond generally to hydrophobic effects, hydrogen bonding or charge interactions.

Whilst the physical viewpoint is largely addressed by biophysicists [22,48,82], the chemical viewpoint is in vogue nowadays by the increasing of molecular simulations works [18,83,84].

1.4.1 Lipids interacting with membrane proteins

Regardless of the approach, lipid organisation can be, in general, affected by two types of proteins: soluble or membrane proteins. On the one hand, soluble proteins can recognize specifically different headgroups or associate due to bulk chemical properties (e.g. polar headgroup charge). They can have several functions, such as being in charge of the regulation of many cell signalling processes [79]. Additionally, they can modify cell membrane characteristics, e.g. adsorption of proteins can induce domain formation [85]. On the other hand, membrane proteins may experience and/or exert influence at three different lipid levels (Figure 7):

I. Bulk lipids: constitute the ensemble of lipids far from the protein, which do not display direct molecular interaction with it. In consequence, their impact on the protein is relatively non-specific [77]. They can be considered as the executants of the effects related to the described biophysical approach [76].

II. Annular lipids or boundary lipids: they encompass all lipids in closer contact to the protein, which organize forming an annular shell of lipids around it [86]. The interaction of these lipids with a membrane protein is higher as compared to bulk lipids. Indeed, it has been shown by spin-label SPR that this first shell of lipids is motionally restricted as compared to bulk lipids [87]. However, the exchange rate between annular lipids and the bulk phase is fast, indicating a lipid-protein binding affinity relatively weak [87]. This fast recovery of annular lipids can be explained because not only

specific species are important in the shell, but also some particular physical properties that can be achieved by more than one phospholipid species (although affinities might prove to be different between them) [77].

Annular lipids seem to associate to proteins by van der Waals forces arising between acyl chains and grooves formed by specific arrangements of amino acid side-chains on the hydrophobic protein surface. However, interactions of polar headgroup moieties with amino acids at the protein-lipid interface cannot be excluded [79]. The binding stoichiometry of these lipids is related to the size and structure of the TMs of the protein. Proof of this is the fact that not only defined stoichiometries have been described, but also the selectivity of different membrane proteins for specific phospholipids has been found [88]. Moreover, annular lipids work as mediators between bulk lipids and protein, covering the roughness of the protein surface and, importantly, integrating and sealing it into the membrane barrier [78] in a cooperative way [16].

III. Integral protein or non-annular lipids: they present the greater specificity for proteins and integrate a very small number of lipid molecules that act like co-factors [77]. They are bound to TM α-helices either within a protein or at protein-protein interfaces in multi-subunit proteins and present high affinity to hydrophobic cavities and clefts [77].

In some cases, non-annular lipid-binding sites have been found to be extremely well conserved (e.g. cytochrome c oxidase [89]). Such high degree of conservation suggests important structural, functional, or assembly roles of these bound lipids. The precise defined roles are still not completely understood, but there is evidence that their presence is important in the stabilization of interactions between subunits in multi-subunit complexes. Additionally, non-annular lipids can mediate interactions between different protein complexes, allow for good rearrangement of TM α-helices during conformational changes and act as a sealant that allows proteins to integrate correctly in the membrane [79,89].

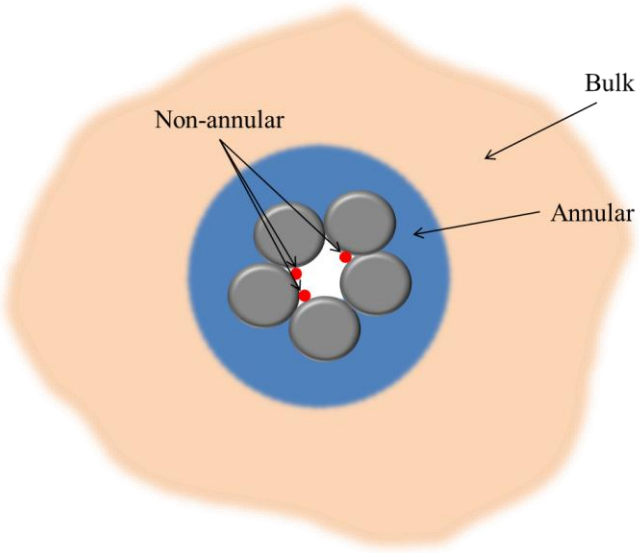

Figure 7. Cartoon exemplifying the putative position of different types of phospholipids exerting influence on a membrane protein embedded in a lipid bilayer: lipids far away from the protein or bulk lipids, annular lipids organized forming a shell around a membrane protein, and non-annular lipids which are bound specifically with the membrane protein.

The relation between a membrane protein and annular and non-annular lipids give rise to interactions that can be explained by the chemical approach, where molecular-molecular interplay is the most relevant characteristic. This tight interaction is evidenced by the lipid presence in resolved high-resolution crystal structures of membrane proteins. This is the case especially for non-annular lipids which, due to their strong binding to the protein, remain immobilized (at least part of the lipid molecule) and are reproducibly co-purified alongside the protein. Interestingly, crystallographic data has revealed the appetence of non-annular lipids to adhere to TM domains in unusual positions, e.g., with the headgroup below the membrane plane and/or non-perpendicular to the bilayer [78]. Some annular lipids have also been resolved in crystals, but they are always found in a highly disordered organisation, as it is the case of the bacteriorhodopsin trimer [90].

1.4.2 Lipid-protein interaction parameters

Many biophysical and chemical parameters have been described to affect reciprocally membrane proteins and lipids (bulk, annular and non-annular). Some of the most important are reported to give some insights into the lipid-protein interaction subject.

Biophysical lipid-protein interaction parameters

- **General bulk phospholipid composition.** Properties of the bulk lipids influence TM helix-helix interactions in several ways: they can modulate changes in helix tilt or orientation, changes on conformation or helix-helix interactions, and even changes in the assembly of larger protein oligomeric complexes [74]. This may be caused by subsequent modifications in the acyl chain order and fluidity of the lipid bilayer, in the nature of a lipid headgroup or in the lateral or transversal bilayer asymmetry which create local lipid domains with defined properties [91].
- **Hydrophobic match.** As previously described, a relevant property of a lipid bilayer is the thickness of its hydrophobic core, which corresponds to the separation between the glycerol backbone regions on the two bilayer leaflets [15]. When a membrane protein is embedded within a bilayer, it is assumed that the hydrophobic thickness of the bilayer adjusts to match well with the hydrophobic thickness of the protein, due to the high energetic cost of exposing apolar regions to water [51,75]. Any hydrophobic mismatch between the two thicknesses would be expected to lead to a distortion of the lipid bilayer, or the protein (e.g. by tilting the helix to reduce the protein effective length [74]), or both, or even to the exclusion of the membrane protein out of the system [77]. It can also provoke protein self-association or conformational change. Alternatively, the avoiding of hydrophobic mismatch may result in the possibility of sorting, selection, or enrichment of certain lipids near the protein [51,92]. Although hydrophobic matching might be a purely physical effect, specific interactions are possible and, in this case, may over-rule the matching effect.
- **Gel to liquid crystalline phase transition.** The L_β to L_α phase transition involves many changes in the physical properties of a lipid bilayer (e.g. fluidity, thickness) which might be expected to affect the activity of membrane proteins [77]. Indeed, some membrane proteins might prefer one or the other phase, leading to a partition of the proteins almost exclusively in one of the phases [93]. Due to the higher fluidity which permits less energetic conformational changes, most of the described cases indicate protein preference for L_α phase [74,94], although in some particular cases L_β phase is also preferred [95].
- **Membrane viscosity.** The resistance to motion (changes in shape of proteins when performing their functions) through a liquid (in this case, the lipid bilayer) can be expressed in terms of viscosity. In a lipid bilayer the resistance to motion is

predominantly processed from the lipid fatty acyl chains. The idea that changes in membrane viscosity may affect the protein function is related to the ancient hypothesis of the "homeoviscous adaptation" of the membrane [96]. In there, it was thought that an exact viscosity parameter of the lipid component in the membrane was held constant for optimal functioning of the membrane. In this sense, it postulated that organisms can alter their lipid composition in order to maintain constant this parameter. However, as further proposed by Lee [77], although organisms modify their membrane composition as an adaptation to temperature and so to changes on the viscosity of their membranes, it might not be true, as a general rule, to say that this maintains a constant viscosity in the membrane.

- **Protein stabilization of lamellar phases.** The presence of TMPs tends to stabilize the lamellar phase in lipids that present tendency to organise in non-bilayer forming phases. This is because the hydrophobic span of the protein matches that of the lipid membrane in the lamellar phase. Protein forces phospholipids with non-bilayer tendencies to be in a bilayer state and thus leads to curvature frustration. As explained in section 1.2.2, this stored stress in the membrane is important since it can modulate protein activity via the heterogeneous transverse profile of lateral pressure across the membrane or via the formation of local non-bilayer structures [48,77]. In turn, the insertion of an integral protein can release this stored stress for example through the positioning of the acyl chains placed nearby the protein and filling spaces bellow the helix. For instance, the presence of Cytochrome c oxidase causes cardiolipin to organise in a bilayer structure under conditions (presence of Ca^{2+}) where normally it would adopt an hexagonal phase [97].

Chemical lipid-protein interaction parameters

- **Chaperonin-like function in insertion and orientation of TM helices.** Each TMP presents a particular topological organisation with certain number of TMs displaying a specific orientation with respect to the plane of the lipid bilayer. In general, the topological organization of a membrane protein is well established, especially in cases where the X-ray structure of the protein is available. On the contrary, the process of membrane protein topogenesis and the factors that influence it are less well defined. In this sense, primal amino acid sequence of a membrane protein encodes a set of topogenic signals, which are decoded by processes not completely understood. Hence, not only the primary structure is determinant for a good tertiary structuring. Correct

folding involves proper control and alignment in the interactions of individual TM helices, multiple TMs, and the ensemble with the surrounding phospholipids [91]. Indeed, there are studies pointing out the importance of specific phospholipids acting as lipid chaperones for some membrane proteins as it has been demonstrated for lactose permease (LacY) of *E. coli* [6].

- **Non-annular lipid highly specialized functions.** The presence of non-annular lipids forming a complex with a membrane protein can be transduced in very diverse and specific functions. For example, they can be keys for the formation of helix-helix association (guide assembly) and orientation of TM helices, or they can be directly involved in the molecular mechanism of the protein, e.g., enzymatic activity or transport processes across the membrane [79].
- **Structure of the annular lipid headgroup region.** It defines the region closer to a membrane protein and can affect the correct formation of secondary structures such as α-helix and β-sheet. This is explained because the polypeptide backbone has requirements for polar residues permitting hydrogen bonding. Hence, the region has been referred to as a catalyst for the formation of secondary structure by peptides [77,98]. Also, the lipid headgroup region can affect the activity of a membrane protein when changing the concentrations of charged molecules or ions close to the surface of the membrane [77].

Finally, a last case which involves both physical and chemical characteristics is the formation of lateral heterogenic domains through the segregation and clustering of lipids and proteins. From *ex vivo* studies it is clear that lipid-lipid interactions can lead to the formation of domains, but there are evidences confirming that the presence of proteins can also affect or trigger this process. For example, lipid *raft* domains which are found in mammalian cells are not considered anymore as structures originated solely from lipid-lipid interactions (cholesterol, saturated phosphatidylcholines, and sphingomyelin), since the protein-lipids interactions have been identified as equally important in the formation, maintenance, and dynamics of these domains [13]. Another example could be the recent findings where microdomains independents of cholesterol or lipid phases appeared when the membrane was in contact to syntaxin-1A membrane protein [99].

The presence of phase separation triggered by biophysical forces seems to be largely driven by lipids and respond to general properties of the interaction partners (size,

rigidity, charge, etc.). It yields to domains highly dynamic which vary from ten to hundreds of nanometers in size [5]. On the contrary, stable or meso-stable assemblies can also be generated by specific, chemical high-affinity molecular interactions between lipids, protein and carbohydrates. In this case the obtained domains might be larger, longer-lived and include static scaffold-based assemblies [5].

Phospholipids and membrane proteins have co-evolved simultaneously in nature, which is evidenced by the high interplay that they exhibit. In this sense, it is clear that many membrane proteins present high specificity for particular phospholipids or for specific phospholipid characteristics and, in consequence, one individual membrane protein seems prepared to be expressed in a precise type of lipid bilayer composition. However, many membrane protein structures have been conserved throughout all domains of life, whereas lipid membrane composition can show remarkable diversity from organism to organism [100]. This might indicate that although the specificity of protein-lipid interactions is well-demonstrated, membrane proteins evidence some degree of fundamental tolerance in remodelling in lipid composition. This tolerance has permitted the emergence of new species without having to extensively remodel the associated membranes proteins, but it has also favoured that a single cell changes its membrane lipid composition in response to changing environments [100]. However, as pointed out by Zhou and Cross [101], yet modifying lipid composition there are many biophysical properties of the membrane environment that remain largely unchanged (e.g. bilayer hydrophobicity and thickness) and can be maintained in different mixtures of lipids, trying to adapt them to the precise needs of each membrane protein. Moreover, different lateral and transversal compartmentalization of phospholipids in a bilayer can create discrete domains with alternative physical parameters, and thus a given bulk composition of a lipid membrane might not be significant of the overall existing different microenvironments. And eventually, the great diversity of different lipids in cell and its constant adjust of membrane composition makes it to seem unlikely that fundamental physiological processes should not be regulated by such a complex lipid repertoire. Indeed, all these points restore the controversy on this subject to the same unsolved questions again and again: to which extent lipids exert their role on protein membrane functioning? And why the cell bothers to synthesise so many lipids? [36,102,103].

1.5 LacY and its surrounding environment

Lactose permease (LacY), a protein present in the inner membrane of the gram-negative bacterium *E. coli*, is the TMP studied in this thesis. Consequently, the phospholipids of interest correspond to mixtures mimicking the composition of the inner membrane of this bacterium.

1.5.1 The inner membrane of *Escherichia coli*

Thanks to the combination of multi-headgroups and different hydrophobic tails, lipids display large chemical diversity in cells. Proof of this heterogeneity is the presence of distinct lipid composition on different cell types and cellular organelles. This high diversity may be to some extent a response to diet (diet-induced variation, which modifies more particularly the composition of fatty acid hydrocarbon chains [72]), although the overall pattern is precisely regulated by the cells and require well-controlled metabolic systems [81,104].

This thesis is directed to the study of the inner membrane of *E. coli*. This cell membrane presents a phospholipid composition of approximately 70% phosphatidylethanolamine (PE), 20% phosphatidylglycerol (PG), and 5% cardiolipin (CL) [102]. PE and PG are sorts of phospholipid headgroups and, therefore, indicate two phospholipid families. This means that in spite of a polar headgroup composition relatively constant in this membrane [102], the presence of different species with different hydrocarbonated acyl chains can be finely tuned by the cell in order to adapt to different environmental circumstances (e.g. rising the growth temperature decreases the quantity of unsaturated fatty acids) [10]. Regarding CL, it shows a structure of diphosphatidylglycerol. CL can form non-bilayer structures in presence of divalent cations and thus it has important functions on membrane stability and fusion [105]. Additionally, it interacts with a large number of membrane proteins. For instance, its presence is critical to functional activation of certain enzymes, e.g. those involved in oxidative phosphorylation [106].

Nevertheless, the main strategy employed in this thesis has been to consider binary mixtures of PE and PG phospholipids generally at a molar ratio of 3:1 in order to mimic the naturally occurring composition. In some experiments PE has also been replaced by

phosphatidylcholine (PC), which is the main phospholipid present in eukaryote cell membranes [3].

1.5.2 Lactose permease

LacY belongs to the major facilitator superfamily (MFS), the largest family of secondary transporters which include TMPs of several species, most of them catalysing active transport of a wide range of substrates by transducing the energy stored in a H^+ electrochemical gradient ($\Delta\tilde{\mu}_i$) into a concentration gradient ($\Delta\mu_s$) of substrate [107–109].

The gene encoding LacY was the first gene of a transport TMP cloned into a recombinant plasmid and sequenced [108]. As a consequence, LacY has been largely studied and it has been considered as a paradigm for secondary transport proteins in order to explore the mechanism of energy transduction [108]. Indeed, this mechanism related to biological membranes is one of the most interesting, intriguing and still unsolved problems in biology. It has been postulated for a variety of different phenomena (e.g., secondary active transport, oxidative phosphorylation, rotation of the bacterial flagellar motor) that the used driving force to perform their functions comes from a bulk-phase, transmembrane electrochemical ion gradient [110]. However, questions about the molecular mechanisms explaining how this Gibbs energy stored in such gradients can be transduced into work or into chemical energy are still uncertain [108].

Additionally, the mechanisms of many biological machines involved in energy transduction seem to be related, since different proteins have been included in structurally similar families. Hence, the study of a paradigm protein such as LacY might be important to understand other related proteins, which, importantly, can play important roles in human disease (e.g., cystic fibrosis, resistance to antibiotics and chemotherapeutic drugs, gastric ulcer, glucose/galactose malabsorption) and take part in the mechanism of action of a large number of drugs [108,111].

LacY is one of the most extensively studied cytoplasmic membrane proteins. It is composed of 417 amino acid residues and is functional as a monomer [108]. LacY works catalyzing the coupled stoichiometric transport of a galactopyranoside and a H^+ (galactoside/H^+ symport). The direction of transport is dependent upon the polarity of the sugar concentration gradient (downhill sugar/uphill H^+) or the H^+ electrochemical gradient (downhill H^+/uphill sugar) [109]. Just as the majority of MFS proteins, the secondary structure of LacY consists of 12 TM α-helices, crossing the membrane in a zigzag fashion, which are connected by 11 relatively hydrophilic, periplasmic and cytoplasmic loops, with both the amino and the carboxyl terminus on the cytoplasmic surface.

LacY's tertiary structure has been resolved from X-ray diffraction in the last decade after the achievement of diverse LacY crystals. First, the structure of the C154G conformationally restricted mutant was solved (3.5 Å resolution) [112] (Figure 8) and not long after the wild-type structure was also completed (4 Å resolution) [113]. Interestingly, both proteins were found to be in the same conformation and no striking structural differences could be appreciated between them. X-ray diffraction revealed that LacY shows a helical content of 86% (80% within the membrane) [108]. In addition, the 12 TM α-helices are shaped irregularly and organized into two pseudosymmetrical six-helix bundles (N- and C-terminal) connected by a long loop between helices VI and VII. In a side view, the monomer displays a diameter of 6 nm and is heart-shaped with a large internal hydrophobic cavity open only to the cytoplasmic side, where the binding site has been observed in the approximate middle of the molecule. Due to this cavity facing the cytoplasm, this conformation is known as the inward facing conformational state of LacY [108]. Importantly, the finding that this conformational state is present in bacteria excludes the possibility of a non-native structure resulting from non-physiological crystallization conditions [114,115].

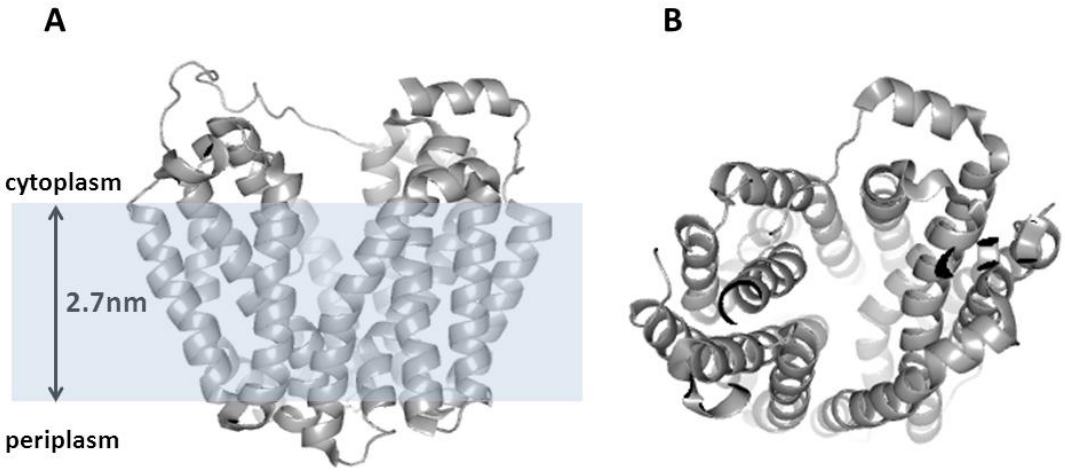

Figure 8. Side-view (**A**) and top-view (**B**) of the crystal structure of inward-facing C154G LacY. Based on PDB ID: 1PV6.

The X-ray structure of LacY provided critical information regarding the overall folding of the protein and the sugar-binding site. What is more, residues already identified as important for correct function could be localized. In that field, the extensive work of professor Kaback [108,111,115] has been determinant. In his laboratory, each of the 417 amino acyl side chains in LacY has been mutated [109], and functional analyses of the mutants revealed that fewer than 10 side chains are irreplaceable or very important in the symport mechanism (Figure 9): E126 (helix IV), R144 (helix V), and W151 (helix V) are directly involved in galactoside recognition and binding; Y236 (helix VII), E269 (helix VIII), and H322 (helix X) are involved in both H^+ translocation and affinity for sugar; and R302 (helix IX) and E325 (helix X) play important roles in H^+ translocation [108,111,116]. As shown in the crystal structures of LacY [112,113,117], these residues are located at the apex of the central hydrophilic cavity and distributed so that the side chains important for sugar recognition are predominantly in the N-terminal helix bundle, and the side chains that form the H^+-binding site are mainly in the C-terminal bundle [108].

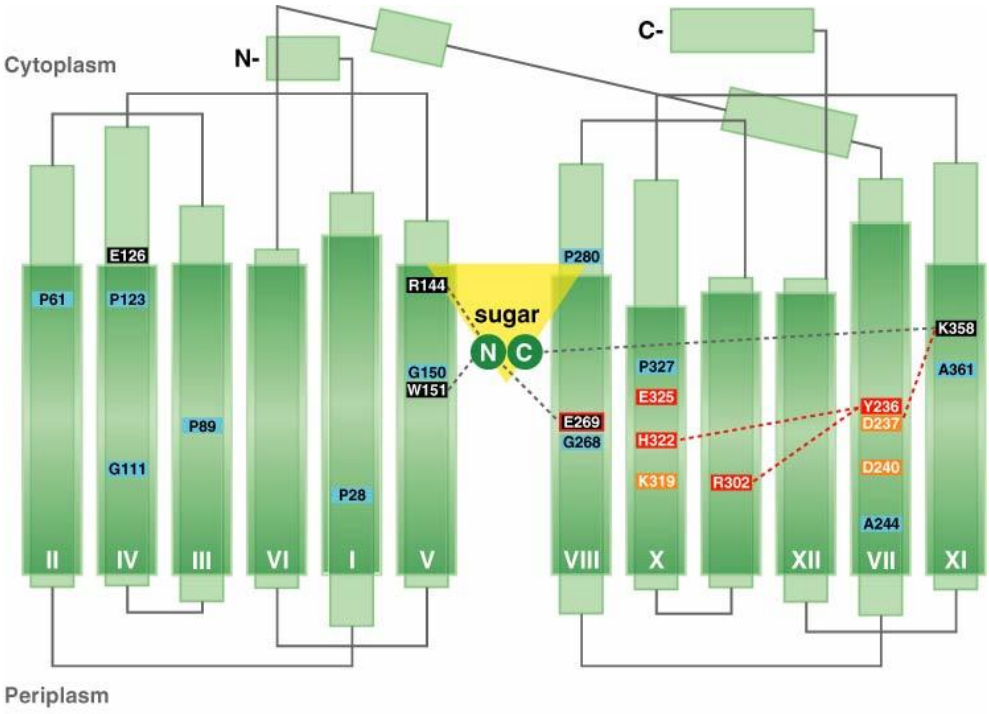

Figure 9. Secondary structure model of LacY derived from the wild-type X-ray structure. The helices traversing the membrane are depicted as dark green rectangles. Light green rectangles indicate hydrophilic domains external to the membrane which connect the different TMs. Lines connecting TMs indicate connectivity between helices. Important residues for the protein are signalled: blue rectangles are residues at the kinks in the TMs, black rectangles are residues involved in substrate binding, red rectangles are residues involved in H^+ translocation, and orange rectangles are residues forming salt-bridges. Glu-269 (black rectangle bordered in red) is involved in both substrate binding and H^+ translocation. An inverted yellow triangle designs the hydrophilic cavity and sugar is depicted by two green circles, with N and C representing the moieties that interact with the N- and C- terminal halves of LacY, respectively (*Figure from Guan et al., 2006* [108]*).*

The mechanism of symport in LacY, although extensively studied, is still being refined [83,109,115,118]. However, there are several biochemical and biophysical data evidencing an alternating access mechanism [115,119], which swaps the molecule from the well-known inward-facing conformation to another less known outward-facing conformation. Accordingly, the catalytic cycle of the transporter does not involve significant movement of sugar- and H^+-binding sites relative to the membrane. Rather, the protein essentially moves around the sugar, alternatively exposing both sites to either side of the membrane [108]. The structure of the outward-facing conformation of LacY, although studied by molecular simulations [120,121] is to date poorly understood, as well as the dynamics and structural changes that underlie the transitions between the inward-facing and outward-facing conformations [83]. A proposal on the mechanism of action can be seen in Figure 10.

Finally, evidences have been gathered on the tight influence that surrounding phospholipids exert on the functional activity of the protein [122].

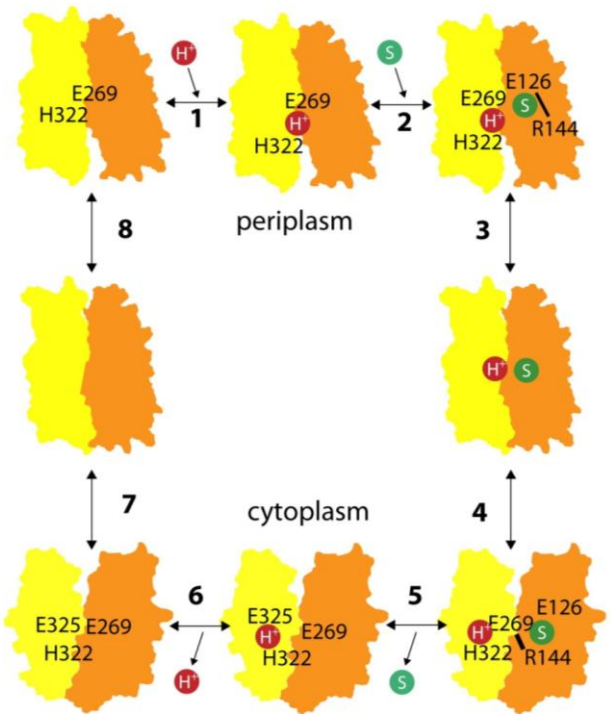

Figure 10. The eight steep LacY reaction cycle for lactose/H^+ symport beginning with an outward-facing conformation: **step 1** represents protonation of LacY, where H322 and E269 participate closely. Importantly, E269 constitutes a link between the H^+-translocation site and the sugar-binding site. In **step 2**, E126 and R144 in the N-terminal domain are absolutely required for sugar binding to protonated LacY, which initiates the outward-to-inward facing transition of LacY in **step 3** and **step 4**. The transition includes several relocations such as the proton movement towards its final acceptor, E325. Substrate release in **step 5** leads to structural rearrangements that cause the final deprotonation of LacY in **step 6**. After releasing a H^+ to the cytoplasm, LacY assumes again an outward-facing conformation (**steps 7 and 8**) *(Figure from Andersson et al., 2012* [83]*).*

1.5.3 LacY-phospholipid interaction

All MFS transporters seem to be tightly coupled to its bilayer environment [83,123–125]. Indeed, the relation between LacY and the surrounding phospholipids has been extensively studied and lipids have been found to affect at various stages of the protein assemblage and activity.

As early as the 70s it was already known that LacY requires a membrane in L_α phase for full transport activity [126,127]. In these pioneer experiments, the phospholipid

membrane was found to play a role in the frequency with which conformational fluctuations occurred in LacY and not in the energetics of the process, something that would agree with the current model of LacY alternating access [76]. Accordingly, LacY reconstitution in supported lipid bilayers has been found to take place preferentially in L_α phases as evidenced by AFM imaging [128].

Studies analysing the effect of the surrounding membrane on LacY can be divided in three types: (i) studies inquiring about the annular region of the protein, (ii) studies looking for the residues involved in the protein-phospholipid interaction, and (iii) studies concerning phospholipid requirements for correct functioning and folding of LacY. In this last section special mention has to be done to Dowhan's group [122], which has devoted plenty of efforts in understanding the role of phospholipids *in vitro* and *in vivo* in the special case of LacY. Their findings might presumably be extrapolated to a wide variety of other TM proteins.

1.5.3.1 The annular region

The presence of an annular region surrounding LacY was first described through the segregation of pyrene-labelled phospholipids in the vicinity of the protein [129]. In this study, the segregation was strongly influenced by the structure of hydrophobic chains, whereas headgroup interactions were less obvious. However, as it was discovered afterwards [130], these measurements were done in POPG proteoliposomes which is a non-biomimetic matrix where the protein is not correctly folded. Therefore, the capability of LacY to recruit lipids in its surroundings was confirmed, but further results were not representative.

Later on, Picas et al. [131–133] working again with pyrene-labelled phospholipids analysed the FRET phenomenon appearing between labelled phospholipids and a single-tryptophan mutant of LacY. By these means, they reported the presence of POPG in the annular region of the protein when it was inserted in POPE:POPG (3:1, mol/mol) proteoliposomes, although POPE was found to be always the main species in this region. In addition, when comparing POPE:POPG at molar ratios of 3:1, 1:1 and 1:3, the first composition presented the best values of FRET efficiency for POPE and thus the optimal matching between phospholipids and LacY. Finally, LacY selectivity for PE seemed to be constrained also to the membrane fluidity. Hence, when LacY was

embedded in a PE:PG mixture with both phospholipids in L_α phase, LacY tended to be surrounded by PE; but when PE was in L_β phase and PG was in L_α phase (the case of a DPPE:POPG mixture), LacY clearly preferred to recruit PG.

1.5.3.2 The residues involved in LacY – phospholipid specific interaction

In the 90's a ion pair in LacY structure (K358 and D237) was identified as important for an efficient insertion of the protein into the membrane, but not for the activity [134,135]. Mutants lacking this charge pair were defective in a step between translation and insertion into the membrane, but they could be stable once inserted. Indeed, molecular dynamic (MD) simulations performed not long ago [83] showed that both residues may interact via a salt bridge that stay intact during protein conformational changes. Therefore, the charge pair is likely to play a role in LacY folding at a stage prior to the complete insertion into the membrane.

In the same study [83], LacY was modelled in two different lipid matrices: POPE and DMPC. Surprisingly, after deprotonation of the protein, only LacY embedded in POPE lipids presented the required conformational changes to start the alternating cycle. In DMPC lipids deprotonated LacY was detached from lipid headgroups and was deficient in starting large-scale conformational changes. These results suggested that LacY needs to be tightly connected to surrounding phospholipids to display structural dynamics necessary for function, while a protein disconnected from lipid headgroups appears static and presumably unable to meet the dynamic demands of transport. Additionally, the main anchor points between the protein and POPE amines were identified, localizing the eight most prevalent hydrogen bond interactions (PE with D44, E139, D190, E255, T310, E314, N371, and E374). Interestingly, D68 residue was not identified among them.

D68 position is described in further detail in section 4.1.2.3, but, briefly, it has been identified as the more relevant PE-interacting residue by Lensink et al. [136]. In this molecular modelling and dynamics study performed with LacY embedded in POPE, POPG and POPC matrices, instead of identifying direct H-bonds they were more interested in the detection of salt bridges between two LacY residues and a phospholipid. Four salt bridges were found with POPE, two with POPC and only one with POPG. The interaction D68-phospholipid-K69 was the most significant salt bridge

identified, and it appeared with the amine group in POPE (non-, mono-, and dimethylated) and also, although weaker, with the choline group in POPC. Conversely, the simulations of LacY in a POPG bilayer showed no affinity of the glycerol side chain to the acidic D68, and POPG was found to bind the phosphate groups of its neighbouring lipids.

These overall results show that MD simulation techniques should be carefully considered since they depend strongly in the used methodology, as well as the depart constraints and structure. However, they provide very interesting information and evidence large differences in LacY systems only by changing the bilayer composition. In any event, extra studies are required concerning residues involved in the sensing of the phospholipid environment, especially to further elucidate if phospholipids play a global or a local (residue-specific) effect on LacY.

1.5.3.3 Phospholipid requirements for correct functioning and folding of LacY

Early studies [137] indicated an important role for lipid composition in LacY function. They showed the requirement of LacY for PE for maximal activity when inserted into membranes containing anionic lipids such as PG and CL, whereas mono- and dimethylation in PE reduced transport activity. They also proved that liposomes lacking PE and containing PG and CL, or only DOPC could support energy-independent downhill transport, but not uphill transport. And, additionally, PE could be replaced by bovine phosphatidylserine (PS) maintaining to some extent the activity, which suggested that hydrogen-bonding ability of the amine in the headgroup might be required for uphill transport. However, almost 30 years of research have shown that the situation is largely more complicated.

The starting point for Dowhan and Bogdanov studies was the possibility that these *in vitro* results did not reflect *in vivo* requirements for LacY. Hence, apart from working with proteoliposomes, Dowhan et al. developed a large library of genetically modified *E. coli* strains. They performed mutations in the enzymes that define the phospholipid biosynthesis allowing thus the tuning of the cell lipid composition and even the insertion of foreign lipid species in *E. coli* [6,122].

Then, the PE requirement for uphill transport described by Chen et al. [137] in *in vitro* experiments could be reproduced *in vivo* and *in vitro*. Hence, it was observed that PE-lacking lipid compositions (only containing CL and PG) did not support uphill transport. After declining the possibility that this was caused by an alteration of the membrane potential [138], a presence of a structural defect in the protein was discovered. Indeed, mapping the topology of LacY in PE-lacking membrane compositions revealed a topological misfolding (Figure 11) [139,140]. Interestingly, these structural defects were reversible by post-assembly exposure of LacY to PE [141] which leaded to the idea of PE acting as a possible lipid chaperone. In any event, it was the beginning of an extensive research focused in relating the lipid composition of *E. coli*, the possibility to carry on uphill transport and the topological characteristics of the protein.

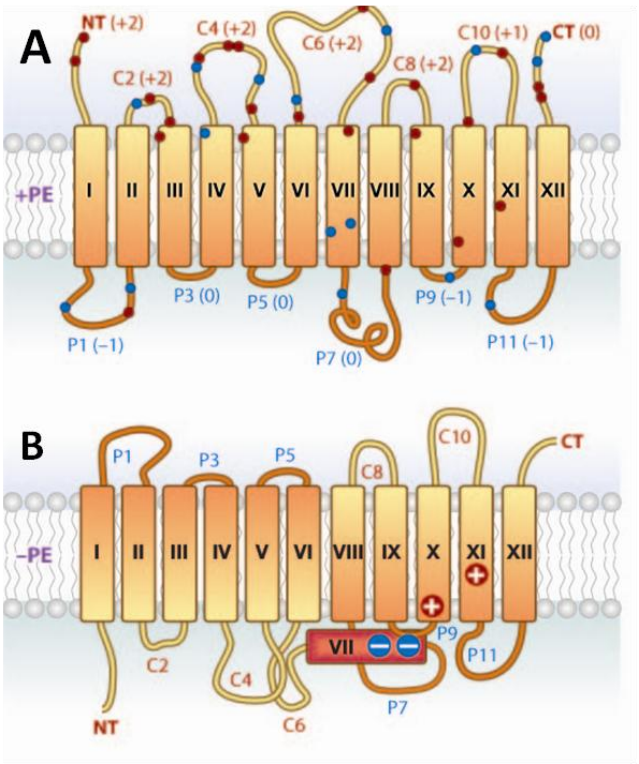

Figure 11. Topological organization of LacY as a function of the membrane lipid composition. LacY assembled in *E. coli* with wild-type phospholipid composition (**A**), and assembled in an *E. coli* mutant lacking PE in the membrane (**B**). Rectangles define TMs oriented with the cytoplasm above the figure. Loops connecting TMs are extramembrane periplasmic (P) or cytoplasmic (C) domains. NT and CT state for N-terminus and C-terminus, respectively. The net charge of each extramembrane domain is indicated next to the domain name. Spots show approximate locations of negatively (blue) and positively (red) charged residues. Topology in B in relation to A presents helices I–VI inverted with respect to helices VIII–XII, which still exhibit native topology. Helix VII (red) is exposed to the periplasm, resulting in the misfolding of the periplasmically exposed domain P7 *(Modified from Dowhan et al., 2009* [6]*).*

As a summary, it was observed *in vivo* and *in vitro* that the uphill functionality of LacY could be re-established after the addition (or the *in vivo* synthesis) of the following lipid species: total *E. coli* phospholipids, commercial bilayer prone PE and the neutral glycolipid GlcDAG. On the contrary, PG and CL (natural or foreign) did not recover the uphill functionality. Monomethyl- and dimethyl-PE were progressively less effective and the neutral glycolipid GlcGlcDAG was completely ineffective [122].

Interesting was the case of PC, which did not show uphill function in proteoliposomes of DOPC [130,137]. Unexpectedly, when PC replaced PE in *E. coli* cells, uphill transport occurred normally [142]. The reason that explained this difference seemed to be related to the lipid acyl chain composition: PC (and also PE) synthesized by *E. coli* are primarily saturated in the 1-position and unsaturated in the 2-position, whilst DOPC contains two unsaturated acyl chains. This hypothesis was confirmed by performing *in vitro* studies with chemically synthesized PCs containing at least one saturated fatty acid and observing how this composition indeed restored LacY uphill transport [140]. Further analyses showed that with the same fatty acid composition, a higher uphill transport activity was observed when using PE-based compared with PC-based phospholipids. In addition, uphill transport activities were observed in the following order: POPE > POPC > DOPE >>DOPC proteoliposomes, indicating that PE is also dependent on the fatty acid composition. This pointed for the first time to an independent influence of both lipid headgroup and fatty acid composition and, eventually, intrinsic curvature of the lipid species [140].

Before PC and GlcDAG had been revealed to suit LacY requirements, initial findings appeared to corroborate Chen's interpretation and indicated the requirement for zwitterionic bilayer-forming phospholipids, with an ionisable amine for proper LacY folding and function. However, these new findings modify the interpretation and rather point to the requirement for a bilayer prone lipid environment with a net neutral charge which might be the most determinant characteristic. Clearly the highly negative surface charge contributed by PG and CL under physiological conditions does not support LacY complete function and requires some attenuation by net neutral lipids. The fact that the neutral GlcGlcDAG is not effective seems to be related to steric effects of its large headgroup that may prevent proper interaction with LacY [122,136].

To conclude, the lipid requirements for supporting native function of LacY are complicated and not fully resolved yet. Downhill transport is not lipid or topological dependent [122,142]. Conversely, uphill transport is highly dependent on LacY correct topology, although it can occur in proteins presenting local subtle defects in its structure, as it is the case of PE-lacking cells expressing PC [142] and GlcDAG [143]. Finally, the effect of lipids on LacY activity involves the role of both the hydrophilic headgroup and the hydrophobic fatty acid moiety of the phospholipid [140].

Furthermore, these new results claim for a revision of well-established concepts in different membrane proteins that show a requirement for PE in order to display uphill transport. In fact, most of the *in vitro* reconstitution studies employ either PC from soybeans, which is highly enriched in unsaturated fatty acids, or synthetic DOPC. Therefore, requirement of heteroacids as found for LacY should be tested in these transporters (e.g. PutP from *E. coli*, LmrP from *Lactococcus lactis*, leucine permease from *Pseudomonas aeruginosa*, branched chain amino acid transport by the transporter from *Streptococcus cremoris*, ABC transporter HorA from *Lactococcus lactis*) [140].

On the other hand, and considering PE as the only native phospholipid supporting uphill activity and correct LacY folding, a huge amount of data has revealed PE as the first phospholipid found to present a chaperonin-like function [138,144]. Chaperones, which were thought to be exclusively proteins, are molecules that bind transiently to substrates to assist their proper folding. They interact non-covalently with non-native folding intermediates, but never with native or totally unfolded molecules. Accordingly:

- PE is required during initial assembly of LacY to establish its proper conformation, but once the information imparted, PE is no longer needed to maintain LacY structure.
- PE only interacts with folding intermediates of the protein, since LacY synthesised in PE-lacking cells can recover the topology when partially denaturalized in presence of SDS and PE, whilst simple exposure to PE does not modify the protein.
- PE-lacking cells could insert LacY in the membrane, but it was found to be incorrectly folded. Therefore, the phospholipid is not required for a good insertion yield or initial folding of LacY, but it is essential in a post-insertion folding step to assure final correct topology.

All described evidences point to an effect of PE in LacY folding solely lipid-driven, spontaneous and governed by thermodynamic considerations [6,139]. Moreover, PE re-naturalizing capacity over LacY derived from PE-lacking cells and reconstituted into proteoliposomes indicates a topogenic influence independent of protein folding history or other protein factors [130]. Thus, PE and probably other phospholipids can interact with proteins in a chaperonin-like way and act as determinants of final structural organization during late folding events outside the translocon [122]. This may indicate that final topological organization in a membrane protein is also dependent on the lipid composition of the host organism and not only on the protein sequence.

One possible explanation for this chaperonin-like role in PE has derived from experiments analysing the incorrect structure of LacY in PE-lacking cells. In fact, the absence of PE seems to perturb delicate charge balances existing in the protein which allow helices to be in the hydrophobic core and loops to be correctly placed in the periplasm or in the cytoplasm. Indeed, as described by the "positive-inside rule" [122,145], a loop with an overall positive charge might be retained in the cytoplasm, whilst a negative predominance in a fragment translocates it to the periplasm. Therefore, a role for net-neutral lipids like PE (but also PC and GlcDAG) is to control this equilibrium of charges [6,146,147]. The whole idea has led to the charge balance hypothesis [6,148] that defends the co-evolution of membrane proteins and lipids in order to maintain a good balance in the net charge of the whole membrane surface.

A final new interesting concept presented by Vitrac et al. [149] comes from recent experiments where interconversion between different topological conformers of LacY was observed in a PE dose-dependent manner. Hence, by increasing or decreasing PE levels in LacY *in vivo* [150] or *in vitro* [149] different degrees of LacY unfolding were found. This demonstrates that membrane protein topology is not static and can be changed simply by modifying membrane lipid composition in a manner independent of other cellular factors. Indeed, these findings conduct to the attractive possibility that membrane protein organization can be sensitive to changes in the lipid environment, which may occur locally in cell processes such as cell division, intracellular trafficking of proteins, membrane fission and fusion, metabolic changes, etc.

Chapter 2. Objectives

Once introduced the state of the art in the field, the main objective of the thesis was directed to investigate the interplay between LacY and its surrounding phospholipid environment in model membranes. Specifically the detailed objectives were the following:

a. Unveil the molecular properties governing the selectivity between LacY and the phospholipids present in the annular region.

b. Determine the composition of this annular region.

c. Determine the influence of the bulk phospholipids in LacY insertion.

d. Investigate the influence of LacY insertion in the physicochemical properties of the bulk phospholipids.

e. Investigate the impact of different phospholipid matrices in the proper insertion, packing and binding capabilities of LacY.

f. Investigate the importance of the aspartic acid in position 68 of LacY in the interaction between LacY and the phospholipid PE.

Chapter 3. Characterization of the lipid system

3.1 The lipid system of interest

The approach to mimic the inner membrane of *E. coli* consists in the use of binary mixtures of phosphatidylethanolamine (PE) and phosphatidylglycerol (PG) at different molar ratios. The estimated biomimetic molar ratio is PE:PG 3:1 mol/mol [65,151,152], although some other compositions have been studied in order to analyse the influence that both family of phospholipids exert to the mixture. Hence, the studied mixtures in this research are the following:

I. POPE:POPG, DOPE:POPG and DPPE:POPG all of them at 3:1 molar ratio: these mixtures were studied with the aim to characterize three lipid matrices with different degrees of PE acyl chain unsaturation for further analysis of LacY-phospholipid interaction.

II. POPE:POPG at 3:1, 1:1, and 1:3 molar ratios: these mixtures were studied with the aim to bring light to the influence of the PG presence in the most biomimetic system, POPE:POPG (3:1, mol/mol) [153].

The lipid mixtures have been studied through three different model membrane systems: monolayers, liposomes, and SLBs; the three of them resumed in section 1.2.3. A brief description of all the used phospholipids is presented below.

3.1.1 PE

PE (Figure 12) is characterised by being a headgroup which gives rise to zwitterionic phospholipids. It is small as compared to the acyl chain moiety, which results in a global phospholipid shape of a truncated cone. This structure confers to PE phospholipids two characteristics: (i) a negative C_0 [154] and (ii) the possibility of undergoing bilayer to non-bilayer physical transitions at relatively high temperatures [22,102,155]. Additionally, because of the ionisable amine of this headgroup, all PE phospholipids have the ability to establish hydrogen bonds, both as donors and as acceptors. This is important, since it allows intermolecular binding and leads to the formation of large and stable PE networks [84,156,157].

PE phospholipids are present in both eukaryotic and prokaryotic membranes, where they participate in a large variety of tasks such as fusion, vesiculation and curvature of bilayers, as well as other biological processes like cell division [151].

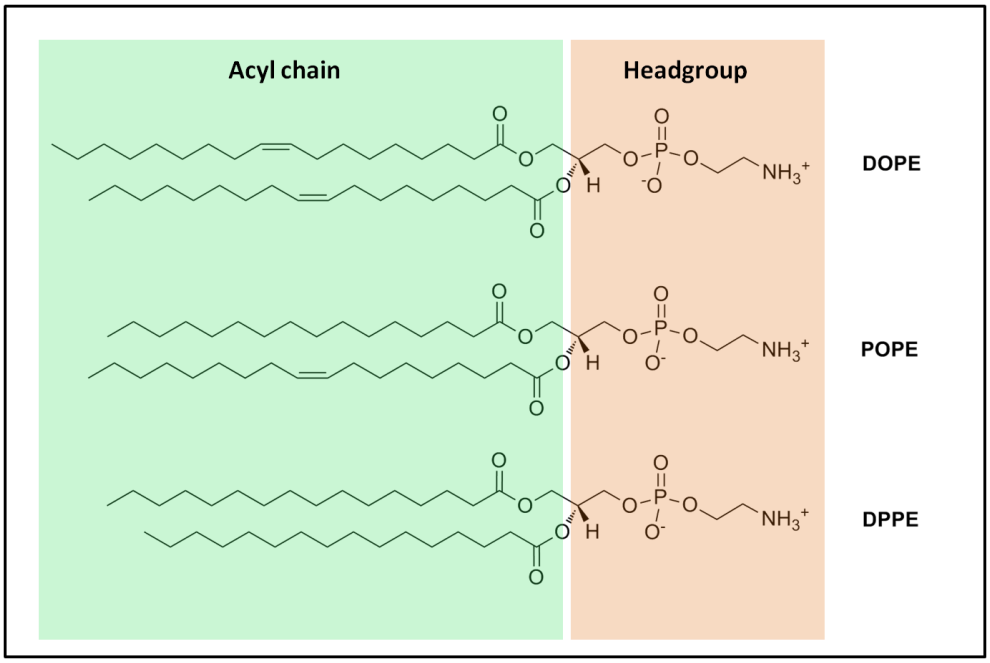

Figure 12. Molecular structures of DOPE, POPE and DPPE. The common PE headgroup is evidenced on the right part of the structures. Acyl chains varying its degree of unsaturation can be observed on the left.

- **POPE:** 1-palmitoyl-2-oleoyl-*sn*-glycero-3-phosphoethanolamine (see structure in Figure 12) is a heteroacid phospholipid formed by a PE headgroup and two different

fatty acyl chains. One of them, palmitoyl, in position *sn*-1 relative to the glycerol, has 16 carbon atoms and is completely saturated. Conversely, oleoyl, in position *sn*-2, is formed by an 18 carbon atoms chain and presents a *cis* unsaturation at the carbon 9. POPE is part of the most common PEs in the inner membrane of *E. coli*, since the most usual phospholipid configuration for all biomembranes corresponds to a saturated *sn*-1 chain and a mono- or polyunsaturated *sn*-2 chain [153].

- **DOPE:** 1,2-dioleoyl-*sn*-glycero-3-phosphoethanolamine (see structure in Figure 12) is an homoacid phospholipid formed by a PE headgroup and two identical acyl chains. Both acyl chains are oleoyl structures with 18 carbon atoms and a *cis* unsaturation at the carbon 9.
- **DPPE**: 1,2-palmitoyl-*sn*-glycero-3-phosphoethanolamine (see structure in Figure 12) is an homoacid phospholipid formed by a PE headgroup and two identical acyl chains. Both acyl chains are palmitoyl structures with 16 carbon atoms completely saturated.

3.1.2 PG

PG (Figure 13) is a lipid headgroup which gives rise to phospholipids with a negative net charge at pH > 5 [158]. It has a cylindrical molecular shape and so, a tendency to form flat bilayers even at high temperatures [158]. The hydroxyl group present in its structure allows PG phospholipids to be acceptors and donors of hydrogen bonds, just as POPE [84,159,160]. However, in this case the interlipid interactions are weakened by the electrostatic repulsion of negatively charged PGs [84]. Indeed, the charge presence makes PG very sensitive to the ionic strength of the aqueous solution, e.g. intermolecular bridging with divalent cations has to be considered [3].

PG phospholipids are typically present in higher plants and bacterial membranes. Whereas PE is the most abundant phospholipid in the inner membrane of *E. coli*, PG is the main species in *Staphylococcus aureus*. Eukaryotic membranes display low amounts of PG, for instance in mitochondria or in red blood cells [84]. It is thought that PGs, as well as other charged lipids, function both as membrane stabilizers and destabilizers for instance by decreasing protrusions in the membrane formed by PE molecules [151].

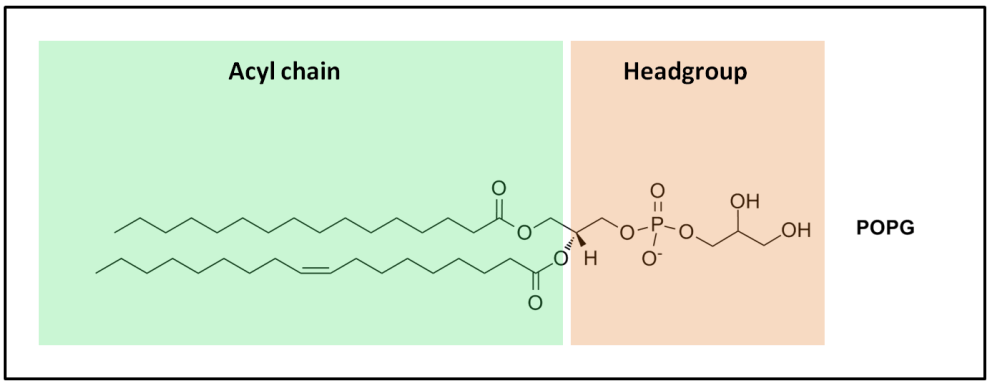

Figure 13. Molecular structure of POPG. PG headgroup is indicated on the right moiety of the molecule, whilst acyl chains are on the left.

- **POPG:** 1-palmitoyl-2-oleoyl-*sn*-glycero-3-phosphoglycerol (see structure in Figure 13) is a heteroacid phospholipid formed by a PG and the same acyl chains described for POPE.

3.2 Techniques to characterize the system

3.2.1 Langmuir isotherms

As specified in section 1.2.3, a membrane model system to study the cell membrane *ex vivo* is the lipid monolayer, which can be physically analysed by performing isotherms.

The obtaining and the study of lipid monolayers can be achieved by using a Langmuir trough (Figure 14), an instrument that allows the organization of amphiphilic molecules into lipid monolayers at the interphase of two phases (air-liquid or liquid-liquid). The Langmuir trough can accurately measure the surface area (A) and the surface pressure (π) and is used for analysing the behaviour of monolayers upon compressing or expanding its area and thus modifying the area per molecule. In addition, it permits the transfer of these monolayers into solid substrates by dipping/rising them through the monolayer.

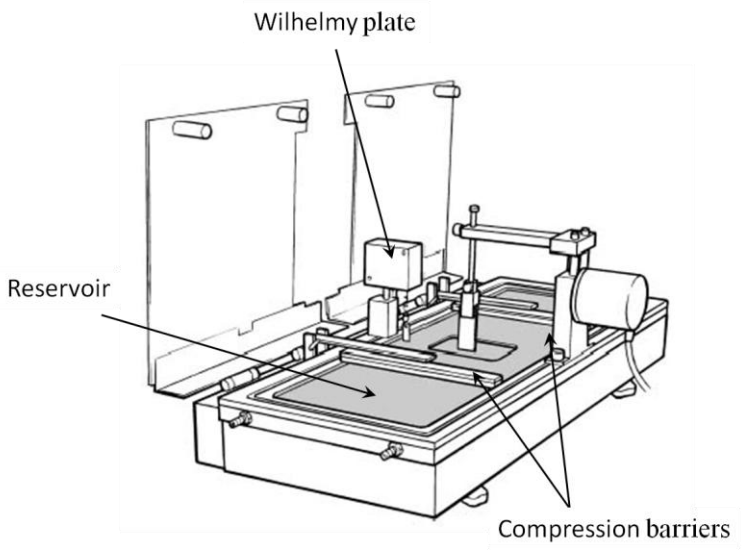

Figure 14. Schema of a Langmuir trough. The apparatus is composed of a rectangular reservoir made of Teflon® where the subphase is contained; two compression barriers which confine the amphiphilic molecules in the desired area of interphase by sweeping them; a Wilhelmy plate, the surface pressure sensor, which measures changes in water surface tension caused by the presence of lipid molecules; and an electronic interface (not depicted) which has a feedback system to control both surface area and surface pressure getting advantage of the compression barriers motor and the surface pressure sensor.

Once the confined monolayer is obtained, a π-area isotherm can be performed. It is operated at a constant temperature and consists of a slow lateral compression of the monolayer at a constant velocity while π and A are monitored. The isotherm can be considered as a fingerprint of a specific lipid or lipid mixture under certain experimental conditions and it is a way to obtain specific information on the packing and organization of lipid molecules [161].

Briefly, π is a measure used to analyse the reduction on surface tension (i.e. energy per area unit to generate more surface) of a liquid caused by the presence of some agents in its surface. It can be defined as [3]

$$\pi = \gamma_0 - \gamma$$

where γ and γ_0 are the surface tension in presence and absence, respectively, of the surface agent. In this sense, π values provide means to analyse the lateral compactness of an amphiphilic molecule through the extent of reduction of surface tension. Indeed, the more molecules of surface active agent present, the higher is π.

A π-area isotherm shows different regions depending on the compactness of the molecule (Figure 15), similarly to what happens in the aggregation of 3D matter [161].

At large areas the monolayer is found in what is called the **gaseous (G) phase**: molecules are widely spaced, interact weakly and behave similar to gas molecules in two-dimensional space. Indeed, the recorded π is nearly zero which indicates that the molecules are not affecting the surface tension of the subphase.

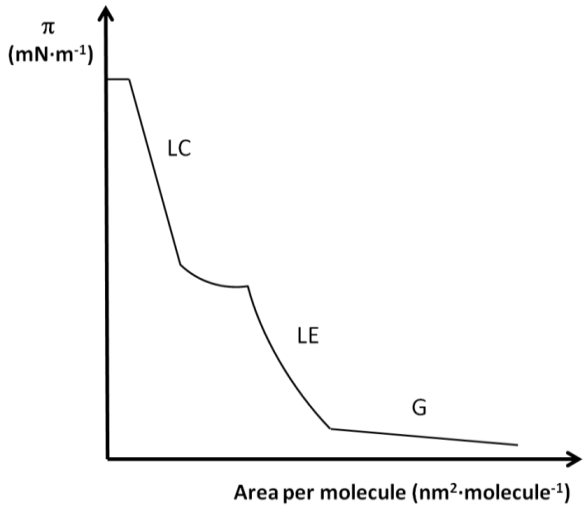

Figure 15. Hypothetic example of a surface pressure – area isotherm from the gas (G) to the liquid-expanded (LE) and the liquid-condensed (LC) phases up to the collapse of the monolayer.

Upon lateral compression of the monolayer with the Langmuir trough barriers, molecules begin to interact. At a certain point, π starts to increase (and consequently the area per molecule starts to decrease) as a result of the restriction in the freedom of movement arisen when molecules or domains of molecules start to press one against another. This stage is called **liquid-expanded (LE) phase**, since the behaviour of molecules is comparable to that of a liquid in three dimensions and it is often assimilated to lipids in the L_α phase. Still compressing, π keeps on rising as molecules become more tightly packed. At some point, a bend in the isotherm can be observed indicating another change in state: from now on the monolayer behaves like a solid-like sheet and is organized in the so-called **liquid condensed (LC) phase**. Here molecules are ideally perfectly compacted and oriented, while occupying very small area per molecule. Hence, any increase in the confinement may lead to large increases in π.

Further compression of the monolayer beyond the LC phase results in a fall in π values which indicates the collapse of the monolayer. It occurs under a specific nominal

pressure which the monolayer cannot stand. Therefore, the monolayer breaks up and material can be pushed down to the bulk liquid or up to the air forming phospholipid multilayers.

Beyond the extraction of information related to the organization of phospholipids upon compression, an isotherm permits as well the obtaining of thermodynamic parameters of the system such as the isothermal compressibility modulus (C_s) or the Gibbs excess energy (G^E) in mixed isotherms (more specified 3.3.1).

3.2.2 Laurdan fluorescence

Fluorescence basic principles

Liposomes, another membrane model (section 1.2.3) can be analysed using fluorescence spectroscopy techniques. Fluorescence phenomenon is a particular type of luminescence, which encloses all emission of light produced by a physic system due to the transition from an excited state to a fundamental state and not resulting from heat dissipation or other relaxation mechanisms. In the case of fluorescence, it appears when a molecule is capable of being excited by a photon and then emitting another photon in a different wavelength (λ). Any molecule able to present fluorescence emission is called fluorophore. Fluorophores typically contain several combined aromatic groups, or planar or cyclic molecules with numerous π bounds, which present special energetic orbital dispositions that allow this re-emitting of light upon light excitation. Finally, fluorophores can be intrinsic (they are part of the studied system) or extrinsic (they are added to the sample) [162].

Hence, a fluorophore emitting fluorescence results from a three stage process (see the simple electronic-state diagram or Jablonski diagram depicted in Figure 16) [162]:

I. Excitation: A photon of an energy hv_{ex} that matches a possible electronic transition within the studied molecule is supplied by an external source (e.g. incandescent lamp or laser) and absorbed by the fluorphore, which suffers a transition from a relaxed state (S_0) to an electronic singlet state (S_1).

II. Excited-state lifetime: an electron of the fluorophore has been promoted to a higher energy orbital in stage I (e.g. $S_0 \rightarrow S_1$) and remains excited for a finite time (typically 1-10 nanoseconds). During this time, the molecule can be subject to a multitude of possible interactions with its molecular environment. Additionally, it can deexcitate partially yielding a relaxed singlet excited state.

III. Fluorescence emission: from the excited state S_1 molecules may return to the ground state (S_o) by emitting a photon of energy $h\nu_{em}$. Due to energy dissipation during the excited-state lifetime, the energy of this photon is lower than the energy displayed by the excitation photon. The difference in energy or wavelength between both the exciting and the emitted photos is called the Stokes shift. It is fundamental to achieve good sensitivity in fluorescence detection because it allows emission photons to be detected against background excitation photons.

Furthermore, not all the excited molecules return to the ground state, since they can undergo 'non-radiative relaxation' due to other processes such as collisional quenching, intersystem crossing or vibrational relaxation. The fluorescence quantum yield, i.e. the ratio of number of fluorescence emitted to the number of photons absorbed, is also a parameter characteristic of a fluorophore and it represents a measure of the relative extent to which fluorescence occurs.

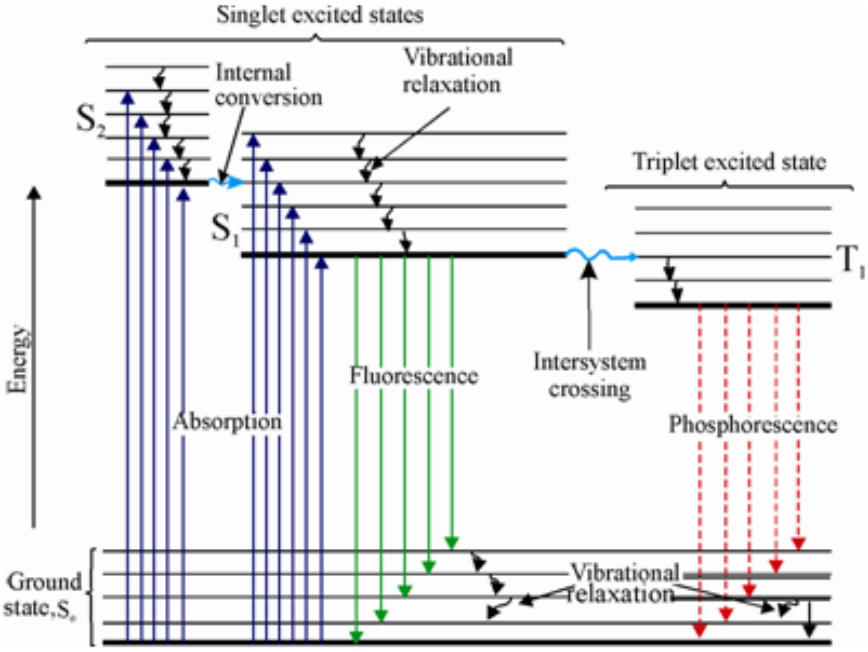

Figure 16. Jablonski diagram showing the phenomenon of fluorescence and phosphorescence between the ground state (S_0) and two singled excited states (S_1 and S_2) or a tripled excited states (T_1) *(www.expertsmind.com).*

Figure 16 presents this process in discrete electronic transitions as it would occur for single atoms, with the interplay of photons of specific energy (hv_{ex} and hv_{em}). Instead, in polyatomic molecules in solution this is replaced by broad energy spectra: the fluorescence excitation spectrum and the fluorescence emission spectrum, respectively. From them, maximum excitation wavelength (λ_{ex}) and maximum emission wavelength (λ_{em}) can be identified, which are characteristics of a fluorophore in a determined chemical environment.

Laurdan fluorophore

Laurdan (6-dodecanoyl-2-dimethylamino-naphthalene) (structure in Figure 17A) is the most commonly used molecule of all membrane probes developed by Weber and Farris [163]. It is a naphthalene derivative that presents the advantageous characteristic of being solvatochromic, i.e. being sensitive to the polarity and the molecular dynamics of dipoles in its environment [164,165]. This is possible thanks to the naphthalene moiety of the molecule that possesses a dipole moment due to a partial charge separation between the 2-dimethylamino and the 6-carbonyl residues [166]. This dipole moment can increase when the molecule is excited and may cause reorientation of the

surrounding solvent dipoles. The energy required for solvent reorientation decreases the probe's excited state energy, which results in an emission of less energetic photons. Therefore, Laurdan's emission spectrum may vary in a continuous red shift as the polarity of the environment increases.

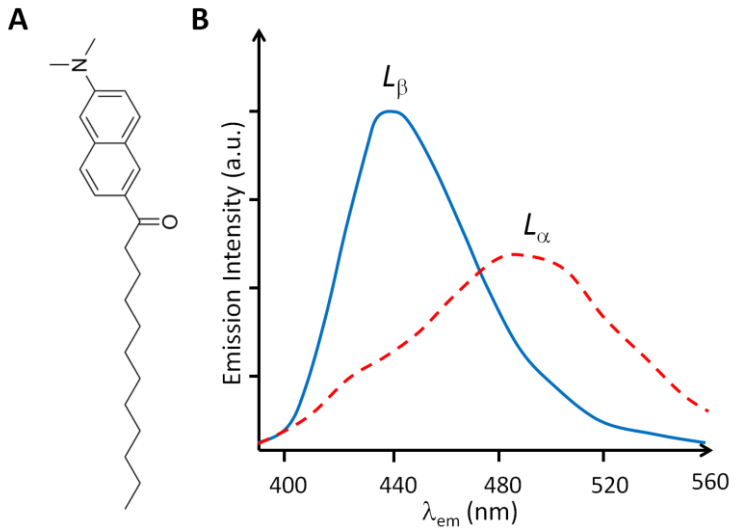

Figure 17. Laurdan probe molecular structure (**A**) and Laurdan emission spectrum (**B**). Continuous line shows a bluer emission occurring when Laurdan is embedded in phospholipids in L_β phase and discontinuous line corresponds to a reddish emission when Laurdan is embedded in phospholipids in L_α phase.

In addition, due to Laurdan amphiphilicity this fluorophore is capable to locate itself in a strategic position when inserted in lipid bilayers: it is localized at the hydrophilic-hydrophobic interface of the bilayer [167], with its lauric acid moiety at the phospholipid acyl chain region and its naphthalene moiety at the level of the phospholipid glycerol backbone. This is a privileged situation, since in this context Laurdan can be very sensitive to the level of hydration of the headgroup phospholipid region. Hence, fluorescent spectrum shifts indicate differences in the number and/or mobility of water molecules present at the level of the phospholipid glycerol backbones [165] and, thus, are directly related to the physical state of the surrounding phospholipids (e.g. packing, lateral organization). This makes Laurdan a very sensitive fluorophore to membrane phase transitions and other alterations of membrane fluidity such as the coexistence of phases [168,169].

In consequence, when incorporated into lipid bilayers, the λ_{em} of Laurdan depends on the phase state of the phospholipids, being bluer in solvent-non-relaxed states (λ_{em} around 440 nm when surrounded by phospholipids in L_β phase) and redder in solvent-relaxed states (λ_{em} around 490 nm when surrounded by phospholipids in L_α phase) (Figure 17B) [164,165]. Moreover, Laurdan exhibits a temperature-dependent redder shift of the emission maximum upon increasing temperature within the L_α phase, whilst in L_β phase this temperature-dependent behaviour does not occur. This shift of the emission spectrum, which allows T_m calculation, is attributed to the dipolar relaxation process occurring only in more mobile phases where the phospholipids are less tightly packed and consequently there is more presence of water around the phospholipid headgroups [170].

Thus, as it is described in 3.3.1, the use of Laurdan fluorescent probes permits to calculate the T_m of a phospholipid system and, at the same time, to detect at a specific temperature the presence of domains of different composition coexisting in the membrane.

3.2.3 Differential scanning calorimetry

Differential scanning calorimetry (DSC) represents another suitable technique to study the thermotropic behaviour of liposomes. DSC is a thermoanalytical technique that monitors and characterizes changes in physical state in polymorphic materials (such as lipids) as well as perturbations on pure materials by the interactions with other different substances. DSC analyses the difference in the amount of heat required to increase the temperature of a sample and an inert reference that are heated independently. For example, the heat for the L_β-L_α phospholipids transition would be required in excess over the heat required to maintain the same temperature in the reference [3].

The ability to determine transition temperatures and excess capacity heats makes DSC a valuable tool in constructing phase diagrams for mixtures of materials (e.g. a phase diagram for a binary system of two lipid components). The most commonly used phase diagrams of binary lipid mixtures are temperature (T)/composition (χ) diagrams, in which pressure is constant (most often atmospheric pressure). To construct this type of phase diagram (Figure 18), for each composition the temperatures at which melting

initiates (T_{onset}) and is finished (T_{offset}) are represented. Then, lines connecting these temperatures are drawn separating regions corresponding to different stable phases (before melting, after melting and coexistence of domains in both phases). The shapes of these lines depend on the thermodynamic characteristics of mixing and melting of the individual components [3].

Ideally, for a given (χ, T) point inside a two-phase region, a tie-line can be drawn, which is a straight line connecting the point under consideration to the nearby phase boundaries. Then, from the values in abscissas of the intersection points with the phase boundaries the compositions of the phases in equilibrium can be obtained. Additionally, the lever rule can be applied to obtain the proportion of each phase in the mixture from the relative distances along the tie-line between the considered point and the intersections with each phase line [171] (see example in Figure 18).

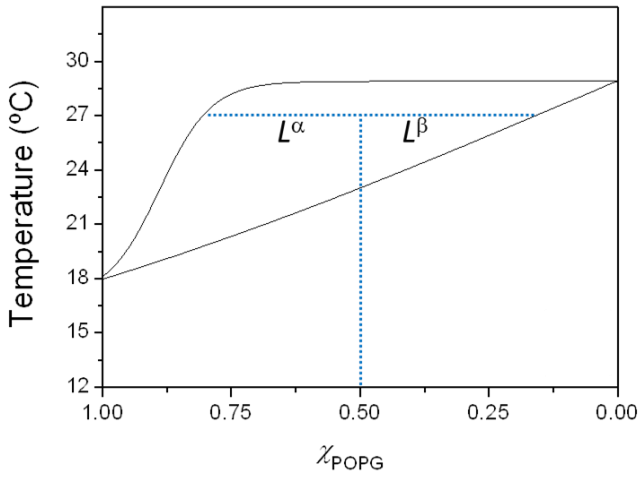

Figure 18. Representative procedure to calculate the proportion of L_{α} and L_{β} at a desired molar fraction by applying the lever rule on a two-component phase diagram *(Figure from results in 3.3.2)*.

3.2.4 Atomic force microscopy

SLB, the last of the employed artificial systems can be exhaustively studied by means of atomic force microscopy (AFM). AFM [172], a near-field microscopy technique initiated in the 80s, belongs to the family of the scanning probes microscopes (SPMs). SPMs, developed after the invention of scanning tunnelling microscopy in 1983 [173],

are characterized by being non-optical microscopes. Instead, they are based in the sensing of near-field physical interactions between two elements placed extremely close: the instrument probe and the surface of interest. In the case of AFM (Figure 19) the probe is a sharp tip attached to a sensitive cantilever and the sample or the probe are attached to a piezoelectric scanner which ensures three-dimensional positioning with high accuracy. When approaching the tip to the sample and prior to physical contact, the cantilever deflects at the appearance of short-range forces acting between both surfaces. These forces, which can be attractive or repulsive and depend on the nature of the interaction (e.g. chemical forces, van der Waals forces, electrostatic forces, capillary forces, friction forces) [174] permit, using a feedback system, to keep the probe at a constant force from the sample, while it scans its surface. In AFM the most used feedback system consists in focusing a laser beam on the back side of the cantilever and in detecting the reflected beam by means of a position sensor, which is usually a quartered photodiode. The position is sent to the electronic interface which, in turn, controls the tip-sample distance and informs the piezoelectric scanner to correct it or not. Therefore, the corresponding correcting movement of the piezoactuator is what generates the topographical image [175].

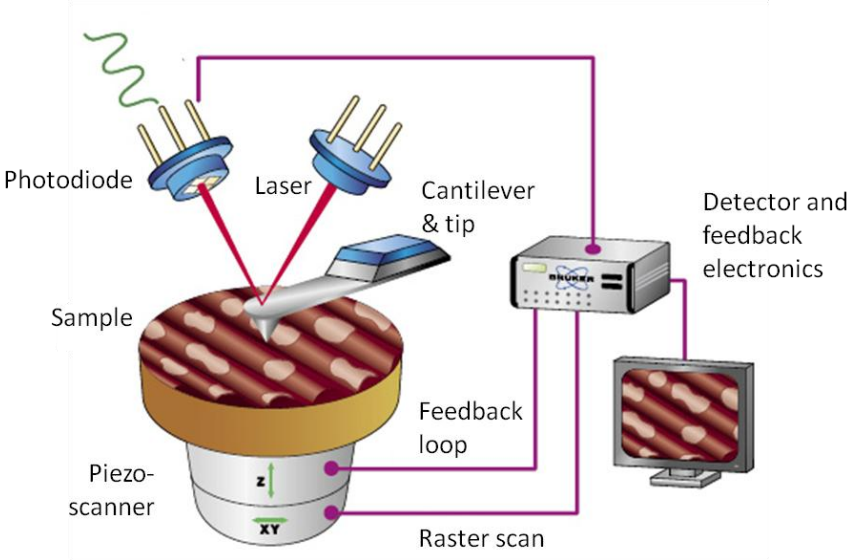

Figure 19. Schema representing the principal elements constituting an AFM instrument: the piezo scanner, the sample, the cantilever and the tip, the laser beam, the photodiode and the detector electronics (*Modified from blog.brukerafmprobes.com*).

The sample is scanned line per line in order to obtain a topographical record of its surface in what is called the AFM topographic mode. The most commons topographic modes used in AFM are (i) the constant-force mode, in which the sample height is adjusted to keep constant the deflection of the cantilever, and so is the force that the tip applies to the sample; and (ii) the intermittent contact or Tapping® mode, in which the tip oscillates near its resonance frequency over the surface and the feedback controls the amplitude and phase of this oscillation. This latter mode reduces the arising of lateral forces during imaging due to minor contact tip-sample (the tip touches the sample surface only at the maximal amplitude) and is thus advantageous for imaging "soft" materials such as biological samples.

Beyond this firstly developed topographic mode, other working modes have been progressively introduced by taking advantage of the tip-sample interaction. For instance, a wide spread AFM mode intended to gain insight into the nanomechanical characteristics of samples at sub-nanonewton resolution [55,176] is the force-spectroscopy (FS) mode. In this mode, the tip focuses in a precise point and ramps in "z" against the sample, while the cantilever deflection is recorded as a function of the vertical displacement of the scanner. Therefore, the tip first approaches, pushes the sample and then retracts. This results in a cantilever-deflection versus scanner-displacement curves, which can be transformed into a force-distance (FD) curve using appropriate corrections.

Hence, AFM is a very powerful technique for the characterization of samples at the nanometer scale. It allows the imaging of conducting and non-conducting samples (contrary to STM) in liquid under physiological conditions (sample preparation is much more easy than in electron microscopy techniques, for example), and it presents a good sub-nanometer resolution in the vertical (0.1 nm) and the lateral (1 nm) axis [55]. Furthermore, the AFM technique is in constant evolution from the initial topography performance to the current new modes where the tip is used as a nano-actuator to manipulate and modify the samples, or even to the improved high-speed AFM [177]. For instance, a few glimpses on future advances in AFM technology might be the idea of a lab-on-a-tip based on the development of modified AFM tips to further play with the tip-sample interaction [178]; the coupling of AFM with other powerful techniques such as the tip-enhanced Raman Spectroscopy (TERS) [179] or the development of tiny AFMs aimed to be used *in situ* to directly diagnose patients [180].

Imaging SLBs

AFM is a very powerful technique to characterize SLB model systems in terms of topography and nanomechanics. The topographic AFM mode permits the analysis of the bilayer organization at the nanometer scale and is especially interesting because it allows the investigation of the lateral domain formation in membranes. Indeed, AFM is among the most used techniques for the study of domains in the nanometer range, yet from artificial membranes [33,93,181,182] or from natural sources [37,38,183,184]. Moreover, AFM has the capability of following dynamic processes. For instance, the modifications of the membrane to the addition of active-membrane compounds can be monitored [169] as well as the changes in bilayer morphology induced by modifications in buffer [185] or in temperature [186–188]. Similarly, the analysis of the behaviour of L_β and L_α lipid phases upon temperature rising can be used to construct phase diagrams of different lipid mixtures [189], as it is done in 3.3.2 for the binary lipid matrix POPE:POPG.

Regarding nanomechanical analysis, FS mode is useful to elucidate intrinsic characteristics of a single lipid system or a lipid matrix [62]. FD curves performed on SLBs show common patterns (Figure 20). In the approach part of the curve, the cantilever is brought close to the sample surface where it exerts a wide range of forces. When van der Waals attraction forces exceed the gradient of the tip spring constant and repulsive forces, a sudden jump of the tip to the surface is sometimes observed, which is referred as **jump-to-contact** [190,191]. Now the tip-sample contact is reached and the piezo displacement continues pushing the sample and bending upwards the cantilever. This is graphically a continuous line with a slope that prolongs until the appearance of a discontinuity. It appears upon the failure of the bilayer and indicates the penetration of the tip into the membrane [192]. The force at which this second jump occurs is attributed to the maximum force the membrane can withstand before breaking and is known as the **breakthrough force** or **yield threshold** (F_y) [193,194]. After that, the tip starts pressing the substrate surface, which is reflected in the plot by a continuous line displaying a slope different from the one obtained in the process of bilayer pushing. Finally, during the retract part of the curve the cantilever is pulled away from the sample but needs additional force to come back to its starting position. This pull-off force between the tip and the bilayer is called **adhesion force** (F_{adh}) [65,195].

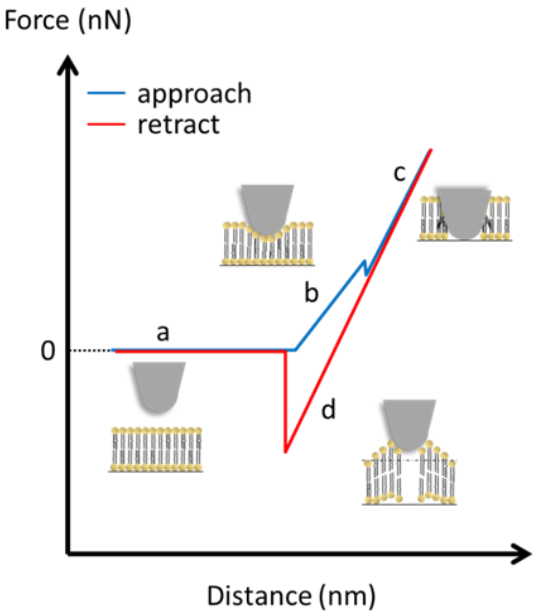

Figure 20. Schematic representation of a typical force-distance curve on a lipid bilayer. First, tip approaches (blue line) to the surface (**a**), it touches the surface, it begins to press down the SLB (**b**) until the force is enough to punch the bilayer (breakthrough force) and the tip continues pressing the substrate surface (**c**). Afterwards, the tip begins to separate (red line) from the mica surface (**d**) until the tip is completely free from the sample (adhesion force) and the tip moves away from the sample (**a**) *(Figure from results in 3.3.2).*

FD curves are directly dependent on the geometry and chemistry of tip and substrate, but also on the nature of the surrounding medium [196]. However, the obtained nanomechanical information has been proposed as a molecular fingerprint of the bilayer mechanical stability under certain experimental conditions [193,197].

3.3 Experimental results

3.3.1 Acyl chain differences in phosphatidylethanolamine determine domain formation and LacY distribution in biomimetic model membranes

Suárez-Germà, C., Montero, M. T., Ignés-Mullol, J., Hernández-Borrell, J., Domènech, Ò. (**2011**).
The Journal of Physical Chemistry B, 115(44), 12778-84.

3.3.1.1 Summary

PE and PG are the two main components of the inner membrane of *E. coli*. It is well-known that the inner membrane contains phospholipids with a nearly constant polar headgroup composition. However, bacteria can regulate the degree of unsaturation of the acyl chains in order to adapt to different external stimuli [10]. It can result in changes in membrane ordering (e.g. in terms of phase separation) that can largely affect membrane protein distribution [94] and induce changes in lipid composition of the annular region [132,133,198]. Studies on model membranes of mixtures of PE and PG, mimicking the proportions found in *E. coli*, can provide essential information on the phospholipid organization in biological membranes and may help in the understanding of membrane proteins activity. In this investigation we studied how different PEs differing in acyl chain saturation influence the formation of laterally segregated domains. Three different phospholipid systems were studied: DOPE:POPG, POPE:POPG, and DPPE:POPG at a molar ratio of 3:1. Lipid mixtures were analysed at 24 and 37 ºC through three different model membranes: monolayers, liposomes, and SLBs.

The first artificial system, lipid monolayers, was analysed in a Langmuir trough by performing isotherms. Pure component isotherms showed that, as expected, for identical headgroup molecules the more unsaturated hydrocarbon chains, the higher area per molecule displayed the monolayer at both temperatures. In addition, when comparing

molecules with identical acyl chains but different headgroups (POPE and POPG) we observed that POPG displayed higher area per molecule at both temperatures, which could be attributed to a larger headgroup structure combined with the repulsion existing between POPG molecules due to its negative charge. Regarding two components monolayers, it is clear that the addition of POPG to the pure PE lipids leaded to remarkable changes in the features of all isotherms. At a π = 30 $mN \cdot m^{-1}$, a pressure considered to be representative for a biomembrane [80] all the mixed monolayers showed higher area per molecule than their corresponding pure monolayers, although the global tendency was maintained (the mixture with the most saturated PE presented the most compressed monolayer). Interestingly, only DPPE:POPG mixture at both temperatures presented two collapse pressures instead of one. Since these collapse pressures did not coincide with those from the pure compounds, the observations might be evidence of the lateral segregation of the system in two different lipid domains, both enriched in one of the components. Accordingly, DPPE:POPG presented positive excess Gibbs energy (G^E) values indicating repulsive interactions between both compounds in this mixture, whilst POPE:POPG and DOPE:POPG showed negative values.

Liposomes, the second artificial membrane system, were incubated with Laurdan probe in order to exploit Laurdan fluorescent properties. From this fluorescence analysis we extracted the following information: DOPE:POPG was in L_α phase from 3 to 65 ºC and the T_m of POPE:POPG and DPPE:POPG were established in 23.3 and 51.1 ºC, respectively. On the other hand, the mixture DPPE:POPG (3:1, mol/mol) was the only studied system showing coexistence of L_β and L_α phases of different compositions from 21.3 to 49.0 ºC. This finding is consistent with the information obtained from the compression isotherms that suggested phase separation.

Finally, SLBs of the studied lipid mixtures were analysed by AFM at 24 and 37 ºC. Again, the only observed phase separated system was, at both temperatures, DPPE:POPG lipid mixture.

In conclusion, data from three different techniques, Langmuir isotherms, Laurdan generalized polarization, and AFM evidenced that only the DPPE:POPG system exhibited coexistence between gel (L_β) and fluid (L_α) phases of different composition at both 24 and 37 ºC . In the POPE:POPG system the L_β/L_α coexistence appeared at 27 ºC. Therefore, in order to investigate the distribution of LacY among phospholipid phases,

we used AFM to explore the distribution of LacY in SLBs of the three phospholipid systems at 27 ºC, where DOPE:POPG displayed L_α phase and POPE:POPG and DPPE:POPG exhibited L_β/L_α coexistence. The results demonstrated the preferential insertion of LacY in fluid phases.

3.3.1.2 Highlights

- DPPE:POPG (3:1, mol/mol) isotherm was the only analysed isotherm displaying two collapses. Since the collapse pressures did not coincide with the collapse pressures of pure DPPE and POPG isotherms, it evidenced the lateral segregation of the system in two different lipid domains, both enriched in one of the components. Accordingly, DPPE:POPG (3:1, mol/mol) presented positive excess Gibbs energy (G^E) values indicating repulsive interactions between both compounds in this mixture, whilst POPE:POPG and DOPE:POPG showed negative values.
- DOPE:POPG (3:1, mol/mol) liposomes were found in L_α from 3 to 65 ºC as analysed by Laurdan fluorescence. In addition, the T_m of POPE:POPG and DPPE:POPG liposomes (both at 3:1, mol/mol) were established in 23.3 and 51.1 ºC, respectively.
- DPPE:POPG (3:1, mol/mol) was the only studied system showing coexistence of L_β and L_α phases of different composition in liposomes from 21.3 to 49.0 ºC as described by Laurdan fluorescence, and in SLBs at 24 and 37 ºC as observed by AFM.
- LacY presented preferential insertion into fluid phases as evidenced from its partition into low domains when inserted in POPE:POPG (3:1, mol/mol) and DPPE:POPG (3:1, mol/mol) at 27 ºC, temperature at which both phospholipid systems presented phase separation.

THE JOURNAL OF PHYSICAL CHEMISTRY B

ARTICLE

pubs.acs.org/JPCB

Acyl Chain Differences in Phosphatidylethanolamine Determine Domain Formation and LacY Distribution in Biomimetic Model Membranes

Carme Suárez-Germà,[†] M.Teresa Montero,[†] Jordi Ignés-Mullol,[‡] Jordi Hernández-Borrell,[*,†] and Òscar Domènech[†]

[†]Department of Physical Chemistry, Faculty of Pharmacy, and [‡]Faculty of Chemistry, IN[2]UB, University of Barcelona, E-08028-Barcelona, Spain

ABSTRACT: Phosphatidylethanolamine (PE) and phosphatidylglycerol (PG) are the two main components of the inner membrane of *Escherichia coli*. It is well-known that inner membrane contains phospholipids with a nearly constant polar headgroup composition. However, bacteria can regulate the degree of unsaturation of the acyl chains in order to adapt to different external stimuli. Studies on model membranes of mixtures of PE and PG, mimicking the proportions found in *E. coli*, can provide essential information on the phospholipid organization in biological membranes and may help in the understanding of membrane proteins activity, such as lactose permease (LacY) of *E. coli*. In this work we have studied how different phosphatidylethanolamines differing in acyl chain saturation influence the formation of laterally segregated domains. Three different phospholipid systems were studied: DOPE:POPG, POPE:POPG, and DPPE:POPG at molar ratios of 3:1. Lipid mixtures were analyzed at 24 and 37 °C through three different model membranes: monolayers, liposomes, and supported lipid bilayers (SLBs). Data from three different techniques, Langmuir isotherms, Laurdan generalized polarization, and atomic force microscopy (AFM), evidenced that only the DPPE:POPG system exhibited coexistence between gel (L_β) and fluid (L_α) phases at both 24 and 37 °C . In the POPE:POPG system the L_β/L_α coexistence appears at 27 °C. Therefore, in order to investigate the distribution of LacY among phospholipid phases, we have used AFM to explore the distribution of LacY in SLBs of the three phospholipid systems at 27 °C, where the DOPE:POPG is in L_α phase and POPE:POPG and DPPE:POPG exhibit L_β/L_α coexistence. The results demonstrate the preferential insertion of LacY in fluid phase.

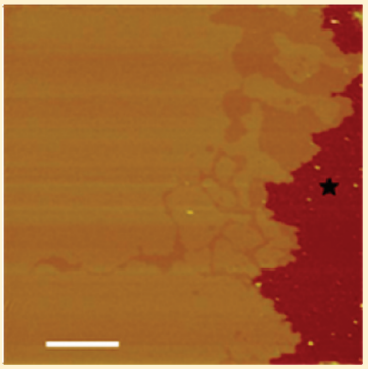

INTRODUCTION

Besides its high content in proteins, the inner lipid bilayer of *Escherichia coli* is composed of three main phospholipids: phosphatidylethanolamine (PE, zwitterionic, 74% of the total molar phospholipid content), phosphatidylglycerol (PG, bearing a negative charge, 19%), and cardiolipin (CL, bearing two negative charges, 3%).[1] Phospholipids, however, are not regarded anymore as a mere barrier but as components that exert strong influence over the activity and structure of membrane proteins.[2−4] Hence the investigation on interactions between lipids and specific proteins in biomembranes becomes of crucial interest for understanding physiological and pathological situations related to protein membrane activity.[5] As illustrated by the mechanosensitive channel proteins,[6] it is plausible to assume that basic physicochemical properties such as lateral compressibility, hydrophobic mismatch, or proton bridging capabilities of phospholipids surrounding transmembrane proteins may influence[7] or be part[8] of the transport phenomena. On the other hand, biomembranes are, as a whole, very dynamic structures where different assemblies occur, including lateral separation in domains[9,10] or selective segregation of particular species in the presence of membrane proteins.[11] Lateral heterogeneity is considered to play a major role in cell and developmental biology. It has been related to signal transduction, cellular adhesion, protein folding and activation or membrane fusion.[12,13] In signal transduction processes, for instance, it is crucial to understand how protein receptors in the surface of the cell adopt their tertiary structures. In this particular field the earlier works of Khorana's group on photoreceptors become illustrative.[14,15] In general, however, there are at the present few doubts on the influence of membrane lipids on the structure and organization of membrane proteins.[16]

In these regards, we have shown, on one hand, that on the basis of FRET measurements in proteoliposomes of mixed 1-palmitoyl-2-oleoyl-*sn*-glycero-3-phosphoglycerol (POPG) and PEs differing in the saturation degree of the acyl chains, lactose permease (LacY) of *E. coli*, a paradigm for the secondary transport,[5,17] prefers PE instead of PG in the annular region.[18,19] On the other hand, using the binary mixture of POPG with 1-palmitoyl-2-oleoyl-*sn*-glycero-3-phosphoethanolamine (POPE), atomic force microscopy (AFM) observations of supported lipid bilayers (SLBs) evidenced that LacY inserts preferentially into the fluid phase (L_α) instead of inserting into the gel phase (L_β).[20]

Received: July 6, 2011
Revised: September 27, 2011
Published: September 30, 2011

However, naturally occurring phospholipids found under physiological conditions feature mixed acyl chains, one saturated (at the *sn*-1 position) and the other unsaturated (at the *sn*-2 position) linked to the glycerol backbone. While the PE/PG ratio may remain nearly constant upon different situations, bacteria can regulate the composition and the degree of unsaturation of the acyl chains to adapt to different external stimuli.[21] As a result, phase separation may occur, which will affect lateral distribution of transmembrane proteins[22] and induce changes in lipid composition in the annular region.[11,18,19] Therefore, it becomes relevant to investigate and compare whether binary mixtures of PG and PE with different acyl composition form laterally segregated domains in monolayers, liposomes, and SLBs.

In this work, we have investigated the mixing properties of the binary mixtures of POPG with either the heteroacid POPE or the saturated homoacid 1,2-palmitoyl-*sn*-glycero-3-phosphoethanolamine (DPPE), or the unsaturated homoacid 1,2-oleoyl-*sn*-glycero-3-phosphoethanolamine (DOPE). The characterization of these systems in monolayers, liposomes, and SLBs may provide means to understand the interaction and specific selectivity between phospholipid species and membrane proteins. Thereafter we have investigated the distribution of LacY in these systems.

EXPERIMENTAL METHODS

1,2-Palmitoyl-*sn*-glycero-3-phosphoethanolamine (DPPE), 1,2-oleoyl-*sn*-glycero-3-phosphoethanolamine (DOPE), 1-palmitoyl-2-oleoyl-*sn*-glycero-3-phosphoethanola-mine (POPE), and 1-palmitoyl-2-oleoyl-*sn*-glycero-3-[phospho-rac-(1-glycerol)] (sodium salt) (POPG) were purchased from Avanti Polar Lipids (Alabaster, AL). Laurdan (6-dodecanoyl-2-dimethyl-aminonaphthalene) was purchased from Molecular Probes (Invitrogen, Carlsbad, CA). All other common chemicals, ACS grade, were purchased from Sigma (St. Louis, MO). Buffer used throughout the experiments was 20 mM HEPES (pH 7.40) and 150 mM NaCl prepared in ultrapure water (Milli-Q reverse osmosis system, 18.2 MΩ cm resistivity). For SLB formation, the buffer was supplemented with 10 mM $CaCl_2$. Lactose permease (LacY) was obtained from bacterial culture, extracted, and purified according to procedures described elsewhere.[18−20]

Surface Pressure−Area Isotherms. Monolayers differing on lipid composition were prepared in a 312 DMC Langmuir−Blodgett trough manufactured by NIMA Technology Ltd. (Coventry, England). The trough (total area, 137 cm^2) was placed on a vibration-isolated table (Newport, Irvine, CA) and enclosed in an environmental chamber. The resolution of the surface pressure measurement was ±0.1 mN m^{-1}. Temperature was maintained via an external circulating water bath (±0.2 °C). Before each experiment, the trough was washed with ethanol and rinsed thoroughly with purified water.

Experiments were performed as described in a previous paper.[23] The corresponding aliquot of chloroform−methanol (2:1, v/v) lipid solution was spread onto the subphase with a Hamilton microsyringe. A 15 min period was required for solvent to evaporate before each experiment. The compression barrier speed was 5 cm^2 min^{-1}. Every surface pressure−area (π−A) isotherm was repeated three times minimum, with the isotherms showing satisfactory reproducibility.

Surface thermodynamic analysis of the mixed monolayers at 30 mN m^{-1} was done in order to analyze miscibility and interactions between their components. The interaction between two phospholipid components in a mixed monolayer, at a constant surface pressure π and temperature, can be evaluated from the calculation of the excess Gibbs energy (G^E), which is given by

$$G^E = \int_0^\pi [A_{12} - \chi_1 A_1 - \chi_2 A_2]\, d\pi \quad (1)$$

where A_{12} is the average area per molecule of the mixed monolayer at a given pressure, A_1 and A_2 are the area per molecule of the pure components at this pressure, and χ_1 and χ_2 are the mole fractions of each component.

Stability of the mixed monolayers was verified by computing the values of the Gibbs energy of mixing ($\Delta_{mix}G$),

$$\Delta_{mix}G = \Delta_{mix}G^{id} + G^E \quad (2)$$

where the first term, the ideal Gibbs energy of mixing ($\Delta_{mix}G^{id}$), is given by

$$\Delta_{mix}G^{id} = RT(\chi_1 \ln \chi_1 + \chi_2 \ln \chi_2) \quad (3)$$

where R is the universal gas constant and T is the temperature.

The inverse of the isothermal compressibility or elastic modulus of area compressibility (C_s^{-1}) was calculated using

$$C_s^{-1} = (-A)\left(\frac{\partial \pi}{\partial A}\right)_{T,n} \quad (4)$$

The derivative of the experimental data was computed by fitting a straight line to a window of area width of 0.2 nm^2 $molec^{-1}$ around any given surface pressure value, so that experimental noise was filtered out.

Large Unilamellar Vesicle Formation. Liposomes of DOPE:POPG (3:1, mol/mol), POPE:POPG (3:1, mol/mol), and DPPE:POPG (3:1, mol/mol) were prepared according to methods previously described.[18,19] Chloroform−methanol (2:1, v/v) solutions containing appropriate amounts of each phospholipid were dried under a stream of oxygen-free N_2 in a conical tube. The resulting thin film was kept under high vacuum for approximately 3 h to remove organic solvent traces. Multilamellar liposomes (MLVs) were formed by redispersing the films with the above-mentioned buffer, applying successive cycles of freezing and thawing below and above the phase transition of the phospholipids, and vortexing for 2 min. Finally, large unilamellar vesicles (LUVs) were obtained by extrusion of the MLVs through 100 nm pore polycarbonate filters (Mini-extruder, Avanti, and Nucleopore filters).

Fluorescence Measurements. Bilayer fluidity was monitored using dipolar relaxation of Laurdan. Briefly, Laurdan is a polarity sensitive probe that tends to locate at the glycerol backbone of the bilayer with the lauric acid tail anchored in the phospholipid acyl chain region.[24] Upon excitation, the dipole moment of Laurdan increases noticeably, and water molecules in the vicinity of the probe reorient around this new dipole. When the membrane is in a fluid phase, the reorientation rate is faster than the emission process, and consequently, a red-shift is observed in the emission spectrum of Laurdan. When the bilayer packing increases, part of the water molecules is excluded from the bilayer and the dipolar relaxation of the remaining water molecules is slower, leading to a fluorescent spectrum that is significantly less shifted to the red.[25]

We monitored the bilayer fluidity-dependent fluorescence spectral shift of Laurdan due to dipolar relaxation phenomena. Determinations were carried out using an SLM-Aminco 8100 spectrofluorimeter equipped with a jacketed cuvette holder. The temperature (±0.2 °C) was controlled using a circulating bath

(Haake K20, Germany). The excitation and emission slits were 4 and 4 nm and 8 and 8 nm, respectively. The lipid concentration in the liposome suspension was adjusted to 250 μM, and Laurdan was added to give a lipid/probe ratio of 300. Generalized polarization (GP_{ex}) from emission spectra was calculated using

$$GP_{ex} = \frac{I_{440} - I_{490}}{I_{440} + I_{490}} \quad (5)$$

where I_{440} and I_{490} are the fluorescence intensities at emission wavelengths of 440 nm (gel phase, L_β) and 490 nm (liquid crystalline phase, L_α), respectively.

GP_{ex} values as a function of temperature were fitted to a Boltzmann-like equation

$$GP_{ex} = GP^2_{ex} + \frac{GP^1_{ex} - GP^2_{ex}}{1 + \exp\left\{\frac{T_m - T}{m}\right\}} \quad (6)$$

where $GP^1{}_{ex}$ and $GP^2{}_{ex}$ are the maximum and minimum values of GP_{ex}, T_m is the gel to fluid phase transition temperature of the studied composition, T is the temperature, and m is the slope of the transition that gives information about the cooperativity of the process.

Supported Lipid Bilayers and Atomic Force Microscopy. The spread of the SLBs was obtained by using the vesicle fusion technique as described elsewhere.[26] Briefly, 80 μL of LUVs, in 20 mM Hepes pH 7.40, 150 mM NaCl, and 10 mM $CaCl_2$ buffer, were deposited onto freshly cleaved mica disks mounted on a Teflon O-ring. Samples were incubated at 50 °C for 2 h in an oven preventing the water evaporation from the sample using a water reservoir, before being washed with 10 mM Hepes pH 7.40, 150 mM NaCl. Proteoliposomes (at a lipid to protein ratio of 40) were prepared following the same protocol, but incubation did not exceed 37 °C. The tip was immediately immersed into the liquid cell. To perform all these experiments it was necessary to drift equilibrate and thermally stabilize the cantilever for 30 min in the presence of buffer.

Liquid AFM imaging was performed using a Multimode Microscope controlled by a Nanoscope V electronics (Digital Instruments, Santa Barbara, CA), in tapping mode acquisition (TM-AFM) at minimum vertical force, maximizing the amplitude set point value and maintaining the vibration amplitude as low as possible. V-shaped Si_3N_4 cantilevers (MLCT-AUNM, Veeco) with a nominal spring constant of 0.10 N m^{-1} were used. Variable temperature experiments were performed by incorporating a temperature controller stage (Digital Instruments, Santa Barbara, CA) to the piezo-scanner. This device allows the maintenance of the sample holder at a fixed temperature (range, from room temperature up to 62.5 °C; resolution, 0.1 °C; temperature drift, <0.5 °C).

■ RESULTS AND DISCUSSION

Lipid monolayers constitute a convenient model system to investigate the interactions and physicochemical properties of phospholipids forming biological membranes. Thus, lateral pressure in biomembranes has been postulated as a mechanism for modulation of transmembrane protein function.[27,28] For this reason we have used Langmuir monolayers to investigate intermolecular interactions between the major phospholipid components, PE and PG, of the inner *E. coli* membrane.[1] In particular these experiments have been delineated to gather information on

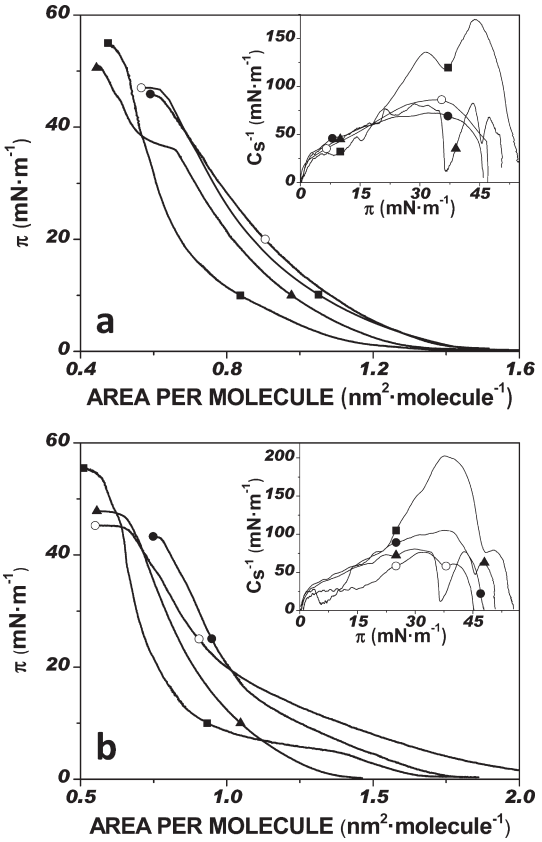

Figure 1. Surface pressure−area isotherms of pure DPPE (■), POPE (▲), POPG (○), and DOPE (●) at (a) 24 °C and (b) 37 °C. Insets show the elastic moduli of area compressibility (C_s^{-1}) corresponding to each isotherm.

the structural relevance of the saturation degree of the acyl chains of PE.

The surface pressure−area (π−A) compression isotherms of the pure phospholipids at 24 and 37 °C are shown in Figure 1 along with C_s^{-1} values (insets). As expected, PE monolayers show higher area per molecule the more unsaturated hydrocarbon chains they contain. These data emphasize the fact that acyl chains play a predominant role in the overall packing of the monolayer which is determined by the degree of unsaturation of the acyl chains. Thus, the existence of a C−C double bond leads to the formation of a kink, producing chain shortening. Besides, it also generates higher intermolecular steric effects increasing the distances between individual molecules. The effect is at the maximum when both acyl chains are unsaturated. This can be observed in Figure 1 where DOPE shows the largest monolayer intermolecular distances. Conversely, DPPE, with both acyl chains saturated, remains as the more compressed molecule. An intermediate situation was found for POPE. These monolayer features are consistent with results found in the literature.[29−32] As discussed by Wydro and Witkowska,[29] while a DPPE monolayer at 24 °C features a liquid expanded (LE) to solid (S) phase transition at ∼37 mN m^{-1}, DOPE is always in the LE phase. These behaviors are consistent with the values of the compression modulus shown in the inset of Figure 1. The POPE isotherm shows, in turn, the characteristic LE−LC phase transition at ∼36 mN m^{-1} whose nanostructure and characteristics have been previously discussed.[33] It is known that POPG is always in the

LE phase above 20 °C.[34,35] Thus, at 37 °C POPE and DOPE monolayers are in the LE phase while DPPE shows a LE−LC phase transition at ∼4.7 mN m^{-1}. When comparing PE and PG headgroups with the same hydrocarbon chain, PE shows at 24 and 37 °C higher areas per molecule at surface pressures below 40 mN m^{-1}. This is attributable to the negative charge born by the PG headgroups and to the size of each headgroup. Besides, both PE amino and PG hydroxyl headgroups are able to form intermolecular hydrogen bonds at physiological pH conditions.[36] However, PG−PG interactions are weaker than those arising between PE zwitterions. Indeed, it is known that PE headgroups tightly interact, creating a hydrogen bond network which confers rigidity to the monolayer.[23]

Lipid mixtures DPPE:POPG, POPE:POPG, and DOPE:POPG (3:1, mol/mol) were also studied using Langmuir monolayers. For these mixed systems, $\pi-A$ compression isotherms are shown in Figure 2 along with the C_s^{-1} values (insets). The addition of POPG to the pure PE lipids led to remarkable changes in the features of all isotherms. At a surface pressure of 30 mN m^{-1}, a pressure considered as representative for a bilayer,[28] all the mixed monolayers showed lower area per molecule than their corresponding pure phospholipid components. As expected, these monolayers showed again higher area per molecule as the number of double bonds of PE increased. It is also worth mentioning the special case of the DPPE:POPG isotherm shown in Figure 2, where two transitions occur at both studied temperatures. Well-defined collapse pressures and characteristic plateaus were observed at 61 and 46 mN m^{-1}, at 24 °C, and 58 and 43 mN m^{-1}, at 37 °C, respectively. This behavior can be more precisely observed by analyzing the C_s^{-1} values plotted in the insets of Figure 2. Since the pressures at which these features occur do not coincide with the collapse pressure of the pure components, the existence of pure DPPE and POPG domains can be excluded. Most likely these observations are evidence of the lateral segregation in two different lipid domains, both enriched in one of the components.

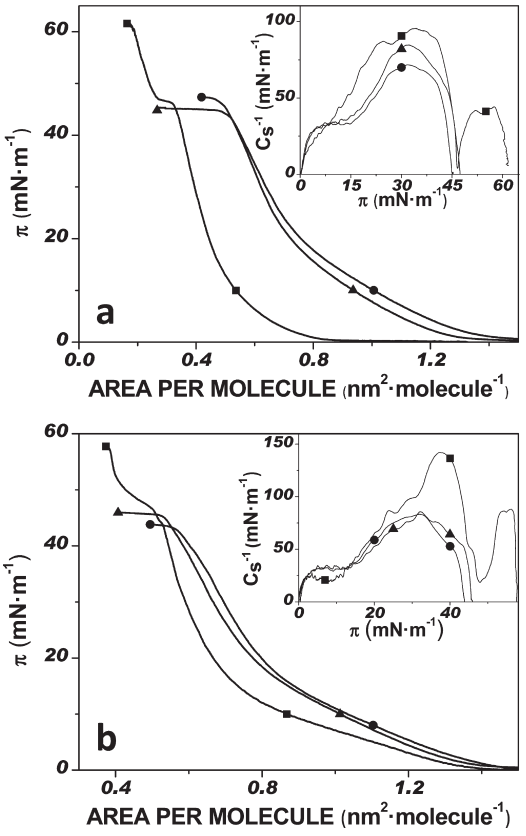

Figure 2. Surface pressure−area isotherms of DPPE:POPG (3:1, mol/mol) (■), POPE:POPG (3:1, mol/mol) (▲), and DOPE:POPG (3:1, mol/mol) (●) at (a) 24 °C and (b) 37 °C. Insets show the elastic moduli of area compressibility (C_s^{-1}) corresponding to each isotherm.

In Table 1 the values of C_s^{-1}, G^E, and $\Delta_{mix}G$ calculated at 30 mN m^{-1} are listed. The low negative deviations of these values observed for POPE:POPG and DOPE:POPG indicate the existence of attractive interactions and confirm the stability of these systems. Conversely, positive and larger values of G^E are found at both temperatures in the DPPE:POPG mixture which is strong evidence of repulsive interactions between both components. This may result in partial miscibility of the components and in their organization in phase separation. Concerning miscibility studies, we have proved by AFM that there is a clear influence between the phase separation in monolayers and the domains observed in bilayers blistered by double deposition of monolayers.[37] Hence, it becomes relevant to investigate the existence of phase separation in the bilayers formed with the same phospholipids used in the monolayer study. To further characterize the specific behavior of the mixed systems, liposomes were used to investigate possible phase separation and also to establish T_m by exploiting Laurdan fluorescence properties. Thus, changes in fluorescence intensity of the probe as a function of temperature and excitation wavelength (λ_{ex}) in the range of temperatures from 3 to 65 °C were studied. As it can be seen in Figure 3, DOPE:POPG (3:1, mol/mol) lipid mixture was found in L_α phase throughout the range of temperatures used in the experiment. However the T_m of this system could not be established due to technical limitations because both pure DOPE and pure POPG have nominal T_m values below 0 °C.

On one hand, the T_m for the mixtures of POPE:POPG (3:1, mol/mol) and DPPE:POPG (3:1, mol/mol) were established at 23.3 and 51.1 °C. Below and above these temperatures L_β and L_α phases are observed, respectively. On the other hand the mixture DPPE:POPG (3:1, mol/mol) was the only studied system showing positive slopes between single L_β and L_α phases. Positive slopes indicate coexistence of L_β and L_α phases. They were observed ranging from 21.3 °C (data not shown) to 49.0 °C, indicating the coexistence of two phases in this range of temperatures. This finding is consistent with the information

Table 1. Mathematical Analysis of the Surface Pressure−Area Isotherms from Figure 2

	24 °C			37 °C		
composition (3:1, mol/mol)	C_s^{-1} (mN m^{-1})	G^E (kJ mol^{-1})	$\Delta_{mix}G$ (kJ mol^{-1})	C_s^{-1} (mN m^{-1})	G^E (kJ mol^{-1})	$\Delta_{mix}G$ (kJ mol^{-1})
DPPE:POPG	91	1.35	−0.04	99	1.30	−0.14
POPE:POPG	82	−0.53	−1.92	81	−0.07	−1.52
DOPE:POPG	70	−0.85	−2.24	77	0.99	−0.45

dx.doi.org/10.1021/jp206369k |J. Phys. Chem. B 2011, 115, 12778–12784

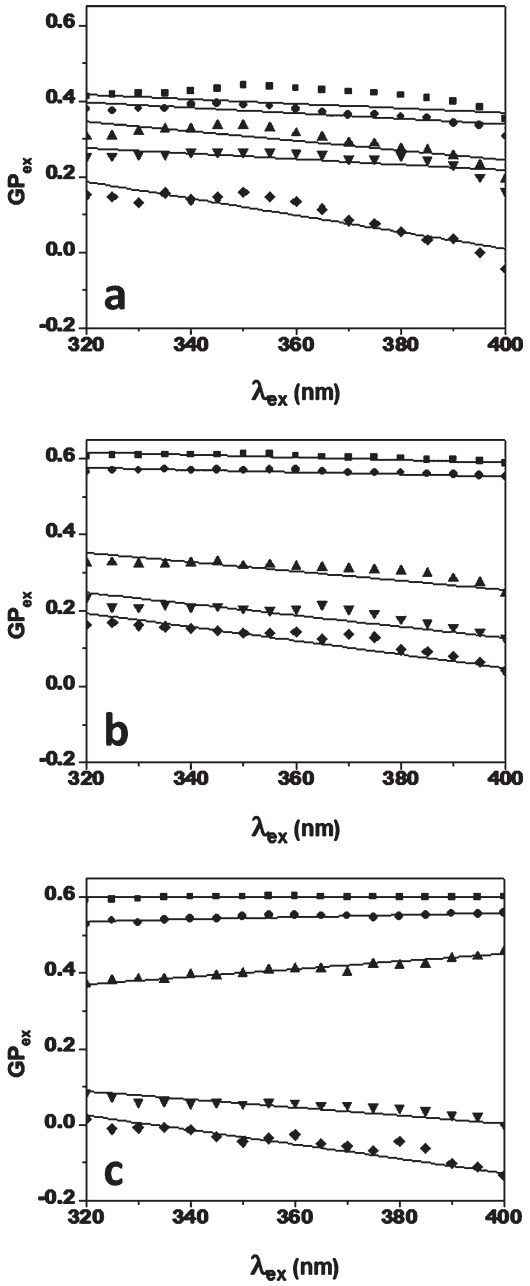

Figure 3. GP_{ex} as a function of λ_{ex} for (a) DOPE:POPG (3:1, mol/mol) (■ = 3.2 °C, ● = 8.0 °C, ▲= 18 °C, ▼= 26.5 °C, triangle pointing left = 38.9 °C), (b) POPE:POPG (3:1, mol/mol) (■ = 2.7 °C, ● = 16.4 °C, ▲= 24.3 °C, ▼= 32.7 °C, ♦ = 41.0 °C), and (c) DPPE:POPG (3:1, mol/mol) (■ = 10.7 °C, ● = 23.8 °C, ▲= 43.0 °C, ▼= 56.0 °C, ♦ = 64.6 °C).

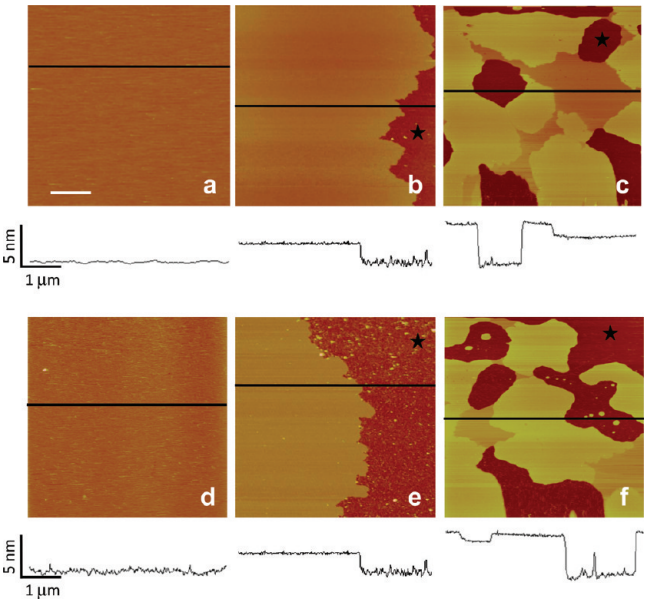

Figure 4. Topography AFM images of SPBs at 24 °C: (a) DOPE:POPG (3:1, mol/mol), (b) POPE:POPG (3:1, mol/mol), and (c) DPPE:POPG (3:1, mol/mol). At 37 °C: (d) DOPE:POPG (3:1, mol/mol), (e) POPE:POPG (3:1, mol/mol), and (f) DPPE:POPG (3:1, mol/mol). Black star indicates mica substrate. Scale bar = 1 μm. Z scale = 20 nm.

obtained from the compression isotherms that suggest phase separation.

Figure 4 shows the AFM characterization at 24 and 37 °C of SLBs of the different phospholipid systems On one hand, the topographic images shown in Figure 4a,d, corresponding to SLBs obtained by extension of DOPE:POPG (3:1, mol/mol) liposomes, feature a homogeneous layer. According to the nominal T_m of both phospholipids, these layers correspond to SLBs in L_α phase. The layer thickness, however, could not be inferred from line profile analysis because of complete coverage of the mica substrate and absence of defects. Similar features are observed in Figure 4b, where the SLBs of POPE:POPG at 24 and 37 °C exhibited also a homogeneous layer. Taking the substrate as reference, the thickness of the POPE:POPG bilayer (3:1, mol/mol) could be established in 3.4 ± 0.3 nm (n = 50) and 3.0 ± 0.3 nm (n = 50) at 24 and 37 °C, respectively. These values are slightly lower than others previously obtained for the same system,[26] which could be attributed to the absence of calcium in the present experiments. Additionally, in that work it has been demonstrated by DSC that the POPE:POPG system undergoes a L_β to L_α transition at 21 °C, which coincides with the value found from our GP_{ex} experiments (see above). It is noteworthy that because of the presence of the mica substrate SLBs feature two decoupled phase transitions. Thus, the value of T_m obtained from DSC of liposomes is interpreted as the representative for the melting of the proximal leaflet in SLBs. Indeed in SLBs this value is shifted to higher temperatures.[38] A detailed investigation of the thermal response of POPE:POPG SLBs under different conditions has been published by Seeger and co-workers.[39] In good comparison with the observations of these authors and in agreement with our previously reported observations, two laterally segregated domains for the POPE:POPG system at 27 °C can be seen in Figure 5.[37] On the other hand, laterally segregated domains for the SLBs of DPPE:POPG (3:1, mol/mol) are observed, that according to Laurdan experiments should be assigned to segregated L_β and L_α phases. The characteristic thicknesses, taking mica as a reference for the line profile analysis, were 5.7 ± 0.3 nm and 7.6 ± 0.3 nm for the thinner and thicker lipid domains at 24 °C, and 5.8 ± 0.3 nm and 7.2 ± 0.3 nm at 37 °C, respectively. These values are higher than expected in comparison with the heights obtained for POPE:POPG. Since the values for pure DPPE bilayers found in literature are ~5.4 nm,[40] the formation of multilayers should be somehow excluded. Most likely the discrepancies would arise because of other factors as the

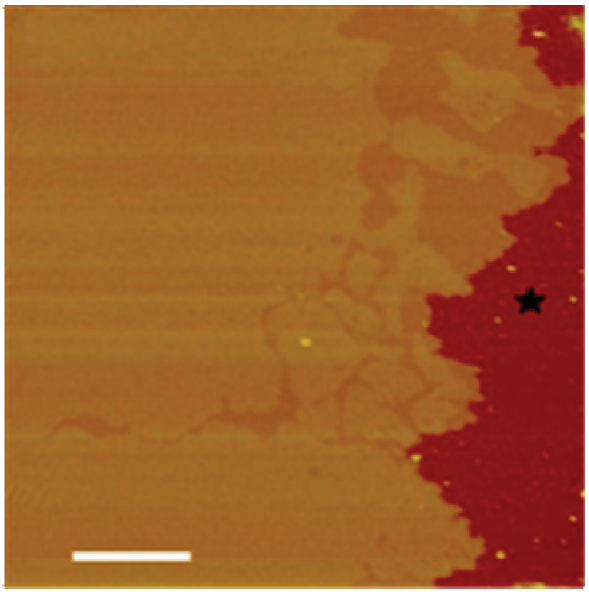

Figure 5. Topography AFM images of POPE:POPG (3:1, mol/mol) at 27 °C. Black star indicates mica substrate. Scale bar = 1 μm. Z scale = 20 nm.

force applied or a possible repulsion between the tip and the L_β phase in the DPPE:POPG system.[26] At this point further discussion is not possible without knowing the exact composition of the domains.

There is a general consensus on the matching between the hydrophobic thickness of the phospholipid bilayer and the transmembrane segments of the protein membranes. This theoretical concept[41] has received experimental support for LacY[42] or melibiose permease (MelB) of *E. coli*.[43] The seminal work based on the use of pyrene-labeled lipids, which are able to form excimers, suggested the enrichment of phospholipids according to this matching principle.[41] However, posterior works based on FRET between a single tryptophan mutant of LacY and pyrene-labeled phospholipids have shown that LacY is able to perform a molecular sorting by recruiting the most abundant lipid in binary mixtures of PE and PG.[18] Importantly, this matching principle is sustained by our data since the thickness of the bilayers, as measured by AFM (see profile analysis in Figure 4), matches well with the estimated hydrophobic thickness of LacY.[17]

Otherwise, it becomes relevant to investigate how the phospholipid composition studied here influences LacY distribution. Indeed, the partitioning of LacY into L_α phases was suggested in earlier works[44] where high concentrations of protein (lipid to protein ratio = 0.5) were used. Here, we have extended these observations to samples prepared at high lipid to protein ratios (less proportion of protein). Thus, when LacY is reconstituted in proteoliposomes of the same composition as the SLBs and observed with AFM at 27 °C, thicker structures protruding from the phospholipid matrices can be distinguished (Figure 6). These entities, most likely ascribable to LacY, protrude 0.8 ± 0.3, 1.4 ± 0.5, and 2.0 ± 0.7 nm from the SLBs of DOPE:POPG (3:1, mol/mol), POPE:POPG (3:1, mol/mol), and DPPE:POPG (3:1, mol/mol), respectively. Although the statistics is short (n = 30), the fact that the protein protrudes more the less saturated the acyl chain species is may be a consequence of different lateral pressure exerted by each phospholipid.[45] Remarkably, these experiments demonstrate that, at lipid to protein ratios compatible with former

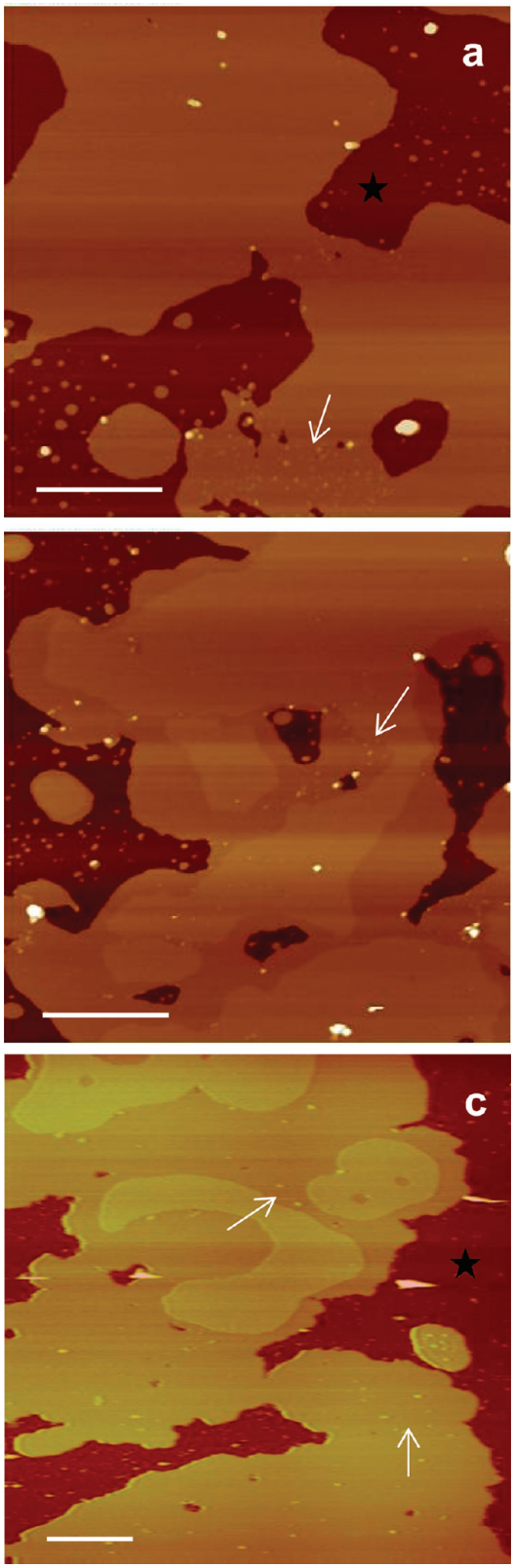

Figure 6. Topography AFM image of extended proteoliposomes of LacY (1.5 μM) at 27 °C: (a) DOPE:POPG (3:1, mol/mol), (b) POPE:POPG (3:1, mol/mol), and (c) DPPE:POPG (3:1, mol/mol). Black star indicates mica substrate. Arrows point to protrusions attributed to the presence of LacY. Scale bar = 500 nm. Z scale = 20 nm.

FRET experiments,[18,19] LacY prefers the L_α phase. This coincides with a general behavior for protein membranes[22] and, remarkably, with the K^+ ion channel (KcsA).[46] As can be seen in Figure 6b,c this preference has been clearly demonstrated here in the systems that form separated phases, that is POPE:POPG and DPPE:POPG.

Indeed, by using FRET tools we have previously shown[18,19] that PG is completely excluded from the annular region in the POPE:POPG system, only partially excluded from the DOPE:POPG matrix, and, conversely, segregated in PG enriched domains in the DPPE:POPG mixture. Results presented in this paper provide support for these interpretations.

CONCLUSIONS

By studying the phase separated mixture of PE and PG, we demonstrate that LacY partitions into fluid phases. Even in the absence of phase diagrams for each binary mixture our results suggest that the fluid phases are enriched in POPG. This is not, however, in contradiction with the fact that LacY shows higher selectivity for PE than PG,[47] providing means for a protein-promoted membrane domain,[11] characterized by a lipid annulus mainly formed by PE.

AUTHOR INFORMATION

Corresponding Author

*E-mail: jordihernandezborrell@ub.edu. Fax: (+34) 934035987. Phone: (+34) 934035986.

ACKNOWLEDGMENT

C.S.-G. is recipient of a FPI fellowship from the Ministerio de Ciencia e Innovación of Spain. This work has been supported by Grant CTQ-2008-03922/BQU from Ministerio de Ciencia e Innovación of Spain.

REFERENCES

(1) Dowhan, W. *Annu. Rev. Biochem.* **1997**, *66*, 199.
(2) Hakizimana, P.; Masureel, M.; Gbaguidi, B.; Ruysschaert, J. M.; Govaerts, C. *J. Biol. Chem.* **2008**, *283*, 9369.
(3) Bogdanov, M.; Mileykovskaya, E.; Dowhan, W. *Subcell. Biochem.* **2008**, *49*, 197.
(4) Schmidt, D.; Jiang, Q. X.; MacKinnon, R. *Nature* **2006**, *444*, 775.
(5) Guan, L.; Kaback, H. R. *Ann. Rev. Biophys. Biomed. Struct.* **2006**, *35*, 67.
(6) Wiggins, P.; Phiplips, R. *Biophys. J.* **2005**, *2*, 880.
(7) Dowhan, W.; Mileykovskaya, E.; Bogdanov, M. *Biochim. Biophys. Acta* **2004**, *1666*, 19.
(8) Haines, T. H.; Dencher, N. A. *FEBS Lett.* **2002**, *528*, 35.
(9) Jacobson, K.; Mouritsen, O. G.; Anderson, R. G. W. *Nat. Cell Biol.* **2007**, *9:1*, 7.
(10) Shultz, Z. D.; Levin, I. W. *Biophys. J.* **2008**, *94*, 3104.
(11) Poveda, J. A.; Fernández, A. M.; Encinar, J. A.; González-Ros, J. M. *Biochim. Biophys. Acta* **2008**, *1778*, 1583.
(12) Brown, D. A.; London, E. *Ann. Rev. Cell. Dev. Biol.* **1998**, *14*, 111.
(13) Simons, K.; Gerl, M. J. *Nat. Rev. Mol. Cell. Biol.* **2010**, *11*, 688.
(14) Ridge, K. D.; Bhattacharya, S.; Nakayama, T. A.; Khorana, H. G. *J. Biol. Chem.* **1992**, *267*, 6770.
(15) Bhattacharya, S.; Ridge, K. D.; Knox, B. E.; Khorana, H. G. *J. Biol. Chem.* **1992**, *267*, 6763.
(16) Nyholm, T. K.; Ozdirekcan, S.; Killian, J. A. *Biochemistry* **2007**, *46*, 1457.
(17) Abramson, J.; Iwata, S.; Kaback, H. R. *Mol. Membr. Biol.* **2004**, *21*, 227.
(18) Picas, L.; Montero, M. T.; Morros, A.; Vázquez-Ibar, J. L.; Hernández-Borrell, J. *Biochim. Biophys. Acta* **2010**, *1798*, 291.
(19) Picas, L.; Suárez-Germà, C.; Montero, M. T.; Vázquez-Ibar, J. L.; Hernández-Borrell, J. *Biochim. Biophys. Acta* **2010**, *1798*, 1707.
(20) Picas, L.; Carretero-Genevrier, A.; Montero, M. T.; Vázquez-Ibar, J. L.; Seantier, B.; Milhiet, P. E.; Hernández-Borrell, J. *Biochim. Biophys. Acta* **2010**, *1798*, 1014.
(21) Morein, S.; Andersson, A. S.; Rilfors, L.; Lindblom, G. *J. Biol. Chem.* **1996**, *271*, 6801.
(22) Houslay, M. D.; Stanley, K. K. *Dynamics of Biological Membranes*; Wiley & Sons: New York, 1982; p116.
(23) Domènech, O.; Sanz, F.; Montero, M. T.; Hernandez-Borrell, J. *Biochim. Biophys. Acta* **2006**, *1758*, 213.
(24) Parassassi, T.; Kransnowska, E. K.; Bagatolli, L.; Gratton, E. *J. Fluoresc.* **1998**, *8:4*, 365.
(25) Domènech, O.; Dufrêne, Y.; Van Bambeke, F.; Tulkens, P. M.; Mingeot-Leclerq, M. P. *Biochim. Biophys. Acta* **2006**, *1758*, 213.
(26) Picas, L.; Montero, M. T.; Morros, A.; Cabañas, M. E.; Seantier, B.; Milhiet, P. E.; Hernández-Borrell, J. *J. Phys. Chem. B* **2009**, *112*, 4646.
(27) Cantor, R. S. *J. Phys. Chem. B* **1997**, *101*, 1723.
(28) Marsh, D. *Biochim. Biophys. Acta* **1996**, *1285*, 183.
(29) Wydro, P.; Witkowska, K. *Colloids Surf., B* **2009**, *72*, 32.
(30) Wydro, P.; Hac-Wydro, K. *J. Phys. Chem. B* **2007**, *111*, 2495.
(31) Saulnier, P.; Foussard, F.; Boury, F.; Proust, J. E. *J. Colloid Interface Sci.* **1989**, *218*, 40.
(32) Brockmann, H. L.; Applegate, K. R.; Momsem, M. M.; King, W. C.; Glomset, J. A. *Biophys. J.* **2003**, *85*, 2384.
(33) Domenech, O.; Ignés-Mullol, J.; Montero, M. T.; Hernández-Borrell, J. *J. Phys. Chem. B* **2007**, *111*, 10946.
(34) Takamoto, D. Y.; Lipp, M. M.; Von Nahmen, A.; Lee, K. Y. C.; Warning, A. J.; Zasadzinski, J. A. *Biophys. J.* **2001**, *81*, 153.
(35) Sánchez-Martín, M. J.; Haro, I.; Alsina, M. A.; Busquets, M. A.; Pujol, M. *J. Phys. Chem. B* **2010**, *114*, 448.
(36) Langmer, M.; Kubica, K. *Chem. Phys. Lipids* **1993**, *102*, 3.
(37) Picas, L.; Suárez-Germà, C.; Montero, M. T.; Hernandez-Borrell, J. *J. Phys. Chem. B* **2010**, *114*, 3543.
(38) Keller, D.; Larsen, N. B.; Moller, I. M.; Mouritsen, O. G. *Phys. Rev. Lett.* **2005**, *94*, 025701.
(39) Seeger, H. M.; Marino, G.; Alessandrini, A.; Facci, P. *Biophys. J.* **2009**, *87*, 1067.
(40) Hui, S. W.; Viswanathan, R.; Zasadzinski, J. A.; Israelachvili, J. N. *Biophys. J.* **1995**, *68*, 171.
(41) Jensen, M. O.; Mouritsen, O. G. *Biochim. Biophys. Acta* **2004**, *1666*, 205.
(42) Lehtonen, J. Y. A.; Kinnunen, P. K. J. *Biophys. J.* **1984**, *46*, 141.
(43) Dumas, F.; Tocanne, J. F.; Leblanc, G.; Lebrun, M. C. *Biochemistry* **2000**, *39*, 4846.
(44) Merino, S.; Domènech, O.; Viñas, M.; Montero, M. T.; Hernández-Borrell, J. *Langmuir* **2005**, *21*, 4642.
(45) Olilla, S.; Hyvonen, M. T.; Vattulainen, I. *J. Phys. Chem. B* **2007**, *111*, 3139.
(46) Seeger, H. K.; Bortolotti, C. A; Alessandrini, A.; Facci, P. *J. Phys. Chem. B* **2009**, *113*, 16654.
(47) Picas, L.; Merino-Montero, S.; Morros, A.; Hernandez-Borrell, J.; Montero, M. T. *J. Fluoresc.* **2007**, *17*, 649.

3.3.2 Combined FS and AFM-based calorimetric studies to reveal the nanostructural organization of biomimetic membranes

Suárez-Germà, C., Morros, A., Montero, M.T., Hernández-Borrell, J., Domènech, Ò.
Submitted to *Soft Matter*

3.3.2.1 Summary

Understanding the physicochemical properties of phospholipid systems is of crucial relevance to understand the relationship between these molecules and membrane proteins embedded in the bilayer. In the model taken, LacY from the inner membrane of *E. coli*, the protein resides within the lipid L_α phase of the membrane [128]. Thus, for better understanding the interplay of LacY with its phospholipid environment, it is imperative to study the phase separation phenomena of a binary mixture that mimics the natural entourage of the protein. Hence, in order to elucidate the influence of the temperature on a given phospholipid mixture, which is directly related to the phase separation appearance, this study conceived the construction of phase diagrams of a binary mixture (POPE:POPG) in the presence of 10 mM of Ca^{2+}. The presence of this cation plays a key role in the adsorption of negatively charged SLBs on mica, systems in plane where the protein has been reconstituted in previous works. In these systems cations can induce physicochemical modifications that require a detailed study. Specifically, liposomes with different mole fractions of POPG were analyzed by differential scanning calorimetry (DSC) and a binary phase diagram of the system was constructed. With the same objective and for comparison, we performed AFM imaging of SLBs with similar compositions at different temperatures, in order to create a binary pseudo-phase diagram specific to this planar membrane model. The construction of the above-mentioned phase diagrams enabled us to grasp better the thermodynamics of the thermal lipid transition from an L_β POPE:POPG phase system to an L_α phase system.

On the one hand, the phase diagram constructed from liposomes using DSC thermograms was constructed. The main conclusions arose from the observation that the non-ideal mixing behavior of the system was enhanced as the POPG proportion increased. On the other hand, AFM observations of SLBs with different POPE:POPG

compositions were conducted at several temperatures in order to construct the second phase diagram and compare it to the one obtained from DSC data. The direct correlation from both diagrams is not possible because the lipid system displays different curvatures in each technique and, additionally, the thermal behavior of SLBs is affected by the presence of the mica substrate. Accordingly, when considering equal compositions the T_m determined from AFM imaging were always higher than those obtained from DSC, and a wider range of temperatures encompassing each transition was detected. In addition, the van't Hoff molar enthalpy (ΔH_{vH}) was higher for SLBs than the enthalpy determined in liposomes, which is explained by the energy spent to counterbalance the existing interaction with the substrate.

The cooperativity unit (N) of the transformation was also calculated. It was found that increasing the proportion of negatively charged phospholipid in the system resulted in a decrease of N. This decreasing of N can be associated to smaller domains undergoing the phase transition at a time, which has been related to the presence of Ca^{2+} interacting and clustering specifically with POPG within the fluid phase.

Finally, further analysis of the lipid phases was performed using FS mode. Thus, the nanomechanics of the two lipid phases were determined at 27 ºC and at different POPG mole fractions. The obtained magnitudes were the breakthrough force (F_y) and the adhesion force (F_{adh}) of the different phases. For completeness, the continuum nucleation model was fitted to the F_y data in order to calculate Γ (related to the line tension of the molecules in the periphery of a hole) and S (the spreading pressure associated with the energy per unit area gained by the layer when filling a hole formed after a rupture). Γ values raised as the POPG content increased and were correlated to the domain size. Hence, higher Γ values may correspond to higher electrostatic repulsion between neighboring molecules and thus, lead to a decrease in the length of the boundary regions and a reduction in domain size. Regarding the parameter S, it showed negative values as described for POPG and POPE in other studies [193]. Results reflected a higher absolute value of S as POPG content increased, which emphasizes that, the more domains become enriched in POPG, the more difficult it is for the film to spread into the gap between the tip and the substrate. Additionally, differential results for L_α and L_β were correlated with the specific composition of each phase, which can be inferred from the obtained AFM phase diagram.

Concerning F_{adh} forces, at low POPG content F_{adh} rose with the increasing of χ_{POPG} and were higher for L_β than for L_α. Conversely, at high POPG content the tendency was inversed and L_α presented elevated F_{adh} values.

Interestingly, all the results seemed largely influenced by the amount of negatively charged lipids, something that agrees with DSC findings. Thus, compositions with higher content of POPG and, especially, L_α phases where POPG was more prominent, displayed properties pointing to the stiffening of the system upon the enrichment of POPG, most likely due to the clustering of POPG phospholipids by the Ca^{2+} ions which compacted and rigidified the bilayer.

3.3.2.2 Highlights

- A phase diagram of POPE:POPG SLBs was constructed from AFM observations. When compared to the liposomes phase diagram constructed from DSC data, the former was displaced at higher T_m, higher enthalpy values and presented wider temperature transitions.
- At 27 ºC, SLBs differing in POPG molar ratio presented lipid phase nanomechanical characteristics directly related to the POPG content. This was observed from increasing Γ values and decreasing S values upon the enlargement of POPG in the system. Additionally, F_y and F_{adh} in L_β and L_α displayed inverted trends in $\chi_{POPG} = 0.75$ as compared to $\chi_{POPG} < 0.75$.
- The evidenced effects related to the POPG increasing are likely explained by the stiffening of the system due to the presence of calcium: the cation interacts with the negative headgroup of the phospholipid creating a PG-PG network, which leads to a decreased area per molecule and a more compact bilayer.

Article submitted to Soft Matter

Combined FS and AFM-based calorimetric studies to reveal the nanostructural organization of biomimetic membranes[§]

C. Suárez-Germà[±]*, A. Morros[¥],
M.T. Montero[±]*, J. Hernández-Borrell[±]*, Ò. Domènech[±]*[#],

Understanding the behavior of phospholipid systems is of crucial relevance when trying to deepen our understanding of the relationship between these compounds and a possible embedded membrane protein. Here we studied a binary lipid matrix of 1-palmitoyl-2-oleoyl-*sn*-glycero-3-phosphoethanolamine (POPE) and 1-palmitoyl-2-oleoyl-*sn*-glycero-3-phospho-(1'-*rac*-glycerol) (POPG), a composition that mimics the inner membrane of *Escherichia coli*. More specifically, liposomes with varying fractions of POPG were analyzed by differential scanning calorimetry (DSC) and a binary phase diagram of the system was created. Additionally, we performed atomic force microscopy (AFM) imaging of supported lipid bilayers (SLBs) of similar compositions at different temperatures, in order to create a pseudo-binary phase diagram specific to this membrane model. AFM study of SLBs is of particular interest, as it is conceived as the most adequate technique not only for studying lipid bilayer systems but also for imaging and even nanomanipulating inserted membrane proteins. The construction of the above-mentioned phase diagram enabled us to grasp better the thermodynamics of the thermal lipid transition from a gel-like POPE:POPG phase system to a more fluid phase system. Finally, AFM force spectroscopy (FS) was used to determine the nanomechanics of these two lipid phases at 27 ºC and at different POPG fractions. The resulting data correlated with the specific composition of each phase, which was calculated from the AFM phase diagram obtained. All the experiments were done in the presence of 10 mM of calcium, as this ion is commonly used when performing AFM with negatively charged phospholipids.

[¥]Unitat de Biofísica, Departament de Bioquímica i Biologia Molecular, Facultat de Medicina and Centre d'Estudis en Biofísica (CEB), UAB; *Departament de Fisicoquímica, Facultat de Farmàcia, UB; [±]Institut de Nanociència i Nanotecnologia IN[2]UB, Barcelona, Catalonia, Spain; [#]corresponding autor: odomenech@ub.edu
[§]Electronic Supplementary Information (ESI) available: SI for the extended material and methods and SII for a supplementary AFM and zeta potential data.

1. Introduction

In strictly physical terms, the plasma membrane can be seen as the boundary region that separates the discrete mass of the cytoplasm from its outer environment. This membrane, consisting mainly of a phospholipid bilayer and proteins interacting in various ways, is recognized as a heterogeneous structure that provides the basis not only for cell compartmentalization but also for specific metabolic processes to take place, among which are processes from signal or energy transduction to transport of drugs and metabolites, viral and bacterial infections, or tissue development and metastasis. In this respect, characterization of the physicochemical properties of the plasma membrane is crucial to understanding the molecular aspects behind these processes. Biological membranes contain a complex mixture of lipid species that, depending on their molecular structure and physicochemical conditions, such as pH, temperature (*T*) or ionic strength (*I*), may show phase separation and become laterally segregated into nano- or micro-domains.[1] How the physical properties of phospholipid bilayers (e.g. phase segregation, lipid curvature, elasticity) are related to those found in natural biomembranes is, at the least, intriguing. Although the universality of the phospholipid bilayer can be postulated, to assume that behavior observed in model systems occurs in natural membranes remains a matter of debate in the field of membrane biophysics. Thus, as phospholipids belong to mesomorphic matter, they can have

several physical states, depending on the physicochemical conditions. In excess water, phospholipids form fully solvated lipid bilayers, which undergo the known phase transition from the solid-like gel state (L_β) to the fluid liquid-crystalline state (L_α) at a definite transition temperature (T_m) that is specific to each species and phospholipid mixture.[2]

Integral membrane proteins have one or more segments that are embedded in the phospholipid bilayer, where they interact strongly and selectively[3] with the surrounding lipids. Indeed, there is evidence indicating that the activity and folding of some integral proteins depend on the physicochemical properties of neighboring phospholipids.[4] Furthermore, most of the integral membrane proteins reside almost exclusively within the L_α phase[5] and, though this is sometimes controversial, there is evidence that some proteins are excluded from the L_β phase.[6] In a very illuminating paper from Facci's group,[7] such behavior was conclusively demonstrated through atomic force microscopy (AFM) observations, when the channel protein KcsA was reconstituted in supported lipid bilayers (SLBs) of 1-palmitoyl-2-oleoyl-*sn*-glycero-3-phosphoethanolamine (POPE) and palmitoyl-2-oleoyl-*sn*-glycero-3-phospho-(1'-*rac*-glycerol) (POPG) and the temperature was reduced below the T_m of the phospholipid mixture. Then, KcsA monomers were observed to be excluded from the solid-like domain (defined there as L_o) and remained segregated in the fluid phase (defined there as L_d) and at the edge between fluid and gel phase boundaries (see Figure 4 in Seeger's paper). Besides, all integral membrane proteins are surrounded by a layer of phospholipids, the so-called "annular region", which provides the adequate lateral pressure[8] and fluidity to seal the membrane during the structural changes in the protein during transport events. It should be noted that, as shown in the case of lactose permease (LacY) of *Escherichia coli* (*E. coli*), the recruitment of one of the phospholipid species by the protein is dependent on the POPE:POPG molar ratio, which is commonly accepted as the biomimetic binary lipid mixture for LacY.[9] Although a POPE:POPG phase diagram constructed from differential scanning calorimetry (DSC) measurements of liposomes in absence of Ca^{2+} is available,[10] it has become imperative to build a phase diagram for the same system that enables us to predict, at least approximately, the composition of each phase in SLBs in presence of calcium. AFM of SLBs provides topographic information on the lipid bilayers, with the advantage of working in a liquid environment.[11] Furthermore, when working in force spectroscopy (FS) mode, AFM can throw light on the nanomechanical properties of the relevant lipid planar systems, mainly the breakthrough or yield threshold force (F_y) and the adhesion force (F_{adh}).[12-14] In fact, FS has been tested as a suitable technique to distinguish between SLBs of several pure and mixed phospholipid compositions through F_y values.[15,16] The formation of SLBs of negatively charged systems like POPE:POPG requires the presence of divalent cations to screen the negative charge borne by mica,[17,18] in order to provide stability to the system.[19] The purpose of this research paper is two-fold: first, to gain more insight into the nanostructure and nanomechanics of SLBs of POPE:POPG in presence of Ca^{2+}; and secondly, to build and compare binary phase diagrams for the POPE:POPG system obtained either from liposomes through DSC data or from SLBs through AFM observations.

2. Results and Discussion

2.1. Constructing diagrams from DSC data and AFM imaging

The phase behavior of the POPE:POPG binary system was investigated by DSC. To build a phase diagram for the POPE:POPG system, the onset and completion temperatures (T_{onset} and T_{offset}, respectively) from the endotherms of a series of mixtures have to be determined. Figure 1 shows the response function of multilamellar vesicles in presence of 10 mM of Ca^{2+} of different POPE:POPG mixtures as a function of temperature. As observed from normalized endotherms, the T_m, the temperature at the maximum heat capacity, remains withheld nearly 24 ºC up to the equimolar of both phospholipids. Further increase in the molar ratio of POPG results in a significant decrease in the T_m. Remarkably, endotherms are slightly asymmetric, skewed to the low temperature side in all cases and becoming clearly asymmetric at $\chi_{POPG} > 0.50$. Indeed, this behavior indicates an enhanced non-ideal mixing behavior of the system as the POPG proportion increases.

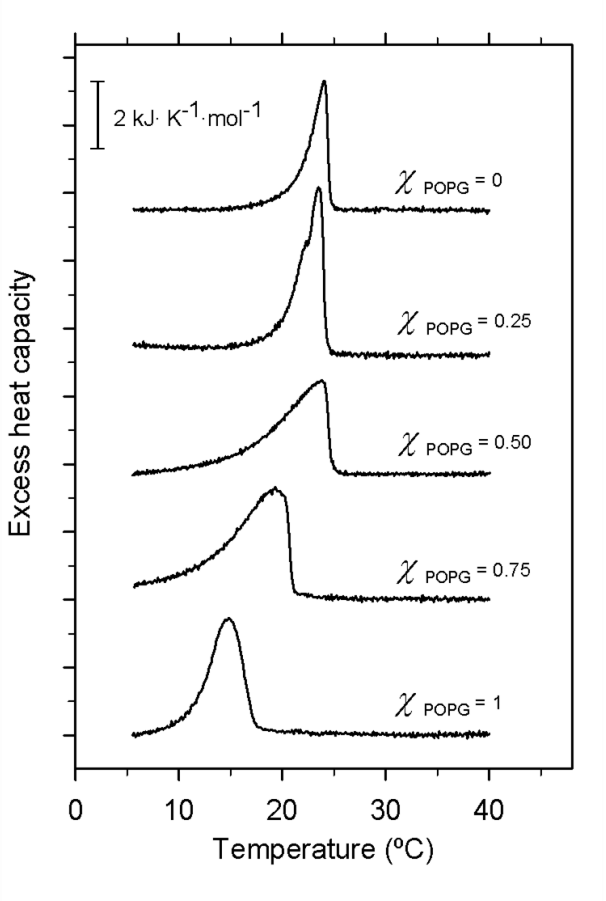

Fig. 1 Normalized excess heat capacity profiles for large multilamellar liposomes of POPE:POPG mixtures at the indicated molar ratios. The total phospholipid concentration was 2.0 mg·mL^{-1} and the heating scan rate was 0.44 ºC·min^{-1}.

Mathematical adjustments performed on individual endotherms (see Supplementary Materials SI) allowed the determination of the thermodynamic parameters of the transition: T_m and the enthalpy involved in the process of transformation ($\Delta_{transf}H$), from the L_β to the L_α phase (Table 1).

Table 1. Thermodynamic parameters obtained from the thermograms and from fitting the AFM data to the van't Hoff equation.

		χ_{POPG}		
		0.25	0.50	0.75
T_m (ºC)	DSC	23.50 ± 0.15	23.70 ± 0.13	19.30 ± 0.10
	AFM	27.80 ± 0.12	24.35 ± 0.15	25.85 ± 0.03
$\Delta_{transf}H$ (kJ·mol^{-1})	DSC	17.7 ± 0.2	18.9 ± 0.2	24.7 ± 0.2
	AFM	1560 ± 150	1600 ± 300	980 ± 30
N	$\frac{\Delta H_{AFM}}{\Delta H_{DSC}}$	87	85	40

Figure 2A shows the binary phase diagram obtained from the endotherms constructed after connecting the corresponding T_{onset} (open circles) and T_{offset} (full circles). As observed, this pseudo-phase diagram is S-shaped, which indicates a substantial deviation from the ideal mixing behavior at all the molar fractions analyzed. The diagram is quite consistent with a previous phase diagram derived by Pozo-Navas et al.[10] for the same system in absence of Ca^{2+}. Actually, the shift of the T_m towards lower temperatures, most precisely for those liposome mixtures containing high POPG proportions, was reported earlier.[21,22]

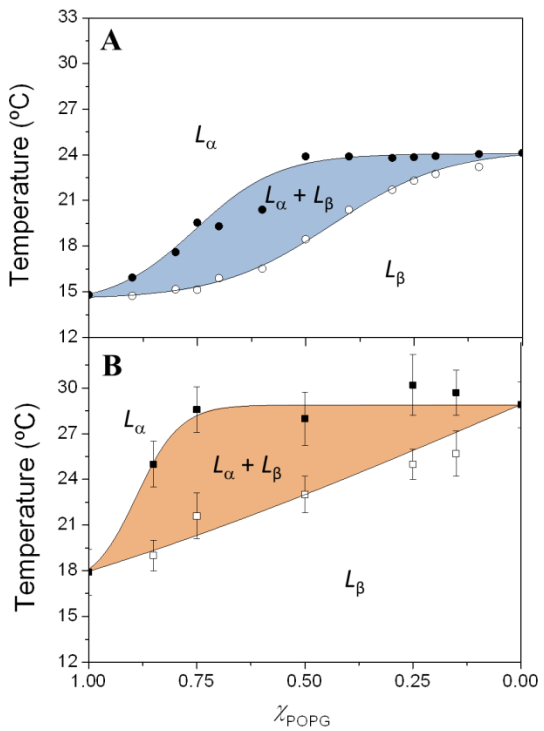

Fig. 2 A) Phase diagram for POPE:POPG mixtures obtained from the heat capacity curves shown in Figure 1. Empty circles correspond to the experimental T_{onset} and filled circles to the T_{offset} of the main phase transition. B) Phase diagram of POPE:POPG mixtures obtained from the AFM topography images. Empty circles correspond to the experimental T where the first L_α domain appeared and filled circles correspond to the experimental T where the last L_β domain vanished. Error bars correspond to standard deviations in at least three replicate experiments.

An interesting feature of the diagram is the quite horizontal segment of the *solidus* line from $\chi_{POPG} > 0.7$, which is consistent with the occurrence of a miscibility gap within the L_β phase. This behavior means that, for the present system and for $\chi_{POPG} > 0.7$, the formation of two gel lipid sub-domains with different compositions ($L_{\beta1}$ and $L_{\beta2}$) should be considered.[23,24] However, to probe the existence of these two gel phases X-ray diffraction or other techniques different

of DSC should be applied. In any event, such investigation is out of the scopes of the present research.

It has been shown that SLBs of POPE:POPG prepared either by the vesicle fusion technique[25] or Langmuir-Blodgget double deposition[26] display expected L_α/L_β phase coexistence at room temperature. In the present study, AFM observations of SLBs with different mole fractions of POPG have been conducted at several temperatures, to construct a phase diagram (Figure 2B) and compare it to the phase diagram obtained from DSC data (Figure 2A). Of course the comparison between both pseudo-phase diagrams should be taken with caution. First, because the influence of the substrate may play a major role in the lipid behavior. Mica is the more popularized substrate because it is smooth and hydrophilic, but it is worth to mention that other substrates, as fused silica, borosilicate glass or titanium oxide are common. In such cases the pseudo-phase diagram would present probably different trends. Besides it is not only the influence of the substrate but the ionic strength and type of cation[27,28] or osmolarity[29] that may affect the properties of the phase transition. In any case, the use of mica and a precise buffer is justified here by the need to correlate the obtained results with other studies of our group.[5,30] Secondly, it should be noted that, although the temperature was controlled with great accuracy in our AFM experiments (see Supporting Information, SI1), the high sensitivity and accuracy attained with DSC cannot be technically achieved with the actual temperature-control system of the AFM, which anticipates the difficulty for finding a direct correspondence between the phase diagrams obtained from both techniques.

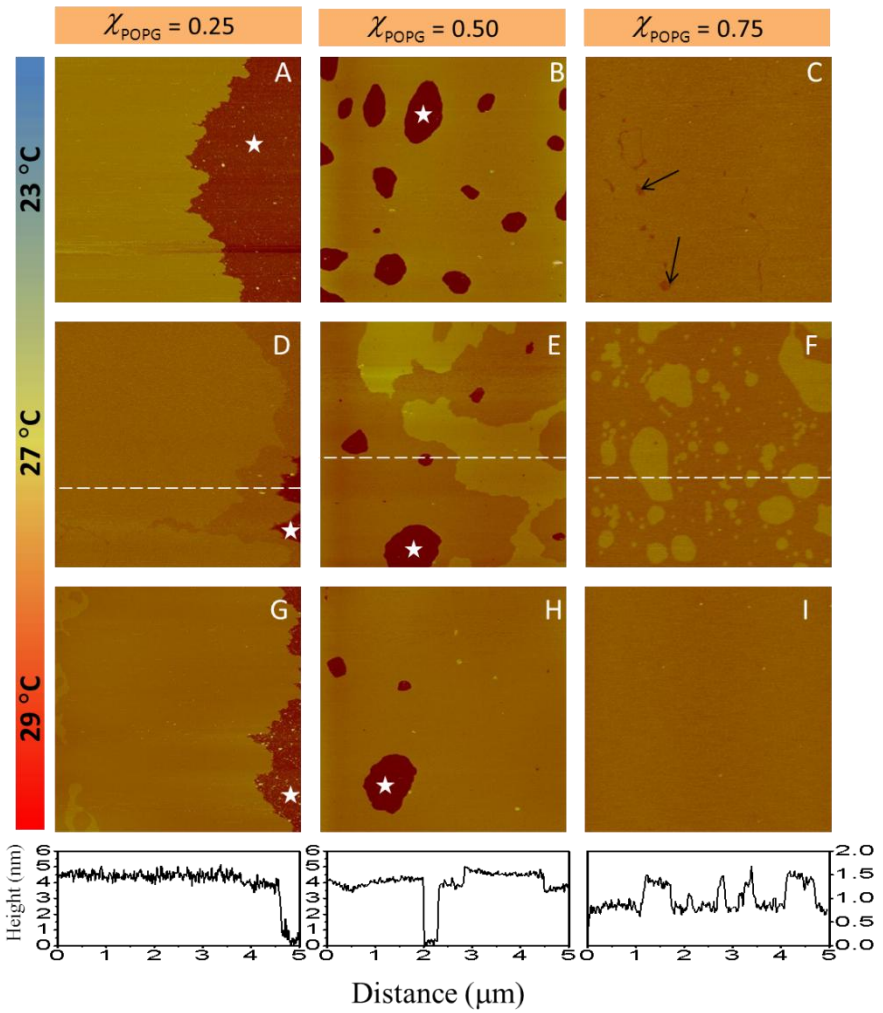

Fig. 3. AFM images of POPE:POPG phospholipid bilayers with χ_{POPG} = 0.25 (A, D, G), χ_{POPG} = 0.50 (B, E, H) and χ_{POPG} = 0.75 (C, F, I) at 23, 27 and 29 ºC. White stars correspond to mica surface, black arrows in image C correspond to L_α domains and white dotted lines correspond to height profiles shown at the bottom of each composition. Z scale bar was 20 nm except for images (C, F, I) that was 10 nm.

Figure 3 shows a selection of AFM topography images of SLBs obtained at three different compositions (χ_{POPG} = 0.25, 0.50 and 0.75) and three temperatures (23, 27 and 29 ºC). Although 37ºC would be desirable because it is considered physiological, at this temperature only one phase would be present. Indeed, *E. coli* has been proved to present populations normally living out of warm-blooded animals[31], and thus studies at room temperature might be also relevant and this provides means for the present study on the phase separation. At 23 ºC, SLBs of χ_{POPG} = 0.25 (Figure 3A) and χ_{POPG} = 0.50 (Figure 3B) show flat and homogenous surfaces with step height differences of 3.4 and 5.4 nm from the bare mica surface, respectively. At this temperature, both images show SLBs in L_β phase. For the SLB with χ_{POPG} = 0.75 (Figure 3C), the step height difference was established at 5.63 nm. In this case, although the surface of the SLBs is rather flat and homogenous, some small patches covering less than 3% of the surface can be observed (see black arrows in the image). Indeed, these patches indicate that, for this temperature and composition, the SLB is close to T_{onset}, so just starting the L_β to L_α phase transition. At 23 ºC we confirmed the shift of the T_{onset} towards higher temperatures than those observed from DSC data. This behavior, previously reported for SLBs,[32,33] is the result of the potential interaction of the proximal leaflet of the SLBs with the mica substrate. In the present study, such interaction is enhanced at higher POPG molar fractions, as a consequence of a bridging effect of Ca^{2+} between POPG and the negatively charged mica surface. Actually, the interaction of the proximal leaflet with mica substrate has been extensively debated.[26,34,35] This interaction would in fact modulate not only the thermotropic behavior of SLBs, but also their topographical features and nanomechanical properties.

At 27 ºC, all SLBs (Figure 3, images D, E and F) have two domains that show the L_α /L_β phase coexistence. The step height difference for the lighter (higher) domains in these images compares well with the value reported at 23 ºC (L_β phase). In turn, the darker (lower) domains are ~0.6 to 1.4 nm lower than those observed at 23 ºC, which is the expected height difference between the L_β and L_α phases. After the temperature was raised to 29 ºC (Figure 3, images H and I), SLBs showed a single domain with an average height that falls within the range expected for L_α phases. Although residual L_β domains are still present in Figure 3G, the L_α phase is, however, the predominant phase. Heights and roughness values obtained for each image shown in Figure 3 are available in a Table given in the Supporting Information, SII4.

After a careful analysis of the topographical images, the phase diagram was constructed from the T_{onset} (open squares) at which the L_α phase appears and the T_{offset} (closed squares), at which the L_β phase vanishes. The pseudo-binary phase diagram is shown in Figure 2B; Table 1 shows the values derived from this data. As can be seen, the T_m determined from AFM imaging were higher than those obtained from DSC. As stated above, this behavior was expected, since it is well known that SLB transition encompasses a higher and wider range of temperatures than transitions observed by performing DSC on liposomes with the same composition. This behavior, extensively discussed by several authors,[14,33,36-38] has been attributed to different effects: *i*) the presence of the substrate in contact with the proximal leaflet of the bilayer; *ii*) the infinite radius of curvature of the SLBs, which decreases the lateral tension between phospholipids in the bilayer*;* and *iii*) the decoupling between the leaflets of the bilayers which results in a double transition. As concluded from detailed investigations on POPE-POPG system reported by Facci's group,[25] the last effect appears to depend on the experimental conditions followed during SLB preparation. In the present study, SLBs were obtained by liposome spreading and incubation of the sample above the T_m of the lipid mixture, under high ionic strength conditions. This is why we did not observe the intermediate phase postulated by Seeger et al.[25] Indeed, in our experiments, only one transition demonstrating the coupling between the two leaflets of our SLBs was observed. However, it is intriguing that in the SLB with χ_{POPG} = 0.5, the difference observed between the T_m obtained from DSC and from AFM studies is less than 1 ºC. This observation suggests that this composition is less affected by the supporting surface. It has been widely reported that negatively charged phospholipids adsorbed onto mica are limited to lateral diffusion because of the interaction between the negative polar head and the substrate.[18] The *liquidus* line (closed squares in Figure 2B) obtained on SLBs does not significantly change on the POPG molar fraction decreasing and is, remarkably, quite similar to the T_m of pure POPE (χ_{POPG} = 0).

Despite it being technically more difficult than DSC, the AFM-based pseudo-phase diagram provides a fast, approximate evaluation of the composition of L_α and L_β phases on SLBs and, thus, a way to estimate the composition of the domains observed in the images

shown in Figure 3. Therefore, by taking a connection line along 27 ºC (the temperature selected for the nanomechanical studies) and applying the lever rule, we can determine the composition of each phase for the biomimetic composition of LacY (χ_{POPG} = 0.25). Thus, we obtain that POPG is distributed as follows: χ_{POPG}^{α} = 0.11 (molar fraction of POPG in the L_α phase) and χ_{POPG}^{β} = 0.14 (molar fraction of POPG in L_β phase). Consequently, POPE's presence in L_α and L_β phases corresponds to χ_{POPE}^{α} = 0.03 and χ_{POPE}^{β} = 0.72, respectively. Thus, the composition χ_{POPG} = 0.25 shows an enrichment of POPG in L_α and an enrichment of POPE in L_β phase. For the sake of clarity an illustration showing the application of the lever phase rule for predicting each composition is provided as Supporting Information, SII5.

2.2. Thermodynamics of the POPE:POPG phase transition onto mica

In a system where only two possible states (L_α and L_β) are assumed, the phase transition of the SLBs onto a surface may be described by an equilibrium constant (*K)* that can be defined as

$$K = \frac{\theta}{1-\theta} \qquad (1)$$

where θ is the fraction of the L_α phase in the SLBs calculated by measuring its area after the AFM images.[25,33,36] According to Mabrey and Sturtevant,[39] *K* can be described as a function of *T* by the integrated form of the van't Hoff equation

$$Ln\ K = -\frac{\Delta H_{vH}}{R}\left(\frac{1}{T} - \frac{1}{T_m}\right) \qquad (2)$$

where *R* is the gas constant, T_m is the transition temperature and ΔH_{vH} is the van't Hoff molar enthalpy. Then, by inserting Equation (2) in (1) we obtain the following expression

$$\theta = \frac{1}{1+\exp\left[-\frac{\Delta H_{vH}}{R}\left(\frac{1}{T}-\frac{1}{T_m}\right)\right]} \qquad (3)$$

which relates θ at a given temperature with the ΔH_{vH} involved in the transition occurring on the surface. θ values were determined at 10 different temperatures and Equation 3 was fitted to the data. For a better comparison, the results obtained from analyzing the thermal behavior of the SLBs are summarized in Table 1 along with the values obtained from DSC experiments. It is thought that, when the temperature of the system increases and the phospholipids undergo the phase transition, part of the energy is used to counterbalance the interactions with the substrate. Therefore, this would explain why the ΔH_{vH} are higher for SLBs than ΔH for liposomes.[17,40] For the SLBs at χ_{POPG} = 0.25 and 0.5, the magnitudes of the ΔH_{vH} are quite similar (~ 1600 kJ·mol^{-1}), but for the SLB at χ_{POPG} = 0.75 it decreases to 980 kJ·mol^{-1}. Such a difference could be attributed to the high negative charge present in the latter composition (see the zeta potential values for each composition provided as Supporting Information, SII6), which increases the electrostatic repulsion between the bilayer and the substrate and results in a decrease of ΔH_{vH}.

The approximate number of lipids experiencing the transition, interpreted as the cooperativity unit,[41] is given by $N = \Delta H_{AFM}/\Delta H_{DSC}$. The *N* values are 87 and 85 for the SLBs with χ_{POPG} = 0.25 and 0.50, respectively, and 40 for the SLB at χ_{POPG} = 0.75. This makes clear that, as the proportion of negatively charged phospholipid increases in the SLBs, the cooperativity unit of the transformation decreases. It is most likely related with the fact that Ca^{2+} induces phase separation because of its ability to bind stoichiometrically to negatively charged phospholipids (e.g. POPG). Thus it results in a reduction of their surface charge and area with consequent increase in the transition temperature and the promotion of a bilayer with a more gel-like nature than in absence of the bivalent cation.[42,43] This behavior may explain the quantitative differences found when comparing with other *N* values obtained in the same system in absence of Ca^{2+}.[25] The decrease in *N* on the increase in the POPG molar fraction might also be related, at least at 23 ºC, with the postulated existence of a miscibility gap in the L_β phase when $\chi_{POPG} > 0.7$.[10,23] It should be noted, however, that the AFM experiments performed on SLBs did not have enough resolution to provide visual evidence for the existence of these two different L_β domains.

2.3. Nanomechanics of SLBs

FS has been extensively used to probe the nanomechanical properties of lipid layers.[26,44,45] Since the pioneer works of Dufrêne,[12,46] FS has become the tool for exploring the nanomechanical properties of pure phospholipid SLBs [15,47] and, more importantly, assessing the nanostructural organization of more complex lipid mixtures.[35,48] Although the biological meaning behind

FS measurements is still controversial,[49] the potential of this technique for revealing the nanomechanics of complex systems, from models to natural membranes[50] and living cells[51,52] is, however, widely accepted. The basic magnitudes extracted from traditional FS experiments (Figure 4) are: *i*) the breakthrough or yield threshold force (F_y), i.e. the force that the bilayer can withstand before being indented; and *ii*) the adhesion force (F_{adh}), i.e. the pull-off force between the tip and the bilayer.[12,26]

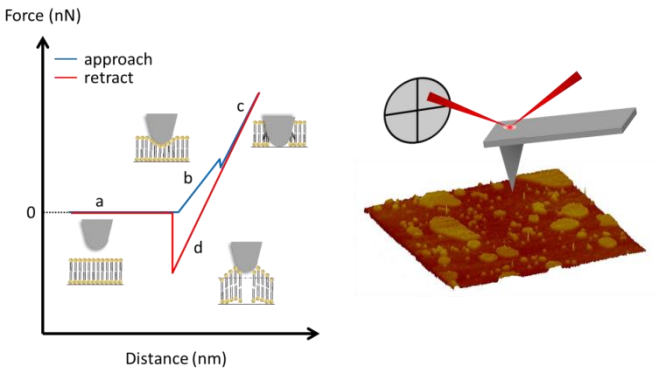

Fig. 4. Schematic representation of the experimental procedure used to obtain threshold and adhesion forces. Right) Topographic images were first acquired to visualize the phospholipid domains and thereafter the AFM tip was centered in the domain chosen for analysis. Left) Typical force curve on a lipid domains. First, tip approaches (blue line) to the surface (a), it touches the surface, it begins to press down the SLB (b) until the force is enough to punch the bilayer (breakthrough force) and the tip continues pressing the mica surface (c). Afterwards, the tip begins to separate (red line) from the mica surface (d) until the tip is completely free from the sample (adhesion force) and the tip moves away from the sample (a).

To clarify further the nature of phase separation in complex biomimetic systems, e.g. displaying phase separation in binary lipid mixtures, we performed FS measurements on SLBs of POPE:POPG at different χ_{POPG}. In terms of biological relevance, we focused the analysis on the biomimetic composition, χ_{POPG} = 0.25. FS measurements were performed at 27 ºC because we wanted to discriminate in FS terms between the L_β and L_α phases.

Distributions of F_y for each lipid domain at each studied composition are shown in Figure 5. For SLBs at χ_{POPG} = 0.25, where the two phases can be spatially resolved (Figure 3D), the mean values of F_y obtained were quite similar for L_β and L_α, 0.250 ± 0.005 nN (Table 2). On the one hand, this value compares well with the one previously obtained for the L_α phase in the same lipid mixture.[30] On the other hand, the value for the L_β phase is lower than that reported in the same study. To rationalize this discrepancy, two related factors should be taken into account: *i*) the higher acquisition temperature (27 ºC), which is some degrees above the temperature used in our earlier study;[30] and *ii*) according to the phase diagram given, whilst at room temperature we are close to the *solidus* line, at 27 ºC we are in the coexistence region (Figure 2B).

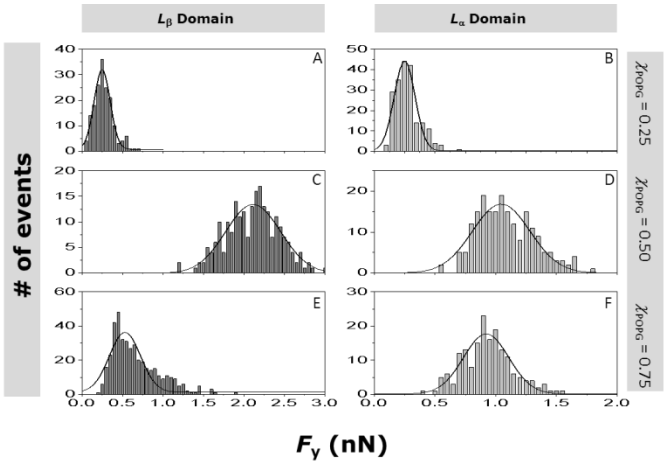

Fig. 5. F_y distribution for χ_{POPG} = 0.25 (A, B), χ_{POPG} = 0.50 (C, D) and χ_{POPG} = 0.75 (E, F), at 27ºC in the L_α and L_β lipid domains. Fits to the continuum nucleation model (eq 4 in SI1) are represented as solid lines.

For the equimolar SLB composition, χ_{POPG} = 0.50 (Figure 3E), the mean F_y values were 2.114 ± 0.016 nN and 1.046 ± 0.016 nN for the L_β and L_α domain, respectively (Table 2). This means that we need ~2 times more energy to indent the L_β than the L_α domain.

Table 2. Mean F_y and F_{adh} values from data presented in Figures 5 and 6 fitted to a Gaussian distribution and calculated Γ and S parameters after fitting data in Figure 5 to the continuum nucleation model. Errors values are standard deviation from the mathematical statistics.

		χ_{POPG}		
		0.25	0.50	0.75
F_y (nN)	L_β	0.250 ± 0.005	2.114 ± 0.016	0.531 ± 0.013
	L_α	0.250 ± 0.006	1.046 ± 0.011	0.922 ± 0.009
F_{adh} (nN)	L_β	0.450 ± 0.006	1.119 ± 0.010	0.54 ± 0.02
	L_α	0.175 ± 0.006	0.278 ± 0.002	1.115 ± 0.019
Γ(nN)	L_β	21.8 ± 1.6	38 ± 2	31.0 ± 1.7
	L_α	19 ± 3	29.9 ± 1.1	28.0 ± 1.0
S (mN·m^{-1})	L_β	-9.53 ± 0.06	-6.61 ± 0.11	-17.8 ± 0.3
	L_α	-6.3 ± 0.2	-9.87 ± 0.03	-7.00 ± 0.09

For SLBs at χ_{POPG} = 0.75 (Figure 3F), the mean F_y value for the L_β phase was 0.531 ± 0.013 nN, whilst the L_α phase had almost twice this value (0.922 ± 0.009 nN). Actually, the observation is in apparent contradiction with a general assumption that higher F_y values are quite closely associated with L_β phases, the results for χ_{POPG} > 0.50 most probably reflect that, for SLBs containing high

amounts of negatively charged lipids, stiffness and electrostatic repulsion variations should be taken into account. Notice that, at this composition, the distribution (Figure 5E) does not fit with the model as well as the other which indicates a different behavior and physicochemical properties at high POPG proportions. Actually, the ratio of the two phases present can be found by using the lever rule. When it is applied in the phase diagram shown in Figure 2B, the amount of POPG estimated for the L_α phase of SLBs at $\chi_{POPG} = 0.75$ rises to 0.74 (Supplementary Material, SII5), which indeed corresponds to almost the entire amount of the POPG present in the system.

As predicted by the lever phase rule, the increase of POPG, in absolute terms, should be more prominent in the L_α than in the L_β phase. This results in smaller domains of the gel-crystalline phase (Figure 3 D-F) and in eventual changes in line tension values.[53] Thus, F_y values would be strongly dependent not only on negative repulsion between POPG molecules, but also on the formation of "solid clusters" within the L_α phase in presence of calcium.[2] As a result, the force needed to indent L_α domains highly enriched in POPG may be greater than the force required to overcome the potential barrier to make a hole in a zwitterionic phospholipid.[54,55] Inspection of the retraction part of force curves performed on SLBs with different χ_{POPG} allows obtaining the corresponding adhesion forces (see left drawing in Figure 4). In a seminal work by Dufrêne et al.,[12] it was shown that F_{adh} are directly related to the strength of the lateral forces between the molecules that provide means for the cohesive forces within the films. However, the actual force required to separate the tip from the lipid may be largely affected by the negative charge borne by POPG and the presence of the Ca^{2+} in the environment. Distributions of F_{adh} for each domain at different POPG mole fractions are shown in Figure 6. Additionally, mean F_{adh} values are summarized in Table 2. For $\chi_{POPG} = 0.25$, two different F_{adh} values, 0.450 ± 0.006 and 0.175 ± 0.006 nN, were obtained for the L_β and L_α domains, respectively. Actually, whilst such behavior was observed for complex mixtures,[56] the converse situation, higher F_{adh} for fluid than ordered phases was reported in neutral phospholipids.[57] Besides, F_{adh} is strongly dependent on the nature and geometry of the tip, surface roughness and preparation procedures[58] among other conditions.[59] Therefore, F_{adh} may not be considered as an intensive property of the SLBs. Then, by taking into account the composition of the fluid phase it is conceivable that L_α might present lower adhesive forces than L_β, which may be related with the clustering of POPG molecules in presence of calcium.[2]

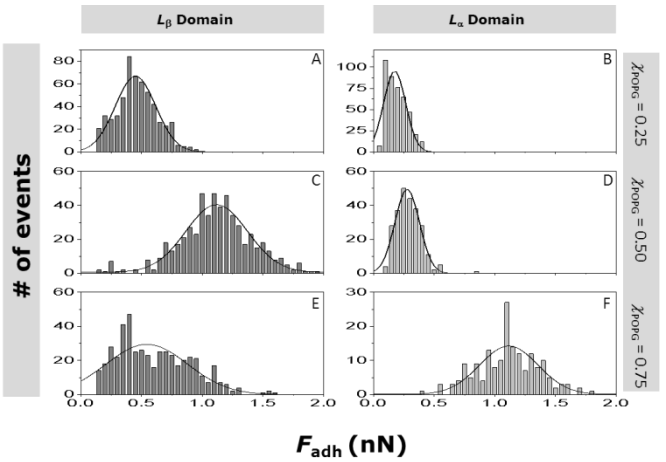

Fig. 6. F_{adh} distribution for $\chi_{POPG} = 0.25$ (A, B), $\chi_{POPG} = 0.50$ (C, D) and $\chi_{POPG} = 0.75$ (E, F), at 27 ºC in the L_α and L_β lipid domains. Fits to a Gaussian distribution are represented as solid lines.

The F_{adh} for the SLB with $\chi_{POPG} = 0.50$ were 1.119 ± 0.020 and 0.278 ± 0.002 nN for the L_β and L_α phases, respectively. Note, however, that for this composition the mean F_{adh} is 4 times higher for the L_β than for the L_α phase. Conversely, the F_{adh} were significantly lower for the L_β phase (0.54 ± 0.02 nN) than for the L_α one (1.115 ± 0.019 nN) when $\chi_{POPG} = 0.75$ (Table 2), which is may be due to a non Gaussian distribution (Figure 6E). Strikingly, for this composition the F_y values for the L_α phase result from a strong repulsion with the tip[30] although the F_{adh} values suggest a strong cohesion of the film. Although the L_α phase is enriched in POPG molecules and the repulsion between the neighbor phospholipids and the AFM tip may occur, there are enough POPE molecules to stabilize the interactions between neighboring lipids.

2.4. Applying the continuum nucleation model

The parameters that determine how the AFM tip can go through the SLB in a force-distance curve have been evaluated in both theoretical and experimental terms.[54,60] A seminal work by Butt and coworkers[54,55] introduced a theory to calculate the activation energy required to form a hole in a lipid film when an AFM tip indents a planar layer. Although this model reduces the system by considering the SLB as a liquid structure in a XY plane, it has been successfully tested on several substrates and conditions.[53,55] Notably, this has also been applied to SLBs, in order to unambiguously assign physical parameters and provide the basis for discrimination between

phospholipid species (homo- and hetero-acids) with different headgroups and, even, different compositions.[42] As discussed by Butt and coworkers,[54] at constant velocity the continuum nucleation model fits the probabilities of distribution of force *P(F)* according to

$$Ln\,P(F) = -\frac{\Omega}{k_c v_0}\int_{F_s}^{F} exp\left(-\frac{c}{(F-F_S)}\right)dF \qquad (4)$$

with

$$c = \frac{2\pi^2\Gamma^2 T}{k_B T} \qquad (5)$$

and

$$F_s = 2\pi RS \qquad (6)$$

where Ω, as a first approximation, can be interpreted as the resonance frequency of the cantilever, k_c is the spring constant of the cantilever, v_0 is the velocity, Γ is a line tension associated with the unsaturated bonds of the molecules in the periphery of the hole, R is the tip radius, k_B is the Boltzmann constant, T is the temperature and S is the spreading pressure associated with the energy per unit area gained by the layer when filling the hole formed after the rupture. Equation 4 can be integrated analytically and the yield probability dP/dF can be expressed as[53]

$$\frac{dP}{dF} = \frac{\Omega}{k_c v_0} exp\left\{-\frac{c}{F'-F_s} - \frac{\Omega}{k_c v_0}\left[exp\left(-\frac{c}{F'-F_s}\right)\left(F'-F_s\right) - cE_i(x)\left(\frac{c}{F'-F_s}\right)\right]\right\} \qquad (7)$$

where

$$E_i(x) = \int_x^{\infty}\frac{e^{-y}}{y}dy \qquad (8)$$

The robustness of the model has been unambiguously demonstrated for lipid bilayers of DOTAP[55] and successfully extended to a wide variety of pure phospholipids and mixtures with cholesterol by Garcia-Manyes et al.[15] To this end, the yield probability dP/dF was adjusted to the experimental data and the fitted parameters are listed in Table 2. Γ values obtained for SLBs at χ_{POPG} = 0.25 and 0.75 were quite similar for both phospholipid domains, ranging from 20 to 30 nN, respectively. It should be noted that the L_β phase showed higher values of Γ for both compositions. Since both POPE and POPG are heteroacid phospholipids with the same acyl chain composition, line tension should arise from the different interaction between the headgroup moieties, mainly entropic and repulsion contributions,[53] and the different composition of lipids that integrate the periphery of the hole. To rationalize these values one should assume that for SLB*s* at χ_{POPG} = 0.75, the phospholipids at the periphery of the hole would probably be more enriched in POPG than in POPE. This assumption is indirectly supported by previous Förster energy transfer experiments performed with proteoliposomes with different POPE:POPG compositions.[9] This would result in an electrostatic repulsion between neighboring molecules, leading to a relative increase in Γ values. This observation corroborates the topographic features observed in Fig. 3F (χ_{POPG} = 0.75), where a decrease in the domain size most probably reflects the increase in the length of the boundary region between the two phases. Then, for the SLB at χ_{POPG} = 0.25, such electrostatic repulsion decreases and, thus, phospholipid molecules would be closer to each other, resulting in the decrease of Γ values. Consequently, the size of the domains will be the largest observed (Figure 3D). When the SLBs are equimolar in composition, χ_{POPG} = 0.5, the values of Γ obtained for the high and low domains were 38 ± 2.0 nN and 29.9 ± 1.1 nN, respectively, which indicates that the gel phase should be more likely to withstand higher indentation forces. In addition, the L_α phase has a similar Γ value as in the case of POPG, with a molar fraction of 0.75. This observation is consistent with the expected enrichment of POPG within the fluid phase, as predicted by using the lever phase rule (χ_{POPG}^{α}=0.46, χ_{POPG}^{β}= 0.03, χ_{POPE}^{α} = 0.11, χ_{POPE}^{β} = 0.39, when χ_{POPG} = 0.5. Conversely, POPE should be the main component of the L_β phase in equimolar composition.

As recently discussed,[15] the parameter S is directly related to the nature of the headgroup, being negative for PE and PG. Thus, the estimated values in this study corroborated qualitatively those reported from previous observations, although in absolute terms they were higher for all compositions and domains (Table 2). The parameter S seems to obey subtle balances between the acyl chain and headgroup composition. Even if this assumption is theoretical and still not experimentally determined, this parameter is most likely to be related to the lateral surface pressure profile.[8,61,62] Negative values of S indicate that the hole formed after AFM indentation during FS experiments is not easily refilled, which means that the SLB loses energy in some way during this process. However, no further defects were observed when performing FS experiments, which might indicate that the kinetics of the process is faster than the velocity of the force curve. The absolute largest and lowest estimated S values correspond to the L_β phase in the SLBs with

χ_{POPG}= 0.75 and to the L_α phase with χ_{POPG} = 0.25 (Table 2). The whole set of *S* values emphasizes how, the more domains become enriched in POPG, the more difficult is for the film to spread into the gap between the tip and the substrate.

2.5. Biological Relevance

To dispose of phase diagrams for mixtures of lipids mimicking biological membranes is important in order to understand how phase properties may affect the membrane physiology and function. It could be interesting, for instance, to get a rationale for the development of membrane disruptive antibiotics, directed specifically to the prokaryotic membrane but with non action against the eukaryotic membrane. Whether the nanostructure of biomembranes is becoming more complex by the compilation of new evidences that transient and permanent lipid-protein associations are present, there is no doubt that the biomembranes are always in fluid phase in order to guarantee their functional properties However, some biological mechanisms seem to depend on the gel state. For instance it is well known that cells modify their membrane composition under stress to adapt to the environment.[63,64] Hence, they respond to changes in temperature, resulting in the increase of low-transition temperature phospholipids. The reason for this is that highly unsaturated phospholipids have enthalpy values similar to those of saturated species. We are investigating thoroughly the possible influence of phospholipids on the activity of LacY of *E. coli*, for which the composition mimicking the inner membrane of the bacteria is provided by POPE and POPG at a 3 to 1 molar ratio. Importantly, for the adaptation of LacY to possible changes occurring in the environment, the knowledge of the POPE:POPG phase diagram becomes of relevance. Thus, by measuring the resonance energy transfer between a single tryptophan mutant of LacY (single-W151/C154G) and pyrene labeled phospholipids we have shown that the protein may recruit either POPE or POPG, depending on the molar phospholipid ratio used to reconstitute the protein.[9] Although FRET experiments in solution[3,9] were carried out using this non-transporting mutant, the findings correlate directly with other observations on the modifications experienced by natural bacterial membranes under stress conditions. Besides, by assuming the existence of an annular region of phospholipids around LacY, we also demonstrated that there is a specific selectivity of LacY for POPE. Similarly, there are studies of mechanosensitive proteins like KcsA[65] that clearly demonstrate the requirement of specific headgroup for the protein activity. Furthermore, a recent study by Weingarth et al.[66] provided strong evidence on non-annular lipid-KcsA specific interactions.

Since many structural resolution and nanomanipulation investigations of membrane proteins are obtained from AFM by using reconstitution procedures into SLBs,[67] it becomes of crucial relevance to dispose of phase diagrams of the lipid mixtures in-plane. This information would be the basis for understanding the distribution of the transmembrane proteins between the different lipid phases, lipid-protein association among other properties observed in membrane models and cell membranes.

3. Materials and Methods

DSC of multilamellar liposomes and AFM of SLBs were combined to study the thermotropic properties of the binary system, POPE:POPG. Sample preparation and experimental procedures have been published elsewhere[20] and details are available in the Supporting Information, SI1.

4. Conclusions

The behaviour of POPE:POPG binary system in the presence of 10 mM of Ca^{2+} has been investigated in this study through the construction of two phase diagrams: one coming from DSC analysis of liposomes and another constructed from SLBs imaging by temperature-controlled AFM. Specifically, obtaining a phase diagram for SLBs is of great relevance for understanding the phase separation phenomena when working with this mixture, widely used as the composition that mimics the inner membrane of *E. coli*. The study was completed with the FS nanomechanical analysis of SLBs varying the χ_{POPG} at 27 ºC. The obtained results evidenced a strong influence of the negatively charged PG in the system, which seems to confirm that Ca^{2+} interacts directly with the PG headgroup promoting a clustering effect. Hence, we showed that the presence of divalent ions in negatively charged bilayers can largely modify the physicochemical behaviour of the system, and therefore, it becomes important to take it into consideration regarding SLBs formation and also possible implications of biological relevance as the interaction with membrane proteins.

Acknowledgements

C. S. G. is recipient of a FPI fellowship from the Ministerio de Economía y Competitividad of Spain. This work has been supported by grant CTQ-2008-03922/BQU from Ministerio de Ciencia e Innovación of Spain. Authors thank the Universitat de Barcelona for financial support. We thank Laura Picas for valuable insights and comments.

References

1 L. A. Bagatolli, *Biochim. Biophys. Acta*, 2006, **1758**, 1556.
2 M. D. Houslay and K. K. Stanley, *Dynamics of biological membranes*, Headington Hill Hall, Chischester, 1982.
3 L. Picas, C. Suárez-Germà, M. T. Montero, J. L. Vázquez-Ibar, J. Hernández-Borrell, M. Prieto and L. M. S. Loura, *Biochim. Biophys. Acta*, 2010, **1798**, 1707.
4 H. Vitrac, M. Bogdanov and W. Dowhan, *Proc. Natl. Acad. Sci. U.S.A.*, 2013, **110**, 9338.
5 L. Picas, A. Carretero-Genevrier, M. T. Montero, J. L. Vázquez-Ibar, B. Seantier, P. E. Milhiet and J. Hernández-Borrell, *Biochim. Biophys. Acta*, 2010, **1798**, 1014.
6 A. G. Lee, *Biochim. Biophys. Acta*, 2004, **1666**, 62.
7 H. M. Seeger, C. A. Bortolotti, A. Alessandrini and P. Facci, *J. Phys. Chem. B*, 2009, **113**, 16654.
8 D. Marsh, *Biochim. Biophys. Acta*, 2008, **1778**, 1545.
9 L. Picas, M. T. Montero, A. Morros, J. L. Vázquez-Ibar and J. Hernández-Borrell, *Biochim. Biophys. Acta*, 2010, **1798**, 291.
10 B. Pozo Navas, K. Lohner, G. Deutsch, E. Sevcsik, K. A. Riske, R. Dimova, P. Garidel and G. Pabst, *Biochim. Biophys. Acta*, 2005, **1716**, 40.
11 L. Picas, P. Milhiet and J. Hernández-Borrell, *Chem. Phys. Lipids*, 2012, **165**, 845.
12 Y. F. Dufrêne, W. R. Barger, J. D. Green and G. U. Lee, *Langmuir*, 1997, **13**, 4779.
13 S. Garcia-Manyes, Ò. Domènech, F. Sanz, M. T. Montero and J. Hernández-Borrell, *Biochim. Biophys. Acta*, 2007, **1768**, 1190.
14 G. Oncins, L. Picas, J. Hernández-Borrell, S. Garcia-Manyes and F. Sanz, *Biophys. J.*, 2007, **93**, 2713.
15 S. Garcia-Manyes, L. Redondo-Morata, G. Oncins and F. Sanz, *J. Am. Chem. Soc.*, 2010, **132**, 12874.
16 L. Redondo-Morata, G. Oncins and F. Sanz, *Biophys. J.*, 2012, **102**, 66.
17 R. P. Richter, N. Maury and A. R. Brisson, *Langmuir*, 2005, **21**, 299.
18 I. Reviakine and A. Brisson, *Langmuir*, 2000, **16**, 1806.
19 L. Redondo-Morata, M. I. Giannotti and F. Sanz, in *in Atomic Force Microscopy in Liquid*, Wiley-VCH Verlag GmbH & Co. KGaA, 2012, pp.259-284.
20 C. Suárez-Germà, M. T. Montero, J. Ignés-Mullol, J. Hernández-Borrell and Ò. Domènech, *J. Phys. Chem. B*, 2011, **115**, 12778.
21 K. Harlos and H. Eibl, *Biochemistry*, 1980, **19**, 895.
22 B. D. Fleming and K. M. W. Keough, *Can. J. Biochem. Cell Biol.*, 1983, **61**, 882.
23 P. Garidel, C. Johann and A. Blume, *J. Therm. Anal. Calorim.*, 2005, **82**, 447.
24 P. Garidel, C. Johann, L. Mennicke and A. Blume, *Eur. Biophy. J.*, 1997, **26**, 447.
25 H. M. Seeger, G. Marino, A. Alessandrini and P. Facci, *Biophys. J.*, 2009, **97**, 1067.
26 L. Picas, C. Suárez-Germà, M. T. Montero and J. Hernández-Borrell, *J. Phys. Chem. B*, 2010, **114**, 3543.
27 B. Seantier and B. Kasemo, *Langmuir*, 2009, **25**, 5767.
28 S. Garcia-Manyes, G. Oncins and F. Sanz, *Biophys. J.*, 2005, **89**, 1812.
29 N. Hain, M. Gallego and I. Reviakine, *Langmuir*, 2013, **29**, 2282.
30 L. Picas, M. T. Montero, A. Morros, M. E. Cabañas, B. Seantier, P. E. Milhiet and J. Hernández-Borrell, *J. Phys. Chem. B*, 2009, **113**, 4648.
31 S. Ishii and M. J. Sadowsky, *Microbes Environ.*, 2008, **23**, 101.
32 S. Garcia-Manyes, G. Oncins and F. Sanz, *Biophys. J.*, 2005, **89**, 4261.
33 D. Keller, N. B. Larsen, I. M. Müller and O. G. Mouritsen, *Phys. Rev. Lett.*, 2005, **94**, 025701.
34 S. Garcia-Manyes, G. Oncins and F. Sanz, *Biophys. J.*, 2005, **89**, 1812.
35 S. J. Attwood, Y. Choi and Z. Leonenko, *Int. J. Mol. Sci.*, 2013, **14**, 3514.
36 F. Tokumasu, A. J. Jin, G. W. Feigenson and J. A. Dvorak, *Ultramicroscopy*, 2003, **97**, 217.
37 M. Giocondi, L. Pacheco, P. E. Milhiet and C. Le Grimellec, *Ultramicroscopy*, 2001, **86**, 151.
38 J. Yang and J. Appleyard, *J. Phy.s Chem. B*, 2000, **104**, 8097.
39 S. Mabrey and J. M. Sturtevant, *Proc. Natl. Acad. Sci. U.S.A.*, 1976, **73**, 3862.
40 H. Yokoyama, K. Ikeda, M. Wakabayashi, Y. Ishihama and M. Nakano, *Langmuir*, 2013, **29**, 857.
41 R. B. Gennis, *Biomembranes: Structure and Function*, Springer-Verlag New York, New York, 1989.
42 S. Tokutomi, R. Lew and S. Ohnishi, *Biochim. Biophys. Acta*, 1981, **643**, 276.
43 U. R. Pedersen, C. Leidy, P. Westh and G. H. Peters, *Biochim. Biophys. Acta*, 2006, **1758**, 573.
44 S. Garcia-Manyes and F. Sanz, *Biochim. Biophys. Acta*, 2010, **1798**, 741.
45 A. Alessandrini and P. Facci, *Micron*, 2012, **43**, 1212.
46 Y. Dufrêne F., T. Boland, J. Schneider W., W. Barger R. and G. Lee U., *Faraday Discuss.*, 1999, **111**, 79.
47 E. Drolle, R. Gaikwad and Z. Leonenko, *Biophys. J.*, 2012, **103**, L27.
48 L. Redondo-Morata, M. I. Giannotti and F. Sanz, *Langmuir*, 2012, **28**, 12851.
49 A. Alessandrini, H. M. Seeger, A. Di Cerbo, T. Caramaschi and P. Facci, *Soft Matter*, 2011, **7**, 7054.
50 G. Francius, Ò. Domènech, M. P. Mingeot-Leclercq and Y. Dufrene, *J. Bacteriol.*, 2008, **190**, 7904.
51 S. E. Cross, Y. Jin, J. Rao and J. K. Gimzewski, *Nat. Nanotechnol*, 2007, **2**, 780.
52 Y. F. Dufrene, *Nat. Rev. Micro.*, 2008, **6**, 674.
53 A. J. García-Sáez, S. Chiantia, J. Salgado and P. Schwille, *Biophys. J.*, 2007, **93**, 103.
54 H. Butt and V. Franz, *Phys. Rev. E.*, 2002, **66**, 031601.
55 V. Franz, S. Loi, H. Müller, E. Bamberg and H. Butt, *Colloids Surf. B*, 2002, **23**, 191.
56 R. M. A. Sullan, J. K. Li and S. Zou, *Langmuir*, 2009, **25**, 7471.

57 Z. Leonenko, E. Finot and D. Cramb, in , ed. ed. A. Dopico, Humana Press, 2007, pp.601-609.
58 A. Trunfio-Sfarghiu, Y. Berthier, M. Meurisse and J. Rieu, *Langmuir*, 2008, **24**, 8765.
59 J. Israelachvili, *Electrostatic Forces Between Surfaces in Liquid*, Academic Press, London, 2002.
60 S. Loi, G. Sun, V. Franz and H. Butt, *Phys. Rev. E*, 2002, **66**, 031602.
61 S. Ollila, M. T. Hyvönen and I. Vattulainen, *J. Phys. Chem. B*, 2007, **111**, 3139.
62 S. M. Bezrukov, *Curr.Opin. Colloid Int.*, 2000, **5**, 237.
63 T. J. Denich, L. A. Beaudette, H. Lee and J. T. Trevors, *J. Microbiol. Meth.*, 2003, **52**, 149.
64 M. Sinensky, *Proc. Natl. Acad. Sci. U.S.A.*, 1974, **71**, 522.
65 D. Schmidt, Q. Jiang and R. MacKinnon, *Nature*, 2006, **444**, 775.
66 M. Weingarth, A. Prokofyev, d. C. van, D. Nand, A. M. J. J. Bonvin, O. Pongs and M. Baldus, *J. Am. Chem. Soc.*, 2013, **135**, 3983.
67 P. Milhiet, F. Gubellini, A. Berquand, P. Dosset, J. Rigaud, C. Le Grimellec and D. Lévy, *Biophys. J.*, 2006, **91**, 3268.

Supporting information I

Materials and Methods

1-palmitoyl-2-oleoyl-*sn*-glycero-3-phosphoethanolamine (POPE) and 1-palmitoyl-2-oleoyl-*sn*-glycero-3-phospho-(1'-*rac*-glycerol) (POPG) specified as 99% pure were purchased from Avanti Polar Lipids (Alabaster, AL, USA). Chloroform and methanol, HPLC grade, and all other commons were purchased from Sigma (St. Louis, MO, USA).

Liposome preparation. Liposomes of POPE:POPG with different molar fractions of POPG were prepared as described elsewhere.[1] Briefly, chloroform-methanol (2:1, v:v) solutions containing the appropriate amounts of each lipid were placed in a conical tube and dried completely under a N_2 stream. The resulting thin film was kept protected from the light and under high vacuum overnight to prevent any trace of organic solvents. Multilamellar vesicles (MLVs) were obtained after hydration of the film with a buffer containing 20 mM Hepes, 150 mM NaCl and 10 mM $CaCl_2$, pH 7.40, applying cycles of freezing and thawing below and above the transition temperature of the phospholipids. Large unilamellar vesicles (LUVs) were obtained by extrusion (Mini-extruder, Avanti Polar Lipids, Alabaster, AL) of the MLVs through filters (Whatman Nederland B.V., Netherlands) with 100 nm of pore diameter. Liposome size and the polydispersity index were measured with a Zetasizer Nano S (Malvern Instruments Ltd., Worcestershire, UK). Electrophoretic mobility to assess the effective surface electrical charge of each lipid composition was determined on MLVs with a Zetasizer Nano ZS90 (Malvern Instruments, UK). Every configuration was determined in triplicate and three measurements per sample were performed.

Differential scanning calorimetry (DSC). DSC experiments were carried out as described elsewhere.[2] Briefly, MLVs used for DSC studies were prepared by redispersion in buffer of the thin film deposited after evaporation of appropriate volumes of stock solutions of POPE and POPG in chloroform. DSC analyses used a MicroCal MC-2 calorimeter and the data obtained were analyzed by the original calorimeter software. Transition temperature (T_m) was taken as the temperature of maximum excess specific heat and was measured to the nearest 0.5 °C. The calorimetric accuracy for T_m and for enthalpy changes was ± 0.1 °C and ± 0.2 kcal·mol^{-1}, respectively. Each sample was scanned in triplicate over the temperature range 5-80 °C at a scan rate of 0.44 °C·min^{-1}.

The phase diagram was constructed from excess heat capacity *vs* temperature curves obtained by DSC. T_{onset} and T_{offset} of the main phase transition were determined as those temperatures corresponding to the intersection between the tangent of the leading edge and the baseline of the thermograms. These temperatures were then corrected by the finite width of the transitions of the pure components weighted with their mole fractions. By connecting the different T_{onset} and T_{offset}, respectively, the *solidus* and *liquidus* curves were defined.

Atomic Force Microscopy Imaging. Atomic Force Microscopy was carried out on a commercial Multimode AFM controlled by Nanoscope V electronics (Bruker AXS Corporation, Madison, WI). MSNL-10 sharpened silicon nitride cantilevers (Bruker AFM Probes, Camarillo, CA) were used with a mean cantilever spring constant of 30 pN·nm^{-1}.

Temperature-controlled experiments were carried out with a Thermal Applications Controller (TAC) (Bruker AXS Corporation, Madison, WI). Temperature deviation between the sample and the TAC was calibrated and controlled with a Dual Type JKTE thermocouple thermometer (Cole Parmer, Vernon Hills, IL), ensuring the real temperature of the sample.

Freshly cleaved mica discs (1 cm^2) mounted on round Teflon discs were glued to steel discs. Liposome suspensions were incubated on mica discs for two hours over the transition temperature of the mixture used. To prevent sample

evaporation, the steel disc containing the mica and the sample was enclosed in a small Petri dish inside a bigger Petri dish with some water at the bottom used as a reservoir. The big Petri dish was then sealed with Teflon ribbon and placed inside an oven (Termaks AS, Bergen, Norway) with temperature control of ± 0.2 °C from the desired temperature.

After incubation, non-adsorbed liposomes were removed by gently rinsing samples with buffer. Samples were then directly mounted on the AFM scanner and allowed to stabilize. When working above room temperature, an o-ring was then incorporated with the aim of enclosing and sealing the sample, in order to avoid further buffer evaporation during experiments. AFM was equipped with an "E" scanner (10 μm) and images were acquired in liquid and under intermittent contact mode at 0° scan angle with a scan rate of 1.5 Hz. The vertical force was maintained at the minimum value, maximizing the amplitude set point value while keeping the vibration amplitude as low as possible. All images were processed by a NanoScope Analysis Software (Bruker AXS Corporation, Santa Barbara, CA).

Force Spectroscopy. Force spectroscopy measurements were performed at a constant velocity of 0.5 $\mu m \cdot s^{-1}$. MSNL cantilevers used in the experiments had a nominal spring constant of 30 $pN \cdot nm^{-1}$. Individual spring constants of the different cantilevers used were determined by the equipartition theorem.[3]

References

1 C. Suárez-Germà; M.T. Montero; J. Ignés-Mullol; J. Hernández-Borrell and Ò- Domènech, *J. Phys. Chem. B*, 2011, **115**, 12778.

2 Ò. Domènech; A. Morros; M.E. Cabañas; M.T. Montero and J. Hernández-Borrell, *Ultramicroscopy*, 2007, **107**, 943.

3 L. Picas; P.E. Milhiet and J. Hernández-Borrell, *Chem. Phys. Lipids*, 2012, **165**, 845.

Supporting information II

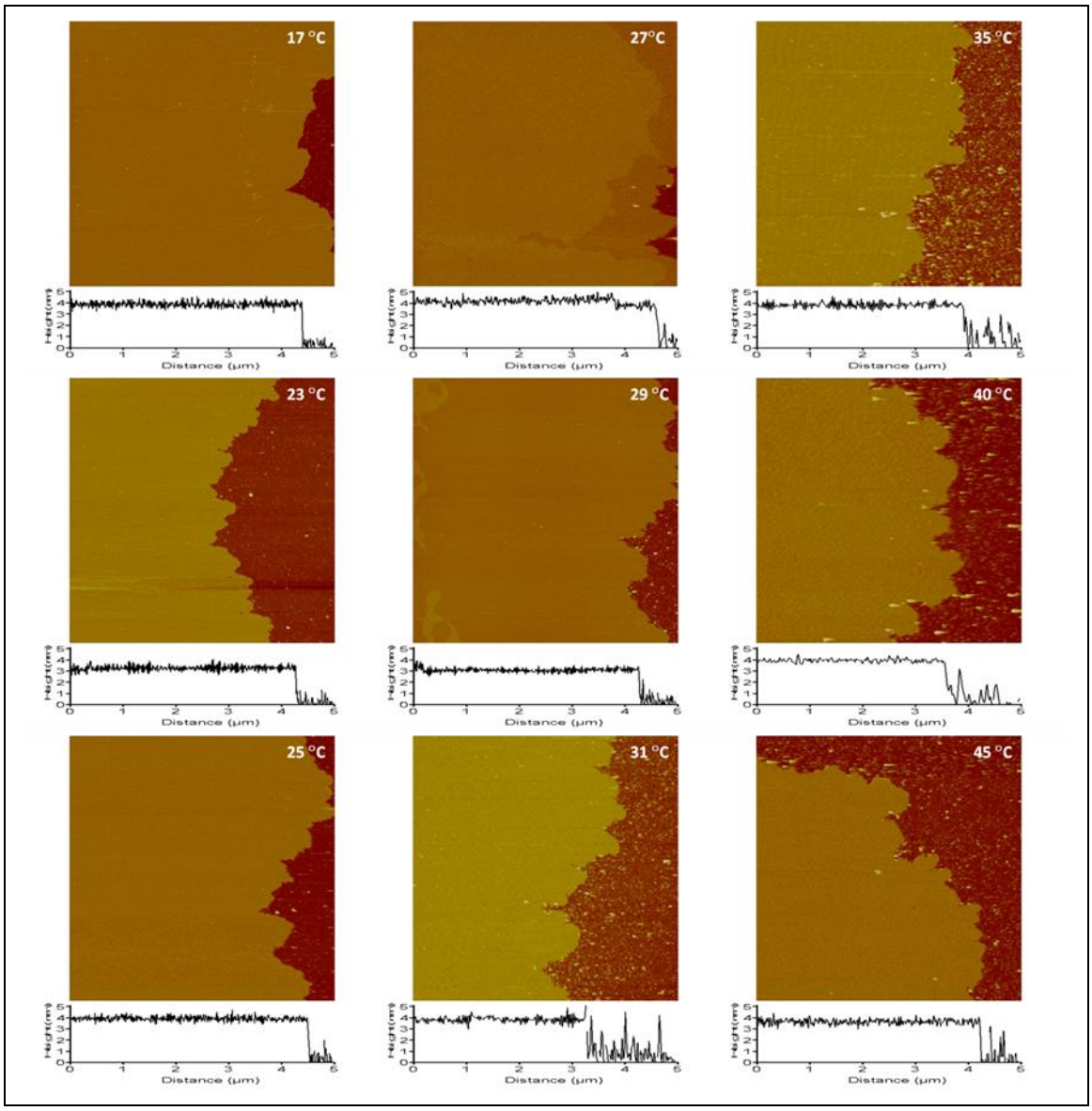

Figure SII1. Ramp temperature of POPE:POPG SLB with χ_{POPG} =0.25 to construct the pseudo-binary phase diagram. AFM topographic images for POPE:POPG SLB with χ_{POPG} = 0.25 from 17ºC to 45ºC. Bottom profile shows a representative height profile from the corresponding image.

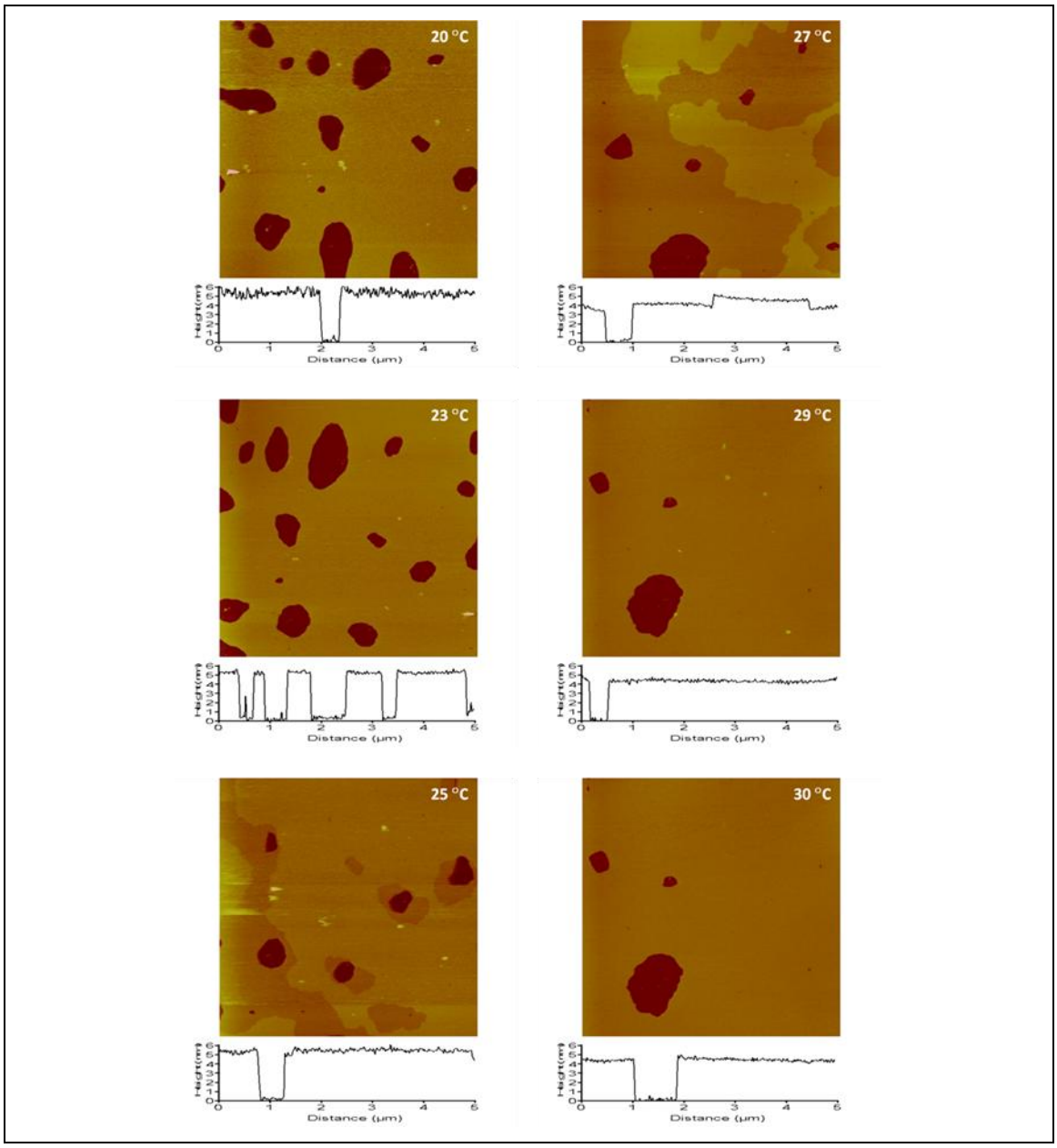

Figure SII2. Ramp temperature of POPE:POPG SLB with χ_{POPG} = 0.50 to construct the pseudo-binary phase diagram. AFM topographic images for POPE:POPG SLB with χ_{POPG} = 0.50 from 20ºC to 30ºC. Bottom profile shows a representative height profile from the corresponding image.

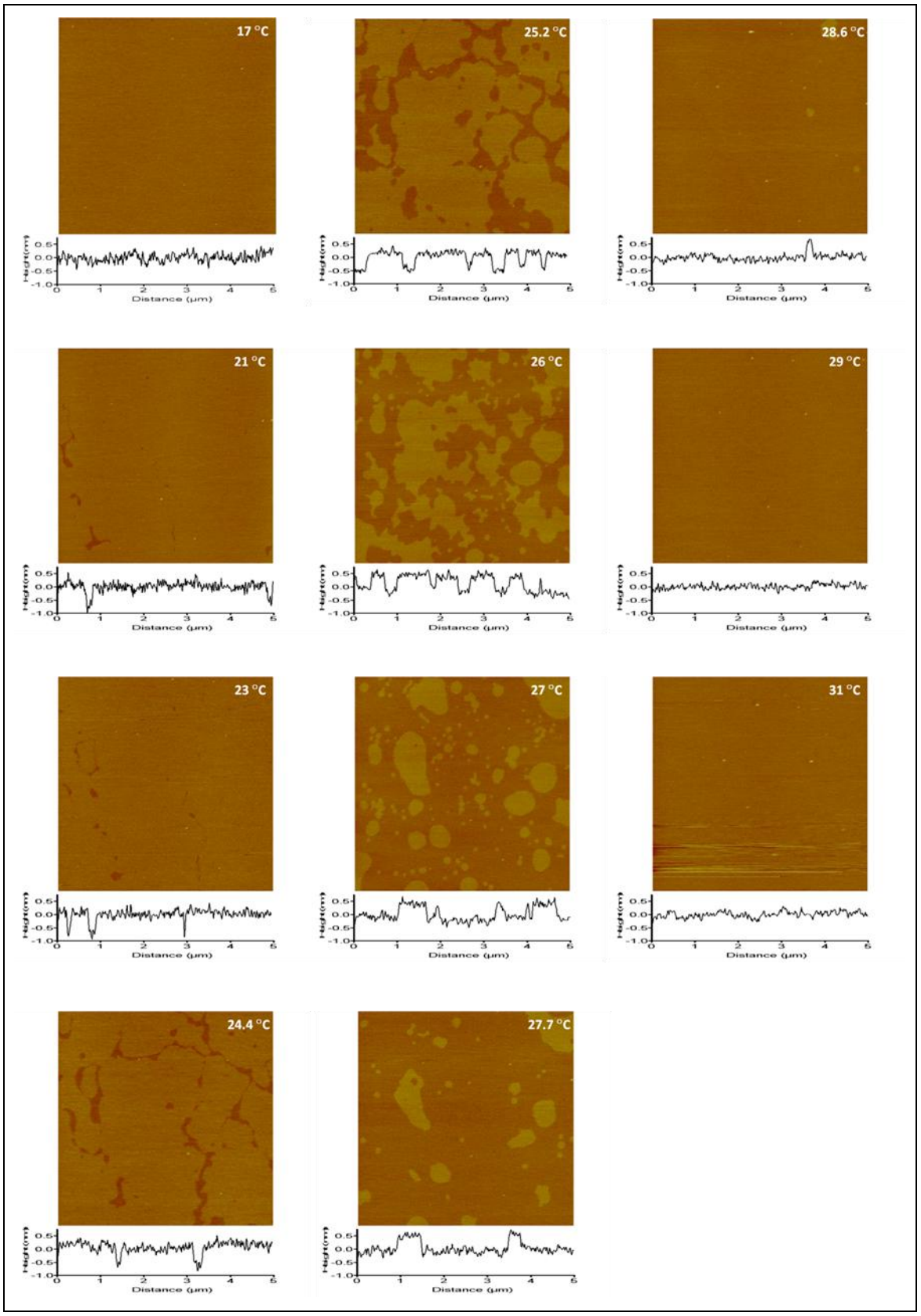

Figure SII3. Ramp temperature of POPE:POPG SLB with χ_{POPG} = 0.75 to construct the pseudo-binary phase diagram. AFM topographic images for POPE:POPG SLB with χ_{POPG} = 0.75 from 17ºC to 31ºC. Bottom profile shows a representative height profile from the corresponding image.

			χ_{POPG}		
		Domain	0.25	0.50	0.75
23 ºC	h (nm)	L_β	3.4 ± 0.3	5.4 ± 0.2	5.63 ± 0.11
		L_α	-	-	-
	Ra (nm)	L_β	0.2	0.11	0.11
		L_α	-	-	-
27 ºC	h (nm)	L_β	3.06 ± 0.12	5.0 ± 0.2	5.60 ± 0.11
		L_α	2.7 ± 0.3	3.9 ± 0.4	5.0 ± 0.2
	Ra (nm)	L_β	0.20	0.11	0.08
		L_α	0.19	0.11	0.08
29 ºC	h (nm)	L_β	-	-	-
		L_α	2.5 ± 0.3	4.5 ± 0.2	5.0 ± 0.2
	Ra (nm)	L_β	-	-	-
		L_α	0.14	0.13	0.13

Figure SII4. Summary of height and roughness values from the topographic images showed in Figure 3. The height values of all SLBs decrease with the increase of the temperature whilst SLBs with higher POPG mole fractions present higher height values, which could indicate the presence of electrostatic repulsion forces between the tip and the top of the SLB.

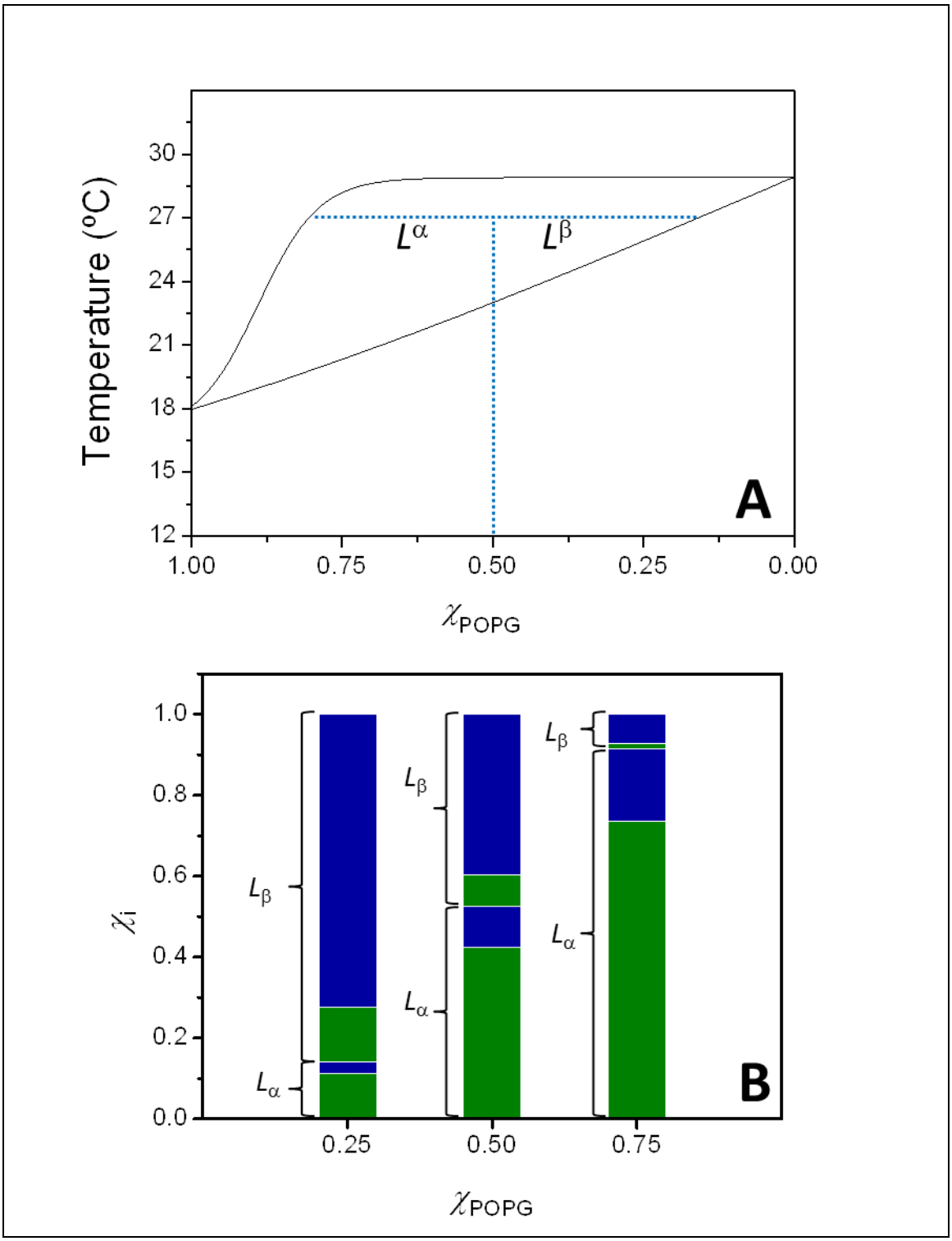

Figure SII5. Measuring the ratio of each lipid in each phase. A) Representative procedure to calculate the proportion of L_{α} and L_{β} at the desired molar fraction applying the lever rule B) For each POPG molar fraction the proportion of POPE and POPG in each phase (L_{α} or L_{β}) was calculated. From all the χ_{POPG} studied it can be seen an enrichment of POPG in the L_{α} phase while in the L_{β} phase this enrichment is in POPE.

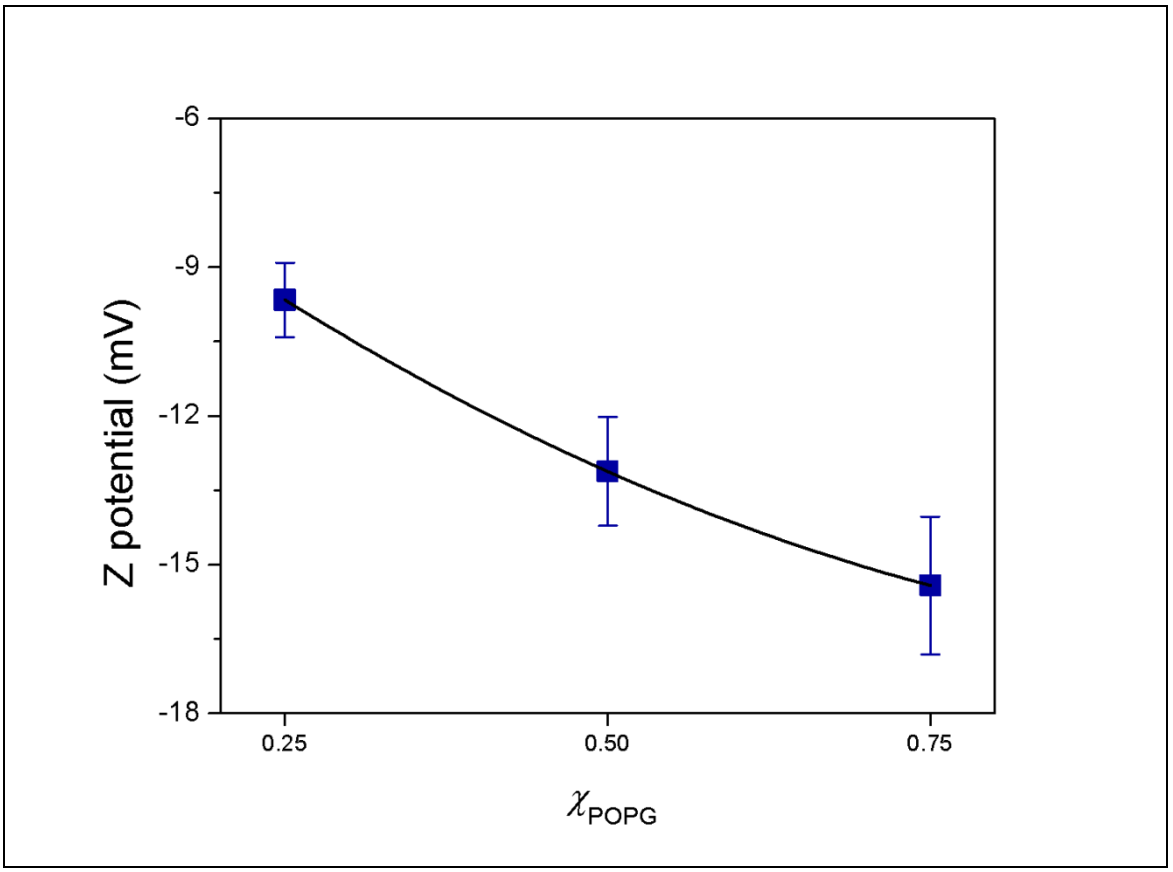

Figure SII6. Zeta potential measures corroborating the negative charge displayed by the SLBs. Zeta potential as a function of the POPG mole fraction at 23ºC. Liposomes in the buffer used (Hepes 20 mM, NaCl 150 mM, pH 7.40, $CaCl_2$ 10 mM) presented negative zeta potential values. The graphic indicates an increasing of the negative charge borne by the lipids in the SLB as the POPG mole fraction increases too.

Chapter 4. Characterization of the LacY-phospholipid interaction

4.1 The system of interest

4.1.1 Lipid matrices

The lipid matrices used in the study of LacY-phospholipid interactions are similar to those described in Chapter 3. The only difference is the use of phosphatidylcholine (PC) phospholipids in order to study the LacY differential headgroup selectivity. Hence, only PC species will be introduced in this section.

4.1.1.1 PC

PC (Figure 21) is a lipid headgroup which give rise to zwitterionic phospholipids. PC phospholipids present higher cross sectional area than PE ones (the choline methylated group is larger than the ammonium group), which results in a cylindrical molecular shape and a tendency to the lamellar packing. Due to the lack of hydrogen bond donors in its structure, PC headgroup cannot perform intermolecular hydrogen bonding. This restrains the intermolecular bonding to weak interactions with negatively charged

phosphate or to carbonyl groups of adjacent PC molecules by forming charge pairs [84,199].

PCs are the most abundant lipids in animal cell membranes, where they are commonly found in the exoplasmic or outer leaflet. However, they are absent in the membranes of most bacteria, including *E. coli*.

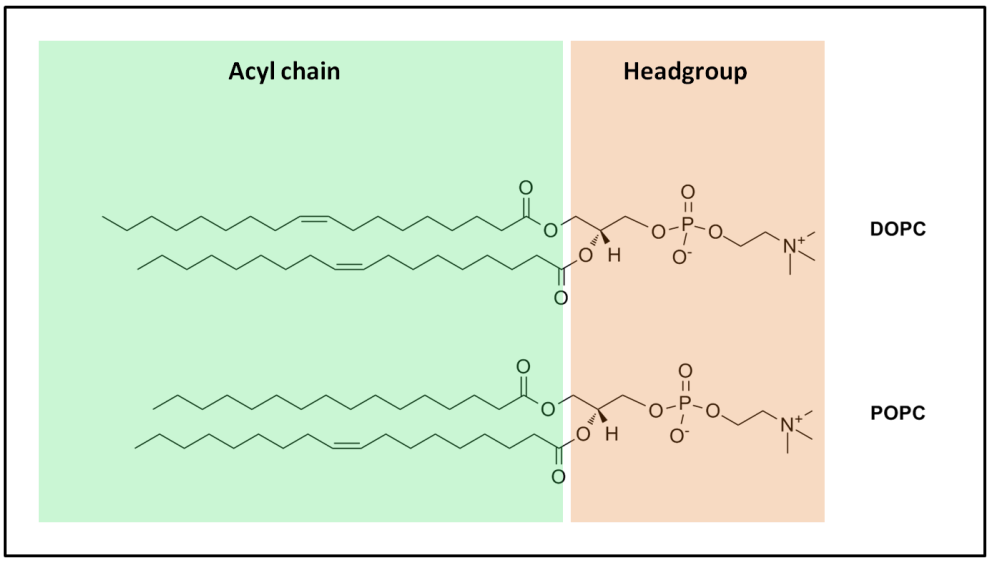

Figure 21. Molecular structures of DOPC and POPC. The common PC headgroup is evidenced on the right part of the structures. Acyl chains varying its degree of unsaturation can be observed on the left.

- **POPC:** 1-palmitoyl-2-oleoyl-*sn*-glycero-3-phosphocholine (see structure in Figure 21) is a heteroacid phospholipid formed by a PC headgroup and two different fatty acyl chains. One of them, palmitoyl, in position *sn*-1 relative to the glycerol, has 16 carbon atoms and is completely saturated. Conversely, oleoyl, in position *sn*-2, is formed by an 18 carbon atoms chain and presents a *cis* unsaturation at the carbon 9.
- **DOPC:** 1,2-dioleoyl-*sn*-glycero-3-phosphocholine (see structure in Figure 21) is a homoacid phospholipid formed by a PC headgroup and two identical acyl chains. Both acyl chains are oleoyl structures with 18 carbon atoms and a *cis* unsaturation at the carbon 9 as shown for POPC.

4.1.2 LacY

The LacY mutant mainly used in this thesis was obtained after the transformation in *E. coli* cells of plasmid pCS19 encoding single-W151/C154G LacY kindly donated by Dr. H. Ronald Kaback from UCLA. Additionally, single-151W/C154G/D68C LacY mutant (see mutated sites in Figure 22) was obtained using the Quickchange Site-Directed Mutagenesis Kit (Stratagene, La Jolla, CA) in *E. coli* cells containing the aforementioned plasmid. The resultant plasmid pCS19 encoding single-W151/C154G/D68C LacY construct was confirmed by DNA sequencing. The purification of both LacY mutants was achieved as described in sections from 4.3.1 to 4.3.4.

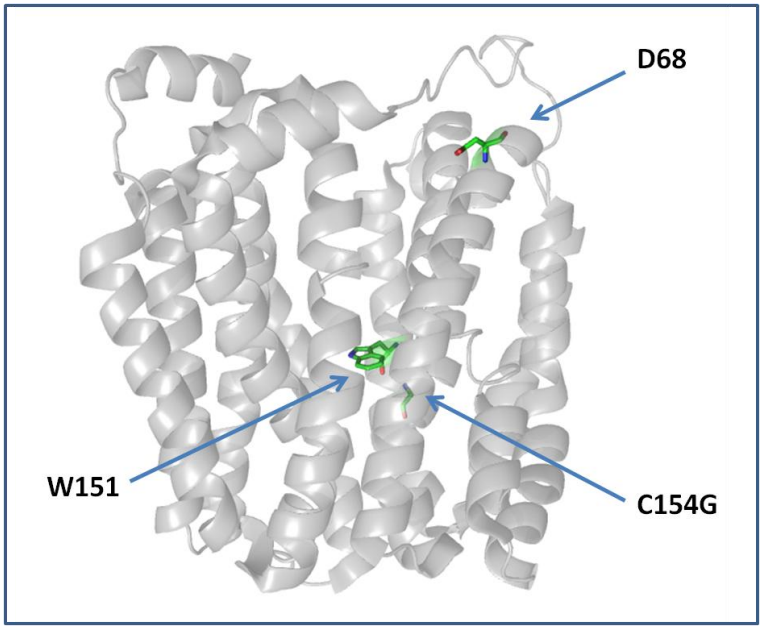

Figure 22. Location of D68 (helix II), W151 and C154G (both at helix V) in a X-ray structure of LacY C154G. Based on PDB ID: 1PV6.

4.1.2.1 Single-W151 LacY mutant

Tryptophan in position 151 (W151) (Figure 22) is one of the important but not irreplaceable amino acids in LacY [108]. It is located in helix V close to R144, in a hydrophilic environment [200]. Upon sugar binding, W151 becomes less exposed to aqueous solvent and a direct stacking interaction between the galactopyranosyl and the indole rings has been described from fluorescence experiments [200,201] and X-ray

data [112]. This hydrophobic interaction is likely to orient the sugar ring so that hydrogen bonds can be formed with side chains of the protein [108]. From all these evidences, W151 is thought to be important in substrate binding and specificity [200]. In addition, W151 forms a hydrogen bond with E269, a key residue that plays a dual role in substrate binding and proton coupling [108,201].

Single-W151 LacY was obtained by replacing the other five tryptophans with tyrosine residues [200] in a mutant that also contained a C154G mutation (described in the following section). The mutant was first designed to take advantage of the fluorescent properties of W to further investigate the role of the position 151 [200,201]. However, due to the unique characteristics of this position regarding emplacement (approximately in the middle of the molecule) and function (it becomes inaccessible when substrate is present), single-W151 mutant has also been exploited to explore entire LacY characteristics [131–133,202].

4.1.2.2 C154G LacY mutant

LacY C154G mutant (see Figure 22), firstly described by Smirnova et al. [203] is a conformationally restricted mutant of the protein. Working with this mutant represents two main advantages as compared to the wild type: it shows good thermostability and exhibits little tendency to aggregate in detergent [203]. Particular benefit was taken from this enhanced protein stability when this mutant was used to obtain the first X-ray crystal of LacY [112]. However, C154G mutation in LacY provokes secondary changes in the protein functioning.

In fact, C154G LacY mutant binds sugar as well as the wild-type but exhibits little or no transport activity [203]. In wild-type, sugar binding induces closing of the cytoplasmic cavity with opening of a hydrophilic clef on the periplasmic side, which is the key for the sugar transport across the membrane. Conversely, although the severely restricted C154G undergoes closing of the cytoplasmic cavity after ligand binding, the periplasmic cleft appears to be paralyzed in an open state [204]. The mechanism leading to this trapped conformation seems to be a tighter packing in helix V due to the presence of glycine which hinders the helix movement needed for the structural transition [120].

In any case, this mutant has been largely employed to study LacY [69,83,128,200,205,206] and, despite its lack of transport activity, it is normally assumed that its structure is indistinguishable from the global structure of the wild-type protein.

4.1.2.3 D68C LacY mutant

Aspartic acid in position 68 (D68) is a well conserved residue in the MFS family which is thought to be part of the motif GXXXD(R/K)XGR(R/K) in the first intracellular loop linking helices II and III [207,208]. This motif has been shown to play an important role in transport by mutational analysis [207–209]. In addition, in MFS proteins such as LmrP it has been postulated that D68 position can establish a hydrogen bond with a surrounding phospholipid DOPE (and single- and double-methylated DOPE, but not DOPC), which might be important for the protein for the proper sensing of the proton gradient. Thus, substrate binding and transport are lost in LmrP D68X mutants [210].

In the specific case of LacY, X-ray data showed that although the motif is conserved, D68 is not placed in the II/III loop, but at the cytoplasmic end of helix II and within bonding distance of K131 at the end of helix IV (Figure 22) [211]. D68 role is anyway important in this emplacement, since different D68 and K131 mutants have been analyzed and all the tested replacements for D68 are inactive while K131 is more permissive [211]. However, second-site suppressor mutations can recover the protein activity indicating that this carboxyl side chain is not absolutely required for symport.

D68X mutants bind substrate normally but present a loss of transport activity likely caused by the decreased probability of opening the hydrophilic pathway on the periplasmic side of LacY upon sugar binding [211]. In fact, it can be explained by the strength of the interaction between D68 and K131. This interaction, although weak, exhibits marked sensitivity to changes in the nature of the side chains. Therefore, it has been postulated that any mutation can strengthen this interaction and inhibit the dynamics of LacY [211].

Furthermore, the possible interaction of this residue with surrounding PEs as it happens with LmrP has also been proposed. As mentioned, in the crystal structure D68 is directed toward the inside of the protein to interact with K131. However, performing

molecular dynamic (MD) simulations and after dynamic stabilization of a system containing LacY embedded in a phospholipid matrix, Lensink et al. [136] described the presence of an important salt bridge between D68, a phospholipid molecule, and K69. It appeared after the rotation of D68 side chain to bind the amine group of the POPE, or the choline group of POPC (although this interaction was weaker), but no binding was present in the case of POPG. From these studies, D68 was identified as the most relevant PE-interacting residue. Strikingly, Andersson et al. [83] also studied phospholipid-LacY interactions using MD simulations techniques and although eight residues were identified as the most lipid-interacting amino acids, none of them turned out to be D68. Hence, although the importance of this position regarding crucial conformational changes seems clear for LacY, the possible link between D68 with the phospholipid environment reminds a subject for further study.

4.1.3 LacY-phospholipid systems

In order to analyse protein-lipid interactions, two different LacY-phospholipid systems have been used (i) the formation of proteoliposomes to be analysed by fluorescence techniques, and (ii) the formation of SLBs to be analysed using AFM.

4.1.3.1 Proteoliposomes

Proteoliposomes are liposomes with one or more different membrane proteins inserted within the bilayer in a specific lipid-to-protein ratio (LPR). They have been obtained following methods largely studied and developed by Rigaud et al. [212,213] which involve removing the detergent from a micellar solution containing the purified protein and a suitable combination of lipids. Although other techniques for membrane protein reconstitution into liposomes are available (organic solvent-mediated-reconstitution, mechanical means including sonication or French-press...), detergent-mediated reconstitution is the most used strategy, since most membrane proteins need detergents to be extracted, purified and solubilised without losing their tertiary structure and activity [214].

Hence, the procedure to obtain proteoliposomes involves initial protein-detergent and lipid-detergent solutions which are combined to obtain a lipid-protein-detergent micellar

solution. Then, detergent is gradually eliminated. This removal results in the progressive formation of closed lipid bilayers in which the proteins eventually incorporate to finally form proteoliposomes [213].

There also exist various methods for detergent removal, namely dialysis, gel chromatography, dilution and hydrophobic adsorption onto polystyrene beads. Here, the latter detergent depletion technique was chosen. It is based on the use of macroporous divinyl benzene cross-linked polystyrene non-polar beads (Bio-beads SM2®) with a high surface area for adsorbing organic materials from an aqueous solution, which is done through hydrophobic bonding. Bio-beads SM2® are mainly used in a batch procedure, taking advantage of their preferential affinity for detergents over phospholipids and proteins [214]. Complete detergent removal and minimization of protein and phospholipid loses can be carefully controlled depending on the biobead-to-detergent ratio and the time of contact of the biobeads with the micellar system [213].

Since the very first time LacY was reconstituted into proteoliposomes in a fully functional state [152], this technique has been extensively used in the literature, either at high LPRs as a strategy to obtain 2D crystallization and thus structural information of the protein [215,216] or at lower protein densities in order to perform other experiments related to functionality and lipid-protein interaction [131,140].

4.1.3.2 SLBs with reconstituted membrane proteins

Another strategy to study lipid-protein interactions is the AFM analysis of proteolipid sheets (PLSs), i.e. supported lipid SLBs with reconstituted membrane proteins. There exist numerous ways to prepare these systems being the more used the Langmuir-Blodgett/Schaefer approach, the *in situ* incorporation of proteins in already preformed SLBs, and the vesicle fusion technique [93].

The Langmuir-Blodgett/Schaefer approach, although technically challenging, has been successfully used to obtain 2D crystals of membrane proteins in what is known as the lipid-layer approach [217]. Regarding the *in situ* incorporation, it is a quite straightforward technique developed by Milhiet's group [218], which is very suitable to obtain domains with high protein concentration. It is achieved from purified membrane proteins that are directly incorporated into SLBs previously destabilised by detergents.

Finally, the vesicle fusion technique is the selected approach in this thesis. It permits the extension of native mixtures of lipids and proteins coming from membrane extractions [219] as well as the extension of proteoliposomes obtained from purified membrane proteins and selected lipid compositions [34,216]. The main parameters controlling the process of extension of the proteoliposomes are the density of proteins (highly crowded vesicles leads to protein aggregation or to vesicles too small for AFM studies), the size of the vesicles, the lipid composition, the time and temperature of deposition and the nature of the support.

4.2 Techniques to characterize the system

4.2.1 FRET fluorescence

Förster resonance energy transfer (FRET) is a photophysical process named after Theodor Förster, the scientific who revealed the theoretical basis for nonradioactive energy transfer [220]. Curiously, he was partly motivated by his familiarity with photosynthetic systems, which are one of the most fascinating examples of FRET in nature.

FRET is radiationless and can occur in the excited state under some specific conditions (Figure 23). The process implies the transmission of an energy quantum from its site of absorption, an initially excited fluorophore that is called the donor (D), to the site of its utilization in a molecule called the acceptor (A). The D typically emits at shorter wavelengths than the A and the electronic emission spectrum overlaps with the excitation spectrum of the A, which can be a non-fluorescent molecule. The FRET process occurs without an intermediate photon from D to A. Instead, both molecules are coupled by long-range dipole-dipole interactions which are the responsible of the energy transfer. In addition, it occurs without conversion to thermal energy and without the D and A coming into a kinetic collision [162,221].

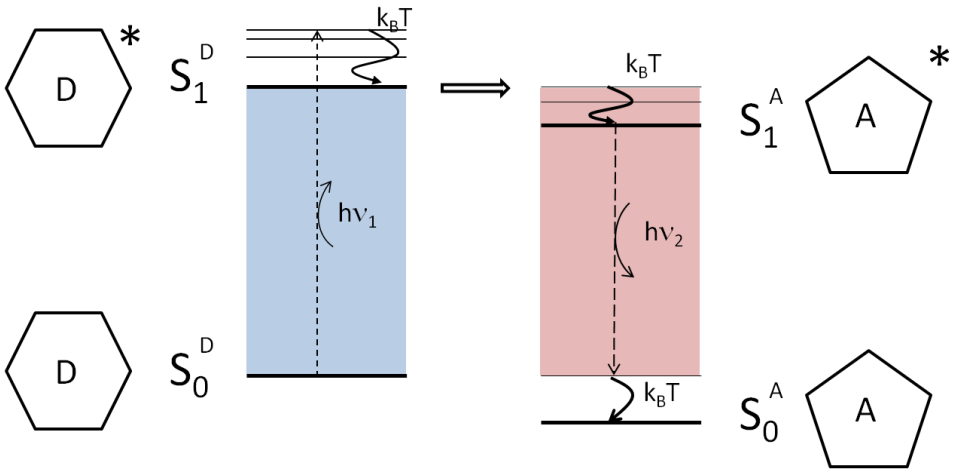

Figure 23. Schema depicting the Förster resonance energy transfer (FRET) process through the energetic levels of two molecules, the donor (D) and the acceptor (A), which present the requirements to act as FRET pairs.

Therefore, FRET is one of the numerous ways that an excited fluorophore can undergo to lose its excitation energy. It can be represented as follows

$$D + A + h\nu_E \rightarrow D^* + A \overset{k_T}{\rightarrow} D + A^*$$

where k_T is the rate of energy transfer [221]. The appearance of the energy transfer as well as its rate depends upon the extent of spectral overlap of the emission spectrum of the D with the excitation spectrum of the A, the quantum yield of the D, the relative orientation of the D and A transition dipoles, and the D-A distance. More important, distances where the energy transfer occurs are in the scale of biological macromolecules. Indeed, the distance at which FRET is 50% efficient, called the Förster distance, is typically in the range of 0.5-10 nm and comparable to the diameter of many proteins, the thickness of biological membranes and the distance between sites on multisubunit proteins. Additionally, the process takes place mostly independent of the intervening solvent and/or macromolecule [162,220].

The most readily accessible measure of FRET is the transfer efficiency, *E*, which can be obtained using the relative fluorescence intensity of the donor, in the absence (I_D) and presence (I_{DA}) of acceptor,

$$E = 1 - \frac{I_{DA}}{I_D} = 1 - \frac{\int_0^\infty i_{DA}(t)dt}{\int_0^\infty i_D(t)dt}$$

This equation is only applicable to D-A pairs which are separated by a fixed distance. However, a single fixed donor-acceptor distance is not found for mixtures of donors and acceptors in solution, nor for donors and acceptors dispersed randomly in membranes. More complex expressions are required in these cases [162,222].

For all these characteristics, FRET has been widely used as a "spectroscopic ruler" for measurements in biological systems, taking advantage of its capability to detect distances between molecules which are either close one to another or moving relative to each other in the nanometric range. As a result, FRET applications extend from spectroscopic measurements [65,223] to imaging experiments in the fluorescence microscope [224,225] and single molecule experiments [226]. In membrane science FRET has revealed as a very interesting method to investigate membrane biophysics [227,228], but especially as an excellent tool for the study of protein-lipid interactions [222,229,230].

4.2.1.1 Pyrene labelled phospholipids

Pyrene is a polycyclic aromatic fluorophore (Figure 24). Its most characteristic features are a long excited state lifetime and a concentration-dependent formation of excimers. Excimers, which describe excited pyrene dimmers, are structures arisen from the particular photophysical behaviour of the molecule. Thus, a monomeric excited-state pyrene (monomer, M) can relax radiatively to ground state by emission of photons with a maximum wavelength at $\simeq$ 375 nm, the exact peak energy and spectral fine structure depending on the solvent polarity. During excited lifetime, M can also collide with a ground-state pyrene and form a characteristic temporary complex named excimer (E). This complex relaxes back to two ground-state pyrenes by emitting a photon with a maximum wavelength centred at $\simeq$ 470 nm. The presence of both species, related by the excimer-to-monomer (E/M) ratio mainly depends on the rate of collisions between different pyrene molecules [129,231].

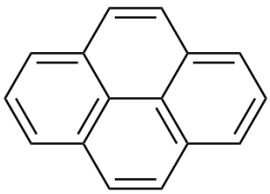

Figure 24. Pyrene structure.

Interestingly, the pyrene molecule can also act as an acceptor in a FRET process. For instance, the pyrene excitation spectrum overlaps extensively with the tryptophan emission spectrum (Figure 25) [231]. In this case, pyrene-tryptophan pairs displays a Förster distance of 2.1 – 2.7 nm [222].

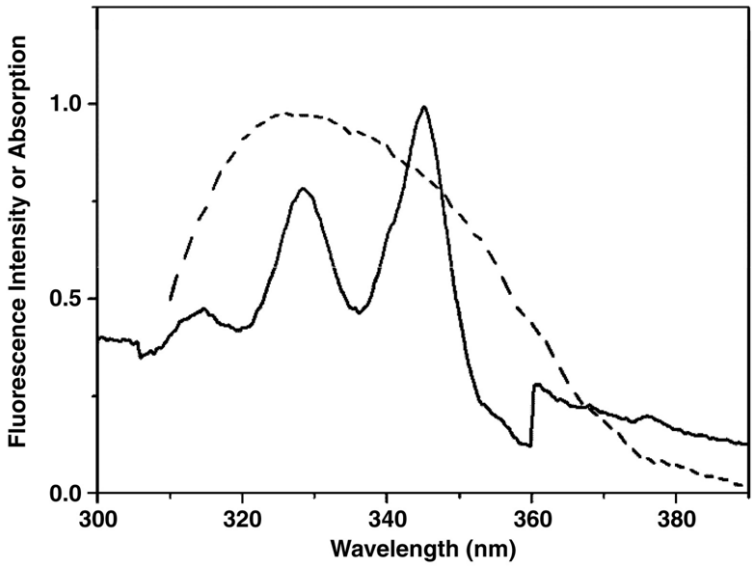

Figure 25. Overlap between the emission spectrum of the LacY mutant single-W151/G154C (dashed line) and the excitation spectrum of proteoliposomes containing PG phospholipids labelled with pyrene at the acyl chain (solid line) *(Figure from Picas et al., 2010* [132]*).*

All those capabilities make pyrene a very interesting molecule for the study of the properties of biomembranes and membrane models [129]. Such studies are normally carried out by employing fluorescent phospholipid analogues that mimic the natural membrane components. Hence, the use of pyrene-labelled phospholipids (Figure 26) offers several advantages [232], since they lead to a system less sterically perturbed thanks to a probe that is an integral part of a system component. In addition, the hydrophobic characteristics of pyrene facilitate the insertion of the labelled-

phospholipid into the membrane. However, some perturbation of the system appears unavoidably and intrinsic to the use of fluorophores [233]. In pyrene-labelled phospholipids the fluorophore is usually attached to the distal end of the acyl chain (Figure 26A), thus replacing one of the lipid fatty acid chains. Alternatively, it can be also attached to the phospholipid headgroup (Figure 26B). However, the use of such derivatives is more delicate since the hydrophobic pyrene moiety in the headgroup might alter the physical properties of the labelled lipid molecule [231].

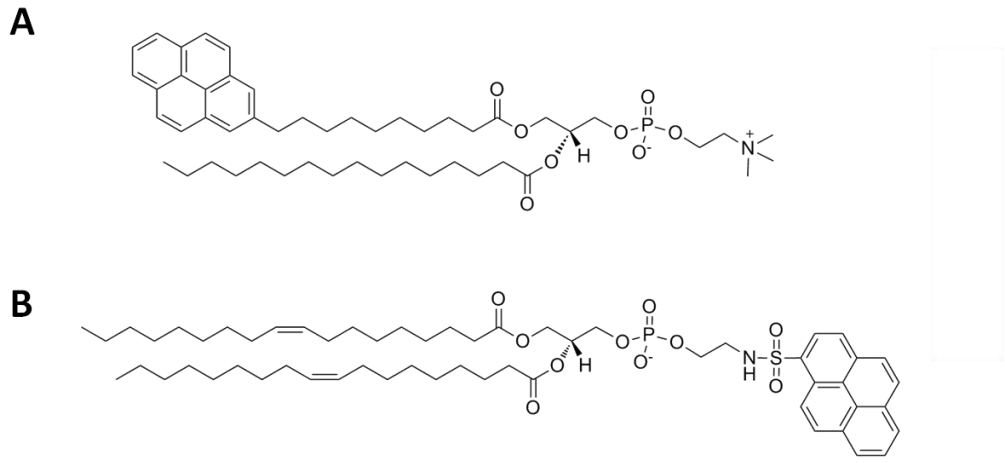

Figure 26. Structure of PE phospholipids labelled with a pyrene at the acyl chain (**A**) and at the headgroup (**B**). They correspond to the fluorophores employed in sections 4.3.1-4.3.3.

When working with pyrene-labelled phospholipids, the obtained E/M ratio, related to the collision rate of pyrene moieties, might reflect the lateral mobility of the analogues, as well as the local concentration of the fluorophore in the membrane [129,231]. Hence, the probe is a suitable and sensitive tool for studying a variety of biophysical phenomena like lateral diffusion, phase behaviour and dynamics of lipids [231,234].

Finally, the possibility of performing FRET between pyrene-labelled phospholipids and tryptophan remains very attractive. Being this amino acid the most important intrinsic fluorophore in proteins, the use of pyrene-labelled phospholipids may support the simultaneous study of (i) the bilayer fluidity and organization through the E/M ratio data (Figure 27A) and/or, (ii) the lipid-protein interactions when the protein of interest contains at least one tryptophan residue in its structure (Figure 27B).

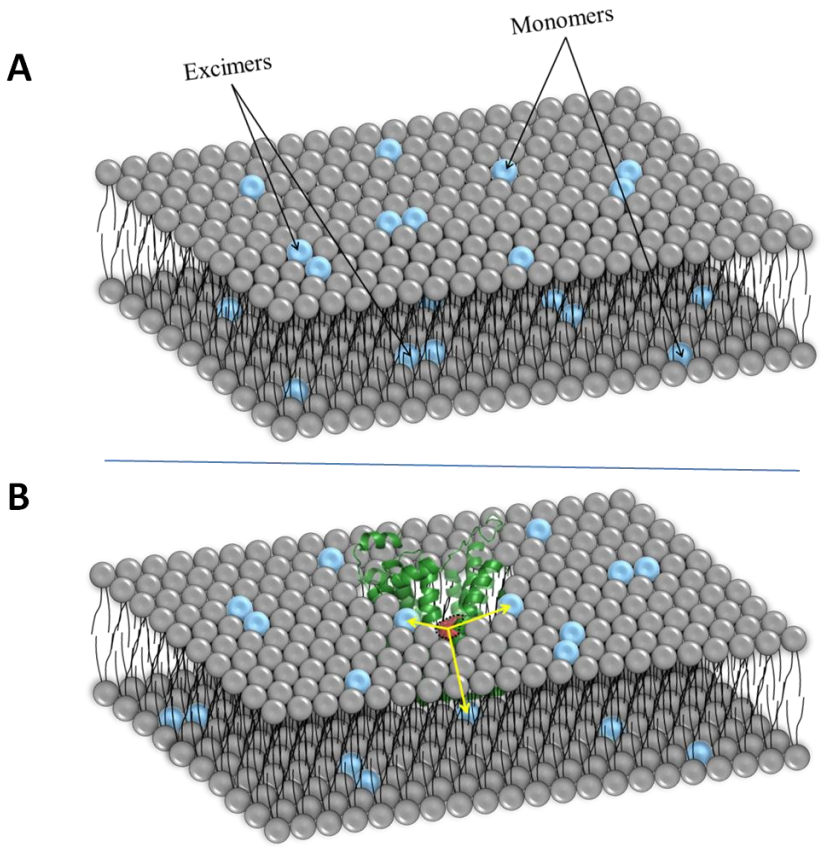

Figure 27. Processes occurring when pyrene-labelled phospholipids are added to a phospholipid bilayer with reconstituted single-tryptophan proteins: formation of pyrene excimers occurring when two pyrene-labelled phospholipids are close one to another (**A**), and FRET energy transfer from the tryptophan (red) to pyrene-labelled phospholipids (blue) placed within Förster distance (**B**).

4.2.2 Atomic force microscopy in lipid-protein systems

AFM is the only microscopy technique that allows the analysis of membrane proteins at subnanometer resolution and under physiological conditions [235]. It enables the imaging of membrane proteins with a powerful performance, reaching even lateral resolutions of ≃0.5 nm and vertical resolutions of ≃0.1 nm [236]. Additionally, the characteristics of membrane proteins naturally immobilised in lipid membrane largely facilitate the use of this SPM technique. With the development of high resolution and high speed AFM, the technique has evolved until achievements such as the direct observation of membrane protein functioning [177,237] or even the track of protein diffusion in the lipid bilayer [238].

In this thesis, conventional AFM has been used to study PLSs. It has been carried out using topography imaging and force spectroscopy (already explained in 3.2.4). Force-volume and molecular unfolding or single-molecule force spectroscopy have also been employed.

Force-volume (FV) imaging is an AFM mode that combines the force measurement with the topographic image. It is performed through the simultaneous measure of topography and interaction forces, which can be obtained by periodically indenting the AFM tip into the sample when scanning its surface features. Therefore, in the FV mode each (x, y) position is associated with a FD curve in z, creating thus a force density map that can be directly correlated to topography.

This technique has been used to examine polymer properties [239] and produce elasticity maps of heterogeneous materials such as biominerals [240], polymer composites [239,241], and living cells [242]. In membrane science FV has been mainly focused on the study of large areas with coexistence of components [243,244]. In addition, by chemically modifying the AFM tip with a ligand (chemical force microscopy), FV imaging has been successfully employed to create complete maps of recognition sites in samples, e.g. in living cells surfaces [245,246], or purified proteins [247,248].

Finally, although this approach is slower than some recently developed techniques such as the Peakforce® AFM, it remains interesting due to easier tuning of applied forces and more precise measurement of force curves. This ensures that in soft samples, the proper topography of undisturbed layers is measured with force curves corresponding to interactions between the tip and the intact bilayer [244]. However, the main drawback of the technique is that the slow acquisition time directly compromises the lateral resolution of the AFM image and the drift [55].

Molecule unfolding with AFM is an advanced application of force spectroscopy which can be directed to many different biomolecules. In the case of protein unfolding this technique allows the study of the mechanical properties of the molecule. In fact, protein unfolding is a huge area in biophysics and biochemistry that studies the behaviour of a protein assembly under different stresses such as chemical, thermal or mechanical. Protein unfolding with AFM is performed through a mechanical process. Other techniques such as optical or magnetic tweezers also study the protein unfolding under

mechanical stress, although AFM is the one presenting higher accessibility, simplicity and best ease to work with membrane proteins [249]. Interestingly, AFM protein unfolding is, in principle, assumed to be a single-molecule experiment and so it implies the study of only one molecule at a time. After a significant number of events, a distribution of single observable events can be obtained, while distributions from average values are characteristics of bulk experiments [249].

When performing the protein unfolding, the initial distribution of the sample is unknown and therefore the "fishing" for samples is usually done randomly by systematic scanning of the substrate. Additionally, a protein can by picked up at random positions of its surface [73] which makes the process highly stochastic. A way to improve the reproducibility of the experiments is to perform what is called the specific unfolding, e.g. by functionalizing tips and/or modifying proteins to ensure a single interaction point between both components.

The AFM molecule unfolding consists in a process similar to a FD curve where the AFM tip is pressed against the sample. The main difference is that, in this case one or more proteins may potentially adsorb to the tip upon withdrawing. Then, as the tip-surface distance increases, the molecule starts to be stretched and it shows an opposing force which results in a nonlinear restoring force. This force increases until critical bonds are broken. Once this point is reached, the protein segment unfolds and is unravelled. This sudden increase in the length of the molecule normally drops the force to basal levels, which results in a typical force peak. If the tip continues withdrawing, subsequent protein segments may continue their unfolding thus creating the characteristic sawtooth peaks profile (see Figure 28). Hence, changes in cantilever deflection and force needed to unfold the protein are recorded and the curve of interest is obtained by plotting force versus tip-sample separation. The resulting FD curve reveals forces required to pull the molecule out of the lipid membrane [249].

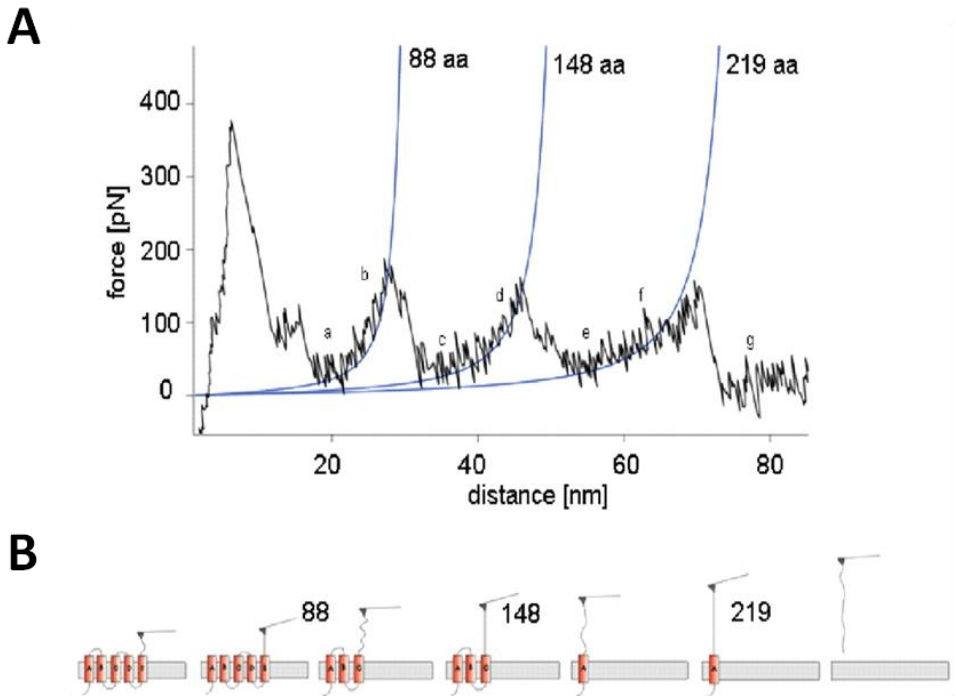

Figure 28. Typical spectrum obtained from an unfolding experiment of bacteriorhodopsin with the main peaks fitted using the worm-like chain model (**A**). Peaks correlated to the unfolding of secondary structure elements of the bacteriorhodopsin (**B**) *(Modified from Marisco et al., 2006* [250]*).*

In order to facilitate the analysis, the protein unfolding behaviour under mechanical stress is normally assimilated to the nonlinear force-extension relationship of a polymer being stretched. The behaviour of stretched polymers is well described by elasticity models of semiflexible polymers. The most widely used model is the interpolated approximation to the Worm-like chain (WLC), which has been successfully applied to model the elasticity of proteins, DNA, and RNA on stretching [249].

The WLC model considers a polymer as a flexible chain of length L_c (contour length) and predicts the restoring force F. Another parameter, the persistence length (p), is related to the flexibility of the molecule (i.e. the distance through which the orientation of the polymer remains correlated). In the case of proteins $p \simeq 0.4$ nm, which is the average value of the length of a single amino acid [251]. The analytical expression of the interpolated approximation to the WLC model [252] can be expressed as follows

$$F(x) = \frac{k_B T}{p}\left[\frac{1}{4}\left(1 - \frac{x}{L}\right)^{-2} - \frac{1}{4} + \frac{x}{L}\right]$$

where $F(x)$ is the force at a distance x, k_B is the Boltzmann constant, and T is the temperature. Then, by applying this equation to each of the unfolding peaks it is possible to obtain the increase in contour length for each unfolding event, which would correspond to the increase in length of the unfolded protein segment. Finally, by dividing this number by the length contribution of each amino acid, the number of amino acids found in the unfolded region can be obtained.

The particular case of membrane proteins unfolding involves the simultaneous study of intramolecular (between protein residues) and intermolecular (protein-lipid) interactions. For the unfolding, the forces to overcome are typically weak interactions, e.g. hydrogen bonding, hydrophobic forces, ionic and van der Wals interactions, which are in a whole collectively strong enough to hold the structure together. Therefore, the fine details of unfolding pathways require high force resolution like the one AFM can provide [253].

Furthermore, the mechanical unfolding pathways of membrane proteins are different than those found for water-soluble proteins. Whereas water-soluble proteins unfold cooperatively, when unfolding membrane proteins they present sequential unfolding steps, which indicates the presence of unfolding intermediates and constitute an unfolding pathway [254]. This phenomenon has been interpreted as a response to the separate contributions from intramolecular interactions that stabilize individual structural segments and from contributions from intermolecular interactions such as those represented by tertiary contacts (e.g protein-lipid interplay) [255]. Finally, one membrane protein can unfold with different characteristic pathways which are sensitive to environmental conditions [254].

4.3 Experimental results

4.3.1 Membrane protein−lipid selectivity: enhancing sensitivity for modeling FRET data

Suárez-Germà, C., Loura, L. M. S., Prieto, M., Domènech, Ò., Montero, M. T., Rodríguez-Banqueri, A., Vázquez-Ibar, J. L., Hernández-Borrell, J. (**2012**).
The Journal of Physical Chemistry B, 116(8), 2438-45.

4.3.1.1 Summary

FRET is a powerful method for the characterization of membrane proteins lipid selectivity. It can be used to quantify distances between a single D and a single A molecule; however, for FRET D and A scattered in the bilayer plane, multiple D-A pairs and distances are present. In addition, when studying protein/lipid selectivity, for a single tryptophan used as a D; several lipid acceptors may be located at the boundary region (annular lipids) of the protein. Therefore, in these experiments a theoretical analysis based on binomial distribution of multiple acceptors around the membrane proteins is required. In this study, we performed FRET measurements between an engineered single tryptophan situated in a hydrophilic cavity in the centre of LacY (single-W151/C154G LacY) used as D and pyrene acyl chain-labelled phospholipids (Pyr-PE, Pyr-PG, and Pyr- PC) used as acceptors reconstituted in POPE, POPG, POPC, and DOPC matrices at 25 and 37 °C. Previous studies were done with proteoliposomes reproducing a biomimetic system with PE:PG (3:1, mol/mol) and a χ = 0.0025 of probe [133]. However, this configuration created a severe dilution of the labelled phospholipid and therefore, although significant trends appeared, a rather weak energy transfer was detected. Hence, in order to increase the sensitivity of the method and to ascertain the lipid selectivity for LacY, the protein was reconstituted now in one-component host lipid matrices doped with 1.5% of probe. In addition, the influence of the headgroup and acyl chain composition was investigated.

Binding capabilities of LacY (and consequently correct folding) in the different lipid matrices were ascertained by taking advantage of W151 position which, after binding of a substrate, becomes inaccessible to a fluorescein-maleimide fluorophore. The obtained results indicated that, apart from POPE matrix, in all other lipid compositions LacY displayed a good substrate binding. However, taking into account LacY's normal fluorescent spectra when embedded in a POPE matrix and other bibliographic results [130], a correct topology of LacY in the POPE matrix was assumed.

By analysing the experimental FRET efficiency for Pyr-PE, Pyr-PG, and Pyr-PC in all host matrices at 25 and 37 °C, Pyr-PE was found to be the preferred lipid in the annular region of LacY irrespectively of the temperature and the composition. Next, Pyr-PG was preferred over Pyr-PC in the POPE and POPG matrices at 25 ºC and in the DOPC matrix at both temperatures. On the contrary Pyr-PE>Pyr-PC>Pyr-PG trend occurred in POPE and POPG matrices at 37 °C and in the POPC matrix at both temperatures. Interestingly, Pyr-PC showed higher FRET efficiency in POPC compared to DOPC, indicating a possible influence of the degree of unsaturation of the acyl chains. An opposite behaviour was observed for Pyr-PG, for which the efficiency in DOPC was higher in contrast with POPC matrix.

From fitting the mentioned theoretical model to the experimental FRET efficiencies, two parameters were calculated: the probability (μ) of a site in the annular ring being occupied by a pyrene-labelled phospholipid and the relative association constant (K_s) between the labelled and unlabelled phospholipids. In all cases, both were the highest for Pyr-PE. Especially notable was the relative Pyr-PG enrichment found in the annular region when the matrix was DOPC ($K_s > 1$), since this labelled-phospholipid was excluded from POPC matrix ($K_s \sim 0$). And, curiously, Pyr-PC was enriched in the annular region in a POPC matrix ($K_s > 1$) and excluded from it in a DOPC matrix ($K_s \sim 0$).

Additional information on the annular lipid composition of each system was obtained by exciting W151 of single-W151/C154G LacY and monitoring the emission intensities for monomer and excimer of the pyrene spectra. The obtained excimer-to-monomer (E/M) ratios were always higher for Pyr-PE than for the other labelled phospholipids, at both temperatures and at all phospholipid matrices.

In conclusion, it has been observed by using single component systems that the selectivity of LacY for PE is much higher than that for either PC or PG. That is, with the limitations imposed by the model and the system itself, we confirm that Pyr-PE is able to get closer to or, alternatively, to stay longer near LacY. We report also that when the phospholipids in the annular region of LacY are zwitterionic heteroacids (PE, PC), the probability for anionic PG to be in close proximity is very low. The presented data also suggest that the nature of the hydrophobic moiety and the appropriate acyl chain combination in phospholipids may govern the optimal function of LacY.

4.3.1.2 Highlights

- Selectivity of LacY for different Pyr-PE, Pyr-PG, Pyr-PC was tested in four different pure lipid matrices (POPE, POPG, POPC and DOPC) at 25 and 37 °C. In all compositions and at all temperatures Pyr-PE was the phospholipid predominant in the annular region surrounding the protein. Thus, phospholipids with PE headgroup seem to preferentially constitute the annular region of LacY thanks to its ability to get closer or, alternatively, stay longer near the protein.
- Results in POPG matrix (Pyr-PE>Pyr-PG>Pyr-PC at 25 °C and Pyr-PE>Pyr-PC>Pyr-PG at 37 °C) have to be carefully considered since LacY might be incorrectly folded despite the preserved binding capabilities [130].
- The presence of Pyr-PC in the annular region in POPC but not in DOPC matrices points to a possible influence of the degree of unsaturation of the phospholipid acyl chains in the protein selectivity.

THE JOURNAL OF PHYSICAL CHEMISTRY B

Article

pubs.acs.org/JPCB

Membrane Protein−Lipid Selectivity: Enhancing Sensitivity for Modeling FRET Data

Carme Suárez-Germà,[‡,†] Luís M. S. Loura,[∥] Manuel Prieto,[⊥] Òscar Domènech,[‡,†] M. Teresa Montero,[‡,†] Arturo Rodríguez-Banqueri,[§] José L. Vázquez-Ibar,[§] and Jordi Hernández-Borrell[‡,†,*]

[†]Departament de Fisicoquímica, Facultat de Farmàcia, UB and [‡]Institut de Nanociència i Nanotecnologia IN[2]UB, [§]ICREA and Institut de Recerca Biomèdica, Parc Científic de Barcelona, 08028 Barcelona, Spain

[⊥]Centro de Química-Física Molecular and IN, IST, 1049-001, Lisboa, Portugal

[∥]Faculdade de Farmácia, Universidade de Coimbra, Azinhaga de Santa Comba, 3000-548 Coimbra, Portugal and Centro de Química de Coimbra, 3004-535 Coimbra, Portugal

ABSTRACT: Förster resonance energy transfer (FRET) is a powerful method for the characterization of membrane proteins lipid selectivity. FRET can be used to quantify distances between a single donor and a single acceptor molecule; however, for FRET donors and acceptors scattered in the bilayer plane, multiple donor−acceptor pairs and distances are present. In addition, when studying protein/lipid selectivity, for a single tryptophan used as a donor; several lipid acceptors may be located at the boundary region (annular lipids) of the protein. Therefore, in these experiments, a theoretical analysis based on binomial distribution of multiple acceptors around the membrane proteins is required. In this work, we performed FRET measurements between single tryptophan lactose permease (W151/C154G LacY) of *Escherichia coli* and pyrene-labeled phospholipids (Pyr-PE, Pyr-PG, and Pyr-PC) reconstituted in palmitoyl-2-oleoyl-*sn*-glycero-3-phosphoethanolamine, 1-palmitoyl-2-oleoyl-*sn*-glycero-3-[phospho-*rac*-(1-glycerol)] (sodium salt), 1-palmitoyl-2-oleoyl-*sn*-glycero-3-phospho-choline, and 1,2-dioleoyl-*sn*-glycero-3-phospho-choline at 25 and 37 °C. To increase the sensitivity of the method and to ascertain the lipid selectivity for LacY, we reconstituted the protein in the pure phospholipids doped with 1.5% of labeled phospholipids. From fitting the theoretical model to the experimental FRET efficiencies, two parameters were calculated: the probability of a site in the annular ring being occupied by a labeled pyrene phospholipid and the relative association constant between the labeled and unlabeled phospholipids. The experimental FRET efficiencies have been interpreted taking into account the particular folding of the protein in each phospholipid matrix. Additional information on the annular lipid composition for each system has been obtained by exciting W151/C154G LacY and monitoring the emission intensities for monomer and excimer of the pyrene spectra. The results obtained indicate a higher selectivity of LacY for PE over PG and PC and pointed to a definite role of the acyl chains in the overall phospholipid−protein interaction.

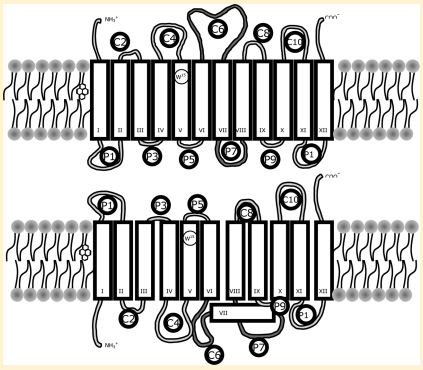

INTRODUCTION

Cell envelopes play an important role in many physiological and pathological processes: signal transduction; transport of drugs and metabolites; energy generation; and development of tissues, including tumor metastasis and viral and bacterial infections, among many others. The cell membrane is presently viewed as a heterogeneous object because of the lateral distribution and segregation of its two fundamental components: phospholipids and proteins. Transmembrane proteins (TMPs) involved in specific transport molecules across the phospholipid bilayer represent 5−10% and 3% of total proteins encoded by bacterial and human genomes, respectively.

A large number of secondary transporters, in which the source of energy for the process of transport depends on the electrochemical potential gradient ($\Delta\tilde{\mu}_i$), of ions such as Na^+ or H^+ contain 12 or 14 transmembrane segments (TMS) (α-helix),[1] crossing the membrane in a zigzag fashion. Many of these proteins play an important role in conferring resistance to drugs (anticancer and antibiotics) in both bacterial and eukaryotic cells. One of the paradigmatic models of membrane transporters is lactose permease (LacY) of *Escherichia coli*.[2] LacY, the secondary structure of which is shown in Figure 1a, is probably the best characterized of all proteins belonging to the 12-TMS group that also includes, among others, the efflux pumps LmrP of *Lactococcus lactis* and NorA of *Staphylococcus aureus*,[3] which actively expel daunomycin and norfloxacin, respectively. In the context of the chemiosmotic theory,[4] LacY utilizes the Gibbs energy stored in $\Delta\tilde{\mu}_{H^+}$ to drive the uphill translocation of galactosides. Although the coupling mechanism is not completely solved, the basic pathway of sugar and H^+ translocation through LacY and across the membrane is known in high detail.[2] TMPs are solvated by membrane lipids. There is

Received: November 3, 2011
Revised: January 31, 2012
Published: February 1, 2012

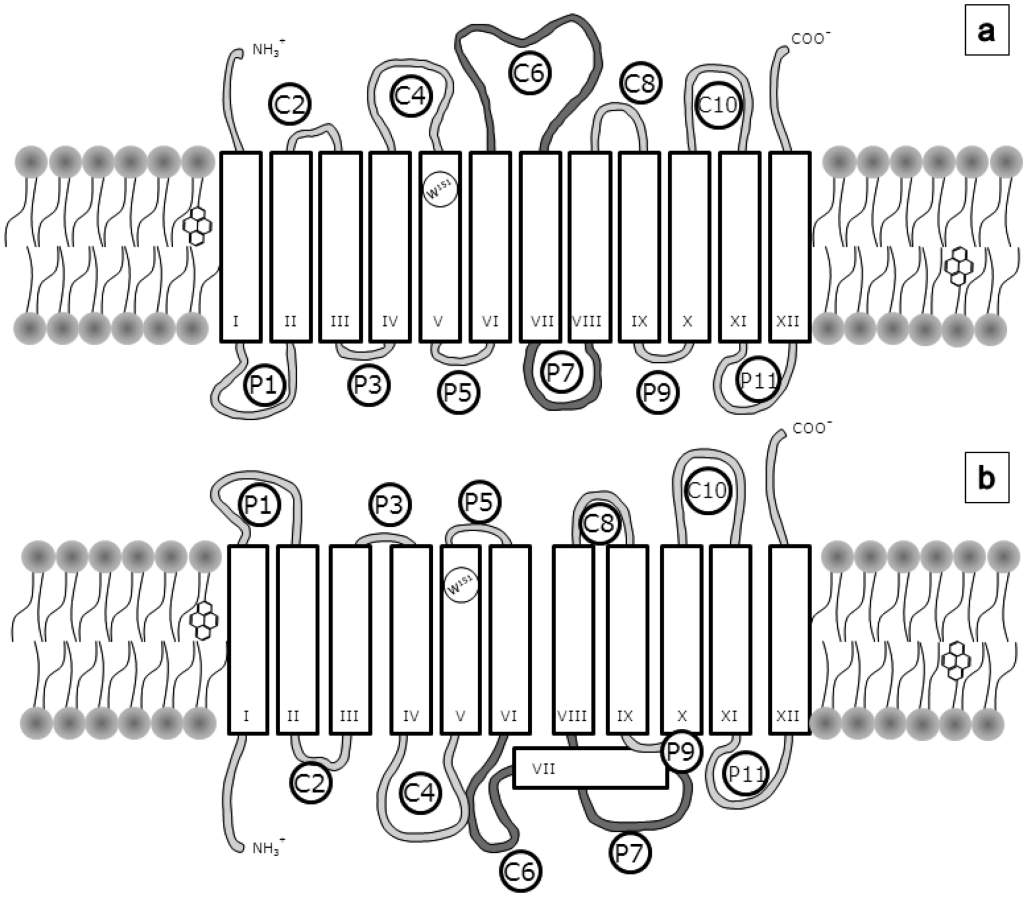

Figure 1. Secondary structure model of lactose permease showing topological organization in the presence (a) and absence (b) of PE or PC. Putative transmembrane helices, connected by extramembrane loops, cytoplasmic (C) and periplasmic (P), are shown in boxes. The approximate positions of the W151 (donor) (helix V) and the position of pyrene labeled molecules (acceptor) in the annular region is also shown. Based on ref 19.

evidence, mainly based on earlier electron spin resonance experiments,[5] supporting the existence of a layer of phospholipids in intimate interaction with the TMPs that are known as annular lipids. In physical terms, this is a boundary region that provides an adequate thickness and lateral pressure to embed the protein following what is referred to in the field as the matching principle.[6]

In previous works,[7,8] we have demonstrated that an adequate method to investigate the composition of the annular region is Förster resonance energy transfer (FRET).[9] The strategy consists of measuring the efficiency of the energy transfer between a single tryptophan (Trp) mutant of LacY (W151/C154G),[10] used as a donor (D), and different pyrene-labeled phospholipids as acceptors (A). The main conclusions drawn were that both phosphoethanolamine (PE) and phosphoglycerol (PG) can be part of the annular region, with PE being the predominant phospholipid. On one hand, these results reinforce the basic consensus on the PE requirement for LacY correct folding and in vivo function.[11] On the other hand, to better mimic the inner bacterial membrane composition, these previous efforts were carried out mostly in PE/PG 3:1 mixtures, a ratio identical to that found in the inner membrane of *E. coli*.[12]

This creates a dilution problem. For example, in an experiment in which the acceptor is labeled PE, even if the annular region would consist solely of PE lipid, the enrichment of labeled PE in this layer would be only of a factor 4/3. Adding to the fact that unspecific FRET to acceptors outside the annular layer is always present, this would imply a rather modest increase in the expected FRET efficiency. Finally, the simple fact that a pyrene acyl chain labeled lipid behaves identically to an unlabeled lipid of the same class is questionable, and this cannot be resolved in an experiment in which the host lipid matrix is a two-component mixture. For these reasons (to gain increased sensitivity and to assess the extent of correct reporting by the acceptor probes of each class), this protein system is readdressed in this paper, using different one-component host lipid matrixes. In addition, the influence of the headgroup and acyl chain composition is investigated.

In this work, we have reconstituted single-W151/C154G LacY in proteoliposomes formed with 1-palmitoyl-2-oleoyl-*sn*-glycero-3-phosphoethanolamine (POPE), 1-palmitoyl-2-oleoyl-*sn*-glycero-3-[phospho-*rac*-(1-glycerol)] (sodium salt) (POPG), 1-palmitoyl-2-oleoyl-*sn*-glycero-3-phospho-choline (POPC) or 1,2-dioleoyl-*sn*-glycero-3-phospho-choline (DOPC). The FRET strategy in the framework of this study consisted in measuring the efficiency of the energy transfer (E) between an engineered single tryptophan situated in a hydrophilic cavity in the center of LacY and three different pyrene-labeled phospholipids used as acceptors that are analogues of PE, PG, and PCs.

dx.doi.org/10.1021/jp2105665 | *J. Phys. Chem. B* 2012, 116, 2438–2445

EXPERIMENTAL METHODS

Materials. *N*-Dodecyl-β-D-maltoside (DDM) was purchased from Anatrace (Maumee, OH, USA). POPE, POPG, POPC, and DOPC were purchased from Avanti Polar Lipids (Alabaster, AL, USA). 1-Hexadecanoyl-2-(1-pyrenedecanoyl)-*sn*-glycero-3-phosphocholine (Pyr-PC), 1-hexadecanoyl-2-(1-pyrenedecanoyl)-*sn*-glycero-3-phosphoglycerol ammonium salt (Pyr-PG), 1-hexadecanoyl-2-(1-pyrenedecanoyl)-*sn*-glycero-3-phosphoethanolamine ammonium salt (Pyr-PE), and fluorescein-5-maleimide were purchased from Invitrogen (Barcelona, Spain). β-D-Galactopyranosyl-1-thio-β-D-galactopyranoside (TDG), isopropyl-1-thio-β-D-galactopyranoside (IPTG), and dithiothreitol (DTT) were obtained from Sigma Chemical Co. (St. Louis, MO, USA), and Bio-Beads SM-2 were purchased from Bio-Rad (Hercules, CA, USA). All other common chemicals were ACS grade.

Bacterial Strains and Protein Purification. These detailed procedures have been described in previous papers.[7,8] Briefly, *E. coli* BL21(DE3) cells (Novagen, Madison, WI, USA) transformed with plasmid pCS19 encoding single-W151/C154G LacY provided by Dr. H. Ronald Kaback (UCLA, USA), were grown in Luria−Bertani broth at 30 °C containing ampicillin (100 μg/mL) and induced at the appropriate moment with 0.5 mM IPTG. Cells were disrupted, and the membrane fraction was harvested by ultracentrifugation. Membranes were solubilized by adding DDM and purified by Co(II) affinity chromatography (Talon Superflow, Palo Alto, CA, USA). Protein eluted with 150 mM imidazole was subjected to gel filtration chromatography using a Superdex 200 20/30 column (GE-Healthcare, UK) equilibrated with 20 mM Tris−HCl (pH 7.5), 0.008% DDM. The protein was concentrated by using Vivaspin 20 concentrators (30 kDa cutoff; Vivascience, Germany) and stored on ice. Protein identification was performed by SDS/PGE electrophoresis, and protein quantitation was carried out using a micro-BCA kit (Pierce, Rockford, IL).

Vesicle Preparation and Protein Reconstitution. Liposomes and proteoliposomes were prepared according to methods published elsewhere[7,8] Briefly, chloroform−methanol (2:1, vol/vol) solutions containing appropriate amounts of both labeled and unlabeled phospholipids were dried under a stream of oxygen-free N_2 in a conical tube. The total concentration of phospholipids was calculated as a function of the desired lipid-to-protein ratio and protein concentration (1.5 μM). The amount of fluorescent probe was $x = 0.015$ for all the experiments. The resulting thin film was kept under high vacuum for ∼3 h to remove any traces of organic solvent. Multilamellar liposomes were obtained following redispersion of the film in 20 mM Hepes, 150 mM NaCl buffer, pH 7.40, and applying successive cycles of freezing and thawing both below and above the phase transition of the phospholipids and sonication for 2 min in a bath sonicator. Afterward, large, unilamellar liposomes supplemented with 0.2% of DDM were incubated overnight at room temperature. Liposomes were subsequently mixed with the solubilized protein and incubated at 4 °C for 30 min with gentle agitation to obtain a lipid-to-protein ratio (w/w) of 40. DDM was extracted by addition of polystyrene beads (Bio-Beads SM-2, Bio-Rad).

Binding Properties of Single-W151/C154G LacY Reconstituted in Vesicles. Substrate recognition by single-W151/C154G LacY reconstituted in lipid vesicles was tested by adapting a previously described protocol[7,8] based on the protection of the substrate against thiol modification of LacY. Briefly, 50 μL of proteoliposomes containing 1.5 μM of single-W151/C154G LacY[13] were incubated at room temperature for 5 min with either TDG or 15 mM L-glucose. Next, the samples were incubated with the fluorescent dye fluorescein-5-maleimide for 10 min at room temperature. The reaction was stopped by adding 5 mM of DTT. To evaluate the extent of LacY labeling, proteoliposomes were solubilized with 1% SDS and subjected to 12% PAGE gel electrophoresis. In-gel fluorescence was evaluated using a G-BOX gel analysis instrument (Syngene, Cambridge, UK) and compared with the total amount of protein after staining the same gel with Coomassie blue.

FRET Methodology. Steady state fluorescence measurements were carried out with an SLM-Aminco 8100 (Urbana, IL, USA) spectrofluorometer. The cuvette holder was thermostatted with a circulating bath (Haake, Germany), which was used to control temperature within 0.1 °C. The fluorescence experiments were performed at 25 and 37 °C. The excitation and emission bandwidths were 4/4 and 8/8 nm, respectively. Annular fluidity was determined as described elsewhere.[14] Pyrene was excited at 338 nm, with fluorescence spectra scanned from 350 to 500 nm. For energy transfer measurements, Trp was excited at 295 nm, and the spectra were recorded from 300 to 500 nm. To calculate the excimer-to-monomer fluorescence ratio (E/M), we used signal intensities at 375 nm (corresponding to the peak of monomer band) and 470 nm (maximum of pyrene excimer band). As described in detail elsewhere,[7,8] single-W151/C154G LacY, the donor, was excited at 295 nm, and emission of the pyrene-labeled phospholipids, the acceptor, was monitored at 338 nm.

FRET efficiencies (E) are calculated according to the equation

$$E = 1 - \frac{I_{DA}}{I_D} = 1 - \frac{\int_0^\infty i_{DA}(t)\,dt}{\int_0^\infty i_D(t)\,dt} \tag{1}$$

where I_D and I_{DA} are the tryptophan emission intensities in the absence or presence of pyrene acceptors, respectively. The reported values of experimental E are the averages of triplicate measurements from five separate reconstitutions. In the case of transmembrane proteins, we have to consider the existence of two different populations of phospholipids, those forming the first shell surrounding the protein, confined in the so-called boundary region, and those of the bulk. Assuming these two populations of A molecules, the fluorescence decay of D molecules can be written as

$$i_{DA}(t) = i_D(t)\,\rho_a(t)\,\rho_r(t) \tag{2}$$

where i_D and i_{DA} are the donor fluorescence decays in absence and presence of acceptor molecules, respectively. Since the number of annular pyrene phospholipids around each protein molecule is expected to follow a binomial population,[15] the annular contribution to the decay can be expressed as

$$\rho_a(t) = \sum_{n=0}^{m} e^{-nk_t t}\binom{m}{n}\mu^n(1-\mu)^{m-n} \tag{3}$$

where m is the number of phospholipid molecules in the first layer surrounding the protein, taken as 46 for LacY;[8] μ is defined as the probability of each site in the annular ring being

dx.doi.org/10.1021/jp2105665 | J. Phys. Chem. B 2012, 116, 2438−2445

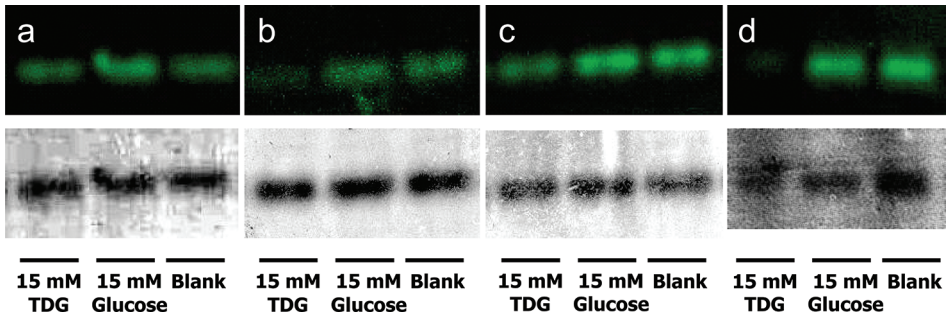

Figure 2. Substrate recognition by single-W151/C154G LacY reconstituted in proteoliposomes. Fluorescein−maleimide labeling of purified single-W151/C154G LacY reconstituted in vesicles composed of (a) POPE, (b) POPG, (c) POPC, and (d) DOPC. As indicated, the experiments were performed in the presence of 15 mM of TDG, 15 mM L-glucose, or no substrate (control). The upper panels (black background) correspond to the fluorescence intensity of fluorescein-labeled protein after being subjected to a 12% SDS−PAGE gel electrophoresis. The lower panels are the same gels after protein staining with Coomassie blue.

occupied by a labeled pyrene phospholipid; and k_t is the rate constant for D−A energy transfer,

$$k_t = \frac{1}{\tau}\left(\frac{R_0}{R}\right)^6 \tag{4}$$

where, in turn, τ is the donor lifetime and R_0 is the Forster radius (3.0 nm for the Trp/pyrene).[16] On the other hand, R, the distance between the D and annular A molecules, can be estimated according to

$$R = \left(w^2 + {R_e}^2\right)^{1/2} \tag{5}$$

where w (estimated as 1.2 nm) is the transverse distance between D (the Trp residue, for which an interfacial location is expected) and A (hydrophobic fluorophore, expected to reside near the bilayer center), and R_e (estimated as 3.0 nm) is the exclusion distance along the bilayer plane between the protein axis and the annular lipid molecules. For this system, the resulting value R = 3.2 nm was considered.[8]

The probability, μ, can be written as

$$\mu = K_s \frac{n_{pyr}}{n_{pyr} + n_{PL}} = K_s X_{pyr} \tag{6}$$

where the n's are the mole numbers of the labeled (n_{pyr}) and nonlabeled (n_{PL}) phospholipids, X_{pyr} is the label mole fraction, and K_s is the relative association constant between the labeled and unlabeled phospholipids. Thus, K_s = 1 denotes equal probability of finding acceptors in the annular region and in the bulk, whereas K_s = 0 means no acceptor in the annular region.

Alternatively

$$\mu = \frac{n_{pyr}^{ann}}{n_{pyr}^{ann} + n_{PL}^{ann}} = X_{pyr}^{ann} \tag{7}$$

By inserting eq 7 into eq 6, we obtain a more intuitive meaning of K_s,

$$X_{pyr}^{ann} = K_s X_{pyr} \tag{8}$$

that is, K_s is the ratio between the acceptor mole fractions in the annular region and in the overall system.

The FRET contribution of acceptors randomly distributed outside the annular region is given by Davenport et al.[17] as

$$\rho_r(t) = \exp\left\{-4n_2\pi l^2 \int_0^{1/\sqrt{l^2+{R_e}^2}} \frac{1-\exp(-tb^3\alpha^6)}{\alpha^3}\, d\alpha\right\} \tag{9}$$

where $b = (R_0/l)^2\tau^{-1/3}$, n_2 is the acceptor density in each leaflet, and l is the distance between the plane of the donors and the plane of the acceptors.

RESULTS AND DISCUSSION

The topological organization of LacY is well established.[18] As can be seen in Figure 1, the protein in its natural topology consists of 12 transmembrane α-helices, crossing the membrane in a zigzag fashion, that are connected by 11 relatively hydrophilic, periplasmic (P) and cytoplasmic (C) loops, with both amino and carboxyl termini on the cytoplasmic surface. It is important to note within the context of the following discussion that in cells and proteoliposomes formed with PG or cardiolipin, LacY adopts an inverted topology (Figure 1b), whereas in the ones containing PE or PC, LacY adopts the natural topology (Figure 1a).[19] In this work, for FRET modeling, LacY has been assimilated to a cylinder with a diameter ~6 nm in which the single tryptophan residue (W151) lies in the center of the cylinder. Despite the limitations of such approach, the model was tested successfully in preceding works,[8] where it was assumed that the single-W151/C154G mutant of LacY is indistinguishable from the global structure of the wild type protein.

With this assumption, we have reconstituted the protein in matrixes including 1.5% of pyrene-labeled phospholipids. This increase in the unlabeled/labeled phospholipid ratio was intended to improve the sensitivity of the FRET measurements to produce efficiencies of $E \approx 0.5$, for which FRET sensitivity to distance is maximal. Since LacY topological organization is sensitive to the lipid environment,[19] it is quite relevant to study the structural organization of the protein when reconstituted in the one-component host lipid matrices used in the present work.

To ascertain the folding of LacY in the different matrices, we used a fluorescence experiment that provides information about the ability of LacY to recognize its specific substrate, TDG.[8] Binding of TDG to LacY protects against the covalent modification of the protein by the fluorescent dye fluorescein−maleimide, whereas the nonsubstrate, L-glucose, does

dx.doi.org/10.1021/jp2105665 | J. Phys. Chem. B 2012, 116, 2438−2445

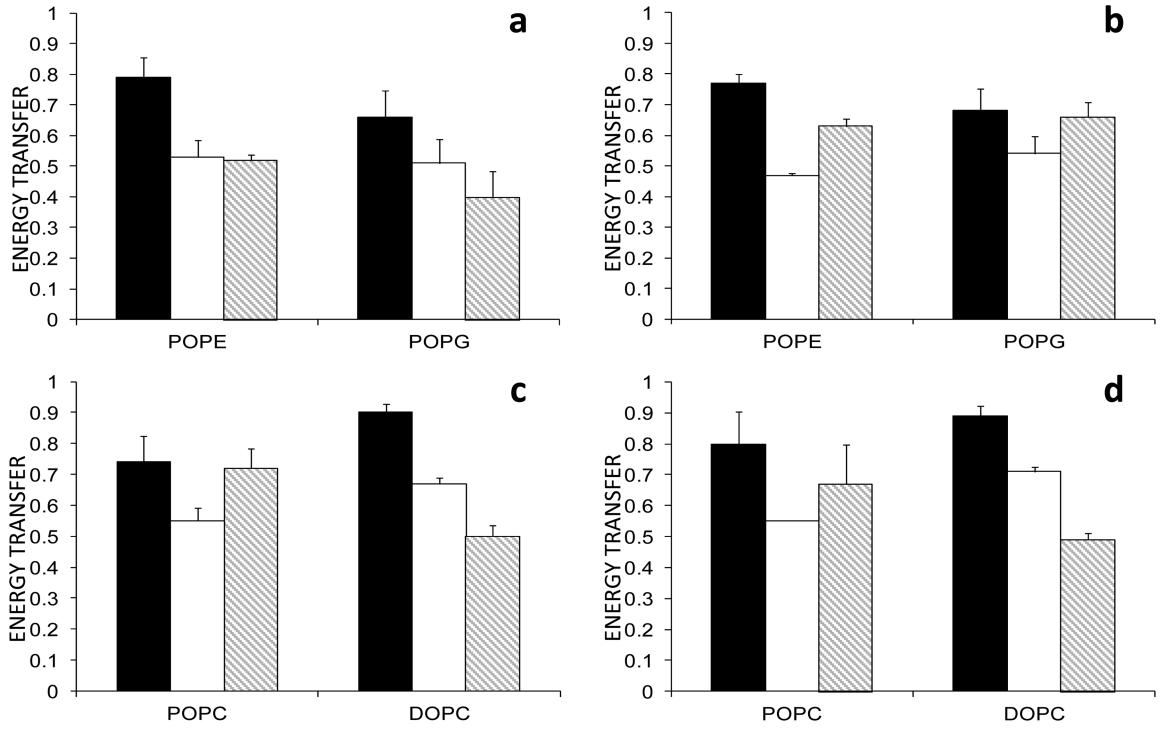

Figure 3. FRET efficiency between W151 and Pyr-PE (black columns), Pyr-PG (white columns) and Pyr-PC (striped columns) in POPE and POPG matrixes at 25 (a) and 37 °C (b) and in POPC and DOPC matrixes at 25 (c) and 37 °C (d). Proteoliposomes (1.5 μM LacY) were doped with 1.5% of the corresponding phospholipids analog label. The error bars stand for $\sigma/\sqrt{n}$, σ being the standard deviation, and n, the number of measurements performed.

Table 1. Experimental Efficiencies, Probabilities of Each Site in the Annular Ring Being Occupied by a Pyrene Labeled Phopholipid and Relative Association Constant toward LacY

		POPE matrix				POPG matrix			
	labeled lipid (1.5%)	experimental E	μ	K_s	K_s/K_s(PE)	experimental E	μ	K_s	K_s/K_s(PE)
25 °C	Pyr-PE	0.79	0.10	6.53	1.00	0.66	0.03	2.00	1.00
	Pyr-PG	0.53	0.00	0.00	0.00	0.51	0.00	0.00	0.00
	Pyr-PC	0.52	0.00	0.00	0.00	0.40	0.00	0.00	0.00
37 °C	Pyr-PE	0.77	0.08	5.53	1.00	0.68	0.04	2.47	1.00
	Pyr-PG	0.47	0.00	0.00	0.15	0.54	0.00	0.00	0.00
	Pyr-PC	0.63	0.02	1.40	0.25	0.66	0.03	2.00	0.81

not show such protection. As can be seen in Figure 2, in addition to the exception of POPE 98.5% lipid composition, TDG binding to LacY reconstituted in all the studied lipid systems partially blocks fluorescein−maleimide labeling. This indicates that the reconstituted protein can selectively recognize the substrate TDG over the nonsubstrate L-glucose.[2] Incidentally, it may be noticed that POPG 98.5% composition shows, in general, paler fluorescence, which may be attributed to the repulsion encountered by the negatively charged fluorescein when approaching the negative matrix, which may somewhat hinder the probe−protein interaction.

Given the functional data shown previously, the absence of TDG protection against fluorescein−maleimide labeling in LacY reconstituted with POPE (Figure 2, upper panel a) is somehow contradictory with the fact that PE is the most abundant phospholipid species (70%) in the inner *E. coli* membrane.[12]It is noteworthy that LacY reconstituted into phospholipids extracted from *E.coli* cytoplasmic membranes composed mainly of PE (up to 75%) is fully functional and shows high levels of active transport.[19] Similar to what it has been reported in other works,[20] fluorescence spectra of LacY reconstituted in PE proteoliposomes was indistinguishable from the proteoliposomes of other compositions. This suggests that the position of the fluorophore, sited near the binding site, remains unaltered and that the global structure is maintained. Then we may assume that LacY adopts a correct topology when reconstituted in 98.5% POPE proteoliposomes.

Regarding matrixes formed with anionic phospholipids, it is well established that LacY cannot carry out uphill but downhill substrate transport.[21] This is due to a change in the topological organization of domains C6 and P7 of LacY (Figure 1b).[19] Nevertheless, the binding site remains unaltered in POPG, since it supports downhill transports and, in our studies, substrate recognition (Figure 2, upper panel b). Furthermore, similar functional behavior (only downhill transport) is found when LacY is reconstituted in proteoliposomes mostly composed of the neutral zwitterionic phospholipid DOPC.[19] However, it has been demonstrated that the protein conserves its physiological topology (Figure 1a).

Figure 3 shows the experimental FRET efficiency for the three Pyr-labeled phospholipids used as acceptors (Pyr-PE, Pyr-PG, and Pyr-PC) in all host lipids at 25 and 37 °C. At first

dx.doi.org/10.1021/jp2105665 | J. Phys. Chem. B 2012, 116, 2438−2445

Table 2. Experimental Efficiencies, Probabilities of Each Site in the Annular Ring Being Occupied by a Pyrene Labeled Phopholipid and Relative Association Constant toward LacY

		POPC matrix				DOPC matrix			
	labeled lipid (1.5%)	experimental E	μ	K_s	K_s/K_s(PE)	experimental E	μ	Ks	K_s/K_s(PE)
25 °C	Pyr-PE	0.74	0.07	4.31	1.00	0.90	0.28	18.50	1.00
	Pyr-PG	0.55	0.00	0.02	0.00	0.67	0.03	2.24	0.12
	Pyr-PC	0.72	0.05	3.63	0.84	0.50	0.00	0.00	0.00
37 °C	Pyr-PE	0.80	0.11	7.08	1.00	0.89	0.25	16.47	1.00
	Pyr-PG	0.55	0.00	0.02	0.00	0.71	0.05	3.60	0.22
	Pyr-PC	0.67	0.03	2.24	0.32	0.49	0.00	0.00	0.00

sight, there is a larger preference for Pyr-PE, irrespective of the temperature and the phospholipid matrix. Pyr-PE is preferred over Pyr-PG, and the latter over Pyr-PC, in the POPE and POPG matrixes at 25 °C (Figure 3a), and in the DOPC matrix at both temperatures (Figures 3a, c). A change in preference, Pyr-PC by Pyr-PG occurs in the POPE and POPG matrixes at 37 °C (Figure 3b) and in the POPC matrix at both temperatures (Figure 3c, d). Interestingly Pyr-PC shows a higher efficiency in POPC than in DOPC, indicating a possible influence of the degree of unsaturation of the acyl chains. An opposite behavior is observed for Pyr-PG, for which the efficiency in DOPC is higher than in the POPC matrix.

In Table 1, the experimental FRET values are listed along with the calculated μ and K_s values. As can be seen, the probability of finding labeled phospholipids at the annular regions (μ) is always the highest, irrespective of the matrix, for Pyr-PE. This behavior reflects the values of the FRET efficiency mentioned above. By inspecting the outcome for K_s values, we notice that the largest values are obtained for Pyr-PE in all matrixes and both temperatures. It is worth mentioning that ideally, $K_s = 1$ for any probe that mimics the nonlabeled phospholipids, and values between 1 and 3 have been reported.[9] Therefore, these high values of K_s obtained for Pyr-PE may indicate either an annular region extremely enriched in the label or that Pyr-PE does not mimic well the unlabeled phospholipid. Although this may be a handicap, if one compares across probes in the same host lipid, it becomes clear that there is an effect of preference of Pyr- PE for PE over PG and PC. Since the probes are all equal except for the headgroup, and for comparing the different probes in the same host lipid, K_s/K_s (PE) ratios are provided in Table 1.

In the POPE matrix, μ values indicate that Pyr-PG is excluded at both temperatures and that Pyr-PC is excluded at 25 °C and shows a small enrichment at 37 °C. Since $K_s = 0$ means no acceptor in the annular region, it becomes clear that at 25 °C, Pyr-PG and Pyr-PC are completely excluded. Although Pyr-PG behaves in the same way at 37 °C, LacY shows an increased preference for Pyr-PC at this temperature. The overall results in the POPE matrix, in which LacY is folded closely to the in vivo conditions (Figure 1a), point to the fact that Pyr-PE should be in closer proximity than the other labels. On the other hand, notice that μ and K_s for Pyr-PE in the POPG matrix are compatible with a moderate enrichment of the label in the annular region. Notice that Pyr-PG is depleted from the annular region at both temperatures when the host phospholipid is POPG. Similarly, we can observe that Pyr-PC is also depleted when hosted by POPG at 25 °C and that a very slight enrichment is observed at 37 °C.

All these observations may be likely related to the inverted topology of domains C6 and P7 of LacY (see Figure 1b) when reconstituted in POPG proteoliposomes.[19] Our FRET measurements in POPE and POPG matrixes confirm the preference of LacY for PE and its probable predominance in the annular ring.[7,8] This may indirectly support a hypothetical interaction between the PE headgroup and some specific residue of the protein.[23,24] Importantly, recent observations have shown that uphill transport occurs in *E. coli*, in which PE has been completely exchanged by PC.[25] Since in PE and PC matrixes LacY exhibits its natural topology (Figure 1a), this intriguing observation points to a more complex molecular interaction between the protein and the annular phospholipids. Hence, FRET measurements in PC matrixes (Table 2) become of interest given the fact that despite its natural topology in these matrixes, LacY shows only downhill transport in DOPC proteoliposomes.[19] Pyr-PG is slightly enriched in the annular region when the matrix is DOPC ($K_s > 1$) but is excluded from it in a POPC matrix ($K_s \sim 0$). However, the most interesting result is possibly that, according to the K_s values, Pyr-PC is enriched in the annular region in a POPC matrix ($K_s > 1$) and excluded from it in a DOPC matrix ($K_s \sim 0$).

Given that DOPC and POPC share the same headgroup and have very similar hydrophobic lengths in the bilayer (2.48 nm for DOPC vs 2.54 nm for POPC),[26] this difference is probably related to the different specific curvature of the two lipid species. It has been reported that whereas proper topology of LacY depends on a dilution of high negative surface charge density (and hence, probably the decreased affinity of the protein for PG), rather than on spontaneous curvature (C_0),[27] the latter appears to be crucial regarding uphill transport of lactose by LacY in vivo,[28] with negative curvature lipids such as PE being required. C_0 (POPC) is essentially zero, and DOPC, due to its additional unsaturated acyl chain, has a negative specific curvature (C_0(DOPC) = −0.11 nm^{-1}).[26] Although its value is still far from the nonbilayer lipid DOPE (C_0(DOPE) = −0.35 nm^{-1}),[26] it may justify the preference of properly reconstituted LacY for DOPC rather than POPC, and hence, the differential behavior in DOPC and POPC matrixes regarding selectivity for labeled probes.

In addition, DOPC is also much closer to PE on hydratation properties. The fact that an opposite trend is observed for Pyr-PG (Table 2) is suspicious and probably related to the above-mentioned improper organization of LacY in PG. Interestingly, according to theoretical calculations,[29] although repulsive contributions in the core of the membrane are similar (∼166 bar and ∼200 bar for POPC and DOPC, respectively), the repulsive forces at the headgroups level are much higher for POPC (∼675 bar) than for DOPC (∼266 bar). Therefore, whatever the precise mechanism involved in the phospholipid−protein interplay may be, there would be a subtle balance among the forces evolved from physicochemical properties of the molecules.

dx.doi.org/10.1021/jp2105665 | J. Phys. Chem. B 2012, 116, 2438−2445

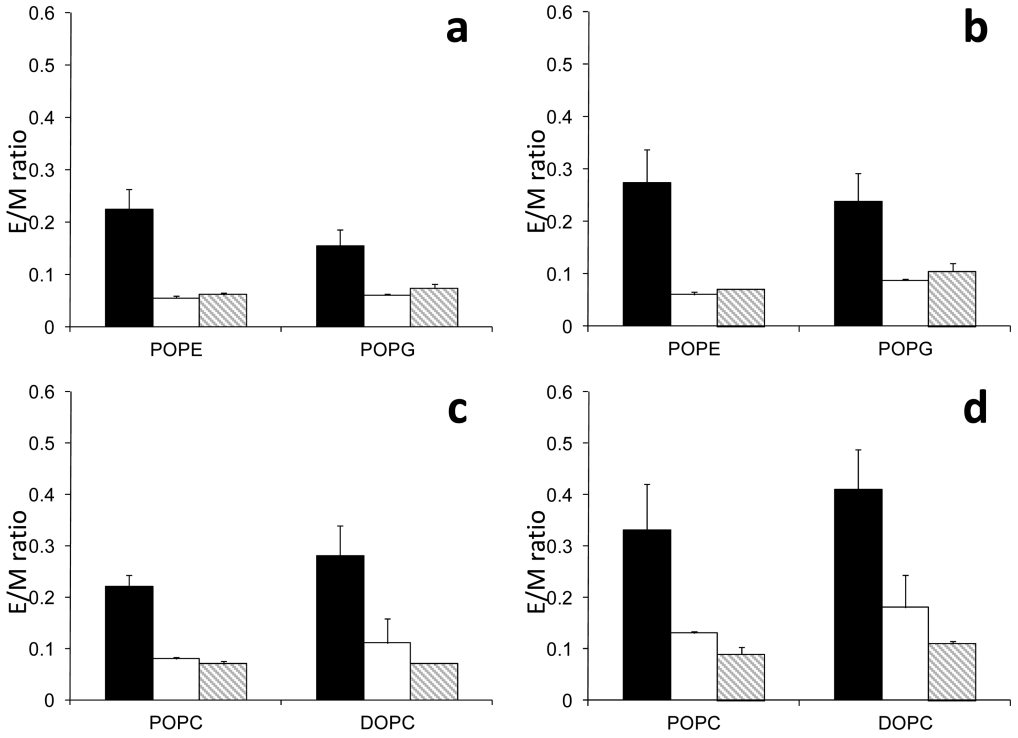

Figure 4. E/M ratios from the annular labeled lipids: Pyr-PE (black columns), Pyr-PG (white columns) and Pyr-PC (stripped columns) of 1.5 μM LacY proteoliposomes of POPE and POPG at 25 °C (A) and 37 °C (B); and POPC and DOPC at 25 °C (C) and 37 °C (D). The error bars stand for $\sigma/\sqrt{n}$, σ being the standard deviation, and n, the number of measurements performed.

The excited-state pyrene molecules display two characteristic peaks in the fluorescence spectra, for the monomer and excimer, respectively. The specific E/M ratio will result in the collision rate of the pyrene molecules. Thus, additional information can be obtained by exciting the single tryptophan of W151/C154G LacY and monitoring the emission intensities for M and E of the pyrene spectra because only the labeled molecules surrounding the protein, annular lipids, will be selectively excited. Consequently, the E/M ratio will provide information on the annular lipid proportion for each system.

The E/M ratios reported by the pyrene probes in the corresponding host phospholipids under study are shown in Figure 4. As can be seen, theses ratios were always higher for Pyr-PE than for the other labeled phospholipids, at both temperatures and all phospholipid matrixes. Notice that slight differences in the E/M ratios for Pyr-PG and Pyr-PC are observed in the POPE and POPG matrices (Figure 4a, b) and that Pyr-PG shows slightly higher E/M ratios than Pyr-PC in the POPC and DOPC matrixes (Figure 4c, d). Although caution should be taken with such conclusion, on the basis of the assumption that labeled and unlabeled phospholipids behave similarly, these overall results are in agreement with the overall FRET observations and support the idea that LacY is preferentially surrounded by PE rather than by the other phospholipids and that acyl chains may play a definite role in the transport processes.

CONCLUSIONS

In this work, we have observed by using single component systems that the selectivity of LacY for PE is much higher than that for either PC or PG. That is, with the limitations imposed by the model and the system itself, we do confirm that Pyr-PE is able to get closer to or, alternatively, spend more time next to the LacY. We report also that when the phospholipids in the annulus of the LacY are zwitterionic (PE) or neutral (PC) heteroacids, the probability for anionic PG to be in close proximity is very low. The presented data also suggest that the nature of the hydrophobic moiety and the appropriate heterological combination of phospholipids may govern the optimal function of LacY.

AUTHOR INFORMATION

Corresponding Author

*Phone: (+34) 934035986. Fax: (+34) 934035987. E-mail: jordihernandezborrell@ub.edu.

Notes

The authors declare no competing financial interest.

ACKNOWLEDGMENTS

C.S.G. is the recipient of a FPI fellowship from the Ministerio de Ciencia e Innovación of Spain. Special thanks to the Reviewers for valuable comments. This work has been supported by Grant CTQ-2008-03922/BQU from the Ministerio de Ciencia e Innovación of Spain. L.M.S.L. and M.P. acknowledge funding by FEDER (COMPETE program), and by FCT (Fundação para a Ciência e a Tecnologia), project references PTDC/QUI-BIQ/099947/2008 and FCOMP-01-0124-FEDER-010787 (FCT PTDC/QUI-QUI/098198/2008).

REFERENCES

(1) Pao, S.; Paulsen, I. T.; Saier, M. H. *Microbiol. Mol. Biol. Rev.* **1998**, *62*, 1.

(2) Guan, L.; Kaback, H. R. *Ann. Rev. Biophys. Biomed. Struct.* **2006**, *35*, 67.

(3) Paulsen, I. T.; Brown, M. H.; Skurray, R. A. *Microbiol. Rev.* **1996**, *60*, 575.

(4) Mitchel, P. *Chemiosmotic Coupling and Energy Transduction*; Glynn Res. Ltd.: Bodmin, U. K., 1968.
(5) Marsh, D.; Horváth, L. I. *Biochim. Biophys. Acta* **1998**, *1376*, 267.
(6) Mouritsen, O. G.; Bloom, M. *Biophys. J.* **1984**, *46*, 141.
(7) Picas, L.; Montero, M. T.; Morros, A.; Vázquez-Ibar, J. L.; Hernández-Borrell, J. *Biochim. Biophys. Acta* **2010**, *1798*, 291.
(8) Picas, L.; Suárez-Germà, C.; Montero, M. T.; Vázquez-Ibar, J. L.; Hernández-Borrell, J.; Prieto, M.; Loura, L. M. S. *Biochim. Biophys. Acta* **2010**, *1798*, 1707.
(9) Loura, L. M. S.; Prieto, M.; Fernandes, F. *Eur. Biophys. J.* **2010**, *39*, 565.
(10) Vázquez-Ibar, J. L.; Guan, L.; Svrakic, M.; Kaback, H. R. *Proc. Natl. Acad. Sci. U.S.A.* **2003**, *100*, 12706.
(11) Dowhan, W.; Bogdanov, M. *Annu. Rev. Biochem.* **2009**, *78*, 515.
(12) Dowhan, W. *Annu. Rev. Biochem.* **1997**, *66*, 199.
(13) Vazquez Ibar, J. J.; Weinglass, A. B.; Kaback, H. R. *Proc. Natl. Acad. Sci. U.S.A.* **2002**, *99*, 3487.
(14) Mason, R. P.; Jacob, R. F.; Walter, M. F.; Mason, P. E.; Avdulov, N. A.; Chochina, S. V.; Igbavboa, U.; Wood, W. G. *J. Biol. Chem.* **1999**, *274*, 18801.
(15) Fernandes, F.; Loura, L. M. S.; Koehorst, R.; Spruijt, R. B.; Hemminga, M. A.; Fedorov, A.; Prieto, M. *Biophys. J.* **2004**, *87*, 344.
(16) Tahara, Y.; Murata, M.; Ohnishi, S.; Fujiyoshi, Y.; Kikuchi, M.; Yamamoto, Y. *Biochemistry* **1992**, *31*, 8747.
(17) Davenport, L.; Dale, R. E.; Bisby, R. H.; Cundall, R. B. *Biochemistry* **1985**, *24*, 4097.
(18) Bogdanov, M.; Xile, J.; Dowhan., W. *J. Biol. Chem.* **2009**, *284*, 9637.
(19) Wang, X.; Bogdanov, M.; Dowhan, W. *EMBO J.* **2002**, *21*, 5673.
(20) Alvis, J. S.; Williamson, I. M.; East, J. M.; Lee, A. G. *Biophys. J.* **2003**, *85*, 3828.
(21) Page, M. J. P.; Rosenbusch, J. P.; Yamato, I. *J. Biol. Chem.* **1988**, *263*, 15897.
(22) Hakizimana, P.; Masureel, M.; Gbaguidi, B.; Ruysschaert, J. M.; Govaerts, C. *J. Biol. Chem.* **2008**, *283*, 9369.
(23) Chen, C. C.; Wilson, T. H. *J. Biol. Chem.* **1984**, *259*, 10150.
(24) Soubias, O.; Teague, W. E. Jr.; Hines, K. G.; Mitchell, D. C.; Gawrisch, K. *Biophys. J.* **2010**, *99*, 817.
(25) Bogdanov, M.; Heackock, P.; Guan, Z.; Dowhan, W. *Proc. Natl. Acad. Sci. U.S.A.* **2010**, *107*, 15057.
(26) Bogdanov, M.; Xie, J.; Heacock, P.; Dowhan, W. *J. Cell Biol.* **2008**, *182*, 925.
(27) Wikström, M.; Kelly, A. A.; Georgiev, A.; Eriksson, H. M.; Klement, M. R.; Bogdanov, M.; Dowhan, W.; Wieslander, A. *J. Biol. Chem.* **2009**, *284*, 954.
(28) Ollila, S.; Hyvönen, M. T.; Vattulainen, I. *J. Phys. Chem. B* **2007**, *111*, 3139.
(29) Ollila, S.; Róg, T.; Karttunen, M.; Vattulainen, I. *J. Struct. Biol.* **2007**, *159*, 311.

4.3.2 Phosphatidylethanolamine−lactose permease interaction: a comparative study based on FRET

Suárez-Germà, C., Loura, L. M. S., Domènech, Ò., Montero, M. T., Vázquez-Ibar, J. L., Hernández-Borrell, J. (**2012**).
The Journal of Physical Chemistry B, 116(48), 14023-8.

4.3.2.1 Summary

In the present study we investigated the selectivity of LacY for its surrounding phospholipids when reconstituted in binary mixtures of POPE, DPPE, or DOPE with POPG at a 3:1 molar ratio. FRET measurements were performed to investigate the selectivity between a single tryptophan mutant of LacY used as D, and two analogues of PE and PG labelled with pyrene in the acyl chains (Pyr-PE and Pyr-PG) used as acceptors. As a difference from previous works, the donor was W151 from single-W151/C154G LacY, but with an additional mutation (D68C) in which an aspartic acid residue was replaced by a cysteine. It has been reported that the replacement of the aspartic acid in position 68 by cysteine inhibits active transport in LacY [211]. Moreover, this highly conserved residue in MFS has been proposed as the main mediator of the interaction between PE and the protein [136]. Thus, we aimed to elucidate the phospholipid composition of the annular region of this mutant, and to determine whether the mutation performed, induced changes in the protein−lipid affinity. Additionally, results were fitted to a model consisting in a theoretical analysis of FRET results based on a binomial distribution of multiple acceptors around a membrane protein.

Proper binding capabilities of the mutant in the studied matrices were assessed in proteoliposomes by a method that takes advantage of W151 (see 4.3.1). Thus, in all lipid matrices the protein was considered to be correctly inserted and folded in the membrane.

When performing FRET measurements, transfer efficiencies for Pyr-PE were always higher than for Pyr-PG. The values of the probability of each site in the annular ring being occupied by a label (μ) were similar at the studied temperatures (24 and 37 °C),

suggesting that the lipid environment was not significantly affected when modifying the temperature.

By comparing the results with those obtained for single-W151/C154G LacY, it was observed that the mutation in the 68 residue indeed changed the selectivity of the protein for the phospholipids. As a matter of fact, normalized values of FRET efficiency were similar for both mutants in DOPE:POPG (3:1, mol/mol), and lower and higher normalized values were observed in POPE:POPG (3:1, mol/mol) and DPPE:POPG (3:1, mol/mol), respectively, for the systems where the 68 residue was mutated into cysteine. These results support the preference for PE in systems in the L_α phase as well as a higher relative affinity between POPE and single-W151/C154G than between POPE and single-W151/C154G/D68C. Unexpectedly, while the model could not be applicable for DPPE:POPG (3:1, mol/mol) system when the D was single-W151/C154G LacY, efficient energy transfer occurred when using the single-W151/C154G/D68C mutant. Hence, this last mutant was able to recruit Pyr-PE in its vicinity even in the presence of phase separation. Thus, while the lipid selectivity for wild-type D68 was DOPE ~ POPE >> DPPE, the mutation to cysteine increased the protein selectivity for DOPE over POPE and DPPE (DOPE>POPE>DPPE). This observation reinforces the implication of the acyl chains in the LacY-lipid interaction besides the headgroup requirement.

Finally, all the gathered evidences indicate that the introduction of the mutation in the 68 site brings to a change of LacY affinity for POPE. This may lead to a modification in the composition of the phospholipids in close contact with the protein, which might be induced by changes in the conformational dynamics of LacY resulting in a recruitment of the phospholipid species most adaptable to the geometrical needs of the protein.

4.3.2.2 Highlights

- The annular region of single-W151/C154G/D68C LacY has been studied through FRET analysis between W151 and labelled phospholipids (Pyr-PE and Pyr-PG) in DOPE, POPE and DPPE, and POPG lipid matrices (PE:PG 3:1, mol/mol).
- In all the studied lipid compositions, D68C mutant preferentially showed PE over PG in its annular region. This differ from calculations with W151/C154G LacY, in which the protein showed enrichment in PE in all the lipid matrices, except in the

phase separated system DPPE:POPG (3:1, mol/mol) with POPG as the predominant species in the annular region. Thus, this represents a change in the protein-lipid affinity and a modification in the composition of the annular region of the protein, most likely to better adapt to a possible new geometrical organization.

- A higher relative affinity between POPE and single-W151/C154G than between POPE and single-W151/C154G/D68C has been reported. This suggests a possible role for D68 in the PE-LacY interaction.
- D68C mutant affinity for PE presented and acyl chain selectivity as follows: DOPE>POPE>DPPE. This points to possible requirements of the protein for specific acyl chain configurations besides the headgroup requirement.

THE JOURNAL OF PHYSICAL CHEMISTRY B

Article

pubs.acs.org/JPCB

Phosphatidylethanolamine–Lactose Permease Interaction: A Comparative Study Based on FRET

Carme Suárez-Germà,[‡,†] Luís M.S. Loura,[⊥] Òscar Domènech,[‡,†] M. Teresa Montero,[‡,†] José Luís Vázquez-Ibar,[§] and Jordi Hernández-Borrell*[,‡,†]

[†]Departament de Fisicoquímica, Facultat de Farmàcia, Universitat de Barcelona, Spain

[‡]Institut de Nanociència i Nanotecnologia IN[2]UB, 08028 Barcelona, Spain

[§]Unitat de Biofísica, Departament de Bioquímica i Biología Molecular, Facultat de Medicina and Centre d'Estudis en Biofísica (CEB), UAB 08193 Bellaterra, Barcelona, Spain

[⊥]Faculdade de Farmácia, Universidade de Coimbra, Azinhaga de Santa Comba, 3000-548 Coimbra, Portugal and Centro de Química de Coimbra, 3004-535 Coimbra, Portugal

ABSTRACT: In this work we have investigated the selectivity of lactose permease (LacY) of *Escherichia coli* (*E. coli*) for its surrounding phospholipids when reconstituted in binary mixtures of 1-palmitoyl-2-oleoyl-*sn*-glycero-3-phosphoethanolamine (POPE), 1,2-Palmitoyl-*sn*-glycero-3-phosphoethanolamine (DPPE), or 1,2-dioleoyl-*sn*-glycero-3-phosphoethanolamine (DOPE) with 1-palmitoyl-2-oleoyl-*sn*-glycero-3-(phospho-*rac*-(1-glycerol)) (POPG). Förster resonance energy transfer (FRET) measurements have been performed to investigate the selectivity between a single tryptophan mutant of LacY used as donor (D), and two analogues of POPE and POPG labeled with pyrene in the acyl chains (Pyr-PE and Pyr-PG) used as acceptors. As a difference from previous works, now the donor has been single-W151/C154G/D68C LacY. It has been reported that the replacement of the aspartic acid in position 68 by cysteine inhibits active transport in LacY. The objectives of this work were to elucidate the phospholipid composition of the annular region of this mutant and to determine whether the mutation performed, D68C, induced changes in the protein–lipid selectivity. FRET efficiencies for Pyr-PE were always higher than for Pyr-PG. The values of the probability of each site in the annular ring being occupied by a label (μ) were similar at the studied temperatures (24 °C and 37 °C), suggesting that the lipid environment is not significantly affected when increasing the temperature. By comparing the results with those obtained for single-W151/C154G LacY, we observe that the mutation in the 68 residue indeed changes the selectivity of the protein for the phospholipids. This might be probably due to a change in the conformational dynamics of LacY.

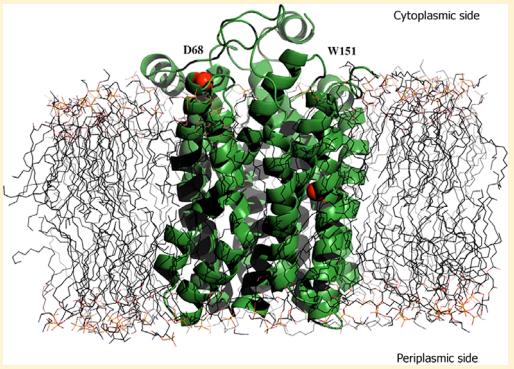

INTRODUCTION

Cell envelopes play an important role in many physiological and pathological processes: signal transduction, transport of drugs and metabolites, energy generation, and development of tissues, among many others. The cell membrane is presently viewed as a heterogeneous object because of the lateral distribution and segregation of its two fundamental components: phospholipids and proteins. Transmembrane proteins (TMs) involved in specific transport of molecules across the phospholipid bilayer account for 5–10% and 3% of total proteins encoded by bacterial and human genomes, respectively. Among the secondary transporters, where the source of energy for the process of transport depends on electrochemical potential gradient of ions such as Na^+ or H^+, one of the most studied groups is formed by the 12-TMS family characterized by the presence of 12 transmembrane segments (α-helix).[1,2] Many of these proteins are the therapeutic targets of several drugs and play an important role in conferring drug resistance (to anticancer drugs and antibiotics) in both bacteria and eukaryotic cells. One of the paradigmatic models of the transport protein is lactose permease (LacY) from *Escherichia coli*,[3] the best characterized of all proteins belonging to the 12-TMS group that also includes the LmrP efflux pump in *Lactococcus lactis*[4] or NorA of *Staphylococcus aureus*,[5] that actively expel daunomycin and norfloxacin, respectively. LacY is a lactose cotransporter (symporter) against gradient (uphill) that is coupled with the proton electrochemical potential gradient. The three-dimensional structure of the C154G mutant of LacY[6] and other LacY mutants[7−9] obtained by X-ray diffraction have definitively contributed on the understanding of the mechanism of lactose/H^+ cotransport.[3]

Actually, LacY was the first symporter to be solubilized from membrane, purified to homogeneity,[10] and shown to catalyze all the translocation reactions typical of the transport system in

Received: October 1, 2012
Revised: November 7, 2012
Published: November 8, 2012

vivo.[11] LacY is often reconstituted in native *E. coli* polar phospholipid membrane extracts as well as in binary mixtures of phosphatidylgycerol (PG) and phosphatidylethanolamine (PE) that mimic the inner membrane of the bacteria. The presence of PE is required not only for its function[12] but also for its correct folding in the membrane during biogenesis.[13] Furthermore, the addition of specific phospholipids to the detergent-purified protein has been recognized as the key for obtaining suitable crystals for X-ray diffraction[14] a fact that emphasizes the strong interplay between LacY and phospholipids.

It has been hypothesized[4,15] that the aspartic acid 68 (D68), a highly conserved residue in the major facilitator superfamily (MFS), where LacY belongs, mediates the interaction between PE and transporters of this superfamily. It has been demonstrated that this residue is important for the protein to be sensitive to the proton gradient but also that it plays a role in facilitating conformational changes needed for substrate translocation.[16] In fact, although D68 position is very sensitive to replacement, several second-site activity revertants have been described,[17] which suggests that D68 is not absolutely irreplaceable for the transport mechanism. D68 mutants are still able to bind substrate, but its translocation is locked. On this basis, the proposed mechanism is that the D68 mutation decreases the probability of opening of the hydrophilic pathway on the periplasmic side of LacY upon sugar binding. This is reinforced by the findings that not only the negative charge of the aspartic acid but also the structure of the amino acid is important in this position. In this regard, even the most conservative replacement, D68E, inactivates LacY transport.[18] This is because D68 interacts with K131 forming a weak H bonding pair which enables LacY dynamics. On the contrary, replacement of position 68 with glutamate results in a stronger charge-pair interaction with lysine 131, thus preventing the necessary chain reorganization for sugar-induced opening of the periplasmic cavity. In this regard, Lensink et al.[15] performed LacY molecular dynamics (MD) simulation studies to investigate specific protein−lipid interactions. These authors found only one lipid-mediated salt bridge between conserved residues in LacY, D68 being the crucial amino acid in this interaction. This bond involves two residues, D68 and K69, and a phospholipid, preferably PE over single and double methylated PE. Interestingly, it has been shown that PC interacts also, weaker than the unmethylated PE, and that PG is never involved in the interaction. Importantly, these results are the first to suggest a possible mechanism for the direct interaction between PE and a member of the MFS transporters.

In previous works[19−21] we have exploited Förster resonance energy transfer (FRET) to study lipid selectivity between a single tryptophan mutant of LacY (W151/C154G), used as donor (D), and different phospholipids labeled with pyrene in the acyl chains that are used as acceptors (A). In the present work we have used W151/C154G and delineated a new mutant W151/C154G/D68C, in which the aspartic acid residue has been replaced by cysteine. The strategy consists of measuring the FRET efficiency between the single tryptophan mutants reconstituted in PE:PG 3:1, mol/mol matrixes, and two different acyl-chain pyrene-labeled phospholipids used as acceptors, Pyr-PG or Pyr-PE. The objectives of these experiments are 2-fold: (i) to ascertain the composition of the annular lipids that surround LacY; (ii) to investigate if the D68C mutation will result in changes in such affinity.

2. MATERIALS AND METHODS

N-Dodecyl-β-D-maltoside (DDM) was purchased from Anatrace (Maumee, OH). 1,2-Palmitoyl-*sn*-glycero-3-phosphoethanolamine (DPPE), 1,2-dioleoyl-*sn*-glycero-3-phosphoethanolamine (DOPE), 1-palmitoyl-2-oleoyl-*sn*-glycero-3-phosphoethanolamine (POPE), and 1-palmitoyl-2-oleoyl-*sn*-glycero-3-(phospho-*rac*-(1-glycerol)) (sodium salt) (POPG) were purchased from Avanti Polar Lipids (Alabaster, AL). 1-Hexadecanoyl-2-(1-pyrenedecanoyl)-*sn*-glycero-3-phosphoglycerol ammonium salt (Pyr-PG) and 1-hexadecanoyl-2-(1-pyrenedecanoyl)-*sn*-glycero-3-phosphoethanolamine ammonium salt (Pyr-PE) were purchased from Invitrogen (Barcelona, Spain). Isopropyl 1-thio-β-D-galactopyranoside (IPTG) was obtained from Sigma Chemical Co. (St. Louis, MO), and Bio-Beads SM-2 were purchased from Bio-Rad (Hercules, CA). All other common chemicals were ACS grade.

2.1. Bacterial Strains and Protein Purification. Single-151W/C154G/D68C LacY mutant was obtained using the Quickchange Site-Directed Mutagenesis Kit (Stratagene) from *E. coli* BL21(DE3) cells (Novagen, Madison, WI) containing plasmid pCS19 encoding single-W151/C154G LacY donated by Dr. H. Ronald Kaback (UCLA, Los Angeles CA). The resultant plasmid pCS19 encoding single-W151/C154G/D68C LacY construct was confirmed by DNA sequencing. The purification of this mutant was achieved following procedures detailed in previous papers.[19−21] Briefly, *E. coli* was grown in Luria−Bertani broth at 30 °C containing ampicillin (100 μg/mL) and induced at the appropriate moment with 0.5 mM isopropyl 1-thio-β-D-galactopyranoside. Cells were disrupted, and the membrane fraction was harvested by ultracentrifugation. Membranes were solubilized by adding DDM and purified by Co (II) affinity chromatography (Talon Superflow, Palo Alto, CA). Protein eluted with 150 mM imidazole was subjected to gel filtration chromatography using a Superdex 200 10/30 column (GE-Healthcare, UK) equilibrated with 20 mM Tris-HCl (pH 7.5), 0.008% DDM. The protein was concentrated using Vivaspin 20 concentrators (30 kDa cutoff; Vivascience, Germany) and stored on ice. Protein identification was performed by SDS/PGE electrophoresis, and protein quantitation was carried out using a micro-BCA kit (Pierce, Rockford, IL).

2.2. Vesicle Preparation and Protein Reconstitution. Liposomes and proteoliposomes were prepared according to methods published elsewhere.[19−21] Briefly, chloroform−methanol (2:1, vol/vol) solutions containing appropriate amounts of both labeled and unlabeled phospholipids were dried under a stream of oxygen-free N_2 in a conical tube. The total concentration of phospholipids was calculated as a function of the desired lipid-to-protein ratio (LPR) and protein concentration (1.5 μM). The mole fraction of fluorescent probe (relative to total lipid) was $x = 0.0025$ for all the experiments. The resulting thin film was kept under high vacuum for approximately 3 h to remove organic solvent traces. Multilamellar liposomes (MLVs) were obtained following redispersion of the film in 20 mM HEPES, 150 mM NaCl buffer, pH 7.40, and applying successive cycles of freezing and thawing below and above the phase transition of the phospholipids, and sonication for 2 min in a bath sonicator. Afterward, large unilamellar liposomes (LUVs) supplemented with 0.2% of DDM were incubated overnight at room temperature. Liposomes were subsequently mixed with the solubilized protein and incubated at 4 °C for 30 min with

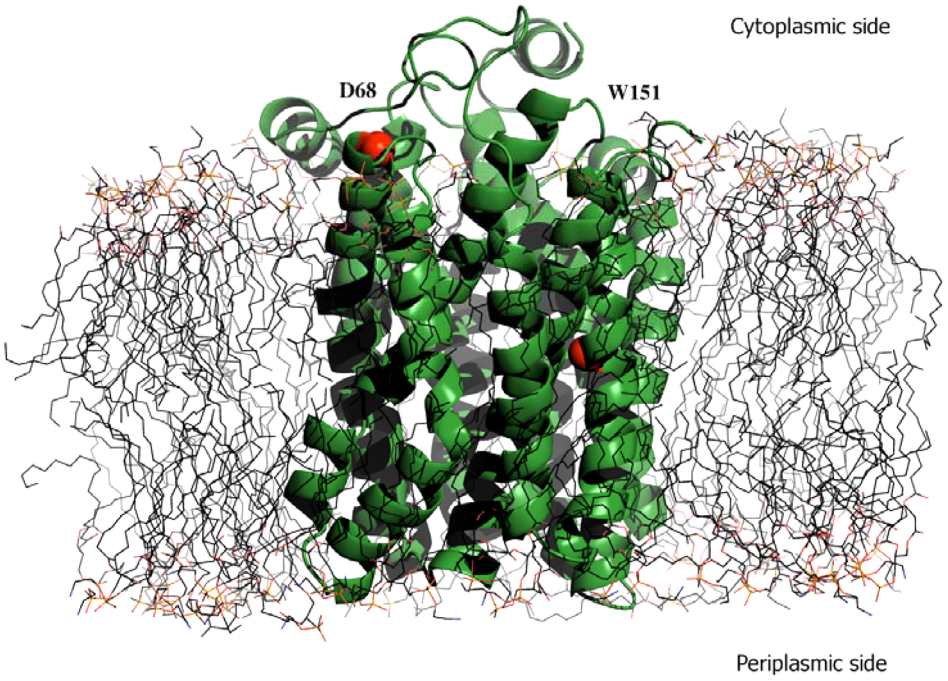

Figure 1. Model of LacY C154G embedded in a POPE matrix. Tryptophan 151 and aspartic acid 68 are highlighted. This model has been constructed using CHARMM-GUI Membrane Builder.

gentle agitation, to obtain a lipid to protein ratio (w/w) of 40. DDM was extracted by addition of polystyrene beads.

2.3. Binding Properties of Single-W151/C154G LacY Reconstituted in Vesicles. Substrate recognition by single-W151/C154G LacY reconstituted in lipid vesicles was tested by adapting a protocol previously described,[20,21] based on the protection of the substrate against thiol modification of LacY. Briefly, 50 μL of proteoliposomes containing 1.5 μM single-W151/C154G/D68C LacY[22] were incubated at room temperature for 5 min with either 15 mM β-D-galactopyranosyl-1-thio-β-D-galactopyranoside (TDG) or 15 mM L-glucose. Next, the samples were incubated with the fluorescent dye fluorescein-5-maleimide for 10 min at room temperature. The reaction was stopped by adding 5 mM DTT. To evaluate the extent of LacY labeling, proteoliposomes were solubilized with 1% SDS and subjected to 12% PAGE gel electrophoresis. In-gel fluorescence was evaluated using a G-BOX gel analysis instrument (Syngene, Cambridge, UK) and compared to the total amount of protein after staining the same gel with Coomassie blue.

2.4. FRET Modeling. Steady-state fluorescence measurements were carried out with an SLM-Aminco 8100 (Urbana, IL) spectrofluorometer. The cuvette holder was thermostatted with a circulating bath (Haake, Germany), which was used to control temperature within 0.1 °C. The fluorescence experiments were performed at 24 °C and 37 °C. The excitation and emission bandwidths were 4/4 and 8/8 nm, respectively. As described in detail elsewhere,[20,21] single tryptophan-LacY mutants (either W151/C154G or W151/C154/D68C), the donors (D), were excited at 295 nm and emission of the pyrene was recovered at 375 nm.

FRET efficiencies (E) are calculated according to the equation

$$E = 1 - \frac{I_{DA}}{I_D} = 1 - \frac{\int_0^\infty i_{DA}(t)\mathrm{d}t}{\int_0^\infty i_D(t)\mathrm{d}t} \tag{1}$$

where I_D and I_{DA} are the tryptophan emission intensities in the absence or presence of pyrene acceptors, respectively. The reported values of experimental E are the averages of triplicate measurements from five separate reconstitutions. The description of the model used to fit the data has been clarified in detail elsewhere.[21] Briefly, we assume the existence of two populations of acceptors (A), one located at the annular shell around the protein and another in the bulk outside it. Then we can write the decay of the fluorescence of the donor D as

$$i_{DA}(t) = i_D(t)\rho_a(t)\rho_r(t) \tag{2}$$

where i_D and i_{DA} are the donor fluorescence decays in the absence and presence of acceptor molecules, respectively. Because the number of annular pyrene phospholipids around each protein molecule is expected to follow a binomial population,[23] the annular contribution to the decay can be expressed as

$$\rho_a(t) = \sum_{n=0}^{m} e^{-nk_t t}\binom{m}{n}\mu^n(1-\mu)^{m-n} \tag{3}$$

where m is the number of phospholipid molecules in the first layer surrounding the protein and k_t is the rate constant for D−A energy transfer, given by

$$k_t = \frac{1}{\tau}\left(\frac{R_0}{R}\right)^6 \tag{4}$$

where in turn τ is the donor lifetime and R_0 is the Forster radius (3.0 nm for the Trp/pyrene),[24] and μ is defined as the probability of each site in the annular ring being occupied by a labeled pyrene phospholipid. This probability can be written more intuitively as

$$\mu = K_s\frac{n_{pyr}}{n_{pyr} + n_{PL}} = K_s X_{pyr} \tag{5}$$

dx.doi.org/10.1021/jp309726v | J. Phys. Chem. B 2012, 116, 14023−14028

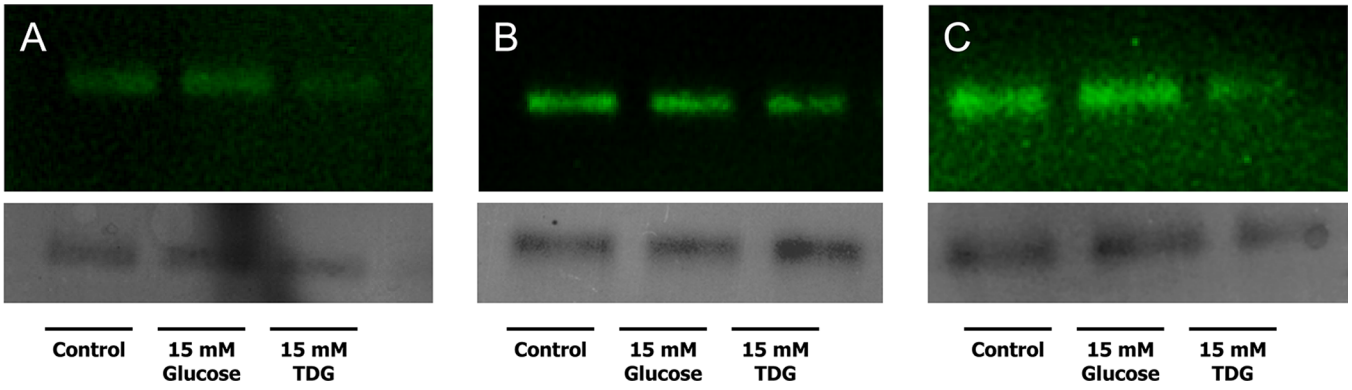

Figure 2. Substrate recognition by single-W151/C154G/D68C LacY reconstituted in DOPE:POPG 3:1 (mol:mol) (A), POPE:POPG 3:1 (mol:mol) (B), and DPPE:POPG 3:1 (mol:mol) (C) proteoliposomes. Fluorescein-maleimide labeling was performed in the presence of 15 mM TDG, 15 mM L-glucose, or no substrate (control). The upper panels (black background) correspond to the fluorescence intensity of fluorescein-labeled protein after being subjected to a 12% SDS−PAGE gel electrophoresis. Lower panels are the same gels after protein staining with Coomassie Blue.

where n are the mole numbers of the labeled (n_{pyr}) and the nonlabeled (n_{PL}) phospholipids, X_{pyr} is the label mole fraction, and K_s is the relative association constant between the labeled and unlabeled phospholipids. Thus, $K_s = 1$ denotes equal probability of finding acceptors in the annular region than in the bulk, whereas $K_s = 0$ means no acceptor in the annular region. Finally, the rate of FRET to acceptors randomly located outside the annular layer ($\rho_r(t)$) is given by

$$\rho_r(t) = \exp\left\{-4n_2\pi l^2 \int_0^{1/\sqrt{l^2+R_e^2}} \frac{1-\exp(-tb^3\alpha^6)}{\alpha^3}\,d\alpha\right\} \quad (6)$$

where $b = (R_0/l)^2\tau^{-1/3}$, n_2 is the acceptor density in each leaflet, and l is the distance between the plane of the donors and the plane of acceptors.

RESULTS AND DISCUSSION

A model of LacY embedded in a bilayer constituted by POPE matrix is shown in Figure 1. The position of W151 that acts as a donor for the FRET experiments is highlighted along with the position of D68, located in helix II facing to the cytoplasmic side of the protein. To assess the folding state of the proteins in the proteoliposomes, binding assays have been performed. Figure 2 shows that for all matrix, β-D-galactopyranosyl 1-thio-β-D-galactopyranoside (TDG) partially blocks fluorescein labeling, indicating that the reconstituted protein can selectively recognize the substrate (TDG over L-glucose) and, therefore, is properly folded in those lipid environments.

A large amount of evidence supports the specific requirement of PE for the proper folding, adequate topology, and activity of LacY.[13,25] Because it is well established that PE may create extensive intermolecular hydrogen bonding, it becomes tentative to hypothesize that a specific interaction between the amine headgroup of PE and some specific amino acid residues of the protein may exist.[4,15] This may be a crucial event that triggers the whole mechanism of active transport. Nevertheless, not only the headgroup is important:[26,27] in recent works where the protein was reconstituted in single phospholipid matrixes[21] and in others based on measuring transport of genetically modified bacteria,[28] the importance of the acyl chain moiety in the interaction between phospholipids and membrane proteins has been pointed out.

The D68 residue, situated at the edge of the interface between helix II and the intracellular loop II-III, is a highly conserved residue in the MFS that has been proposed to mediate the interaction between PE and the protein in the cases of LacY[15] and LmrP,[4] another member of this superfamily. It has been also suggested that this interaction is necessary for the protein to be sensitive to the proton gradient.[4] To further investigate this system, our work's aim is to study if this particular mutation, D68C, would lead to a change of the phospholipid composition intimately interacting with the protein. Particularly, and giving that this mutation inhibits LacY conformational changes after ligand binding,[16] our observations may provide new evidence on the relation between lipid−protein selectivity and conformational mobility of LacY in the membrane.

Figure 3 shows the experimental E values at 25 °C and 37 °C obtained for W151/C154/D68C LacY with both Pyr acyl-labeled phospholipids (Pyr-PE and Pyr-PG) in the three binary phospholipids systems under study (DOPE:POPG, POPE:-POPG, and DPPE:POPG, all at 3:1 molar ratio). Clearly, Pyr-PE is preferred over Pyr-PG, at both temperatures and all phospholipid matrixes. Consequently, the values of μ listed in Table 1 are always the highest for Pyr-PE irrespective of the matrix. These results coincide qualitatively with those observed in POPE:POPG and DOPE:POPG systems, using the W151/C154G mutant of LacY.[20] To rationalize these, we should take in consideration the thermotropic nature of the mixtures used. Thus, while at 25 °C and 37 °C DOPE:POPG remains in the L_α phase and DPPE:POPG exhibits coexistence between the L_α and L_β phases at both temperatures, POPE:POPG still exhibits the L_β phase at 25 °C and L_α phase 37 °C.[29] Because LacY inserts preferentially in fluid phases,[29,30] the negligible variations in the μ values when increasing the temperatures indicate that the lipid environment around W151/C154G/D68C mutant does not change.

For a better comparison Figure 4 shows the normalized values of E between single-W and Pyr-PE (the phospholipid of most interest for these studies) at 37 °C for both LacY versions. As can be seen, the normalized values of E were similar for both mutants in DOPE:POPG, and lower and higher normalized E values were observed in POPE:POPG and DPPE:POPG, respectively, for the systems where the 68 residue has been mutated into cysteine. These results support the preference for

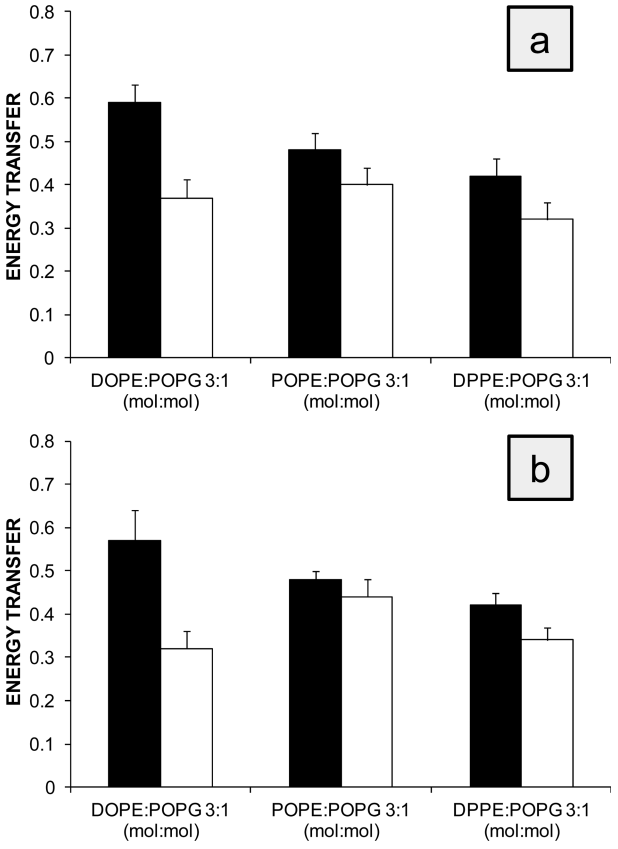

Figure 3. FRET efficiency between W151 of the mutant W151/C154G/D68C LacY and Pyr-PE (black columns) and Pyr-PG (white columns) in different lipid matrixes at 25 °C (a) and 37 °C (b). Proteoliposomes (1.5 μM LacY) of DOPE:POPG 3:1 (mol:mol), POPE:POPG 3:1 (mol:mol), and DPPE:POPG 3:1 (mol:mol) were doped with $x = 0.0025$ of label. The error bars stand for $\sigma/n^{1/2}$, σ being the standard deviation and n the number of measurements performed.

Table 1. Experimental Efficiencies E and Probabilities μ for Each Site in the Single-W/C154G/D68C LacY Annular Ring Being Occupied by a Pyrene Phospholipid

composition (3:1, mol/mol)		experimental E	μ
	25 °C		
DOPE/POPG	Pyr-PE	0.59	0.05
	Pyr-PG	0.37	0.02
POPE/POPG	Pyr-PE	0.48	0.03
	Pyr-PG	0.40	0.02
DPPE/POPG	Pyr-PE	0.42	0.02
	Pyr-PG	0.32	0.01
	37 °C		
DOPE/POPG	Pyr-PE	0.57	0.05
	Pyr-PG	0.32	0.01
POPE/POPG	Pyr-PE	0.48	0.03
	Pyr-PG	0.44	0.03
DPPE/POPG	Pyr-PE	0.42	0.02
	Pyr-PG	0.34	0.01

PE in systems in the L_α phase as well as a higher relative affinity between POPE and W151/C154G than between POPE and W151/C154G/D68C. That is, the introduction of the mutation in the 68 site results in a change of LacY affinity for POPE, leading to a modification in the composition of the phospholipids in close contact with the protein. Interestingly,

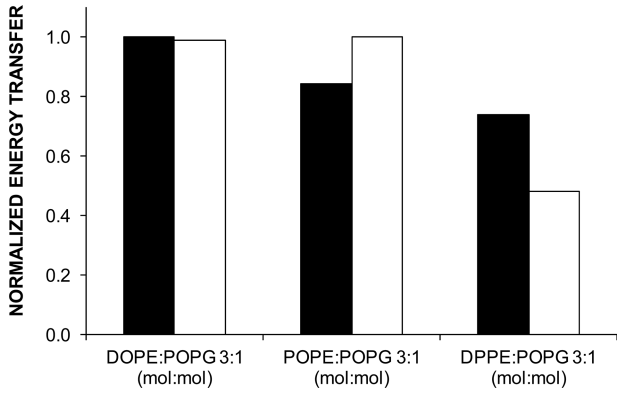

Figure 4. Comparison of normalized FRET efficiency at 37 °C between W151 of the mutant single-W/C154G/D68C LacY and Pyr-PE (black columns) and W151 of the single-W/C154G LacY and Pyr-PE (white columns).

while the model could not be applicable for the DPPE:POPG system when the donor was W151/C154G, efficient energy transfer occurs when using the W151/C154/D68C mutant. Clearly the D68C mutant studied here is able to recruit Pyr-PE to its vicinity even in the presence of phase separation. This is at variance with the W151/C154G. In that case, Pyr-PG presented more efficient FRET values than Pyr-PE in DPPE:POPG as a consequence of L_α and L_β coexistence.[20]

These observations are in concordance with the earlier finding that LacY promotes phospholipid microdomain formation around the protein.[31] The evidence of such a laterally segregated domain was gathered from two types of monomer to excimer ratio measurements: among pyrene-labeled phospholipids and between pyrene-labeled LacY and surrounding pyrene-labeled phospholipids. Although the interpretation was based on the mismatch between the protein and the phospholipids, our results show that the lipid selectivity depends on a complex mechanism of phospholipids adaptation to the protein surface,[26,27] that should be related to the lateral pressure profile of each species[32] and/or intrinsic curvature of the phospholipids.[33] According to MD simulations,[15] however, the specific interaction between PE and aspartic acid 68 could be anticipated. Hence, this mutation (D68C) may hinder the PE-68 residue interaction and consequently modify the protein−lipid affinity.

In conclusion, our results suggest that the mutation in the 68 position positively changes the selectivity of the protein for phospholipids and may induce a change in the conformational dynamics of LacY by recruitment of the phospholipid species most adaptable to the geometrical needs of the protein. Thus, while the lipid selectivity for D68 is DOPE ~ POPE > DPPE, the mutation increases the protein selectivity for DOPE over POPE and DPPE. This observation demonstrates the implication of the acyl chains in the interaction and points to a possible requirement for the heteroacid phospholipids besides the headgroup requirement. Furthermore, it is demonstrated here that although POPE is still present in the boundary of W151/C154G/D68C LacY, the mutation decreases the preference of the protein for this phospholipid. This might support the proposed mechanism that this amino acid is involved in the interaction between the protein and POPE,[4] possibly forming a lipid-mediated salt bridge,[15] an event that can be intimately related with the increase of the open

dx.doi.org/10.1021/jp309726v | J. Phys. Chem. B 2012, 116, 14023−14028

probability of the periplasmic side of LacY upon sugar binding.[16]

AUTHOR INFORMATION

Corresponding Author

*E-mail: jordiborrell@ub.edu.

Notes

The authors declare no competing financial interest.

ACKNOWLEDGMENTS

Special thanks to Dr. Josep M. Campanera for artwork provided and helpful discussions. C.S.G. is a recipient of a FPI fellowship from the Ministerio de Ciencia e Innovación of Spain. This work has been supported by grant CTQ-2008-03922/BQU from Ministerio de Ciencia e Innovación of Spain. C.S.G., O.D., M.T.M., and J.H.B. thank Universitat de Barcelona for financial support. L.M.S.L. acknowledges funding by FEDER (COMPETE program), and by FCT (Fundação para a Ciência e a Tecnologia), project references PTDC/QUI-BIQ/099947/2008, PTDC/QUI-BIQ/112067/2009, and FCOMP-01-0124-FEDER-010787 (FCT PTDC/QUI-QUI/098198/2008).

REFERENCES

(1) Pao, S. S.; Paulsen, I. T.; Saier, M. H. *Microbiol. Mol. Biol. Rev.* **1998**, *62*, 1−34.

(2) Van Bambeke, F.; Balzi, E.; Tulkens, P. M. *Biochem. Pharmacol.* **2000**, *60*, 457−470.

(3) Guan, L.; Kaback, R. H. *Annu. Rev. Biophys. Biomol. Struct.* **2006**, *35*, 67−91.

(4) Hakizimana, P.; Masureel, M.; Gbaguidi, B.; Ruysschaert, J. M. *J. Biol. Chem.* **2008**, *283*, 9369−9376.

(5) Yu, J. L.; Grinius, L.; Hooper, D. C. *J. Bacteriol.* **2002**, *184*, 1370−1377.

(6) Abramson, J.; Simirnova, I.; Kasho, V.; Vernen, G.; Kaback, H. R.; Iwata, S. *Science* **2003**, *301*, 610−615.

(7) Mirza, O.; Guan, L.; Verner, G.; Iwata, S.; Kaback, H. R. *EMBO J.* **2006**, *25*, 1177−1183.

(8) Guan, L.; Mirza, O.; Verner, G.; Iwata, S.; Kaback, H. R. *Proc. Natl. Acad. Sci. U.S.A.* **2007**, *104*, 15294−15298.

(9) Chaptal, V.; Kwon, S.; Sawaya, M. R.; Guan, L.; Kaback, H. R.; Abramson, J. *Proc. Natl. Acad. Sci. U.S.A.* **2011**, *108*, 9361−9366.

(10) Viitanen, P.; Newman, M. J.; Foster, D. L.; Wilson, T. H.; Kaback, H. R. *Methods Enzymol.* **1986**, *125*, 429−452.

(11) Viitanen, P.; Garcia, M. L.; Kaback, H. R. *Proc. Natl. Acad. Sci. U.S.A.* **1984**, *81*, 1629−1633.

(12) Chen, C. C.; Wilson, T. H. *J. Biol. Chem.* **1984**, *259*, 10150−10158.

(13) Dowhan, W.; Bogdanov, M. *Annu. Rev. Biochem.* **2009**, *78*, 515−540.

(14) Guan, L.; Smirnova, I. N.; Verner, G.; Nagamori, S.; Kaback, H. R. *Proc. Natl. Acad. Sci. U.S.A.* **2006**, *103*, 1723−1726.

(15) Lensink, M. F.; Govaerts, C.; Ruysschaert, J. M. *J. Biol. Chem.* **2010**, *285*, 10519−26.

(16) Liu, Z.; Madej, M. J.; Kaback, H. R. *J. Mol. Biol.* **2010**, *396*, 617−626.

(17) Jessen-Marshall, A.; Brooker, R. J. *J. Biol. Chem.* **1996**, *271*, 1400−1404.

(18) Jessen-Marshall, A.; Paul, N. J.; Brooker, R. J. *J. Biol. Chem.* **1995**, *270*, 16251−16257.

(19) Picas, L.; Montero, M. T.; Morros, A.; Vázquez-Ibar, J. L.; Hernández-Borrell, J. *Biochim. Biophys. Acta* **2010**, *1798*, 291−296.

(20) Picas, L.; Suárez-Germà, C.; Montero, M. T.; Vázquez-Ibar, J. L.; Hernández-Borrell, J.; Prieto, M.; Loura, L. M. *Biochim. Biophys. Acta* **2010**, *1798*, 1707−1713.

(21) Suárez-Germà, C.; Loura, L. M.; Prieto, M.; Domènech, O.; Montero, M. T.; Rodríguez-Banqueri, A.; Vázquez-Ibar, J. L.; Hernández-Borrell, J. *J. Phys. Chem. B* **2012**, *116*, 2438−2445.

(22) Vázquez-Ibar, J. L.; Guan, L.; Svrakic, M.; Kaback, H. R. *Proc. Natl. Acad. Sci. U.S.A.* **2003**, *100*, 12706−12711.

(23) Fernandes, F.; Loura, L. M. S.; Koehorst, R.; Spruijt, R. B.; Hemminga, M. A.; Fedorov, A.; Prieto, M. *Biophys. J.* **2004**, *87*, 344−352.

(24) Tahara, Y.; Murata, M.; Ohnishi, S.; Fujiyoshi, Y.; Kikuchi, M.; Yamamoto, Y. *Biochemistry* **1992**, *31*, 8747−8754.

(25) Bogdanov, M.; Dowhan, W. *J. Biol. Chem.* **1995**, *1270*, 732−739.

(26) Cantor, R. S. *J. Phys. Chem.* **1997**, *101*, 1723−1725.

(27) Marsh, D. *Biochim. Biophys. Acta* **2008**, *1778*, 1545−1575.

(28) Bogdanov, M.; Heacock, P.; Guan, Z.; Dowhan, W. *Proc. Natl. Acad. Sci. U.S.A.* **2010**, *107*, 15057−15062.

(29) Picas, L.; Carretero-Genevrier, A.; Montero, M. T.; Vázquez-Ibar, J. L.; Seantier, B.; Milhiet, P.-E.; Hernández-Borrell, J. *Biochim. Biophys. Acta* **2010**, *1798*, 1014−1019.

(30) Suárez-Germà, C.; Montero, M. T.; Ignés-Mullol, J.; Hernández-Borrell, J.; Domènech, O. *Phys. Chem. B* **2011**, *115*, 12778−12784.

(31) Lehtonen, J. Y.; Kinnunen, P. K. J. *Biophys. J.* **1997**, *72*, 1247−1257.

(32) Olilla, S.; Hyvönen, M. T.; Vattulaine, I. *J. Phys. Chem. B* **2007**, *111*, 3139−3150.

(33) Wikström, M.; Kelly, A. A.; Georgiev, A.; Eriksson, H. M.; Klement, M. R.; Bogdanov, M.; Dowhan, W.; Wieslander, A. J. *Biol. Chem.* **2009**, *284*, 954−965.

4.3.3 Phospholipid−lactose permease interaction as reported by a head-labeled pyrene phosphatidylethanolamine: a FRET study

Suárez-Germà, C., Loura, L. M. S., Prieto, M., Domènech, Ò., Campanera, J. M., Montero, M. T., Hernández-Borrell, J. (**2013**).
The Journal of Physical Chemistry B, 117,6741-8.

4.3.3.1 Summary

FRET measurements were performed in preceding works to study the selectivity between a single-tryptophan mutant of LacY (used as D) and phospholipid probes labelled with pyrene at the acyl chain moiety (used as A). In the present study, the reported results were obtained by using the same single-W151/C154G LacY mutant and binary lipid mixtures of PE differing in the acyl chain composition (DOPE, POPE, DPPE) and POPG (PE:PG 3:1, mol/mol) doped with a phospholipid probe labeled with pyrene at the headgroup. The selected lipid mixtures had already been proved suitable for the insertion of LacY (see 4.3.2). The head-labelled phospholipid, 1,2-dioleoyl-*sn*-glycero-3-phosphoethanolamine-N-(1-pyrenesulfonyl) ammonium salt (HPyr-PE) was employed with the aim to study the independent contributions of the acyl chains in the LacY-PE interaction occurring at the annular region. Indeed, recent research has revealed that the effect of lipids on LacY activity involves both the hydrophilic headgroup domain (there is a need for species lacking a net-charge) and the hydrophobic acyl chain domain (POPC and POPE sustain full protein activity, DOPE sustains very low activity, and LacY in DOPC is inactive regarding uphill transport) [140]. In turn, PE headgroup was selected since a large amount of evidence points to this structure as the more adequate to accomplish the specific requirements for proper folding and correct function of the protein [122].

In order to discuss the obtained results, it was important to take into account the fact that the pyrene moiety, which is characterized by a planar structure and high hydrophobicity, may introduce changes in the physicochemical properties of the host bilayer. In particular, the presence of a large entity at the headgroup level, in addition to the lack of hydrogen bonding of the structure, may result in an increase in the surface

area of the bilayer. Thus, the capabilities of HPyr-PE as a good PE reporter were questioned.

In the performed FRET experiments the lowest energy transfer values were obtained for DOPE:POPG (3:1, mol/mol) at both 25 and 37 °C and POPE:POPG (3:1, mol/mol) at 37 °C. In addition, POPE:POPG (3:1, mol/mol) was the only mixture that presented a significant change when the temperature was varied. In agreement with these observations, the probability that a given site in the annular ring is occupied by a labelled pyrene phospholipid (μ) was the highest for DPPE:POPG (3:1, mol/mol) at 25 °C and POPE:POPG (3:1, mol/mol) at 37 °C. The presence of HPyr-PE in the annular region in DOPE:POPG (3:1, mol/mol) was almost negligible at both temperatures. To explain these results it is important to consider LacY preference for L_α phases. Hence, in DPPE:POPG (3:1, mol/mol) a LacY selectivity for a PE over PG headgroup was observed (considering HPyr-PE partitioned in L_α domains due to its unsaturated acyl chains). In the case of POPE:POPG (3:1, mol/mol), high FRET efficiencies in the fully fluid system at 37 °C may indicate that LacY much prefers to be surrounded by PE lipids (including the probe) than POPG. On the contrary, at 25 °C and close to the T_m, the system might display L_α/L_β coexistence and LacY may preferentially locate in PE-impoverished fluid domains. That is why some annular sites could be occupied by POPG and the FRET efficiency was decreased. Finally, DOPE:POPG (3:1, mol/mol) system remained the most complicated to interpret. In this case, low FRET efficiencies and low μ values could be attributed to displacement of the acceptor by DOPE and/or POPG. However, previous works showed preference for DOPE in this same host mixture [65]. Therefore, it is much more likely that this displacement was caused by an enrichment of DOPE rather than POPG in this region. These results could be related to the different spontaneous curvatures (C_0) of each PE species [$-C_0$(HPyr-PE) < $-C_0$(DOPE) < -C_0(POPE)].

When comparing results at 37 °C with previous FRET experiments performed with PE labelled with pyrene in the acyl chain moiety (TPyr-PE), POPE:POPG (3:1, mol/mol) was the only composition presenting equal values of normalized energy transfer efficiency for both labelling forms. DOPE:POPG (3:1, mol/mol) and DPPE:POPG (3:1, mol/mol) presented opposite behaviours: whereas the former mixture presented low normalized energy transfer efficiency with HPyr-PE and high efficiency with TPyr-PE, the second mixture varied in the opposite way. These differences in behaviour of the

head-labelled and tail-labelled pyrene acceptor probes could be probably related to differences in their acyl chain compositions and packing requirements for the bulky pyrene moiety.

In all the systems higher E/M ratios were measured for annular probes relative to probes in the bulk, indicating a segregation of the fluorophore in this region. Additionally, global E/M ratios were lower for HPyr-PE by comparison to E/M ratios obtained using Pyr-PE labelled in the acyl chain. However, both labelling forms showed parallel trends, reflecting pyrene probe enrichment in the annular region of LacY in the phase separated DPPE:POPG (3:1, mol/mol) mixture (probably due to probe partition in one of the domains) and depletion in the DOPE:POPG (3:1, mol/mol) mixture.

The main conclusions raised from these results suggest that (i) for phase-separated systems, LacY would be located in fluid domains nominally enriched in POPG, and if a given proportion of PE is present in this phase, it will be mainly located around the protein; and (ii) in the absence of phase separation, LacY is preferentially surrounded by PE and, in particular, seems to be sensitive to the lipid C_0, with a preference for more negative C_0 values.

4.3.3.2 Highlights

- A PE probe labelled with pyrene at the headgroup (HPyr-PE) was used to investigate the independent contribution of the acyl chains in the LacY-PE interaction. This was done through FRET measurements between the fluorophores and the tryptophan of single-W151/C154G LacY mutant embedded in different biomimetic matrices: DOPE:POPG (3:1, mol/mol), POPE:POPG (3:1, mol/mol), and DPPE:POPG (3:1, mol/mol).
- Specific structure of HPyr-PE as well as results difficult to interpret made arisen the question whether this probe is indeed a good PE reporter.
- From the obtained results, it can be concluded that LacY would be located in fluid domains nominally enriched in POPG, and if a given proportion of PE is present in this phase, it will be mainly located around the protein. Hence, DOPE and POPE might be the main annular components in their respective systems, whilst DPPE would not collocate with the protein. Interestingly, in this last system, HPyr-PE,

bearing two unsaturated chains might be segregated in fluid phases and thus it would be selected preferentially by the protein over POPG.

- In the absence of phase separation LacY is preferentially surrounded by PE (selectivity DOPE > POPE). This could be explained by a preference of the protein for more negative C_0 values. However, caution must be taken regarding these interpretations, especially due to a possible less adequate physico-chemical behaviour of HPyr-PE as a PE lipid reporter.

THE JOURNAL OF PHYSICAL CHEMISTRY B

Article

pubs.acs.org/JPCB

Phospholipid–Lactose Permease Interaction As Reported by a Head-Labeled Pyrene Phosphatidylethanolamine: A FRET Study

Carme Suárez-Germà,[†,‡] Luís M. S. Loura,[∥,⊥] Manuel Prieto,[§] Òscar Domènech,[†,‡] Josep M. Campanera,[†] M. Teresa Montero,[†,‡] and Jordi Hernández-Borrell*[,†,‡]

[†]Departament de Fisicoquímica, Facultat de Farmàcia, and [‡]Institut de Nanociència i Nanotecnologia (IN[2]UB), Universitat de Barcelona, 08028 Barcelona, Spain

[§]Centro de Química-Física Molecular and Institute of Nanoscience and Nanotechnology (IN), Instituto Superior Técnico, Universidade Técnica de Lisboa, 1049-001 Lisboa, Portugal

[∥]Faculdade de Farmácia, Universidade de Coimbra, Azinhaga de Santa Comba, 3000-548 Coimbra, Portugal

[⊥]Centro de Química de Coimbra, 3004-535 Coimbra, Portugal

ABSTRACT: Förster resonance energy transfer (FRET) measurements were performed in preceding works to study the selectivity between a single-tryptophan mutant of lactose permease (LacY) of *Escherichia coli* (used as the donor) and phospholipid probes labeled with pyrene at the acyl chain moiety (used as the acceptor). In the present work, we report the results obtained by using the same LacY mutant (W151/C154G) and binary lipid mixtures of phosphatidylethanolamine (PE) differing in the acyl chain composition and 1-palmitoyl-2-oleoyl-*sn*-glycero-3-[phospho-*rac*-(1-glycerol)] (POPG) (3:1 mol/mol) doped with a phospholipid probe labeled with pyrene at the headgroup. The use of 1,2-dioleoyl-*sn*-glycero-3-phosphoethanolamine-*N*-(1-pyrenesulfonyl) ammonium salt (HPyr-PE), which bears two unsaturated acyl chains, enabled the investigation of the specific interaction between LacY and HPyr-PE. The main conclusions raised from our results suggest that (i) for phase-separated systems, LacY would be located in fluid domains nominally enriched in POPG, and if a given proportion of PE is present in this phase, it will be mainly located around LacY; and (ii) in the absence of phase separation, LacY is preferentially surrounded by PE and, in particular, seems to be sensitive to the lipid spontaneous curvature.

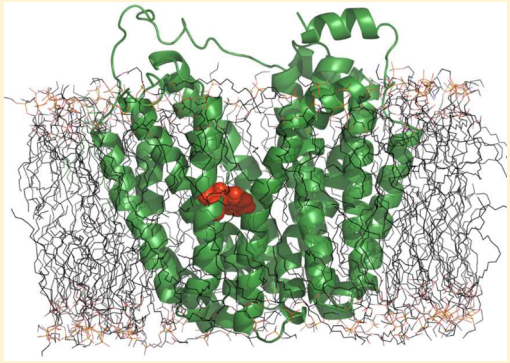

INTRODUCTION

Lactose permease (LacY) is a membrane protein found within the inner membrane of *Escherichia coli* that belongs to the major facilitator superfamily (MFS), a very large group of membrane transporter proteins that are evolutionarily related. LacY is probably the best characterized of the proteins belonging to the 12 transmembrane segment (TMS) α-helix group.[1] The X-ray structure of the protein[2,3] was first obtained from the conformationally constrained C154G mutant.[4] Later, the wild-type permease X-ray structure was elucidated by manipulating the phospholipid content during the crystallization process.[5] LacY cotransports galactopyranosides and H^+ into the bacterial cytoplasm and is considered to be a paradigm for secondary transporters in membranes. Indeed, the protein is the substrate whereby transduction between the energy stored in the electrochemical H^+ gradient ($\Delta\tilde{\mu}_{H^+}$) downhill and the accumulation of galactopyranosides uphill occurs. Remarkably, the phenomenological behavior of the transport is sustained not only by the structure of the protein but also by an extensive number of biophysical and biochemical experiments accumulated over the years.[6] Although some details are not totally understood, there is a consensus on the basic mechanism of lactose/H^+ transport, in which only six side chains from the 417 amino acid residues of the protein are irreplaceable with respect to active transport. In this mechanism, Glu-126 (helix IV) and Arg-144 (helix V) have been identified as crucial parts of the binding site for the substrate, and Glu-269 (helix VIII), Arg-302 (helix IX), His-322 (helix X), and Glu-325 (helix X) have been shown to be irreplaceable with respect to H^+ translocation. In the postulated mechanism, the protonated state is characterized by the H^+ shared between Glu-269 and His-322. It is noteworthy that the protein catalyzes exchange and counterflow without translocation of H^+. It is widely believed that all of the conformational changes undergone by the protein depend on internal H^+ transport throughout the protein that is brought about by transfer between acidic residues. However, the two non-chemiosmotic mechanisms rather suggest that binding of the substrate is the trigger step for the whole mechanism.[1] Recently, a theoretical study showed that LacY displays the structural dynamics required for function only when it is embedded in a 1-palmitoyl-2-oleoyl-*sn*-glycero-3-phosphoethanolamine (POPE) matrix.[7] Indeed, it was largely believed that

Received: March 2, 2013
Revised: May 6, 2013
Published: May 6, 2013

   dx.doi.org/10.1021/jp402152n | *J. Phys. Chem. B* 2013, 117, 6741–6748

protonation of the amino group of phosphatidylethanolamine (PE)[8] is a basic requirement for the function and also for the correct folding of LacY in the membrane during biogenesis.[9] However, new studies[10] revealed that the activity is sustained not only by PE but also by phosphatidylcholine (PC). Significantly, a recent work by Vitrac et al.[11] proved that the effect of lipids on LacY activity involves both the hydrophilic headgroup domain and the hydrophobic fatty acid domain. That work demonstrated the preference of LacY for headgroups with a lack of net charge (independent of the presence of an ionizable amine) and heteroacid acyl chains, a finding that opened the question of the role of the hydrophobic moiety in the permease activity. Actually, a few works, most of them theoretical,[12] had already focused in the importance of the acyl chain composition of the phospholipids in providing adequate adaptation to the protein surface during the conformational changes undergone during the transport.

Pyrene-labeled phospholipids have been widely accepted as good analogues of naturally occurring lipids.[13,14] The photophysical properties of pyrene have been differently exploited in the past to investigate structural features such as the proximity of specific residues[15] and the lipid dynamics in reconstituted LacY proteoliposomes.[16,17] In this regard, Förster resonance energy transfer (FRET) has been successfully used in the investigation of membrane lipid selectivity[18] and particularly in studies of the interactions of LacY with PEs and phosphoglycerol (PG). FRET methodologies have been exploited by our group to prove (i) the selectivity of LacY for POPE in favor of 1-palmitoyl-2-oleoyl-*sn*-glycero-3-phosphoglycerol (POPG)[19] and 1-palmitoyl-l-2-oleoyl-*sn*-glycero-3-phosphocholine (POPC)[20] and (ii) the preference of LacY for fluid phases of the membrane.[21] On this basis, in the present work we performed FRET experiments to measure the efficiency (E) of energy transfer between W151/C154G LacY and 3:1 mol/mol PE/POPG mixtures with differing acyl chain composition of the PE component [1,2-dioleoyl-*sn*-glycero-3-phosphoethanolamine (DOPE), POPE, and 1,2-dipalmitoyl-*sn*-glycero-3-phosphoethanolamine (DPPE)] and containing a probe labeled at the headgroup with pyrene, 1,2-dioleoyl-*sn*-glycero-3-phosphoethanolamine-*N*-1-pyrenesulfonyl ammonium salt (HPyr-PE). The selected lipid mixtures are suitable for the insertion of LacY, as shown previously.[21] This strategy is different to others used previously, in which the pyrene acceptors were attached to the acyl chain moiety.[19−23] Hence, the use of HPyr-PE enables the investigation of the specific interaction between LacY and the probe, which bears two unsaturated acyl chains, in competition with nonfluorescent PE having varying acyl chain compositions, eventually avoiding perturbation due to labeled acyl chains.

MATERIALS AND METHODS

Materials. *N*-Dodecyl-β-D-maltoside (DDM) was purchased from Anatrace (Maumee, OH, USA). DPPE, DOPE, POPE, 1-palmitoyl-2-oleoyl-*sn*-glycero-3-[phospho-*rac*-(1-glycerol)] sodium salt (POPG), and HPyr-PE were purchased from Avanti Polar Lipids (Alabaster, AL, USA). 1-Hexadecanoyl-2-(1-pyrenedecanoyl)-*sn*-glycero-3-phosphoethanolamine ammonium salt (TPyr-PE) was purchased from Invitrogen (Life Technologies Ltd., Paisley, UK). Isopropyl-1-thio-β-D-galactopyranoside (IPTG) was obtained from Sigma Chemical (St. Louis, MO, USA), and polystyrene Bio-Beads SM-2 were purchased from Bio-Rad (Hercules, CA, USA). All other common chemicals were ACS grade.

Bacterial Strains and Protein Purification. These detailed procedures have been described in previous papers.[20,21] Briefly, *E. coli* BL21(DE3) cells (Novagen, Madison, WI, USA) transformed with plasmid pCS19 encoding the single-tryptophan mutant W151/C154G LacY provided by Dr. H. Ronald Kaback (UCLA) were grown in Luria−Bertani broth containing ampicillin (100 μg/mL) at 30 °C and induced at the appropriate moment with 0.5 mM IPTG. The cells were disrupted, and the membrane fraction was harvested by ultracentrifugation. The membranes were solubilized by adding DDM and purified by Co(II) affinity chromatography (Talon Superflow, Palo Alto, CA, USA). Protein eluted with 150 mM imidazole was subjected to gel-filtration chromatography using a Superdex 200 10/300 column (GE-Healthcare, Buckinghamshire, UK) equilibrated with 20 mM Tris-HCl (pH 7.6) containing 0.008% DDM. The protein was concentrated using Vivaspin 20 concentrators (30 kDa cutoff; Vivascience, Göttingen, Germany) and stored on ice. Protein identification was performed by sodium dodecyl sulfate polyacrylamide gel electrophoresis (SDS-PAGE), and protein quantitation was carried out using a Micro BCA kit (Pierce, Rockford, IL).

Vesicle Preparation and Protein Reconstitution. Liposomes and proteoliposomes were prepared according to methods published elsewhere.[20,21] Briefly, 2:1 (v/v) chloroform/methanol solutions containing appropriate amounts of both labeled and unlabeled phospholipids were dried under a stream of oxygen-free N_2 in a conical tube. The total concentration of phospholipids was calculated as a function of the desired lipid/protein ratio (LPR) and protein concentration (1.5 μM). The amount of fluorescent probe was x = 0.0025 for all the experiments. The resulting thin film was kept under high vacuum for ∼3 h to remove organic solvent traces. Multilamellar liposomes (MLVs) were obtained following redispersion of the film in 20 mM HEPES buffer (pH 7.40) containing 150 mM NaCl, application of successive cycles of freezing and thawing below and above the phase transition of the phospholipids, and sonication for 2 min in a bath sonicator. Afterward, large unilamellar liposomes (LUVs) supplemented with 0.2% DDM were incubated overnight at room temperature. The liposomes were subsequently mixed with the solubilized protein and incubated at 4 °C for 30 min with gentle agitation to obtain an LPR (w/w) of 40. DDM was extracted by addition of polystyrene beads. The obtained LUVs presented a diameter of ∼350 nm according to dynamic light scattering measurements.

Fluorescence Measurements. Steady-state fluorescence measurements were carried out with an SLM-Aminco 8100 spectrofluorometer (Urbana, IL, USA). The cuvette holder was thermostatted with a circulating bath (Haake, Germany), which was used to control the temperature within 0.1 °C. The fluorescence experiments were performed at 25 and 37 °C. The excitation/emission bandwidths were 4/4 and 8/8 nm, respectively. As described in detail elsewhere,[20,21] for energy transfer measurements, the W151/C154G LacY mutant, used as the donor (D), was excited at 295 nm, and the pyrene emission of HPyr-PE, used as the acceptor (A), was recovered at 375 nm. Annular fluidity was determined using the annular excimer fluorescence/monomer fluorescence (E/M) ratio, as described elsewhere.[24] Pyrene (HPyr-PE or TPyr-PE) was excited at 295 nm, and the fluorescence spectra were scanned from 350 to 500 nm. To calculate the E/M ratio, we used the signal intensities at 375 nm (corresponding to the peak of the monomer band) and 470 nm (the maximum of the pyrene

dx.doi.org/10.1021/jp402152n | J. Phys. Chem. B 2013, 117, 6741−6748

excimer band). In the case of global fluidity, the bulk E/M ratio was calculated likewise but with direct excitation of the pyrene moiety in HPyr-PE or TPyr-PE at its own excitation peak (338 nm).

FRET Modeling. FRET efficiencies (E) were calculated according to the equation

$$E = 1 - \frac{I_{DA}}{I_D} = 1 - \frac{\int_0^\infty i_{DA}(t)\,dt}{\int_0^\infty i_D(t)\,dt} \quad (1)$$

where I_D and I_{DA} are the integrated tryptophan emission intensities in the absence or presence of the pyrene acceptors, respectively, and $i_D(t)$ and $i_{DA}(t)$ are the corresponding emission intensities at time t. The reported experimental E values are averages of triplicate measurements.

The model used to fit the data has been described in detail elsewhere.[20] Briefly, we assume the existence of two populations of acceptors, those located in the annular shell around the protein (denoted by "a") and those randomly distributed in the bulk outside this shell (denoted by "r"). Then we can write the fluorescence intensity of the donor in the presence of acceptors at time t as

$$i_{DA}(t) = i_D(t)\rho_a(t)\rho_r(t) \quad (2)$$

where $\rho_a(t)$ and $\rho_r(t)$ are the annular and random contributions to the donor fluorescence decay, respectively. Since the number of annular pyrene phospholipids around each protein molecule is expected to follow a binomial population,[18] the annular contribution to the decay can be expressed as

$$\rho_a(t) = \sum_{n=0}^{m} e^{-nk_t t}\binom{m}{n}\mu^n(1-\mu)^{m-n} \quad (3)$$

in which m is the total number of phospholipid molecules in the first layer surrounding the protein, μ is the probability that a given site in the annular ring is occupied by a labeled pyrene phospholipid, and k_t is the rate constant for D−A energy transfer, given by

$$k_t = \frac{1}{\tau}\left(\frac{R_0}{R}\right)^6 \quad (4)$$

where τ is the donor lifetime, R_0 is the Förster radius (3.0 nm for the tryptophan/pyrene),[25] and R is the D−A distance. Finally, the contribution to the decay due to FRET to acceptors randomly located outside the annular layer is given by

$$\rho_r(t) = \exp\left\{-4n_2\pi l^2 \int_0^{1/\sqrt{l^2+R_e^2}} \frac{1-\exp(-tb^3\alpha^6)}{\alpha^3}\,d\alpha\right\} \quad (5)$$

where $b = (R_0/l)^2\tau^{-1/3}$, n_2 is the acceptor density in each leaflet, l is the distance between the plane of the donor and the plane of the acceptor, and R_e is the exclusion distance along the bilayer plane between the protein axis and the annular lipid molecules, which is obtained from the relation $R = (w^2 + R_e^2)^{1/2}$, where $w = 1.2$ nm is the estimated transverse distance between the tryptophan and the bilayer center.[21]

In our previous works, this FRET model was applied to lipids labeled with pyrene on the acyl chains. To adapt it to head-labeled probes, we used molecular modeling tools to derive the necessary geometrical parameters such as R, n_2, and l. The Membrane Builder of the CHARMM-GUI package (http://www.charmm-gui.org/?doc=input/membrane)[26] was used to build two model bilayer systems (POPE and POPG) with the protein (PDB entry 1PV6) inserted in it. The 1PV6/POPE pure bilayer model represents the PE lipid of the experimental mixture and therefore corresponds to the lipid modified with pyrene, whereas the 1PV6/POPG model does the same for the other lipid of the experimental mixture. The following geometrical considerations were taken into account to obtain the geometrical parameters: (i) 39 annular sites were considered for the protein; (ii) two acceptor planes were considered, at slightly different distances (l_1 = 2.10 nm and l_2 = 2.36 nm from the plane of the W151 donors); (iii) the average distance R from W151 to the pyrene moiety of HPyr-PE in the annular sites was taken as 3.8 nm; and (iv) lipid molecular areas of 0.62 and 0.63 nm^2 were used for POPE and POPG, respectively. These structural parameters should be viewed cautiously, as the system was not dynamically equilibrated (that would involve molecular dynamics simulations, which are being considered for future studies) and therefore constitutes only a rough approximation of the atomic details of the system. However, while this may affect the quantitative determination of the μ parameter, it does not hamper a comparative discussion of the experimental FRET energy transfers.

RESULTS

A model of C154G LacY embedded in a POPE matrix is illustrated in Figure 1. The position of W151 that acts as a donor for the FRET experiments is highlighted. The FRET acceptors in this experiment are PE lipids labeled with pyrene on the polar headgroup. On one hand, PE was selected since a large amount of evidence points to this headgroup as more adequate to accomplish the specific requirements for proper folding[9] and correct function of the protein.[27,28] On the other hand, polar-headgroup labeling was selected to respond to recent results pointing to the importance of the acyl chain moiety in the interplay between phospholipids and membrane proteins;[10,11,20] the aim of this configuration was to investigate the independent contributions of the headgroup and the acyl chains in the lipid−protein interaction.

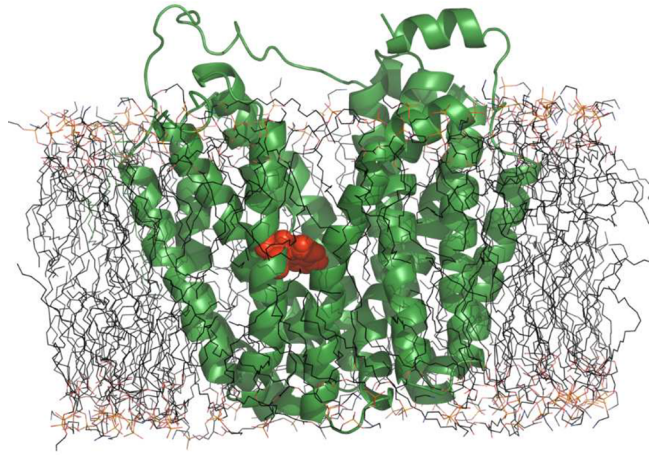

Figure 1. Model of C154G LacY embedded in a POPE matrix. Tryptophan 151 is highlighted in orange. This model was constructed using CHARMM-GUI Membrane Builder.

The FRET methodology developed by Fernandes et al.[18] and reformulated by Suárez-Germà et al.[20] was employed to

dx.doi.org/10.1021/jp402152n | J. Phys. Chem. B 2013, 117, 6741−6748

measure the efficiency of energy transfer between the single-tryptophan mutant W151/C154G LacY and the PE headgroup-labeled analogue HPyr-PE in three different biomimetic binary phospholipid mixtures: DOPE/POPG, POPE/POPG, and DPPE/POPG, each at a 3:1 molar ratio. With such a strategy, information on the selectivity of the protein for the different acyl chains (DO, PO, and DP, respectively) was gathered.[21]

Figure 2 shows the experimental FRET efficiencies obtained at 25 and 37 °C using HPyr-PE as the acceptor. As can be seen,

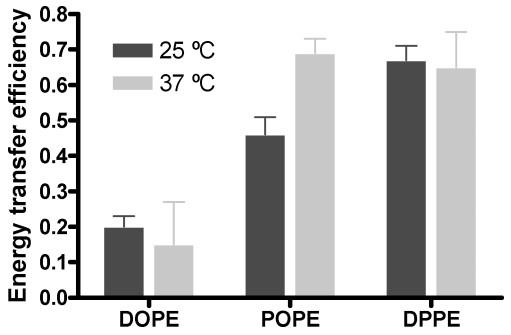

Figure 2. Efficiency of FRET between W151 in LacY and pyrene in headgroup-labeled PE in different lipid matrices at 25 °C (black columns) and 37 °C (gray columns). Proteoliposomes (1.5 μM LacY) of 3:1 (mol/mol) DOPE/POPG, POPE/POPG, and DPPE/POPG were doped with label (x = 0.0025). Error bars stand for $\sigma/\sqrt{n}$, where σ is the standard deviation and n the number of measurements performed.

the lowest FRET values were obtained for DOPE/POPG at both temperatures, while the highest values were found for DPPE/POPG at both 25 and 37 °C and POPE/POPG at 37 °C. In addition, POPE/POPG was the only mixture that presented a significant change when the temperature was varied. In agreement with these observations, the probability that a given site in the annular ring is occupied by a labeled pyrene phospholipid (μ) was the highest for DPPE/POPG at 25 °C (0.22) and POPE/POPG at 37 °C (0.24) (Table 1). The presence of HPyr-PE in the annular region in DOPE/POPG was almost negligible (μ = 0.02 and 0.01 at 25 and 37 °C, respectively; Table 1).

Table 1. Experimental FRET Efficiencies (E) and Calculated Probabilities for Occupancy of a Given Site in the LacY Annular Ring by a Headgroup-Labeled Phospholipid (μ)

T (°C)	mixture[a]	E	μ
25	DOPE/POPG	0.20	0.02
	POPE/POPG	0.46	0.09
	DPPE/POPG	0.67	0.22
37	DOPE/POPG	0.15	0.01
	POPE/POPG	0.69	0.24
	DPPE/POPG	0.65	0.20

[a]Mixture composition: 3:1 (mol/mol) PE/POPG.

In previous works[21] FRET experiments were carried out with identical lipid matrices but with the acceptor fluorophores placed on the acyl moiety of the phospholipid structure. Therefore, it seems interesting now to compare these published results with the ones obtained from FRET between W151 and polar-headgroup-labeled phospholipids. With that purpose, Figure 3 shows a comparison of normalized energy transfer

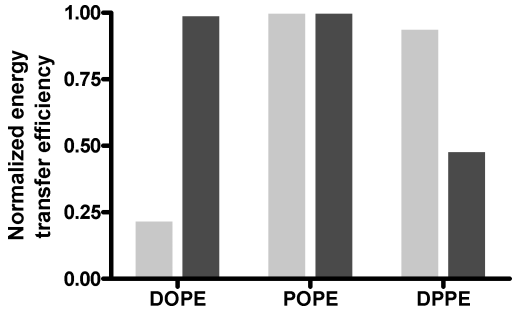

Figure 3. Comparison of normalized efficiencies for FRET between W151 of single-W C154G LacY and PE labeled on the polar headgroup (gray columns) or the acyl chain (black columns) at 37 °C.

efficiencies obtained from the measurements of FRET between W151 of LacY and pyrene in PE labeled on the polar headgroup (HPyr-PE) or the acyl chain (TPyr-PE) at 37 °C. Among the three studied lipid mixtures, POPE/POPG was the only one presenting equal values of the normalized energy transfer efficiency for both labeling forms. DOPE/POPG and DPPE/POPG presented opposite behaviors: whereas the former mixture presented low normalized energy transfer efficiency with HPyr-PE and high efficiency with TPyr-PE, the second mixture varied in the opposite way.

When the pyrene-labeled phospholipids are directly or indirectly excited (at 338 or 295 nm, respectively), the pyrene excimer/monomer (E/M) ratio can provide information on the lateral diffusion and local effective pyrene concentration of the labeled phospholipids in the bulk and the annular region, respectively. The values of these ratios are shown in Figure 4 for 25 and 37 °C using both HPyr-PE and TPyr-PE as probes.

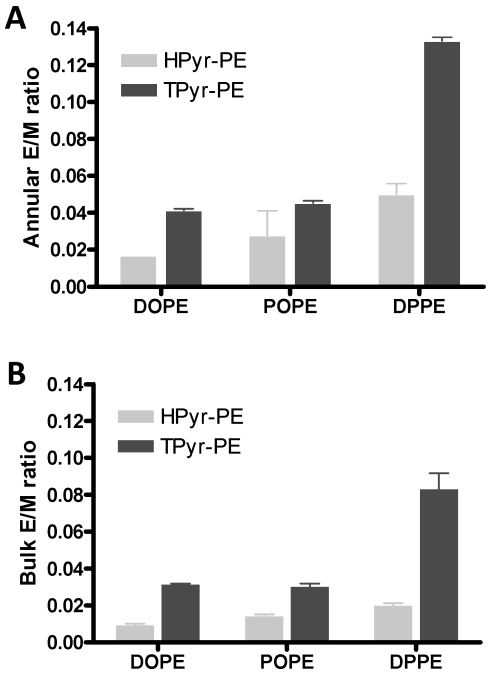

Figure 4. E/M ratios for labeled lipids in (A) the annular region and (B) the bulk at 37 °C for 3:1 (mol/mol) DOPE/POPG, POPE/POPG, and DPPE/POPG lipid mixtures containing headgroup-labeled (gray columns) or acyl-labeled (black columns) Pyr-PE. Error bars stand for $\sigma/\sqrt{n}$, where σ is the standard deviation and n the number of measurements performed.

dx.doi.org/10.1021/jp402152n | J. Phys. Chem. B 2013, 117, 6741−6748

For all of the systems, higher E/M ratios were measured for annular probes (relative to probes in the bulk), DPPE/POPG (relative to DOPE/POPG and POPE/POPG), and TPyr-PE (relative to HPyr-PE).

DISCUSSION

To rationalize the obtained FRET results shown in Figure 2, we should take into consideration the thermotropic nature of the mixtures used and the influence of the presence of pyrene at the headgroup level on the protein−lipid interaction. On one hand, at both 25 and 37 °C, the DOPE/POPG mixture is in the fluid liquid-crystalline (L_α) phase, and DPPE/POPG displays coexistence between the solidlike gel (L_β) state and the L_α phase. However, the situation is more complex for the POPE/POPG system, because the main transition temperature of the POPE/POPG mixture has been measured as 20.9 °C[22] and ∼21.5 °C[29] by differential scanning calorimetry (DSC) and 23 °C by fluorescence methods.[30] The discrepancies among these values are related to differences in methodology and buffers used in these works and to the fact that POPE/POPG shows a broad transition.[22,29,31] Thus, whereas it is clear that POPE/POPG bilayers exist as a single fluid phase at 37 °C, it is likely that some POPE-rich L_β domains might be still present at 25 °C. Within the context of the present work, it is important to recall that LacY inserts preferentially into fluid phases of laterally segregated phospholipid systems.[21,30] On the other hand, we have to take into account the fact that the pyrene moiety, which is characterized by a planar structure and high hydrophobicity, introduces changes in the physicochemical properties of the host bilayer. In particular, the presence of a large entity, the pyrene, at the headgroup level, in addition to the lack of hydrogen bonding of this structure, may result in an increase in the surface area of the bilayer.[32]

In Figure 2, it is apparent that the system for which the FRET efficiency at both temperatures is the highest is DPPE/POPG. When the preference of LacY for the L_α phase is taken into account, this implies the seemingly unphysical result of a preference of HPyr-PE for the L_α PG-rich phase rather than the L_β PE-rich phase. A possible reason for this observation is that the unsaturated acyl chains of HPyr-PE are better accommodated in the fluid phase rather than in the L_β gel, which would supersede the headgroup-effect difference. On the other hand, within the fluid-phase domains, LacY probably interacts preferentially with the PE probe rather than POPG. Thus, the increased FRET efficiency in the DPPE/POPG system stems from colocalization of the probe and protein in the fluid phase of this phase-separated system and indicates a preference of LacY for (i) the fluid phase over the gel phase and (ii) the PE headgroup over the PG headgroup.

We now address the POPE/POPG system. The fact that a high FRET efficiency was obtained at 37 °C primarily indicates that LacY much prefers to be surrounded by the PE lipid (including the HPyr-PE probe) than by POPG, which is in agreement with the results and μ values previously reported when TPyr-PE was used as the probe.[20,21] The difference in the FRET efficiencies at 25 and 37 °C is probably related to the thermotropic behavior of this mixture. Indeed, if the system is in a gel/fluid mixture at room temperature, because of its preference for fluid phases, LacY will show some preference for the PE-impoverished fluid domains. Hence, some annular sites may be occupied by POPG at 25 °C, decreasing the efficiency of FRET to HPyr-PE relative to that in a single fluid phase at 37 °C.

The DOPE/POPG system shows lower FRET efficiencies and lower μ values than expected at both temperatures. In principle, this behavior could be attributed to displacement of the acceptor by DOPE and/or POPG. However, using TPyr-PE, we previously showed that for a 3:1 DOPE/POPG host lipid mixture identical to that studied here, the best agreement was found when the experimental FRET data were obtained using an annular region composition of ∼90 mol % PE (compared with the value of 75% expected on the basis of the matrix composition).[21] Therefore, LacY shows a preference for DOPE over POPG, and if the probe is displaced from the annular sites, it is much more likely that this displacement will be caused by an enrichment of DOPE rather than POPG in this region. On the other hand, as mentioned above, the presence of the bulky pyrene headgroup may result in larger lateral molecular area occupancy at the boundary region and the exclusion of HPyr-PE.[13] In this regard, it becomes relevant to estimate the local concentration of pyrene within this region. Although merely indicative, this concentration can be estimated by calculating the E/M ratio in the annular region. As can be seen in Figure 4A, excimer formation was always the lowest in the DOPE/POPG mixture, even though in all cases the E/M ratios for HPyr-PE were lower than those obtained for TPyr-PE. Remarkably, the obtained E/M ratios, although lower, presented the same trend as the ones obtained for TPyr-PE. Indeed, the DPPE/POPG mixture again showed the highest E/M ratios, which may be explained by differential partitioning of the probe that leads to higher local concentrations of pyrene. These trends in the E/M ratios are thus parallel to those in the FRET efficiency values, and both reflect pyrene probe enrichment in the annular region of LacY in the DPPE/POPG mixture and depletion in the DOPE/POPG mixture. Figure 4B presents the results for pyrene lateral diffusion in the bulk region for TPyr-PE and HPyr-PE. We observe two general patterns: (i) reduced E/M ratios for HPyr-PE compared with TPyr-PE, which is consistent with the annular results, and (ii) substantially lower TPyr-PE and HPyr-PE E/M ratios than obtained for the annular region (Figure 4A), indicating an enrichment of the probe in the environment of the protein region, also in agreement with the obtained FRET results (which indicate that the probability of occupancy of annular sites by probes is much higher than the bulk probe fraction). The whole body of these data suggests that the local concentration of HPyr-PE may be lower in the case of DOPE/POPG in comparison with the other mixtures. Consequently, a difference in the distribution of the label is observed, which could also result in a lower density of the label in the annular region.

Protein−lipid selectivity may arise as a consequence of matching between the hydrophobic lengths of protein and lipid,[33] or it can be affected by the lateral pressure profile across the membrane. The former effect would not be expected to be overly relevant to our results, in that large changes in lipid hydrophobic length would not be expected in our lipid systems, as fluid 16:0 and *cis*-18:1 having similar lengths along the bilayer normal.[34] The latter has been addressed theoretically by Cantor, whose basic lattice model takes into account the contributions of chain energies (bending stiffness), interfacial tension, and headgroup electrostatic interactions in the calculation of the lateral pressure profile,[35] which was in subsequent papers related to protein conformation and aggregation.[36,37] More recently, Marsh demonstrated that the effects of the lateral pressure profile on the conformation/

dx.doi.org/10.1021/jp402152n | J. Phys. Chem. B 2013, 117, 6741−6748

insertion of proteins in membranes are equivalent to the elastic response to the frustrated spontaneous curvature of the component lipid monolayer leaflets.[38,39] Since it has been suggested that the lipid spontaneous curvature (C_0)[40] appears to be crucial in regard to uphill transport of lactose by LacY in vivo,[32] it becomes tempting to relate this parameter to our FRET data. Although the spontaneous curvature is a global property, it can be parametrized in terms of the geometric parameters (volume, effective length, and cross-sectional area) of the constituent lipid molecules. Thus, while DOPE is known for its highly negative spontaneous curvature [C_0(DOPE) = −0.35 nm^{-1}] resulting from its inverted conical shape, with a small headgroup and disordered acyl chains,[41] to our knowledge, the spontaneous curvature of POPE has not been determined. However, replacement of an oleoyl chain in DOPE with a palmitoyl one in POPE should reduce the cross-sectional area, resulting in an increase of the lateral pressure in the hydrophobic region of the lipid;[30] therefore, it would also be expected that $-C_0$(POPE) < $-C_0$(DOPE), similar to what has been observed with POPC (C_0 = 0) and DOPC (C_0 = −0.11 nm^{-1}).[41]

Because HPyr-PE bears two oleoyl acyl chains, just as in DOPE, it would be reasonable to assume that the probe reports the behavior of this latter phospholipid. However, in terms of specific curvature, pyrene labeling on the headgroup will most probably have a severe effect. It has been shown that replacing the headgroup ethanolamine H atoms with methyl groups decreases the absolute value of C_0 [C_0(DOPE-Me) = −0.27 nm^{-1}, C_0(DOPE-Me$_2$) = −0.19 nm^{-1}),[41] which is understandable since these replacements change the shape of DOPE from an truncated cone to something closer to a cylinder. A similar effect could be expected for pyrene labeling on the headgroup, so we may hypothesize that $-C_0$(HPyr-PE) < $-C_0$(DOPE). Thus, DOPE is clearly expected to be the PE lipid component with the most negative spontaneous curvature, compared with POPE and HPyr-PE. The higher FRET efficiency shown by POPE/POPG in Figure 2 seemingly indicates that HPyr-PE and POPE compete for the annular sites of LacY, whereas the low efficiency and μ value for DOPE/POPG at both temperatures reflect, in comparative terms, more extensive occupation of the annular sites by DOPE, with concomitant probe exclusion. Thus, our data seem to confirm that spontaneous curvature is a major determinant of the LacY−lipid interaction, with PE lipids bearing more negative C_0 values being preferred relative to others with a more cylindrical shape. This seems to be at odds with a recent study by Vitrac et al.[11] indicating that POPE provides LacY with significantly higher uphill transport activity than DOPE. It is worth mentioning here that our mutant (LacY/C154G/single-W151) is different from the ones used by Vitrac et al. (C-less LacY/H205C or C-less LacY/F250C); whereas the latter two are fully functional, LacY (C154G) is severely restricted conformationally and does not transport H$^+$.[42,43] However, our results still suggest that in our systems and using this acceptor probe, DOPE is preferably located in the vicinity of LacY in comparison with POPE. A rationalization of these somewhat contradictory results may involve one of the following scenarios: (i) The design of our experiments presents limitations, possibly stemming from less adequate physicochemical behavior of HPyr-PE as a PE lipid reporter. Regarding this matter, it must also be mentioned that the attachment of a fluorophore to the PE headgroup results in a negative charge that is absent in the unlabeled PE lipid, and as demonstrated in our previous works, LacY shows a preference for zwitterionic PE over anionic PG lipids. (ii) Annular lipid composition is not the only determinant (and perhaps not the main determinant) of uphill transport activity. Additionally, the use of the C154G mutant provides information about a specific condition of the protein without taking into account its need for adaptability when facing structural transitions.[44] These latter possibilities reinforce the fact that many aspects of LacY−lipid interactions remain to be clarified.

We now turn our attention to Figure 3, which shows a comparison of the FRET efficiencies at 37 °C for the HPyr-PE and TPyr-PE probes. These differences in behavior of the head-labeled and tail-labeled pyrene acceptor probes are probably related to differences in their acyl chain compositions and packing requirements for the bulky pyrene moiety. In particular, concerning the phase-separated DPPE/POPG system, the very high and very low efficiencies obtained for HPyr-PE and TPyr-PE, respectively, could be attributed to different partitioning of the fluorescent probes in the lipid mixture. It could be expected that because both probes are labeled PEs, they would mimic the PE mixture component and prefer the DPPE-enriched L_β phase. As proposed in a previous work,[23] this hypothesis appears to be valid for TPyr-PE, possibly because this probe has no unsaturated chains and contains an unsubstitued headgroup identical to that of DPPE and therefore would presumably prefer the PE-rich L_β phase over the POPG fluid. This would decrease the colocalization of the probe with the protein, explaining the low FRET efficiencies obtained. On the other hand, because of its unsaturated acyl chains, HPyr-PE would probably much prefer the PG-rich L_α phase over the DPPE-rich gel. Since the main transition temperature of DOPE (which HPyr-PE most resembles) is around −9 °C,[45] LacY and HPyrPE should both be preferentially located inside the fluid domains, resulting in higher FRET efficiencies.

Previous works by our group have shown the preference of LacY for PE over other kinds of phospholipids such as PG and PC.[20,21] This study aimed to elucidate the factors governing the eventual selectivity of LacY among different PE lipids. The two main conclusions are the following: (i) For phase-separated systems, LacY will be located in the fluid domains, and if a given PE is present in this phase (e.g., as a consequence of acyl chain unsaturation), it will colocate with LacY. (ii) In the absence of phase separation, LacY is preferentially surrounded by PE, and in particular, it seems to be sensitive to the lipid spontaneous curvature C_0, with a preference for more negative C_0 values. A more definite clarification of the differential interaction with headgroup-labeled pyrene lipid HPyr-PE will probably involve FRET experiments in pure POPE and DOPE, similar to our recent study with TPyr-PE,[20] though in this kind of experiment the biomimetics of the matrix would inevitably be lost. Additionally, the use of different pyrene-labeled PE lipids as acceptor probes would create the necessity of complementary studies to clarify these probes' behavior, using, for example, molecular dynamics simulations, as recently employed by Loura and Prieto[46] to study free pyrene in bilayers.

AUTHOR INFORMATION

Corresponding Author

*Department of Physical Chemistry, Faculty of Pharmacy, University of Barcelona, Av. Joan XXIII, 08028 Barcelona,

Spain. E-mail: jordiborrell@ub.edu. Fax: (+34) 934035987. Phone: (+34) 934035986.

Notes

The authors declare no competing financial interest.

■ ACKNOWLEDGMENTS

C.S.-G. was the recipient of an FPI Fellowship from the Ministerio de Economía y Competitividad of Spain. This work was supported by Grant CTQ-2008-03922/BQU from the Ministerio de Ciencia e Innovación of Spain. C.S.-G., Ò.D., M.T.M., and J.H.-B. thank the Universitat de Barcelona for financial support. L.M.S.L. and M.P. acknowledge funding by FEDER (COMPETE Program) and Fundação para a Ciência e a Tecnologia (FCT), project references PTDC/QUI-BIQ/099947/2008 and FCOMP-01-0124-FEDER-010787 (FCT PTDC/QUI-QUI/098198/2008).

■ REFERENCES

(1) Guan, L.; Kaback, H. R. Lessons from Lactose Permease. *Annu. Rev. Biophys. Biomol. Struct.* **2006**, *35*, 67−91.
(2) Abramson, J.; Smirnova, I.; Kasho, V.; Verner, G.; Kaback, H. R.; Iwata, S. Structure and Mechanism of the Lactose Permease of *Escherichia coli*. *Science* **2003**, *301*, 610−605.
(3) Mirza, O.; Guan, L.; Verner, G.; Iwata, S.; Kaback, H. R. Structural Evidence for Induced Fit and a Mechanism for Sugar/H^+ Symport in LacY. *EMBO J.* **2006**, *25*, 1177−1183.
(4) Vázquez-Ibar, J. L.; Guan, L.; Svrakic, M.; Kaback, H. R. Exploiting Luminescence Spectroscopy To Elucidate the Interaction between Sugar and a Tryptophan Residue in the Lactose Permease of *Escherichia coli*. *Proc. Natl. Acad. Sci. U.S.A.* **2003**, *100*, 12706−12711.
(5) Guan, L.; Mirza, O.; Verner, G.; Iwata, S.; Kaback, H. R. Structural Determination of Wild-Type Lactose Permease. *Proc. Natl. Acad. Sci. U.S.A.* **2007**, *104*, 15294−15298.
(6) Kaback, H. R.; Wu, J. What To Do While Awaiting Crystals of a Membrane Transport Protein and Thereafter. *Acc. Chem. Res.* **1999**, *32*, 805−813.
(7) Andersson, M.; Bondar, A.-N.; Freites, J. A.; Tobias, D. J.; Kaback, H. R.; White, S. H. Proton-Coupled Dynamics in Lactose Permease. *Structure* **2012**, *20*, 1893−1904.
(8) Chen, C. C.; Wilson, T. H. The Phospholipid Requirement for Activity of the Lactose Carrier of *Escherichia coli*. *J. Biol. Chem.* **1984**, *259*, 10150−10158.
(9) Bogdanov, M.; Dowhan, W. Phospholipid-Assisted Protein Folding: Phosphatidylethanolamine Is Required at a Late Step of the Conformational Maturation of the Polytopic Membrane Protein Lactose Permease. *EMBO J.* **1998**, *17*, 5255−5264.
(10) Bogdanov, M.; Heacock, P.; Guan, Z.; Dowhan, W. Plasticity of Lipid−Protein Interactions in the Function and Topogenesis of the Membrane Protein Lactose Permease from *Escherichia coli*. *Proc. Natl. Acad. Sci. U.S.A.* **2010**, *107*, 15057−15062.
(11) Vitrac, H.; Bogdanov, M.; Dowhan, W. Proper Fatty Acid Composition Rather Than an Ionizable Lipid Amine Is Required for Full Transport Function of Lactose Permease from *Escherichia coli*. *J. Biol. Chem.* **2013**, *288*, 1−24.
(12) Ollila, S.; Hyvönen, M. T.; Vattulainen, I. Polyunsaturation in Lipid Membranes: Dynamic Properties and Lateral Pressure Profiles. *J. Phys. Chem. B* **2007**, *111*, 3139−3150.
(13) Somerharju, P. Pyrene-Labeled Lipids as Tools in Membrane Biophysics and Cell Biology. *Chem. Phys. Lipids* **2002**, *116*, 57−74.
(14) Kinnunen, P. K. J.; Koiv, A.; Mustonen, P. Pyrene-Labelled Lipids as Fluorescent Probes in Studies on Biomembranes and Membrane Models. In *Fluorescence Spectroscopy: New Methods and Applications*; Wolfbeis, O. S., Ed.; Springer: Berlin, 1993; pp 159−169.
(15) Zhao, M.; Zen, K.-C.; Hubbell, W. L.; Kaback, H. R. Proximity between Glu 126 and Arg 144 in the Lactose Permease of *Escherichia coli*. *Biochemistry* **1999**, *38*, 7407−7412.
(16) Jung, K.; Jung, H.; Kaback, H. R. Dynamics of Lactose Permease of *Escherichia coli* Determined by Site-Directed Fluorescence Labeling. *Biochemistry* **1994**, *33*, 3980−3985.
(17) Lehtonen, J. Y.; Kinnunen, P. K. Evidence for Phospholipid Microdomain Formation in Liquid Crystalline Liposomes Reconstituted with *Escherichia coli* Lactose Permease. *Biophys. J.* **1997**, *72*, 1247−1257.
(18) Fernandes, F.; Loura, L. M. S.; Koehorst, R.; Spruijt, R. B.; Hemminga, M. A.; Fedorov, A.; Prieto, M. Quantification of Protein−Lipid Selectivity Using FRET: Application to the M13 Major Coat Protein. *Biophys. J.* **2004**, *87*, 344−352.
(19) Picas, L.; Montero, M. T.; Morros, A.; Vázquez-Ibar, J. L.; Hernández-Borrell, J. Evidence of Phosphatidylethanolamine and Phosphatidylglycerol Presence at the Annular Region of Lactose Permease of *Escherichia coli*. *Biochim. Biophys. Acta* **2009**, *1798*, 291−296.
(20) Suárez-Germà, C.; Loura, L. M. S.; Prieto, M.; Domènech, O.; Montero, M. T.; Rodríguez-Banqueri, A.; Vázquez-Ibar, J. L.; Hernández-Borrell, J. Membrane Protein−Lipid Selectivity: Enhancing Sensitivity for Modeling FRET Data. *J. Phys. Chem. B* **2012**, *116*, 2438−2445.
(21) Picas, L.; Suárez-Germà, C.; Montero, M. T.; Vázquez-Ibar, J. L.; Hernández-Borrell, J.; Prieto, M.; Loura, L. M. S. Lactose Permease Lipid Selectivity Using Förster Resonance Energy Transfer. *Biochim. Biophys. Acta* **2010**, *1798*, 1707−1713.
(22) Picas, L.; Merino-Montero, S.; Morros, A.; Hernández-Borrell, J.; Montero, M. T. Monitoring Pyrene Excimers in Lactose Permease Liposomes: Revealing the Presence of Phosphatidylglycerol in Proximity to an Integral Membrane Protein. *J. Fluoresc.* **2007**, *17*, 649−654.
(23) Suárez-Germà, C.; Loura, L. M. S.; Domènech, O.; Montero, M. T.; Vázquez-Ibar, J. L.; Hernández-Borrell, J. Phosphatidylethanolamine−Lactose Permease Interaction: A Comparative Study Based on FRET. *J. Phys. Chem. B* **2012**, *116*, 14023−14028.
(24) Mason, R. P.; Jacob, R. F.; Walter, M. F.; Mason, P. E.; Avdulov, N. A.; Chochina, S. V.; Igbavboa, U.; Wood, W. G. Distribution and Fluidizing Action of Soluble and Aggregated Amyloid β-Peptide in Rat Synaptic Plasma Membranes. *J. Biol. Chem.* **1999**, *274*, 18801−18807.
(25) Tahara, Y.; Murata, M.; Ohnishi, S.; Fujiyoshi, Y.; Kikuchi, M.; Yamamoto, Y. Functional Signal Peptide Reduces Bilayer Thickness of Phosphatidylcholine Liposomes. *Biochemistry* **1992**, *31*, 8747−8754.
(26) Jo, S.; Lim, J. B.; Klauda, J. B.; Im, W. CHARMM-GUI Membrane Builder for Mixed Bilayers and Its Application to Yeast Membranes. *Biophys. J.* **2009**, *97*, 50−58.
(27) Dowhan, W.; Bogdanov, M. Lipid-Dependent Membrane Protein Topogenesis. *Annu. Rev. Biochem.* **2009**, *78*, 515−540.
(28) Vitrac, H.; Bogdanov, M.; Heacock, P.; Dowhan, W. Lipids and Topological Rules of Membrane Protein Assembly: Balance between Long and Short Range Lipid−Protein Interactions. *J. Biol. Chem.* **2011**, *286*, 15182−15194.
(29) Pozo Navas, B.; Lohner, K.; Deutsch, G.; Sevcsik, E.; Riske, K. A.; Dimova, R.; Garidel, P.; Pabst, G. Composition Dependence of Vesicle Morphology and Mixing Properties in a Bacterial Model Membrane System. *Biochim. Biophys. Acta* **2005**, *1716*, 40−48.
(30) Suárez-Germà, C.; Montero, M. T.; Ignés-Mullol, J.; Hernández-Borrell, J.; Domènech, O. Acyl Chain Differences in Phosphatidylethanolamine Determine Domain Formation and LacY Distribution in Biomimetic Model Membranes. *J. Phys. Chem. B* **2011**, *115*, 12778−12784.
(31) Picas, L.; Montero, M. T.; Morros, A.; Cabañas, M. E.; Seantier, B.; Milhiet, P.-E.; Hernández-Borrell, J. Calcium-Induced Formation of Subdomains in Phosphatidylethanolamine−Phosphatidylglycerol Bilayers: A Combined DSC, ^{31}P NMR, and AFM Study. *J. Phys. Chem. B* **2009**, *113*, 4648−4655.
(32) Wikström, M.; Kelly, A. A.; Georgiev, A.; Eriksson, H. M.; Klement, M. R.; Bogdanov, M.; Dowhan, W.; Wieslander, A. Lipid-Engineered *Escherichia coli* Membranes Reveal Critical Lipid Headgroup Size for Protein Function. *J. Biol. Chem.* **2009**, *284*, 954−965.

(33) Mouritsen, O. G.; Bloom, M. Mattress Model of Lipid−Protein Interactions in Membranes. *Biophys. J.* **1984**, *46*, 141−153.
(34) Marsh, D. *Handbook of Lipid Bilayers*, 2nd ed.; CRC Press: Boca Raton, FL, 2013.
(35) Cantor, R. S. Lipid Composition and the Lateral Pressure Profile in Bilayers. *Biophys. J.* **1999**, *76*, 2625−2639.
(36) Cantor, R. S. The Influence of Membrane Lateral Pressures on Simple Geometric Models of Protein Conformational Equilibria. *Chem. Phys. Lipids* **1999**, *101*, 45−56.
(37) Cantor, R. S. Size Distribution of Barrel-Stave Aggregates of Membrane Peptides: Influence of the Bilayer Lateral Pressure Profile. *Biophys. J.* **2002**, *82*, 2520−2525.
(38) Marsh, D. Lateral Pressure Profile, Spontaneous Curvature Frustration, and the Incorporation and Conformation of Proteins in Membranes. *Biophys. J.* **2007**, *93*, 3884−3899.
(39) Marsh, D. Protein Modulation of Lipids, and Vice-Versa, in Membranes. *Biochim. Biophys. Acta* **2008**, *1778*, 1545−75.
(40) Gruner, S. M. Intrinsic Curvature Hypothesis for Biomembrane Lipid Composition: A Role for Nonbilayer Lipids. *Proc. Natl. Acad. Sci. U.S.A.* **1985**, *82*, 3665−3669.
(41) Soubias, O.; Teague, W. E.; Hines, K. G.; Mitchell, D. C.; Gawrisch, K. Contribution of Membrane Elastic Energy to Rhodopsin Function. *Biophys. J.* **2010**, *99*, 817−824.
(42) Smirnova, I. N.; Kaback, H. R. A Mutation in the Lactose Permease of *Escherichia coli* That Decreases Conformational Flexibility and Increases Protein Stability. *Biochemistry* **2003**, *42*, 3025−3031.
(43) Garcia-Celma, J. J.; Smirnova, I. N.; Kaback, H. R.; Fendler, K. Electrophysiological Characterization of LacY. *Proc. Natl. Acad. Sci. U.S.A.* **2009**, *106*, 7373−7378.
(44) Shaikh, S. A.; Li, J.; Enkavi, G.; Wen, P.-C.; Huang, Z.; Tajkhorshid, E. Visualizing Functional Motions of Membrane Transporters with Molecular Dynamics Simulations. *Biochemistry* **2013**, *52*, 569−587.
(45) Feng, Y.; Yu, Z. W.; Quinn, P. J. Effect of Urea, Dimethylurea, and Tetramethylurea on the Phase Behavior of Dioleoylphosphatidylethanolamine. *Chem. Phys. Lipids* **2002**, *114*, 149−157.
(46) Loura, L. M. S.; Prieto, M. *Springer Ser. Fluoresc.* **2013**, *13*, 71−113.

4.3.4 Effect of lactose permease presence on the structure and nanomechanics of two components supported lipid bilayers

Suárez-Germà, C., Domènech, Ò., Montero, M.T., Hernández-Borrell, J.
Submitted to *Biochimica et Biophysica Acta - Biomembranes*

4.3.4.1 Summary

In this paper we presented a comparative AFM study of SLBs and PLSs of LacY reconstituted in proteoliposomes with a biomimetic lipid composition of the *E. coli* inner membrane. Lipid matrices of two components, PE:PG (3:1, mol/mol), were selected to mimic the inner membrane of the bacteria. The final goal of this work was to investigate how phospholipid species of different acyl chain composition, compactness and stiffness, affect the integration, distribution and nanomechanical properties of LacY; and, at the same time, how the protein affects the matrices when it is reconstituted in binary mixtures of POPE or DPPE with POPG.

SLBs of POPE:POPG (3:1, mol/mol) and DPPE:POPG (3:1, mol/mol) lipid compositions displayed both lateral L_α/L_β phase separation at the studied conditions and they were investigated through AFM in imaging and FS modes. Similar breakthrough forces (F_y) were found in POPE:POPG (3:1, mol/mol) for both L_α and L_β phases, whilst higher adhesion forces (F_{adh}) were found for L_β as compared to L_α. This was in accordance with results obtained in section 3.3.2. DPPE:POPG (3:1, mol/mol) presented higher F_y values in L_β phase than in L_α phase, evidencing a stiffer L_β phase. Regarding F_{adh}, lipid phases in DPPE:POPG (3:1, mol/mol) displayed the same trend than POPE:POPG (3:1, mol/mol) ($F_{adh}(L_\beta) > F_{adh}(L_\alpha)$). In general, F_{adh} and F_y values were higher for DPPE:POPG (3:1, mol/mol) mixture, which was related to the presence of the more saturated DPPE phospholipid.

PLSs of the same lipid compositions but with the presence of LacY displayed two separate, laterally segregated domains: a lower one, flat and featureless, and a higher one, grainy and covered with protruding entities. Both domains were further characterised by FS and FV AFM modes. We detected that lower domains presented F_y values in the range of those obtained for L_β phases in SLBs. Conversely, higher domains

displayed much lower F_y values than L_α phases from pure SLB systems. No major changes were found in F_{adh} trends and, in general, all F_y and F_{adh} values were lower than the ones presented for systems without protein. This last effect might be related to the presence of the protein in the system, but also to the remaining effect of the detergent used to prepare the samples.

Taking the entire set of nanomechanical results together with the analysis of the step heights differences, we could correlate lower phases in PLSs with L_β domains in the SLBs, and therefore with phases formed mostly by lipids. Then, high-stepped phases were correlated to a new fluid phase were protein and phospholipids colocalized. The fact that the protein-lipid L_α phase from PLSs could be punctured more easily than the L_α phase in the SLB reinforced the idea that we were actually observing a new fluid phase that included average bulk properties of protein and its closed solvated phospholipids.

FV data was analyzed by dividing samples in different regions taking as a reference the distance to the domains containing the protein. Hence, it was detected that the further from the domain with protein, the higher the obtained F_{adh} value. It was related either to the presence of the protein which stabilised the lipid bilayer, or to the described trend behaviour for F_{adh} values, were L_β domains presented higher F_{adh} values than L_α domains. This provides support for the coexistence of nearly protein-free L_β phases and LacY-enriched L_α phases.

Finally, the influence of the lipid environment on LacY organisation was studied by performing protein pulling experiments using the AFM tip. Although the experiments were unspecific, positive events were obtained. A possible influence of the lateral surface pressure on this behaviour was suggested by the higher force required to pull LacY from DPPE:POPG (3:1, mol/mol) than from POPE:POPG (3:1, mol/mol) matrix. This seemed to be related to higher forces governing protein-lipid interaction in the presence of DPPE.

4.3.3.2 Highlights

- POPE:POPG (3:1, mol/mol) and DPPE:POPG (3:1, mol/mol) liposomes reconstituted with LacY were extended over mica and the resulting planar systems were analyzed using topographic, FS and FV AFM modes. Once the results compared with lipid systems without protein, a large influence of the protein on the lipid organization was confirmed.
- The influence of the lipid system on the nanomechanics of the LacY insertion was studied by performing unspecific pulling of the protein when embedded in POPE:POPG (3:1, mol/mol) or DPPE:POPG (3:1, mol/mol) systems. Higher forces were required to extract LacY from DPPE:POPG (3:1, mol/mol) than from POPE:POPG (3:1, mol/mol) matrix, which pointed to an influence of the PE phospholipid structure in the whole bilayer-protein interaction. Additionally, it suggested a role for the phospholipid lateral pressure on the forces governing the incorporation of the protein in a given lipid matrix.

Article submitted to Biochimica et Biophysica Acta Biomembranes:

Effect of lactose permease presence on the structure and nanomechanics of two-component supported lipid bilayers

Carme Suárez-Germà, Òscar Domènech,
M. Teresa Montero, Jordi Hernández-Borrell[#]

[#] Departament de Fisicoquímica, Facultat de Farmàcia, UB and Institut de Nanociència i Nanotecnologia IN^{2}UB, Barcelona, Catalonia, Spain.

Abstract

In this paper we present a comparative study of supported lipid bilayers (SLBs) and proteolipid sheets (PLSs) obtained from deposition of lactose permease (LacY) of Escherichia coli proteoliposomes in plane. Lipid matrices of two components, phosphatidylethanolamine (PE) and phosphatidylglycerol (PG), at a 3:1, mol/mol ratio, were selected to mimic the inner membrane of the bacteria. The aim was to investigate how species of different compactness and stiffness affect the integration, distribution and nanomechanical properties of LacY in mixtures of 1-palmitoyl-2-oleoyl-sn-glycero-3-phosphoethanolamine (POPE) or 1,2-palmitoyl-sn-glycero-3-phosphoethanolamine (DPPE) with 1-palmitoyl-2-oleoyl-sn-glycero-3-[phospho-rac-(1-glycerol)] (POPG). Both compositions displayed phase separation and were investigated by atomic force microscopy (AFM) imaging and force-spectroscopy (FS) mode. PLSs displayed two separated, segregated domains with different features that were characterised by FS and force-volume mode. We correlated the nanomechanical characteristics of solid-like gel phase (L_β) and fluid liquid-crystalline phase (L_α) with phases emerging in presence of LacY. We observed that for both compositions, the extended PLSs showed a L_β apparently formed only by lipids, whilst the second domain was enriched in LacY. The influence of the lipid environment on LacY organisation was studied by performing protein unfolding experiments using the AFM tip. Although the pulling experiments were unspecific, positive events were obtained, indicating the influence of the lipid environment when pulling the protein. A possible influence of the lateral surface pressure on this behaviour is suggested by the higher force required to pull LacY from DPPE:POPG than from POPE:POPG matrices. This is related to higher forces governing protein-lipid interaction in presence of DPPE.

[#]Corresponding author: jordiborrell@ub.edu

1. INTRODUCTION

The cytoplasmic membrane is presently viewed as a heterogeneous system because of the lateral segregation of its fundamental building blocks: lipids and proteins [1]. Depending on the physicochemical properties of its components and the variety of interaction forces that may occur between them, this lateral heterogeneity may have different origins. Lateral segregation has been observed using a wide range of biophysical techniques applied to different model membranes [2,3] and cells [4]. Lipid domains have also been observed in prokaryotic cells [5,6], although the size of the nano- and micro-domains remains a matter of controversy [7,8].

In bilayer model systems, at least two types of lateral phase separation phenomena have been described: those arising from lipid-lipid interactions and those induced by proteins. In this regard, it is a matter of debate whether lipid-lipid interactions govern compartmentalisation of the membrane or whether sustained lipid-protein interactions are responsible for the formation of lipid domains around membrane proteins. A particularly interesting example of lipid-protein aggregation in eukaryotic cells is given by "rafts" [9–11], which are conceived of as dynamic platforms where proteins interact and diffuse along the membrane plane. Another example of protein-phospholipid association is the lateral organisation in highly immobilised annular phospholipids around transmembrane proteins that has been observed using electron spin resonance (ESR) [12]. In fact, whether protein determines phospholipid segregation or vice versa is a subtle reflection of the lipid protein interplay [13].

The use of supported lipid bilayers (SLBs) (membranes supported on a solid substrate) offers several advantages for analysing the topography of samples with nanometre lateral resolution by means of atomic force microscopy (AFM). The insertion of membrane proteins in bilayers can be achieved by reconstitution of proteins in proteoliposomes, which are subsequently spread onto a solid surface (often mica). Thus, by selecting a desired lipid composition that mimics the natural membrane, the protein can interact with the bilayer in a similar way to that occurring *in vivo*. On the one hand, AFM is one of the most suitable techniques for observing laterally segregated lipid domains [14] and protein self-segregation [15]. On the other hand, local forces arising either from different lipid domains [16] or single proteins embedded in the bilayer [17] can be sensed by using the AFM tip in force spectroscopy (FS) mode. Hence, AFM topography images combined with FS may provide valuable information not only about protein lateral distribution but also about the influence of the lipid environment on the nanomechanics behind the insertion of membrane proteins in biomimetic systems. It is well-known that the presence of protein within the lipid system is responsible for considerable changes in the organisation and nanomechanics of the entire system [2,18,19]. In fact, the presence of proteins may promote new lipid-protein domains, as well as extend or modulate the coexistence of phase separation by modifying the transition temperature of the lipid mixtures [20].

The lactose permease (LacY) of *Escherichia coli* (*E. coli*), one of the best studied cytoplasmic membrane proteins, is often taken as a paradigm for secondary transport proteins that couple the energy stored in an electrochemical ion gradient to a concentration gradient (ß-galactoside/H^+ symport). LacY belongs to what is termed the major facilitator superfamily, most of whose members are predicted to contain 12 transmembrane segments. The secondary structure of LacY consists of 12 transmembrane α-helices, crossing the membrane in a zigzag fashion, which are

connected by 11 relatively hydrophilic, periplasmic and cytoplasmic loops, with both amino and carboxyl termini on the cytoplasmic surface [21] (Figure 1). A three-dimensional (3D) model of a LacY mutant (C154G) [22] and a reaction mechanism derived from X-ray diffraction studies are available [23]. The physiological activity of LacY is influenced by the physicochemical properties of neighbouring phospholipids. LacY is commonly reconstituted in native *E. coli* polar phospholipid membrane extracts as well as in binary mixtures of phosphatidylglycerol (PG) and phosphatidylethanolamine (PE) that mimic the inner membrane of the bacteria [24]. Recent studies have revealed that the activity of LacY is sustained not only by PE but also by phosphatidylcholine (PC) [25]. This study suggests the involvement of both the hydrophilic head group domain and the hydrophobic fatty acid domain of the phospholipids in the activity of LacY.

The objective of the present study was twofold: (i) to investigate how lipid organisation is affected by the incorporation of LacY into binary mixtures of 1-palmitoyl-2-oleoyl-*sn*-glycero-3-[phospho-*rac*-(1-glycerol)] (POPG) and either the heteroacid 1-palmitoyl-2-oleoyl-*sn*-glycero-3-phosphoethanolamine (POPE) or the saturated homoacid 1,2-palmitoyl-*sn*-glycero-3-phosphoethanolamine (DPPE), and (ii) to investigate the changes induced in the protein when modifying the lipid environment. Since both the POPE:POPG and DPPE:POPG (3:1, mol/mol) phospholipid systems display lateral phase separation at the studied temperature [26], it was of interest to determine whether this property influences the integration of the protein. Hence, we first investigated the topography of these SLBs by AFM and determined the nanomechanical properties from the force curves [27]. These experiments were taken as a reference for the topography, FS and force-volume (FV) analyses performed on proteolipids sheets (PLSs) obtained from the extension of proteoliposomes onto the same solid substrate. Thereafter, we conducted unspecific unfolding experiments in order to investigate how LacY is affected by the surrounding phospholipid matrix.

2. MATERIALS AND METHODS

N-dodecyl-ß-$_D$-maltoside (DDM) was purchased from Anatrace (Maumee, OH, USA). 1-palmitoyl-2-oleoyl-*sn*-glycero-3-phosphoethanolamine (POPE) and 1-palmitoyl-2-oleoyl-*sn*-glycero-3-[phospho-*rac*-(1-glycerol)] (sodium salt) (POPG) were purchased from Avanti Polar Lipids (Alabaster, AL, USA). Isopropyl-1-thio-ß-D-galactopyranoside (IPTG) was obtained from Sigma Chemical Co. (St. Louis, MO, USA) and polystyrene Bio-Beads® SM-2 were purchased from Bio-Rad (Hercules, CA, USA). All other common chemicals were ACS grade.

2.1 Bacterial strains and protein purification

These procedures have been described in detail in previous papers [28,29]. Briefly, *E. coli* BL21(DE3) cells (Novagen, Madison, WI, USA) transformed with plasmid pCS19 encoding the single- tryptophan mutant W151/C154G LacY provided by Dr. H. Ronald Kaback (UCLA, USA) were grown in Luria-Bertani broth containing ampicillin (100 μg/ml) at 30°C and induced at the appropriate moment with 0.5 mM IPTG. The cells were disrupted, and the membrane fraction was harvested by ultracentrifugation. The membranes were solubilised by adding DDM and purified by Co (II) affinity chromatography (Talon Superflow, Palo Alto, CA, USA). Protein eluted with 150 mM

imidazole was subjected to gel-filtration chromatography using a Superdex 200 10/300 column (GE-Healthcare, Buckinghamshire, UK) equilibrated with 20 mM Tris-HCl (pH 7.6) containing 0.008% DDM. The protein was concentrated using Vivaspin 20 concentrators (30 kDa cut off; Vivascience, Göttingen, Germany) and stored on ice. Protein identification was performed by sodium dodecyl sulphate polyacrylamide gel electrophoresis (SDS-PGE) and protein quantitation was carried out using a Micro BCA kit (Pierce, Rockford, IL).

2.2 Vesicle preparation and protein reconstitution

Liposomes and proteoliposomes were prepared according to previously published methods [26,30]. Briefly, 2:1 (v/v) chloroform/methanol solutions containing appropriate amounts of phospholipids were dried under a stream of oxygen-free N_2 in a conical tube. The total concentration of phospholipids was calculated as a function of the desired lipid-to-protein ratio (LPR) and protein concentration (3.16 μM). The resulting thin film was kept under high vacuum for ~ 3 h to remove organic solvent traces. Multilamellar liposomes (MLVs) were obtained following redispersion of the film in TRIS buffer (pH 7.60) containing 150 mM NaCl, application of successive cycles of freezing and thawing below and above the phase transition of the phospholipids and sonication for 2 min in a bath sonicator. Large unilamellar vesicles (LUVs) were obtained by extrusion (Mini-extruder, Avanti Polar Lipids, Alabaster, AL) of the MLV trough filters (Whatman Nederland B.V., Netherlands) using a pore size diameter of 100 nm. To obtain proteoliposomes, LUVs supplemented with 0.5% DDM were incubated overnight at room temperature. Solubilised protein was then added to the mixture, and it was incubated at 4ºC for 30 min to obtain a LPR (w/w) of 0.5. Proteoliposomes were obtained after the extraction of DDM using polystyrene beads.

2.3 Supported lipid bilayers and atomic force microscopy

SLBs were spread by vesicle fusion as described elsewhere [26]. Briefly, liposomes or proteoliposomes in TRIS buffer supplemented with 10 mM $CaCl_2$ were deposited onto freshly cleaved mica disks. Samples were incubated at 37ºC for 2 h in an oven, using a water reservoir to prevent evaporation of the water from the sample. Before imaging, samples were washed with non-calcium-supplemented buffer. To perform the experiments, it was necessary to drift equilibrate and thermally stabilise the cantilever in the presence of buffer. Images were acquired at 22 ± 0.5ºC.

Liquid AFM imaging was performed using a Multimode Microscope controlled by Nanoscope V electronics (Bruker, AXS Corporation, Madison, WI). Sample images were acquired in contact mode at scan frequencies of 4–7 Hz using an optimised feedback parameter and applying minimum vertical force. MSNL-10 V-shaped Si_3N_4 cantilevers (Bruker AFM Probes, Camarillo, CA) with a nominal spring constant of 0.03 $N \cdot m^{-1}$ were used. All images were processed using NanoScope Analysis Software (Bruker AXS Corporation, Santa Barbara, CA).

2.4 Force Spectroscopy and force-volume measurements

AFM in FS mode was used to obtain nanomechanical magnitudes and to perform protein non-specific unfolding. Individual spring constants of the different cantilevers

used were determined using the equipartition theorem. In practical terms the thermal tune calibration was estimated by using the Bruker software provided by the manufacturer. This method gives values which are within the 20% of the values obtained by other methods. Force–distance curves were measured using a constant velocity of 600 nm·s^{-1} between the AFM tip and the sample. When the pulling of the protein was aimed, the force curve was adjusted at low force (0.5-2 nN) pressing the cantilever down for ~1 s. The frequency of the pickups was low in order to avoid possible pick up of two or more proteins simultaneously.

The worm-like chain (WLC) model [31,32], which describes the elastic behaviour of polymer chain elasticity, was used to fit unfolding events found in the force-distance curves, following the expression

$$F(x) = \frac{k_B T}{p}\left[\frac{1}{4}\left(1 - \frac{x}{L}\right)^{-2} - \frac{1}{4} + \frac{x}{L}\right] \quad (1)$$

where F(x) is the force at a distance x, k_B is the Boltzmann constant, p is the persistence length (0.4 nm) [33], L is the contour length of the unfolded polypeptide chain and T is the temperature. Force peak events were observed in nearly 10% of all force curves (from a total of ~2000 in each experiment). In order to fit to WLC model only these force curves with well-defined sawtoothlike peaks were accepted. The criterion used to select the unfolding peaks was based in the value of the root mean square error (RMSE), which is a measure of the difference between the values predicted by the WLC model and the values actually observed. Only curves displaying RMSE values < 0.015 nN were accepted.

AFM in FV mode was used to combine the topographical image with FS information. To this end, FV images were recorded at a relative trigger threshold below the breaktrough force of the samples. FV imaging was performed using AFM tips with a nominal spring constant of 0.03 N/m. Images contained 32x32 pixels and were registered with an imaging scan-rate of 1 Hz.

3. RESULTS AND DISCUSSION

SLBs of POPE:POPG and DPPE:POPG (3:1, mol/mol) are systems that mimic the lipid composition of the inner membrane of *E. coli*. It is well-known that both systems display lateral phase separation at the temperature at which the experiments were conducted [26]. Although it is believed that lipids in natural biomembranes are in fluid liquid-crystalline (L_α) phase, it was considered of interest to investigate the affinity of the protein for the different L_α or solid-like gel (L_β) phases. Therefore, we investigated the topographic and nanomechanical properties of the SLBs of the same composition as that used to reconstitute the protein. AFM topographic images of POPE:POPG (3:1, mol/mol) and DPPE:POPG (3:1 mol/mol) are shown in Figures 2A and 3A, respectively. The POPE:POPG system showed a fully extended flat bilayer that exhibited the expected coexistence of two lipid phases. We assumed that the higher one was the L_β phase and the lower one, the L_α phase. The step height difference between phases was 0.9 ± 0.1 nm, which matches well with the expected values found elsewhere [34,35]. The absolute height of the L_α phase with respect to the mica could be calculated from some occasional defects found in samples, and was established as 3.8 ± 0.3 nm.

In the DPPE:POPG (3:1, mol/mol) mixture, AFM topographic image in Figure 3A, a flat featureless bilayer surface with coexistence of L_α and L_β phases was observed. In this case, the height of the L_α domain was established as 5.0 ± 0.2 nm and the height of the L_β domain as 5.7 ± 0.2 nm, both values in concordance with previous results [26].

The nanomechanical study of the bilayers was conducted by analysing the FS curves. Essentially, two magnitudes were extracted by operating in this mode: (i) the breakthrough force or yield threshold force (F_y), i.e. the force that the bilayer can withstand before being indented, and (ii) the adhesion force (F_{adh}), i.e. the pull-off force between the tip and the bilayer [27,36]. Distribution of the F_y and F_{adh} values obtained for POPE:POPG is shown in Figures 2B and 2C, respectively. The most probable force values obtained from a Gaussian fitting of the data are shown in Table 1. Concerning F_y (Figure 2B), L_α and L_β did not show major differences (0.509 ± 0.008 nN for L_α versus 0.464 ± 0.006 nN for L_β), which is reasonably consistent with previous studies [37] and may be attributed to the composition of the buffer used. However, it was not possible to perform a more precise comparison, since earlier experiments were performed at different temperatures and ionic strengths (in this former study, 10 mM of calcium was present), factors which determine the F_y values obtained [38,39]. It could still be hypothesised that the higher values obtained in the present study might be related to the lack of calcium in the medium, which would result in higher electrostatic repulsion between charged phospholipids and the tip, and thus higher forces would need to be overcome for the breakthrough event to occur [37]. For F_{adh} (Figure 2C), we found similar values for both lipid phases, although L_β showed a slightly higher F_{adh} than L_α (0.292 ± 0.002 nN and 0.205 ± 0.004 nN, respectively). These values are in qualitative agreement with previous studies [40], whilst the quantitative differences were most probably due to variations in ionic strength and temperature. However, the observed trend was the same (L_β F_{adh} > L_α F_{adh}). One possible interpretation for this behaviour would be to relate this to the enhanced stiffening induced by calcium; however, this was not the case in the present study, where the Ca^{2+} concentration was minimised by swabbing it away after SLB formation. Therefore, we conclude that adhesion force seems to be sensitive to the presence of Ca^{2+} in the aqueous layer between the SLB and the mica substrate [41,42].

Figures 3B and 3C show the distribution of the F_y and F_{adh} values obtained for the DPPE:POPG system. The most probable force values obtained by a Gaussian fitting of the data are shown in Table 1. Concerning F_y, L_α and L_β phases withstood forces of 1.78 ± 0.05 nN and 2.421 ± 0.009 nN, respectively. Note that we required 1.4 times more force to indent the L_β than the L_α domain, which was to be expected, since L_β, enriched in DPPE is the stiffer domain [16]. Also as expected, given the nominal composition, both values were significantly higher than those obtained for the POPE:POPG system. This could be anticipated because of the nature of DPPE, a saturated phospholipid that rigidifies and confers a higher packing to the system [26]. In this regard, DPPE not only hardens L_β phase to a high degree, but also L_α, where it might be present to a lesser extent. We observed that whilst the F_{adh} for the L_α domain in DPPE:POPG was quite similar to the one obtained for L_α in POPE:POPG, the values obtained for the L_β phase were higher. This confirms the trend already described for POPE:POPG in Figure 2C.

LacY was reconstituted with phospholipids at a LPR ratio (w/w) of 0.5 and the resulting proteoliposomes were then deposited onto mica. Note that this approach yields supported lipid bilayers where LacY is embedded in a random configuration (either facing the substrate or facing the aqueous media). The LPR used was higher than the

one found in the majority of biological membranes and close to that used for 2D crystallisation [30], and was very suitable for conducting a structural analysis of LacY. The lower LPR values used in previous studies yield isolated and undefined single protein entities [26,35]. The PLSs obtained by the reconstitution of LacY in POPE:POPG and DPPE:POPG are shown in Figures 4A and 5A, respectively. In both cases, two laterally segregated domains were observed. As can be seen in Figure 4A, when LacY was reconstituted in POPE:POPG proteoliposomes there was a lower domain with a step height of 5.2 ± 0.2 nm and a higher domain with a step height of 5.6 ± 0.2 nm. Whilst the lower domain was featureless, the higher domain evidenced some protrusions that could be attributed to the self-segregated protein. This becomes clearer in the insert provided in Figure 4A. Roughness (*Ra*) values were of 0.06 nm for the lower domain and of 0.09 nm for the higher.

Figure 5A shows a proteolipid sheet obtained from deposition of LacY reconstituted in DPPE:POPG proteoliposomes. A bilayer patch can be observed which, as above, also contained two different domains: a lower one which was flat and featureless, and a higher one, grainy and covered in protrusions most probably due to the self-segregation of LacY. The heights for the lower and higher domains were 4.2 ± 0.2 nm and 5.2 ± 0.2 nm, respectively. *Ra* values were of 0.08 nm for the lower domain and of 0.15 nm for the higher.

Conversely to what was observed with lower LPRs [26], it was not possible in this case either to confirm the existence of L_α and L_β lipid phases or to identify single isolated entities of the protein. This was not totally unexpected since we were using an extremely high LPR ratio, and thus forcing self-segregation of the protein. To explain these observations, it can be argued that when LacY is reconstituted in a binary phospholipid mixture that presents L_α and L_β domains, the protein recruits those phospholipid species which best match its structural requirements and provide the most adequate physicochemical environment [43,44]. Transmembrane proteins are solvated by those phospholipids that reduce the mismatch of the lipid-protein boundary and, as evidenced by ESR, by a lipid annular ring in immediate contact with the protein [45]. According to FRET measurements in solution [29], PEs are preferred over POPGs. Hence, the upper domains observed in Figures 4A and 5A may consist of the assemblage of LacY, its close phospholipid annular ring and an extra phospholipid nano-domain. Therefore, it was considered of interest to conduct a comparative analysis of the domains observed in Figures 4A and 5A with those observed in Figures 2A and 3A.

To this end, a first approach to understanding the AFM topographic observations in systems with LacY was to compare the step height differences between the SLBs in Figures 2 and 3 and the lipid and proteolipid domains in Figures 4 and 5. Thus, when considering the POPE:POPG mixture with LacY (Figure 4A), we would expect to find a step height difference of 0.9 ± 0.1 nm between L_α and L_β (as shown in Figure 2A). Strikingly, the actual step height difference found between the two domains in Figure 4A was 0.4 ± 0.4 nm. Therefore, it is conceivable that the highest domain corresponded to the L_α phase enriched with LacY protruding about 1.3 ± 0.5 nm into this lipid composition, which is in accordance with previous results [26]. Hence, the step height difference observed here may be the consequence of self-segregation of the protein within the L_α phase, and consequently, the lower domain might correspond to the L_β phase. The same comparison can be conducted for the DPPE:POPG mixture. In this case, Figure 3A without protein shows a domain height difference of 0.7 ± 0.4 nm.

Here, step height difference is 1.0 ± 0.4 nm and thus LacY protrusion can be established as 1.7 ± 0.8 nm, which is in accordance with previous studies using this same lipid mixture [26]. Hence, the lower domain can be assigned to the L_β phase and the upper domain to a protein-enriched L_α domain.

Other possibilities, such as (i) a protein-free lipid domain corresponding to L_α and a protein-enriched domain corresponding to L_α containing LacY, or (ii) a protein-free lipid domain corresponding to L_α or L_β and a protein-enriched domain corresponding to L_β containing LacY, were discarded because a comparative analysis of step height did not present reliable results. However, it was difficult to go any further with this analysis because the use of detergent in proteoliposome preparation can significantly change bilayer characteristics [15]. For example, it has been reported that for POPE:POPG (3:1, mol/mol) mixtures treated with detergent, height differences between L_α and L_β phases are lower than the height observed before DDM incubation [35].

Like most of the membrane proteins LacY is hydrophobic and also extremely flexible, and is solvated with lipid molecules. Specifically we have demonstrated that LacY shows selectivity for PE phospholipids [46,47]. For this reason, when reconstituted in binary systems containing PE and PG with PEs differing in the acyl chain composition, one with two saturated acyl chains and the other with the *sn*-1 chain unsaturated and *sn*-2 saturated it becomes of interest to investigate: first, the distribution of LacY between domains observed in the SLBs; and secondly, how the pulling of the protein from the PLS is affected by each lipid matrix.

Thus, to further characterise the systems, nanomechanical information was obtained by extracting force magnitudes from the FS curves applied to the domains with and without LacY. The distribution of F_y and F_{adh} values was plotted in the histograms shown in Figures 4B and 4C and Figures 5B and 5C for the POPE:POPG and the DPPE:POPG systems, respectively. For a better comparison, the more probable F_y and F_{adh} values corresponding to these compositions are listed in Table 2.

In the case of PLSs obtained from the extension of LacY reconstituted in POPE:POPG, F_y values for domains with and without LacY were 0.124 ± 0.004 nN and 0.37 ± 0.01 nN, respectively. This indicates that domains without protein were less easily punctured than domains containing LacY. Since F_y values in Figure 2B were similar for L_β and L_α phases, the changes in Figure 4B indicate that the presence of LacY modified bilayer stiffness. Strikingly, domains without protein showed F_y values also lower than those obtained for the L_β phase (see Table 1) which might be attributed to the presence of some traces of detergent used during the purification of the protein [15]. When analysing F_{adh}, no significant differences were found between domains with and without LacY (0.105 ± 0.003 nN versus 0.1193 ± 0.0014 nN, respectively) (Table 2), which matches reasonably well with the values obtained for protein-free SLBs (Table 1). In general, all F_y and F_{adh} values were lower than the ones presented in Figure 2B. This might be related to the presence of the protein in the system, but also to some extent to the remaining effect of the detergent used to prepare the samples.

In the case of LacY reconstituted in DPPE:POPG, the F_y values followed a similar trend to the one observed when LacY was reconstituted in POPE:POPG. Thus, LacY-enriched domains showed significantly lower F_y values than protein-free domains (0.222 ± 0.006 nN and 2.55 ± 0.02 nN, respectively). On the one hand, F_y values in domains without protein compared quite well with F_y values obtained for the L_β domains (Figure 3B), which is consistent with the hypothesis that this domain may be

organised similarly to a L_β phase. On the other hand, domains with LacY showed much lower values than the L_α domains in Figure 3B, following a similar trend to the one found for POPE:POPG protein-enriched domains. Regarding F_{adh}, both values were similar in presence and absence of LacY (0.212 ± 0.002 nN and 0.237 ± 0.007 nN, respectively), which may be more related to the detergent treatment than to the presence of protein. Again, all values were lower for DPPE:POPG extended proteoliposomes than for DPPE:POPG extended liposomes.

Taking the entire set of F_y values together, we can state that for both lipid mixtures used in LacY reconstitution, the forces obtained in lipid regions without the protein were similar to the values obtained for the L_β domains in the lipid SLBs obtained from liposome extension. These results strongly suggest that the shortest domains in Figures 4A and 5A may in fact correspond to L_β phases. Furthermore, height enhancement in domains with LacY may be due to the presence of the protein and the negative curvature tendency of PE [48], the main component of the annular boundary region [47]. In turn, this would lead to greater changes in nanomechanical magnitudes. Thus, F_y values in LacY-enriched domains differ from the same values in protein-free L_α domains. More difficult is a direct interpretation of the F_{adh} values, which were dramatically affected by other factors, such as area of contact and tip characteristics [49]. Interestingly, we observed that protein-lipid L_α phases from proteoliposomes could be punctured more easily than the L_α phase in the lipid alone. This reinforces the idea that we are actually observing a new fluid phase that includes average bulk properties of protein and its closed solvated phospholipids.

To elucidate how the presence of proteins affects the lipid bilayer, we investigated the system using the FV [50] mode. Figures 6A and 6B show the FV topography images for the two lipid matrices studied, POPE:POPG and DPPE:POPG, respectively. In order to analyse the results, we classified the images into different regions depending on the proximity of each region to the protein-containing domains (see Figures 6C and 6D). FV was performed applying low force per pixel (the minimum necessary to avoid bilayer destruction whilst permitting topography recording). F_{adh} values were notably lower than those obtained from the FS mode due to the fact that F_{adh} is related to tip penetration [50]. The F_{adh} values obtained in Figure 6 increased with the distance from the protein-enriched domain, ranging from 115 ± 16 pN and 10.5 ± 0.8 pN for region 1, to 308 ± 15 pN and 24 ± 2 pN, for the region furthest from the protein, for POPE:POPG and DPPE:POPG, respectively. Indeed, the trend was clear for both lipid matrices: the further from the protein domain, the higher the acquired F_{adh} value. This can be related to two factors: (i) the presence of the protein, which creates a sort of network which stabilises the lipid bilayer, and (ii) the behaviour of the SLBs (Figures 2C and 3C), where L_β domains presented higher F_{adh} values than L_α domains. This provides support for the coexistence of protein-free L_β phases and LacY-enriched L_α phases.

Having analysed the topographic and nanomechanical changes induced in SLBs when LacY was reconstituted in binary phospholipid systems, it then seemed reasonable to investigate the modifications induced in LacY when embedded in the POPE:POPG and DPPE:POPG matrices. To this end, we performed unspecific FS by approaching the AFM tip close to the PLS (Figures 4A and 5A). This means that the AFM tip was not chemically functionalised and therefore the protein could be pulled away from any point of its secondary structure. Note that we were not pursuing the complete unfolding of the protein in order to unveil its single molecular force spectroscopy spectrum [51] but rather to investigate the stochastic behaviour of the protein embedded in different

phospholipid environments. Specifically, we wanted to ascertain whether the pattern of unspecific pulling was modified depending on the lipid matrix.

In these kinds of experiment, a large number of force curves is obtained, but positive retraction curves account for less than 10% [52]. The large number of unsuccessful events can probably be attributed to the high hydrophobicity of LacY, which is tightly packed in the lipid matrix. Noteworthy, as discussed elsewhere [53] a membrane protein may adapt to lipids or vice versa depending on each particular membrane protein. Figures 7A and 8A show a representative retracting force-distance curve obtained for LacY embedded in POPE:POPG (7A) and in DPPE:POPG (8A) lipid compositions. The retraction curves displayed characteristic sawtooth peak features, with a nonlinear increase in the force on separation that preceded an abrupt return to zero force. As can be seen whilst there is some periodicity between the peaks no overlapped sawtooth patterns appear, indicating that we are pulling a single protein entity. For each force-distance curve, several sawtooth peaks were obtained. By fitting the WLC model to these peaks (Eq. 1), we determined the force required to unfold a pulled protein segment (unfolding force, F_u) and the approximate number of amino acids that the segment contained.

Although fully extended LacY may present an unfolding curve of about 171.8 nm (427 amino acids considering the His-Tag and 0.4 nm per amino acid residue [33]), the representative retracting force-curve in 7A is shorter, indicating that complete unfolding, as expected for a non-specific pulling and strong lipid-protein interactions, did not occur. Conversely, the representative retracting force-curve in Figure 8A is closer to a complete unfolding of the protein. Indeed, the total lengths of the unfolding curves were highly variable depending on the tip-protein contact point and whether the protein was completely unfolded or not. For this reason, entire unfolding curves could not be overlaid and averaged in this study.

Figures 7B and 8B show the distribution of the F_u values obtained from pulling LacY embedded in POPE:POPG and DPPE:POPG matrices, respectively. As can be seen, the main F_u values were centred in different regions depending on the phospholipid binary system used in reconstitution. The presence of a single peak in both histograms may be indicative of a monomeric protein organisation [54]. The average unfolding rupture forces corresponding to LacY embedded in POPE:POPG and DPPE:POPG were 72.7 ± 3.6 pN and 91.4 ± 4.3 pN, respectively. These values are in agreement with the unfolding from 2 to 6 α-helices (see Figure 1), since it is accepted that the force required to unfold a primarily α-helical segment should range between 15 and 25 pN [54,55]. These findings would appear to indicate that higher force is required to unfold LacY from the DPPE:POPG matrix than from the POPE:POPG matrix. These observations suggest that the forces governing the protein-lipid interaction when DPPE is the predominant lipid are slightly more important than when the main lipid is POPE and thus LacY might be more tightly inserted in this system. That can be related to two former observations: (i) PE has been described as a chaperone for LacY and, at the same time it is thought to be essential for LacY physiological activity [46,56–58]; and (ii) the acyl chain curvature plays a defined role in the adaptation to the surface of the protein [28]. Both observations are in agreement with the fact that flexible proteins like LacY adapt better to more rigid phospholipids as it is the case of DPPE [1,53]. Additionally, this coincides with recent finding of Bogdanov's group that demonstrates the relevance of the acyl chains in the LacY activity [25]. Of course, it is tempting to relate this behaviour to the different lateral pressures [20] exerted by each phospholipid. As we

have previously shown from interfacial phospholipid monolayers, DPPE presents a larger compressibility modulus than POPE [26,59].

Further investigation into the pulling events yielded an estimation of the number of amino acids extracted in each unfolding event. The distributions corresponding to the POPE:POPG and DPPE:POPG matrices are shown in Figures 7C and 8C, respectively. As can be seen, the most probable values obtained by retrieving the tip from the protein-enriched domains observed in the POPE:POPG and DPPE:POPG matrices were 76 ± 3 and 77 ± 4 amino acids, respectively. This would correspond, on average, to a most probable unfolding in a row of 2.3 α-helices for both lipid mixtures (on average, LacY presents 33.2 amino acids per α-helix and contiguous loop, Figure 1). Interestingly, although DPPE:POPG presented the highest F_u value, it showed the same number of amino acids per pulling event as that obtained from retrieving the tip from POPE:POPG. This may indicate that the required force per amino acid in DPPE:POPG is higher than that required in the POPE:POPG composition, reinforcing the hypothesis that the lateral pressure [20] exerted by the phospholipids is a relevant parameter to take into account. This is important, because pulling experiment outputs of transmembrane protein may vary depending on the lipid matrix used for reconstitution. Lastly, the probability of total unfolding of LacY increased the more α-helices (and consequently amino acids) were pulled. Hence, the unfolding length histograms respond to a decrease in the # of events as length increases, which can be seen by the exponential decay fitting performed in Figures 7C and 8C. A similar behaviour was found for other systems [60].

Taken together, the results presented in this paper demonstrate that the presence of a protein greatly modifies lateral phase segregation in lipid systems. Clearly, when LacY is incorporated into the lipid matrices, two phases are present, but different of the pure L_β or L_α phases. However, a comparative height analysis and the nanomechanical analysis performed on each domain strongly suggest that the domain where the protein is not apparent corresponded to a L_β lipid domain, whilst the domain enriched in LacY corresponded to a new domain where the characteristics of the pure L_α phase had been slightly modified. There is a preferential insertion of LacY for these like-fluid domains mainly composed of POPG. Note, however, that this is not in contradiction with the presence of POPE or DPPE (to a lesser extent) at the boundary or annular region of LacY.
This finding is in agreement with previous studies based on FRET measurements. Furthermore, the unspecific unfolding approach employed here, which was not aimed at structural elucidation of the protein, showed a differential behaviour depending on the PE acyl chain composition. These results indicate the important influence of the lateral pressure achieved at core levels, as suggested by molecular dynamic simulations.

Acknowledgements

C. S. G. is the recipient of a FPI fellowship from the Spanish Ministerio de Economía y Competitividad of Spain. This study was supported by grant CTQ-2008-03922/BQU from the Spanish Ministerio de Ciencia e Innovación of Spain. The authors also thank the Universitat de Barcelona for financial support and Laura Picas for valuable insights and comments.

FIGURES AND TABLES

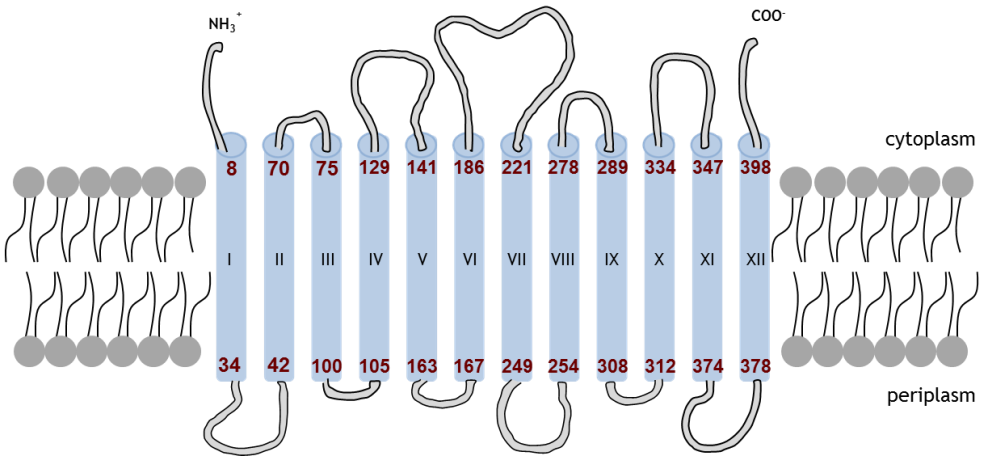

Figure 1. Secondary structure model of lactose permease showing its topological organisation. Red numbers indicate starting and ending amino acid of each transmembrane α-helix. Protein feature based from PDB 1PV6 entry mapped onto a UniProtKB sequence (www.uniprot.org) [21].

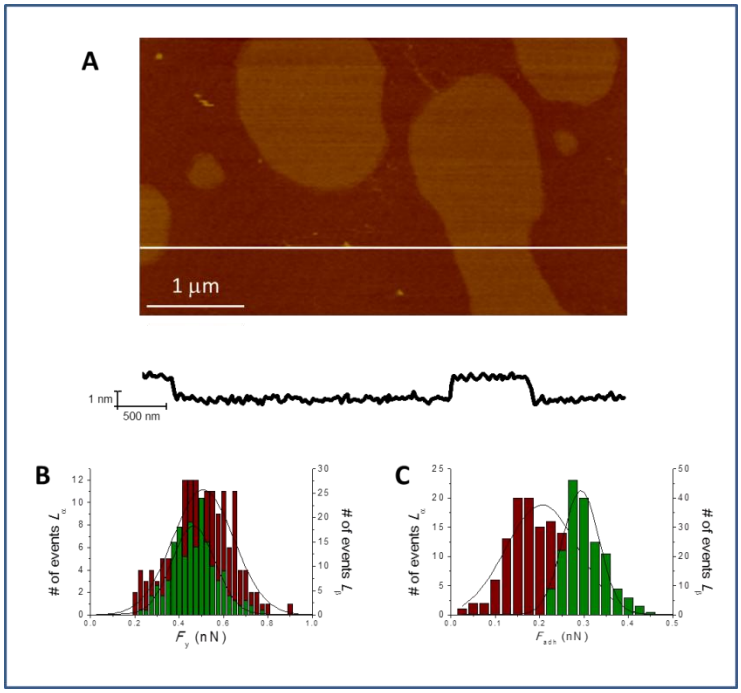

Figure 2. AFM topographic image and height profile analysis of POPE:POPG (3:1, mol/mol) SLB (Z scale = 10 nm) (A). Histograms present the distribution of forces of L_α phase (red) and L_β phase (green) for F_y (B) and F_{adh} (C). Fittings to a Gaussian distribution are represented in solid lines.

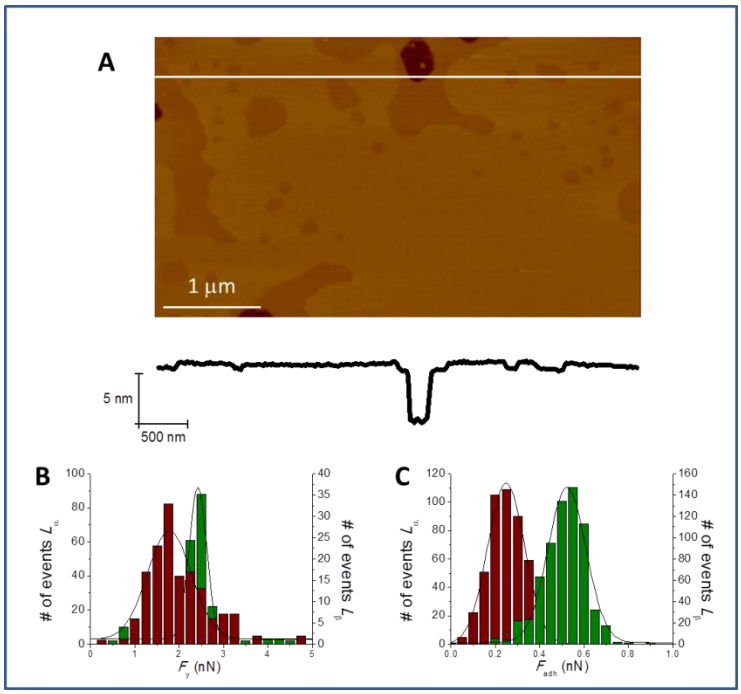

Figure 3. AFM topographic image and height profile analysis of DPPE:POPG (3:1, mol/mol) SLB (Z scale = 10 nm) (A). Histograms present the distribution of forces of L_α phase (red) and L_β phase (green) for F_y (B) and F_{adh} (C). Fittings to a Gaussian distribution are represented in solid lines.

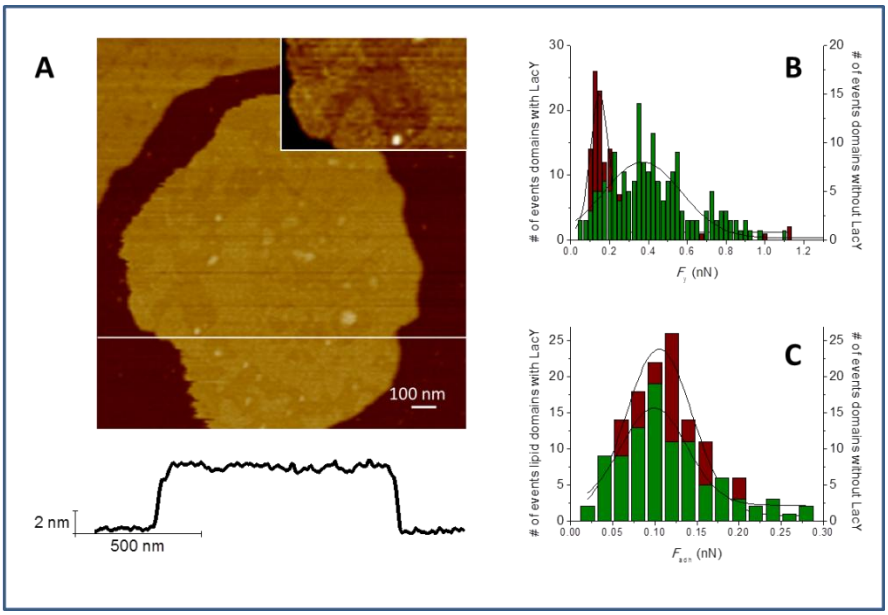

Figure 4. AFM topographic image and height profile analysis of a SLB composed of POPE:POPG (3:1, mol/mol) with LacY at a LPR (w/w) of 0.5 (Z scale = 15 nm) (A). Insert in A presents a magnified image (470 x 280 nm, Z = 3 nm) where domains with LacY can be distinguished from domains without LacY. Histograms present the distribution of forces of domains with LacY (red) and domains without LacY (green) for F_y (B) and F_{adh} (C). Fittings to a Gaussian distribution are represented in solid lines.

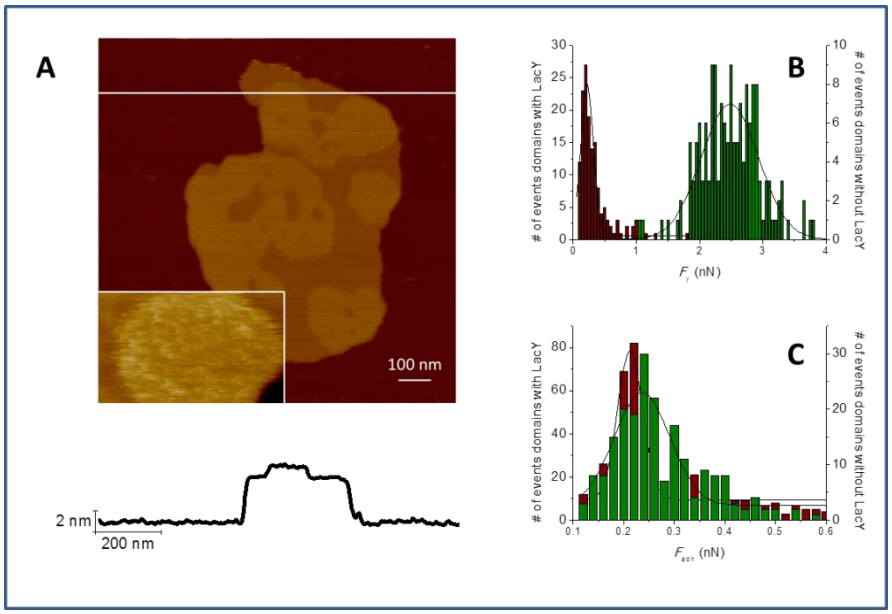

Figure 5. AFM topographic image and height profile analysis of a SLB composed of DPPE:POPG (3:1, mol/mol) with LacY at a LPR of 0.5 (Z scale = 10 nm) (A). Insert in A presents a magnified image (173 x 104 nm, Z = 3 nm) where domains with LacY can be distinguished from domains without LacY. Histograms present the distribution of forces of domains with LacY (red) and domains without LacY (green) for F_y (B) and F_{adh} (C). Fittings to a Gaussian distribution are represented in solid lines.

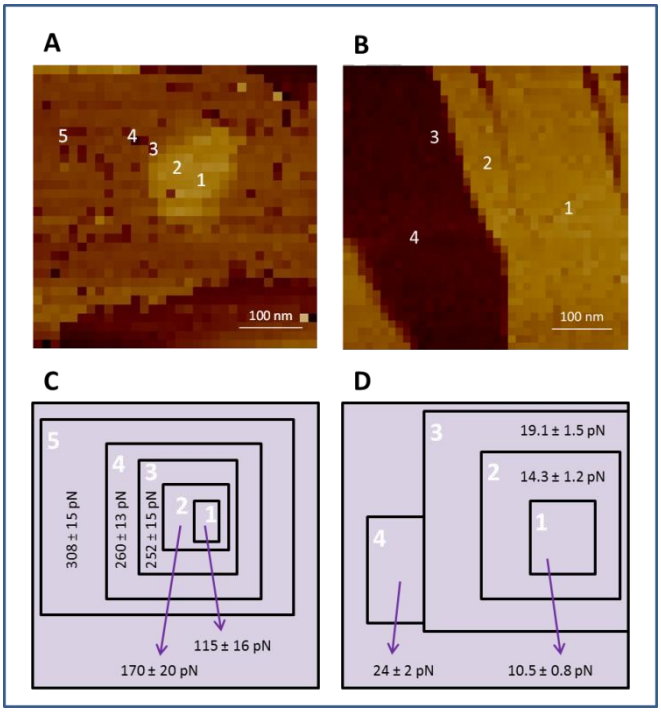

Figure 6. FV AFM topographic images of POPE:POPG (3:1, mol/mol) with LacY (z scale = 15 nm) (A) and DPPE:POPG (3:1, mol/mol) with LacY (z scale = 10 nm) (B). F_{adh} values obtained from image A (C) and B (D). Regions are numbered indicating proximity to the protein starting from zone 1, closer to LacY.

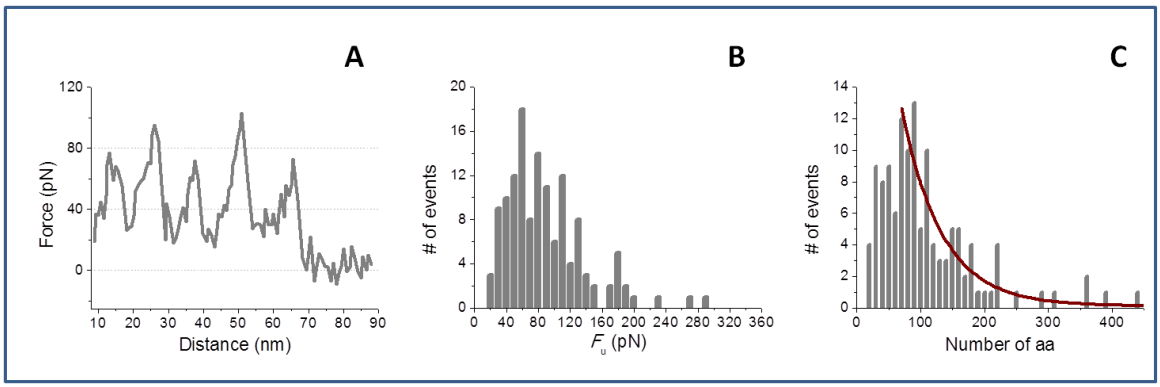

Figure 7. Representative force-distance curve of single LacY unfolding from POPE:POPG (3:1, mol/mol) matrix (A). Distribution of F_u (B) and distribution of force-curve length (C) are shown for LacY in this lipid matrix. Continuous red line corresponds to an exponential fit to the decay.

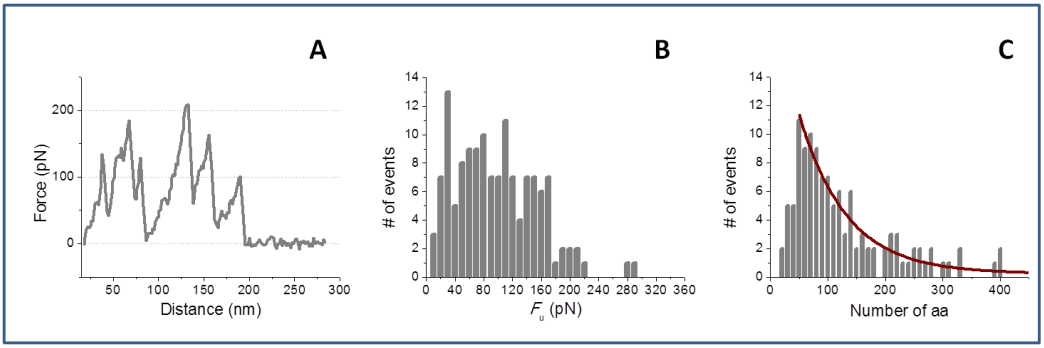

Figure 8. (A) Representative force-distance curve of single LacY unfolding from DPPE:POPG (3:1, mol/mol) matrix (A). Distribution of F_u (B) and distribution of force-curve length (C) are shown for LacY in this lipid matrix. Continuous red line corresponds to an exponential fit to the decay.

Table 1. Mean F_y and F_{adh} values from data presented in Figures 2 and 3, fitted to a Gaussian distribution.

		POPE:POPG (3:1, mol:mol)	DPPE:POPG (3:1, mol:mol)
F_y (nN)	L_α	0.509 ± 0.008	1.78 ± 0.05
	L_β	0.464 ± 0.006	2.421 ± 0.009
F_{adh} (nN)	L_α	0.205 ± 0.004	0.249 ± 0.002
	L_β	0.292 ± 0.002	0.523 ± 0.004

Table 2. Mean F_y and F_{adh} values from data presented in Figures 4 and 5, fitted to a Gaussian distribution

		POPE:POPG (3:1, mol:mol)	DPPE:POPG (3:1, mol:mol)
F_y (nN)	With LacY	0.124 ± 0.004	0.222 ± 0.006
	Without LacY	0.370 ± 0.014	2.55 ± 0.02
F_{adh} (nN)	With LacY	0.105 ± 0.003	0.212 ± 0.002
	Without LacY	0.1193 ± 0.0014	0.237 ± 0.007

REFERENCES

[1] D.M. Engelman, Membranes are more mosaic than fluid, Nature, 438 (2005) 578-580.

[2] M.C. Giocondi, D. Yamamoto, E. Lesniewska, P.E. Milhiet, T. Ando, C. Le Grimellec, Surface topography of membrane domains, Biochim. Biophys. Acta, 1798 (2010) 703-718.

[3] E.I. Goksu, M.L. Longo, Ternary lipid bilayers containing cholesterol in a high curvature silica xerogel environment, Langmuir, 26 (2010) 8614-8624.

[4] D. Lingwood, K. Simons, Lipid rafts as a membrane-organizing principle, Science, 327 (2010) 46-50.

[5] F. Kawai, H. Hara, H. Takamatsu, K. Watabe, K. Matsumoto, Cardiolipin enrichment in spore membranes and its involvement in germination of *Bacillus subtilis* Marburg, Genes Genet. Syst., 81 (2006) 69-76.

[6] E. Mileykovskaya, W. Dowhan, Visualization of phospholipid domains in Escherichia coli by using the cardiolipin-specific fluorescent dye 10-N-nonyl acridine orange, J. Bacteriol., 182 (2000) 1172-1175.

[7] L.M.S. Loura, R.F.M. de Almeida, L.C. Silva, M. Prieto, FRET analysis of domain formation and properties in complex membrane systems, Biochim. Biophys. Acta, 1788 (2009) 209-224.

[8] R. Varma, S. Mayor, GPI-anchored proteins are organized in submicron domains at the cell surface, Nature, 394 (1998) 798-801.

[9] D.A. Brown, E. London, Functions of lipid rafts in biological membranes, Annu. Rev. Cell Dev. Biol., 14 (1998) 111-136.

[10] A. Rietveld, K. Simons, The differential miscibility of lipids as the basis for the formation of functional membrane rafts, Biochim. Biophys. Acta, 1376 (1998) 467-479.

[11] G. van Meer, The different hues of lipid rafts, Science, 296 (2002) 855-857.

[12] A.G. Lee, How lipids affect the activities of integral membrane proteins, Biochim. Biophys. Acta, 1666 (2004) 62-87.

[13] J.A. Poveda, A.M. Fernández, J.A. Encinar, J.M. González-Ros, Protein-promoted membrane domains, Biochim. Biophys. Acta, 1778 (2008) 1583-1590.

[14] P.F. Almeida, W.L. Vaz, T.E. Thompson, Lateral diffusion and percolation in two-phase, two-component lipid bilayers. Topology of the solid-phase domains in-plane and across the lipid bilayer, Biochemistry, 31 (1992) 7198-7210.

[15] A. Berquand, D. Lévy, F. Gubellini, C. Le Grimellec, P.E. Milhiet, Influence of calcium on direct incorporation of membrane proteins into in-plane lipid bilayer, Ultramicroscopy, 107 (2007) 928-933.

[16] S. Garcia-Manyes, L. Redondo-Morata, G. Oncins, F. Sanz, Nanomechanics of lipid bilayers: heads or tails?, J. Am. Chem. Soc., 132 (2010) 12874-12886.

[17] D. Fotiadis, S. Scheuring, S.A. Müller, A. Engel, D.J. Müller, Imaging and manipulation of biological structures with the AFM, Micron, 33 (2002) 385-397.

[18] P.J. Quinn, A lipid matrix model of membrane raft structure, Prog. Lipid Res., 49 (2010) 390-406.

[19] G. van den Bogaart, K. Meyenberg, H.J. Risselada, H. Amin, K.I. Willig, B.E. Hubrich, M. Dier, S.W. Hell, H. Grubmüller, U. Diederichsen, R. Jahn, Membrane protein sequestering by ionic protein-lipid interactions, Nature, 479 (2011) 552-555.

[20] D. Marsh, Protein modulation of lipids, and vice-versa, in membranes, Biochim. Biophys. Acta, 1778 (2008) 1545-1575.

[21] T.U. Consortium, Update on activities at the Universal Protein Resource (UniProt) in 2013, Nucleic Acids Res., 41 (2013) D43-47.

[22] J. Abramson, I. Smirnova, V. Kasho, G. Verner, H.R. Kaback, S. Iwata, Structure and mechanism of the lactose permease of *Escherichia coli*, Science, 301 (2003) 610-615.

[23] L. Guan, H.R. Kaback, Lessons from lactose permease, Annu. Rev. Biophys. Biomol. Struct., 35 (2006) 67-91.

[24] Van Gelder P, F. Dumas, M. Winterhalter, Understanding the function of bacterial outer membrane channels by reconstitution into black lipid membranes, Biophys. Chem., 85 (2000) 153-167.

[25] H. Vitrac, M. Bogdanov, W. Dowhan, Proper fatty acid composition rather than an ionizable lipid amine is required for full transport function of lactose permease from *Escherichia coli*, J. Biol. Chem., 288 (2013) 5873-5885.

[26] C. Suárez-Germà, M.T. Montero, J. Ignés-Mullol, J. Hernández-Borrell, O. Domènech, Acyl chain differences in phosphatidylethanolamine determine domain formation and LacY distribution in biomimetic model membranes, J. Phys. Chem. B, 115 (2011) 12778-12784.

[27] L. Picas, P.E. Milhiet, J. Hernández-Borrell, Atomic force microscopy: a versatile tool to probe the physical and chemical properties of supported membranes at the nanoscale, Chem. Phys. Lipids, 165 (2012) 845-860.

[28] C. Suárez-Germà, L.M.S. Loura, M. Prieto, O. Domènech, J.M. Campanera, M.T. Montero, J. Hernández-Borrell, Phospholipid-lactose permease interaction as reported by a head-labeled pyrene phosphatidylethanolamine: a FRET study, J. Phys. Chem. B, 117 (2013) 6741-6748.

[29] C. Suárez-Germà, L.M.S. Loura, M. Prieto, O. Domènech, M.T. Montero, A. Rodríguez-Banqueri, J.L. Vázquez-Ibar, J. Hernández-Borrell, Membrane protein-lipid selectivity: enhancing sensitivity for modeling FRET data, J. Phys. Chem. B, 116 (2012) 2438-2445.

[30] S. Merino-Montero, Ò. Domènech, M.T. Montero, J. Hernández-Borrell, Preliminary atomic force microscopy study of two-dimensional crystals of lactose permease from *Escherichia coli*, Biophys. Chem., 119 (2006) 78-83.

[31] C. Bustamante, J. Marko, E. Siggia, S. Smith, Entropic elasticity of lambda-phage DNA, Science, 265 (1994) 1599-1600.

[32] A. Janshoff, M. Neitzert, Y. Oberdörfer, H. Fuchs, Force spectroscopy of molecular systems-single molecule spectroscopy of polymers and biomolecules, Angew. Chem. Int. Ed. Engl., 39 (2000) 3212-3237.

[33] S.R.K. Ainavarapu, J. Brujic, H.H. Huang, A.P. Wiita, H. Lu, L. Li, K.A. Walther, M. Carrion-Vazquez, H. Li, J.M. Fernandez, Contour length and refolding rate of a small protein controlled by engineered disulfide bonds, Biophys. J., 92 (2007) 225-233.

[34] M. Giocondi, V. Vié, E. Lesniewska, Phase topology and growth of single domains in lipid bilayers, Langmuir, 17 (2001) 1653-1659.

[35] L. Picas, A. Carretero-Genevrier, M.T. Montero, J.L. Vázquez-Ibar, B. Seantier, P.E. Milhiet, J. Hernández-Borrell, Preferential insertion of lactose permease in phospholipid domains: AFM observations, Biochim. Biophys. Acta, 1798 (2010) 1014-1019.

[36] Y. Dufrêne, W. Barger, J. Green, G. Lee, Nanometer-scale surface properties of mixed phospholipid monolayers and bilayers, Langmuir, 7463 (1997) 4779-4784.

[37] L. Picas, M.T. Montero, A. Morros, M.E. Cabañas, B. Seantier, P.-E. Milhiet, J. Hernández-Borrell, Calcium-induced formation of subdomains in phosphatidylethanolamine-phosphatidylglycerol bilayers: a combined DSC, 31P NMR, and AFM study, J. Phys. Chem. B, 113 (2009) 4648-4655.

[38] A. Alessandrini, H.M. Seeger, A. Di Cerbo, T. Caramaschi, P. Facci, What do we really measure in AFM punch-through experiments on supported lipid bilayers?, Soft Matter, 7 (2011) 7054-7064.

[39] S. Garcia-Manyes, G. Oncins, F. Sanz, Effect of ion-binding and chemical phospholipid structure on the nanomechanics of lipid bilayers studied by force spectroscopy, Biophys. J., 89 (2005) 1812-1826.

[40] R.M.A. Sullan, J.K. Li, S. Zou, Direct correlation of structures and nanomechanical properties of multicomponent lipid bilayers, Langmuir, 25 (2009) 7471-7477.

[41] E. Sackmann, Supported membranes: scientific and practical applications, Science, 271 (1996) 43-48.

[42] P.E. Milhiet, F. Gubellini, A. Berquand, P. Dosset, J.L. Rigaud, C. Le Grimellec, D. Lévy, High-resolution AFM of membrane proteins directly incorporated at high density in planar lipid bilayer, Biophys. J., 91 (2006) 3268-3275.

[43] L. Picas, M.T. Montero, A. Morros, J.L. Vázquez-Ibar, J. Hernández-Borrell, Evidence of phosphatidylethanolamine and phosphatidylglycerol presence at the annular region of lactose permease of *Escherichia coli*, Biochim. Biophys. Acta, 1798 (2009) 291-296.

[44] M. Bogdanov, J. Xie, P. Heacock, W. Dowhan, To flip or not to flip: lipid-protein charge interactions are a determinant of final membrane protein topology, J. Cell Biol., 182 (2008) 925-935.

[45] F.I. Valiyaveetil, Y. Zhou, R. MacKinnon, Lipids in the structure, folding, and function of the KcsA K^+ channel, Biochemistry, 41 (2002) 10771-10777.

[46] L. Picas, C. Suárez-Germà, M.T. Montero, J.L. Vázquez-Ibar, J. Hernández-Borrell, M. Prieto, L.M.S. Loura, Lactose permease lipid selectivity using Förster resonance energy transfer, Biochim. Biophys. Acta, 1798 (2010) 1707-1713.

[47] C. Suárez-Germà, L.M.S. Loura, O. Domènech, M.T. Montero, J.L. Vázquez-Ibar, J. Hernández-Borrell, Phosphatidylethanolamine-lactose permease interaction: a comparative study based on FRET, J. Phys. Chem. B, 116 (2012) 14023-14028.

[48] F. Dumas, J.F. Tocanne, G. Leblanc, M.C. Lebrun, Consequences of hydrophobic mismatch between lipids and melibiose permease on melibiose transport, Biochemistry, 39 (2000) 4846-4854.

[49] J. Israelachvili, Electrostatic Forces Between Surfaces in Liquid, in: Intermolecular and Surface Forces, 3rd ed., Academic Press, San Diego, 2011: pp. 291-340.

[50] H. An, M.R. Nussio, M.G. Huson, N.H. Voelcker, J.G. Shapter, Material properties of lipid microdomains: Force-Volume imaging study of the effect of cholesterol on lipid microdomain rigidity, Biophys. J., 99 (2010) 834-844.

[51] D.J. Muller, AFM : A Nanotool in Membrane Biology, Biochemistry, 47(2008) 7986-7998.

[52] K.T. Sapra, H. Besir, D. Oesterhelt, D.J. Muller, Characterizing molecular interactions in different bacteriorhodopsin assemblies by single-molecule force spectroscopy, J. Mol. Biol., 355 (2006) 640-650.

[53] I. Medalsy, U. Hensen, D.J. Muller, Imaging and Quantifying Chemical and Physical Properties of Native Proteins at Molecular Resolution by Force-Volume AFM, Angew. Chem. Int. Ed. Engl., 50 (2011) 12103-12108.

[54] L.N. Rahman, F. McKay, M. Giuliani, A. Quirk, B. A. Moffatt, G. Harauz, J.R. Dutcher, Interactions of *Thellungiella salsuginea* dehydrins TsDHN-1 and TsDHN-2 with membranes at cold and ambient temperatures-Surface morphology and single-molecule force measurements show phase separation, and reveal tertiary and quaternary associations, Biochim. Biophys. Acta, 1828 (2013) 967-980.

[55] M. Rief, J. Pascual, M. Saraste, H.E. Gaub, Single molecule force spectroscopy of spectrin repeats: low unfolding forces in helix bundles, J. Mol. Biol., 286 (1999) 553-561.

[56] C.C. Chen, T.H. Wilson, The phospholipid requirement for activity of the lactose carrier of *Escherichia coli*, J. Biol. Chem., 259 (1984) 10150-10158.

[57] W. Dowhan, M. Bogdanov, Lipid-dependent membrane protein topogenesis, Annu. Rev. Biochem., 78 (2009) 515-540.

[58] M.F. Lensink, C. Govaerts, J.M. Ruysschaert, Identification of specific lipid-binding sites in integral membrane proteins, J. Biol. Chem., 285 (2010) 10519-10526.

[59] L. Picas, C. Suárez-Germà, M.T. Montero, O. Domènech, J. Hernández-Borrell, Miscibility behavior and nanostructure of monolayers of the main phospholipids of *Escherichia coli* inner membrane, Langmuir, 28 (2011) 701-706.

[60] L.N. Liu, K. Duquesne, F. Oesterhelt, J.N. Sturgis, S. Scheuring, Forces guiding assembly of light-harvesting complex 2 in native membranes, Proc. Natl. Acad. Sci. U.S.A., 108 (2011) 9455-9.

Chapter 5. Discussion

In the present thesis, the working hypothesis to further develop was to assume, based on: (i) electron spin resonance spectroscopy measurements [87]; and (ii) transport experiments carried out with whole cells and proteoliposomes [122]; that there is a direct implication of the phospholipids in the physiological activity of LacY. These phospholipids should be located at the boundary or annular region neighbouring the protein. The main objective of this thesis was to deepen in the elucidation of the physicochemical properties of the lipids in the peripheral region of LacY together with the study of the molecular basis for possible specific protein-lipid interactions. The predominant presence of PE at the annular region of the protein has already been verified by our group [133], confirming cross observations on transport activity [122] and hypothesis of other researchers [136]. Moreover, a minor occupancy of PG has also been reported [131] in agreement with the selective recruitment of phospholipids by LacY in different experimental conditions [132]. However, new approaches were required to finer unveil the nature and the specific physicochemical properties involved in such interactions as well as its biological significance. Consequently, we extended the LacY-phospholipid interaction research to the influence of bulk lipids into the protein insertion (and vice-versa). Hence, we wanted to comprehend the effects induced in the organisation and nanomechanics of lipids when a TMP model such as LacY is inserted in a membrane with binary lipid composition and, at the same time, evaluate changes in the protein properties (structure and folding) when the surrounding lipids are modified. The overall information should give a quite complete insight into the LacY-phospholipid interaction, specially focused in the physicochemical and nanomechanical aspects. Regarding possible studies of non-annular phospholipids [77], their presence

has not been clearly elucidated in LacY yet. Accordingly, in the different X-ray diffraction structures obtained no particular phospholipid was resolved tightly bound to the protein. This does not directly exclude the presence of such kind of phospholipids interacting with the protein, although the LacY ability to present functional activity in different phospholipid conditions may be an indicative of a possible lack of requirement for any non-annular species [140].

The study of LacY annular lipids was achieved by taking advantage of fluorescence techniques with proteoliposomes. More specifically, by exploiting FRET tools between the single tryptophan of the studied mutant (single-W151/C154G LacY) and pyrene-labelled phospholipids added to the vesicles. On the other hand, the investigation of the interaction between bulk lipids and LacY, as well as its consequences in the organisation and nanomechanics of the system were studied using planar models: supported lipid bilayers (SLBs) or planar proteolipid sheets (PLSs). SLBs and PLSs were analysed using topographic and force-spectroscopy (FS) AFM modes.

When working with artificial models the selection of the lipid species forming the lipid membrane is not trivial and represents always the starting point. This means that further studies involving the presence of the protein or the addition of other lipids always imply a greater complication of the system and, thus, it is crucial the previous characterisation of the phospholipid system used as the reference. Therefore, a deep investigation of the lipid systems without the protein is required.

To carry out the experiments we selected lipid mixtures corresponding to simplified biomimetic approaches of the inner membrane of *E. coli*. Hence, we worked with binary mixtures of synthetic PE:PG phospholipids at a molar ratio of 3:1. PE is described as a pivotal phospholipid regarding LacY folding and functioning [6,122] which leads to the presumption of a major role for this species in the system. For this reason we focused on the study of effects related to the PE phospholipid acyl chain composition while maintaining PG species constant. In addition, despite different acyl chain compositions were studied, we concentrated in heteroacid phospholipids because they are predominant configurations in natural membranes [153]. Thus, POPG was the PG compound used in all the matrices and POPE was the most examined PE, being the studied systems POPE:POPG (3:1, mol/mol), DOPE:POPG (3:1, mol/mol), and DPPE:POPG (3:1, mol/mol). Different molar ratios between PE and PG were also

analysed in matrices such as POPE:POPG (3:1, mol/mol), POPE:POPG (1:1, mol/mol) and POPE:POPG (1:3, mol/mol). Finally, although PCs do not show relevant biological significance in the case of the inner membrane of *E. coli*, a recent publication from Bogdanov et al. [142] showed that LacY displays full functional activity when the protein is assembled in mutated *E. coli* where PCs substitute PEs. By contrast, LacY inserted in proteoliposomes containing 70% of DOPC and 30% of PG/CL only displays downhill activity. On account of those results LacY was also reconstituted in PC matrices, which represents a test for the versatility of the protein in adapting to different lipid systems [140]. Moreover, the investigation of PCs with different acyl chains can be useful in order to understand the implications of the phospholipid structure in the LacY-phospholipid interaction.

There are many works showing the preferential insertion of highly mobile proteins in the L_α phase of the lipid matrices [34,94]. Therefore, in a first study described in section 3.3.1 the physicochemical behaviour of DOPE:POPG (3:1, mol/mol), POPE:POPG (3:1, mol/mol) and DPPE:POPG (3:1, mol/mol) lipid systems was addressed with the main objective to investigate the lipid lateral phase separation phenomena. Our results demonstrated that changing PE acyl chains largely modified the behaviour of the lipid systems. Laurdan and AFM measurements evidenced DOPE:POPG (3:1, mol/mol) system in fluid phase all over the studied temperatures (from 3 to 65 ºC). By contrast, DPPE:POPG (3:1, mol/mol) system showed a large range of temperatures with coexistence of L_α and L_β domains with different composition, as shown by AFM at 24 and 37 ºC and by Laurdan measurements which evidenced a coexistence of domains ranging from 21.3 to 49.0 ºC. This was further corroborated by the corresponding isotherms at 24 and 37 ºC displaying two different collapses and thus a laterally segregated system. In the case of POPE:POPG (3:1, mol/mol), L_α and L_β domains only coexisted during the T_m (23.3 ºC, according to Laurdan measurements), as it was further confirmed in the study described in section 3.3.2. Assuming that our mixtures are mimicking but not fully representative of the whole composition of the *E. coli* inner membrane, which is considered to be in L_α phase, the biological meaning of the physical phase separation phenomena can be discussed. Therefore, although drastic changes in temperature are not expected on the regular life of the bacteria, since POPE:POPG (3:1, mol/mol) presents its phase transition close to room temperature this might actually have a biological meaning in some particular situations (e.g. *E. coli* living out of warm-

blooded animals [256]). Besides, the appearance of phase transition in phospholipids can be triggered by other specific factors (e.g. the presence of divalent ions, that normally affects the T_m of a sample [185]) and thus become locally relevant in cells. Additionally, the presence of surrounding membrane proteins or structural cytoskeleton *in vivo* might also modify this behaviour [9]. In any event, DOPE:POPG (3:1, mol/mol) mixture, with a phase transition far from natural conditions (T_m < 3 ºC, according to Laurdan measurements in section 3.3.1) is the system where a possible phase separation would be less relevant in nature.

To assess the importance of such phase separation in the insertion of LacY we reconstituted the protein in proteoliposomes of the very same mixtures (study in 3.3.1). The proteoliposomes were extended over mica and imaged at 27 ºC using AFM. This temperature was chosen because at these conditions POPE:POPG (3:1, mol/mol) and DPPE:POPG (3:1, mol/mol) displayed phase separation. The proteoliposomes were prepared at low LPR in order to avoid possible effects on the phospholipid organisation related to the presence of a high amount of protein. In addition, this configuration allowed a better investigation of the influence of the phase separation in the protein insertion and distribution. In agreement with former studies [128], LacY was mostly observed in L_α phases or sometimes at the boundary regions between both phases, but was excluded from L_β phases in the studied phospholipid matrices. Interestingly, this may indicate that albeit differences in phospholipid acyl chains, length and curvature between these mixtures, all L_α phases were capable to better insert the protein as compared to L_β phases, most likely due to a better hydrophobic matching and adaptation to seal the protein boundaries. However, this does not directly mean that the protein was correctly folded or that it could display full activity in these lipid compositions. Thus, the lack of LacY in L_β phases indicates that the protein can adapt better to POPE:POPG (3:1, mol/mol) and DPPE:POPG (3:1, mol/mol) L_α phases than to L_β phases from the same mixtures. This behaviour can be related to bulk characteristics of the L_α phase in terms of fluidity or, alternatively, to the specific lipid composition of these domains. Indeed, due to its lower melting transition temperature, POPG would presumably be the main component of both fluid phases, something that can contradict the preferential presence of PE at the annular region of the protein. Finally, in the special case of DOPE:POPG (3:1, mol/mol) where the whole system displayed L_α phase, it was interesting to observe the protein mostly self-segregated in an edge of the bilayer patch.

This could point to a high fluidity in the system which permitted the protein to easily diffuse and cluster across the 2D plane of the bilayer.

The presence of LacY in L_α phases where presumably POPG is the predominant species seems to contradict the fact that LacY selects PE in POPE:POPG (3:1, mol/mol) systems as it has been assessed by FRET measurements [133], and other studies indicating the requirement for PE in PE-lacking engineered *E. coli* cells [122]. To further address this problem we constructed a binary phase diagram for the POPE:POPG system (study in 3.3.2). This was important in order to estimate the extent of POPG enrichment in the L_α phase at different temperatures and compositions. Note, however, that a DSC phase diagram from vesicles was already available for this mixture [158]. Unfortunately, such diagram could not be extrapolated to SLB samples, where the infinite curvature of the bilayer together with a high influence of the support creates large physicochemical differences between both model membranes. Hence, the objective was to acquire, despite the limitations of the AFM technique, an AFM pseudo-phase diagram from SLBs to extrapolate information to other studies with the same model membrane system. With this purpose in mind we worked with SLBs in a buffer supplemented with Ca^{2+} because this ion is often used to assist the extension of negative liposomes on a support by the vesicle fusion technique [59], as it is the case of the samples prepared in our studies. Complementarily, a binary phase diagram based on DSC measurements of liposomes was also performed in presence of Ca^{2+} in order to compare it with the binary phase diagram obtained using AFM. As expected, the obtained DSC phase diagram was displaced to lower T_m and presented lower molar enthalpies (ΔH_{DSC}) than their associated van't Hoff molar enthalpies (ΔH_{vH}) calculated from the AFM data. These results confirmed an effect of the mica support on the lipid transition as it has already been described in other works [186,188,189].

In spite of being very useful to interpret SLBs studies of phospholipid mixtures, phase diagrams based in AFM temperature controlled experiments are not frequent in the literature [189,257]. Consequently, the construction of such diagram for the POPE:POPG binary mixture represents a step forward and creates a tool that can be useful to other researchers working with similar phospholipid systems. Additionally, working with SLBs presents the advantage of allowing the AFM topographical and nanomechanical analysis of the system at diverse points of the phase diagram.

Therefore, by performing force-distance (FD) curves we obtained the nanomechanical parameters most commonly used in biomembranes (breakthrough force or F_y and adhesion force or F_{adh}). For completeness, the continuum nucleation model was also fitted to the F_y data in order to calculate Γ (the line tension of the molecules in the periphery of a hole) and S (the spreading pressure associated with the energy per unit area gained by the layer when filling a hole formed after a rupture). All the obtained values were directly associated to the POPG content: (i) increasing Γ values and decreasing S values upon the enlargement of POPG in the system and, (ii) F_y and F_{adh} displaying inverted trends for L_β and L_α in $\chi_{POPG} = 0.75$ as compared to $\chi_{POPG} < 0.75$. These effects related to the POPG increasing were explained by the stiffening of the system due to the presence of calcium: the cation has the ability to interact with the negative headgroup of the phospholipid and create a PG-PG network. This leads to a more rigid bilayer that responds differently to the nanomechanical stimulus.

In the study described in section 4.3.4 we performed again FS analysis of POPE:POPG (3:1, mol/mol). However, in this case no calcium was present when performing the FD curves, since the ion had been swabbed out after the vesicle extension. Interestingly, when comparing both results we realised that similar trends appeared (especially for F_{adh}), which is difficult to justify if the system lacks of Ca^{2+}. In fact, this can be explained by the presence of a buffer layer trapped between the mica and the bilayer during the SLB formation [58,60]. It should be stressed here that Ca^{2+} in this layer can only interact with negative POPG phospholipids placed in the proximal bilayer leaflet, but, surprisingly, this interaction seems to be sufficient to entail global nanomechanical effects in the bilayer.

Focusing on the most biomimetic mixture, POPE:POPG (3:1, mol/mol), the obtained T_m from the AFM binary phase diagram was 27.80 ± 0.12 ºC and the phase transition encompassed a wide range of temperatures, displaying domain coexistence from 25.5 to 30 ºC. Additionally, the diagram was used to estimate the phospholipid composition of the L_α phase at 27 ºC and it confirmed a large enrichment with POPG: it represents 80.7% of this phase. Therefore, taking into account results in 3.3.1 where LacY was embedded preferentially in L_α phases, we can conclude that LacY is inserted in a phase where the main component is POPG. As confirmed in the POPE:POPG (3:1, mol/mol) isotherm at 24 ºC (study in 3.3.1) the system displays good miscibility and thus should present its compounds randomly distributed. Hence, an arbitrary distribution would

signify a high amount of POPG in the annular region of LacY. Instead, the protein prefers POPE in its vicinity as judged by FRET measurements [133]. Therefore, these observations reinforce the idea of a preferential LacY-phospholipid interaction, contrary to a random distribution of phospholipids. Still, POPG may play a role in the system, most likely affecting the bulk properties of the membrane. It could be related to contributions in fluidity, but also in negative charge. Actually, in Bogdanov et al. studies [140], LacY displaying proper transport is always embedded in matrices with up to $\simeq$ 30% of PG and cardiolipin. In any case, the idea of a fluid POPG phase with segregated POPE surrounding LacY might be similar to a hypothesis postulated by London [258]. In this review lateral asymmetry in membrane domains is proposed to happen in diverse ways and at different levels. For instance, a possible way of domain formation is a protein embedded in a fluid phase, but with appetence for a more rigid nanodomain, which would organise only in the annular region close to the protein.

Once the phospholipid systems were extensively analysed, in a second stage we aimed to address the study of the influence between the protein and the lipids. Therefore, as mentioned, we delineated a strategy to study the fluid phase and the insertion of LacY at different levels: the study of the annular lipids was addressed by FRET fluorescence in proteoliposomes under different conditions, and the bulk lipids were studied in phase separated planar PLSs.

The first of the FRET studies (section 4.3.1) aiming the comprehension of the annular region of LacY was delineated with the idea of obtaining direct information about the protein-phospholipid affinity. Thus, LacY was embedded into single-component vesicles. This choice was directed to the elimination of possible factors coming from the biomimetic matrix in order to only focus the attention on the pure structural (chemical) selectivity between LacY and a particular phospholipid species. Moreover, this experimental approach avoided problems present when performing FRET studies in two-component lipid matrices: (i) due to a dilution problem, the probability of finding labelled phospholipids surrounding the protein is decreased and the obtained results are less representative; and (ii) although we normally consider the labelled phospholipid to behave as the unlabelled one and act as a reporter, in fact there are evidences strongly suggesting that we are working with ternary systems [259]. It is true that experiments mimicking the real membrane describe a more realistic situation where all phospholipid species might exert a function in the final organisation of the ensemble, but from a

physicochemical point of view these experiments are complex to analyse due to a system with many variables. So the single-component FRET experiments are crucial as a source of information about LacY capacity to select between a given phospholipid matrix or a precise labelled phospholipid.

Hence, we performed FRET analyses with LacY reconstituted in single phospholipid matrices of POPE, POPG, DOPC and POPC where a χ =0.015 of pyrene acyl chain labelled-PE, -PG or -PC was present. A conceivable obstacle related to the use of non-biomimetic configurations was the possibility of obtaining LacY reconstituted in a non-native topology. It is for instance well-described in systems only containing PG and CL that LacY displays an inverted topology and is not capable to perform uphill activity [130]. However, since downhill activity is preserved, binding capabilities might be conserved. Unfortunately, the mutant employed in our studies, single-W151/C154G LacY cannot execute transport, which limits the possibilities to asses a good membrane insertion to the analysis of the protein substrate recognition. Therefore, although we observed in substrate recognition tests that LacY embedded in a POPG system conserved good binding affinity; other studies confirm that the protein is not correctly folded within this environment [130]. Conversely, when LacY was inserted in DOPC or POPC systems, it presented good binding affinity in our tests and other studies confirm the correct folding of the protein under these conditions [140]. More complicated was the case of POPE because we detected a compromised binding capacity most likely due to the non-lamellar propensity of PE. However, LacY has been reported to work at its best in high amounts of PE [6]. Although it is true that a 98.5% PE matrix as used here has not been tested before in *in vitro* experiments with LacY proteoliposomes, coherent fluorescent spectra were found, suggesting that the position of the fluorophore, sited near the binding site, remains unaltered and that the global structure is maintained.

The obtained FRET results under this particular configuration were of great relevance to understand the preference of LacY for specific phospholipids. Hence, the PE-labelled molecule was the compound that presented higher energy transfer in all the studied mixtures. In addition, when applying the mathematic model developed in collaboration with Dr Loura and Dr Prieto, PE-labelled phospholipids displayed the higher probability (μ) of being found in the annular region and also the higher relative association constant between the labelled and the unlabelled phospholipids (K_s). This is indeed very significant since it assesses a clear preferential LacY-PE interaction and corroborates

previous findings [133]. Thus, this means that whatever is the main lipid surrounding LacY, the protein will always modify the physicochemical properties of the matrix where is embedded to bring closer a phospholipid with a PE headgroup (or, alternatively, PE phospholipids will minimize the energy for a good insertion of the protein in the membrane by segregating closer to the protein). Therefore, it seems to demonstrate that LacY prefers a zwitterionic phospholipid with an ionisable amine. In particular, it has been proved that these characteristics are not essential for the protein functioning since the zwitterionic POPC and the neutral glycolipid GlcDAG can also support full LacY activity [140,143]. Accordingly, in this study the labelled-PC in POPC mixtures presented a significant μ to be placed in the annular region of LacY in certain phospholipid matrices. However, our studies indicated that, whatever is the case, the protein prefers PEs over PCs.

The comparison of the two studied PC containing systems is convenient in order to understand the different reported behaviour of the protein when embedded in POPC or DOPC matrices. Hence, whereas POPC supported the uphill transport activity of the protein [140], just as PC replacing PE *in vivo* in engineered *E. coli* [142]*;* DOPC could only support downhill transport [130]. Unexpectedly but in agreement with these results, in our studies a differential behaviour of labelled-PCs in both systems was described. Thus, labelled-PC was found with higher μ in the annular region of LacY in the case of POPC, whilst LacY in a DOPC matrix presented a probability close to zero of presenting a labelled-PC in its vicinity. The interpretation of the results can be done by considering the probe as a second phospholipid species competing with the unlabelled phospholipid for the same sites in an annular position. Then, low FRET efficiency of labelled-PC in a DOPC matrix indicates that the DOPC phospholipid was capable of displacing the probe out of the annular region of the protein and, therefore, that DOPC is the preferred phospholipid for the protein. On the contrary, POPC could not displace the probe, which points to the following LacY selectivity trend: DOPC>labelled-PC>POPC. This is somehow intriguing, because it seems to indicate that although the protein is not fully active in DOPC phospholipids and fully active in POPC, regarding the fluorescent probes used it presents a major affinity for DOPC than for POPC phospholipids. Assuming that (i) LacY protein embedded in a DOPC matrix cannot perform uphill transport, but is capable of substrate recognition and downhill transport, and (ii) the used s-W151/C154G LacY mutant is arrested in one specific

pseudo inward-conformation; one could think that LacY may be capable to adapt the composition of its annular region depending on the state of the protein. Therefore, it is reasonable to think that LacY may prefer to be surrounded by DOPC when it is in inward-facing conformation, but that the preference for this lipid can be modified during conformational transitions. This would be supported by the high exchange rate described for phospholipids in the annular lipid region [87].

These results from section 4.3.1 are reinforced by those obtained from the study described in 4.3.3, where pyrene PE phospholipids marked in the headgroup (HPyr-PE) were used to analyse the influence of the acyl chain on the system. These experiments were delineated to further understand the influence of the acyl chain composition on the present system, and were performed in binary phospholipid biomimetic matrices (DOPE:POPG, POPE:POPG and DPPE:POPG; 3:1, mol/mol). The results were interpreted taking into account the favoured presence of PE surrounding the protein, as well as all the previous FRET results. Thus, we deduced a tendency indicating the preference for a phospholipid to be located at the annular region of the protein as follows: DOPE>HPyr-PE> POPE. Again DOPE was the preferred phospholipid for LacY. Additionally, these results pointed to a possible importance of the phospholipid spontaneous curvature (C_0) for the LacY selectivity. In fact, the described trend matches an estimated C_0 tendency from the more negative value to the less negative one (see manuscript in 4.3.3). Thus, the data seem to confirm that C_0 is a major determinant of the LacY−lipid interaction, with PE lipids bearing more negative C_0 values being preferred relative to others with a more cylindrical shape.

Studies in 4.3.2 and 4.3.3 were performed using biomimetic phospholipid compositions. By contrast to the single-component strategy, although the two-component matrices cause dilution of the probe and difficulty in interpreting the results, the obtained data is relatively more significant. Therefore, the study with enhanced selectivity (4.3.1) gave us information on the precise LacY-phospholipid affinity, but it omitted the effect of another phospholipid in the mixture. This presence may effectively affect through various means, such as the presence of phase separation and the possible partition of the protein in fluid phases. Indeed, from Laurdan liposome studies in 3.3.1 we know that POPE:POPG (3:1, mol/mol) mixture shows a T_m close to room temperature (23.3 ºC) and DPPE:POPG (3:1, mol/mol) displays coexistence of domains with different composition ranging from 21.3 to 49.0 ºC.

Furthermore, the two described FRET studies (4.3.1, 4.3.3) were focused on revealing information concerning the phospholipids surrounding the protein. In a third FRET study (section 4.3.2) we wanted to centre on the protein structure and try to grasp structural reasons explaining the protein-lipid selectivity. Thus, we based our hypothesis in studies pointing to the amino acid in position 68, an aspartic acid, as the more important residue involved in the PE-protein interaction [136]. The interaction is described to be related to a salt bridge formed between D68, PE and K69. Therefore, it seemed interesting to design FRET experiments which could further investigate these findings. With this aim, the position 68 of our LacY mutant was mutated by placing a cysteine, amino acid which is not capable to perform the mentioned salt bridge. Then, FRET studies were performed between pyrene-labelled phospholipids marked in the acyl chain and the single tryptophan of the new mutant (single-W151/C154G/D68C LacY) embedded in three different biomimetic compositions: DOPE:POPG (3:1, mol/mol), POPE:POPG (3:1, mol/mol) and DPPE:POPG (3:1, mol/mol). This configuration was outlined with the purpose of comparing the obtained results with former ones coming from single-W151/C154G LacY [133].

A common feature in both studies was, interestingly, the presence of higher E/M ratio in annular phospholipids as compared to bulk species, which confirms the segregation of the pyrene-labelled phospholipids in the vicinity of the protein and thus, the formation of an annular region. On the contrary, the pattern of phospholipid affinities was modified when working with the new mutant, namely (i) higher relative affinity between POPE and single-W151/C154G than between POPE and single-W151/C154G/D68C, and (ii) modified affinity trend in DPPE:POPG (3:1, mol/mol) system, where the main component of the annular region was PG in single-W151/C154G, and PE in single-W151/C154G/D68C. In the remaining studied systems PE was found to be the main component of the annular region in single-W151/C154G/D68C as it happened in single-W151/C154G.

Notwithstanding, the D68C mutation did not lead to a new situation with PE completely depleted from the annular region, as it would have been the best case to assess a lack of interaction between PEs and the cysteine in position 68. However, the presence of PE near the protein is not directly indicative of the presence or absence of this link, nor gives information about the strength of a possible interaction. In any event, we observed a general diminution of the selectivity for PEs in this mutant and a change in the

phospholipid selectivity, being suggestive of modifications in the protein-lipid interaction. Therefore, we can confirm that this position exhibits a relationship with the surrounding lipid environment, but we cannot validate it as the most important position regarding PE-LacY interaction.

In summary, all the presented FRET studies point to the presence of a separated phospholipid annular region surrounding LacY as evidenced by enhanced E/M ratios in this region as compared to the bulk lipids. This is in agreement with former fluorescent studies with LacY [129,131,133]. In addition, PE has been corroborated as the main component of the annular region of the protein, although PC could also play a role, at least in the inward-facing configuration. Moreover, evidences have been found suggesting a great importance of the acyl chain structure, as well as geometric characteristics of the phospholipids such as the C_0. Indeed, FRET studies were of extreme importance before further analysing the systems through SLBs using AFM. AFM studies can display a great resolution at the nanoscale level and they present a privileged vision of the insertion of a membrane protein. However, it is complicated to use this technique to obtain information on the annular region of a protein. That is why FRET experiments, along with previous phase behaviour and phase composition studies on phospholipid systems were crucial in order to discuss further results on LacY insertion in planar bilayers.

The next step was the AFM analysis of phase separated systems with the presence of single-W151/C154G LacY at high LPR (study in 4.3.4). Because the biomimetic composition of POPE:POPG (3:1, mol/mol) does not present phase separation at 37 °C, in these studies we worked at room temperature to observe how the presence of protein affects each of the different phases. Additionally, the presence of a phase separated system is necessary in order to obtain regions with packed protein, since a whole fluid phase could lead to the diffusion and dilution of the protein all around the lipid system. The chosen phase separated systems at room temperature were POPE:POPG (3:1, mol/mol) and DPPE:POPG (3:1, mol/mol). The protein was reconstituted to form proteoliposomes which were subsequently extended over mica. Then, the obtained planar systems were analysed through topography, force-spectroscopy (FS) and force-volume (FV) AFM modes. In parallel, the same systems without protein were also studied as controls.

When studying the extended proteoliposomes using AFM, we observed for both phospholipid matrices the presence of two different domains: a flat, lower domain, and a higher one that presented a large number of protrusions. The domains step height was analysed and they turned out to correlate to a lower L_β domain and a higher L_α domain with enhanced step height due to the presence of protein and a possible hydrophobic match between lipids and proteins. Furthermore, FS analysis allowed comparing nanomechanical parameters of lower and higher phases with parameters obtained for L_α and L_β in SLB lipid systems. From these comparisons we observed that the lower domain presented quite similar nanomechanic characteristics to L_β phase, just with few modifications probably due to different preparation processes (in the case of proteoliposomes the system was in contact with detergent and, although rinsed, we cannot exclude a possible remaining concentration in the membrane). Conversely, the higher domain seemed to correspond to a L_α with new characteristics, probably related to the creation of a new phase where average parameters of lipids and proteins were displayed.

Additionally, thanks to the FV mode we could map adhesion forces (F_{adh}) from different zones in an AFM image, giving rise to a clear trend where F_{adh} values decreased the closer the analysed phospholipids were to the protein. This could be explained by a stabilisation effect related to the presence of the protein or alternatively, by differences in F_{adh} found for L_α and L_β phases and previously identified in systems without protein. The results corroborated the hypothesis of a higher domain with the protein embedded in L_α phase and a lower protein-free domain displaying L_β phase.

It is interesting to recall here that from the AFM phase diagram we know that fluid phases in POPE:POPG are mainly composed of POPG. In the case of DPPE:POPG (3:1, mol/mol), due to the high T_m of the DPPE pure system, fluid phases might also be composed mainly of POPG. Since LacY is embedded in these regions we can confirm a bulk role of POPG phospholipid in the protein insertion. Moreover, since the nanomechanical properties of the system undergo changes due to protein insertion, we can also speculate a role for the protein in modifying indirectly these bulk phospholipid properties; although a possible role for the remaining detergent cannot be excluded. However, the effects between LacY and the phospholipids seem to be reciprocal.

Further confirmation of this reciprocity can be attained by performing unspecific pulling experiments of the protein with the AFM tip. Previous experiments of FS and FV on lipids had focused on the effects induced by the protein in the analysed phospholipid systems. Here, stochastic unspecific pulling of LacY embedded in the two studied lipid matrices focused on the protein to give light to the differential forces maintaining LacY inserted in a flat bilayer. Note that both studied lipid systems presented good binding capabilities [133], although this does not directly assess proper LacY folding and topology. Therefore, we do not know if the protein is folded with an identical topology in both systems. In any regard, divergences were found between the two models systems as evidenced by the differential pulling of LacY depending on the surrounding phospholipids. In effect, more force was needed when trying to unfold the protein in DPPE:POPG (3:1, mol/mol) system than in POPE:POPG (3:1, mol/mol) system. This might indicate different interaction forces between LacY and lipids, which could be assessed to different lipid bulk properties or to a different annular region lipid composition. Indeed, from FRET experiments 4.3.1-4.3.3 we know that PE is the main phospholipid in the annular region of POPE:POPG (3:1, mol/mol), whilst PG has been described as the main phospholipid in the DPPE:POPG (3:1, mol/mol) system [133]. This could point to differences derived from a different annular region composition.

Taking into account that (i) POPE:POPG (3:1, mol/mol) is the more biomimetical matrix [153], and (ii) PE, which is needed for proper LacY function, is close to the protein in POPE:POPG (3:1, mol/mol) but not in DPPE:POPG (3:1, mol/mol), it seems interesting to discuss the described harder interaction existing between LacY and DPPE:POPG (3:1, mol/mol) matrix as compared to POPE:POPG (3:1, mol/mol). Thus, major stability is not always a sign for a better activity, as it has been described in LacY for mutations such as C154G [203] or D68E [211]. In those situations different interactions within amino acid side chains of the protein were stabilized, which, unexpectedly, inactivated the protein because the required reorganization of the structure to conduct conformational changes was impeded. Similarly, the stabilization of LacY in DPPE:POPG (3:1, mol/mol) system may not be indicative of a better protein functioning, especially regarding the lack of PE in the annular region of the protein. However, further activity studies are required.

Regarding bulk characteristics, the different pattern in the LacY unspecific pulling depending on the phospholipid matrix suggests that the forces governing the protein-

lipid interaction when DPPE is the predominant lipid are slightly more important than when the main lipid is POPE and thus LacY might be more tightly inserted in this system. This evidences an importance for PE phospholipid, which can be related to the fact that PE has been described as a chaperone for LacY and, at the same time, it is thought to be essential for LacY physiological activity [6,133,136,137]. Additionally, it corroborates that the acyl chain curvature of the phospholipid (C_0) plays a defined role in the adaptation to the surface of the protein, as described in 4.3.1 and 4.3.3, which indirectly reinforces the relevance of the acyl chains in the LacY activity, as it has been postulated by Vitrac et al. [140].

To conclude, regarding POPE:POPG (3:1, mol/mol), the more biomimetic system for LacY, we confirmed by AFM imaging of samples at low and high LPR that the protein inserts preferentially in the L_α phase (studies 3.3.1 and 4.3.4). Additionally, the construction of an AFM pseudo-phase diagram for the binary system allowed us to estimate the composition of this phase at a given temperature, and a major presence of POPG was found at the studied temperatures (study 3.3.2). Regardless of this POPG enrichment in L_α phase, the presence of PE as the preferential phospholipid in the annular region was corroborated by FRET studies which pointed to a selective PE-LacY interaction instead of a random phospholipid positioning (studies 4.3.1-4.3.3). Additionally, a role for the D68 position in the LacY sensing of the lipid environment was found (study 4.3.2). Finally, effects on the nanomechanics of the L_α phase upon the insertion of the protein were described. For instance, the PLS systems displayed lower F_y values than free-protein SLBs, which is indicative of new physicochemical values coming from the average of the lipid and protein bulk properties (study 4.3.4). Furthermore, the interactions of LacY with this POPE:POPG (3:1, mol/mol) L_α phase seemed to present a well-balanced, accurate magnitude to facilitate conformational changes, as it was evidenced from pulling experiments where the force needed to pull the protein in this lipid matrix was lower than the one needed to pull it from the less suitable DPPE:POPG (3:1, mol/mol) system (study 4.3.4).

Chapter 6. Conclusions

This thesis can be framed within the fields of biophysics of biomembranes and physical chemistry, and embedded in the wide field of bionanotechnology. We have studied the existing relationship between a membrane protein, LacY, and its surrounding annular and bulk phospholipids. The partial conclusions of this work can be described as follows:

Characterization of the lipid system

- The physicochemical magnitudes of DOPE:POPG (3:1, mol/mol), POPE:POPG (3:1, mol/mol) and DPPE:POPG (3:1, mol/mol) have been studied by Langmuir isotherms, Laurdan fluorescence of liposomes and AFM imaging of SLBs. Specially, the phase separation phenomena related to the temperature of the system has been investigated, showing DOPE:POPG (3:1, mol/mol) in L_α phase from 3 to 65 ºC, POPE:POPG (3:1, mol/mol) only displaying phase separation around its T_m (23.3 ºC according to Laurdan experiments), and DPPE:POPG (3:1, mol/mol) showing coexistence of domains of different composition from 21.3 to 49 ºC in Laurdan experiments and at 24 and 37 ºC according to AFM analysis.

- To further understand the POPE:POPG system two binary phase diagrams have been constructed in the presence of 10 mM of Ca^{2+}, one obtained from DSC measurements of liposomes in solution and another from SLBs topographical analysis through temperature-controlled AFM. The AFM phase diagram enables the comprehension of the phase composition in other SLBs experiments performed at any χ_{POPG} and T.

- The AFM nanomechanical analysis of POPE:POPG system varying the χ_{POPG} content at 27 ºC and in presence of 10 mM of Ca^{2+} showed large variations in F_y, F_{adh}, Γ and S upon the increasing of the POPG content. This has been attributed to the interaction of the POPG headgroup with the divalent ion. Additionally, the presence of the cation in the remaining buffer layer between the bilayer and the substrate has been revealed to have important effects on a system with negatively charged phospholipids and where calcium has been removed after the extension.

Characterization of the LacY-phospholipid interaction

- The sensitivity for modelling FRET data obtained in membrane protein-lipid selectivity assays has been enhanced by using pure lipid matrices with χ = 0.015 of labelled-phospholipid. This configuration has been useful to unveil preferential LacY-phospholipid interactions.

- The knowledge about the physicochemical magnitudes governing the selectivity between LacY and the phospholipids configuring the annular region has been expanded by using FRET experiments. Regarding headgroup preferences, it has been described that the protein favours zwitterionic phospholipids, with preference for PE over PC. However, in a phase separated system LacY tends to be in L_α phases and it can be surrounded by PG if PE or PC are not present in the phase. Regarding acyl chain preferences, it seems proved that the protein in inward-facing conformation prefers DOPE > POPE > DPPE. This preference trend can be related to the requirement of phospholipids displaying a negative C_0 for the correct insertion and sealing of the protein in the bilayer.

- The importance of the aspartic acid in position 68 of LacY sequence has been confirmed. From our studies, since phospholipid preferences were modified in D68 mutants, this position seems to show a role in the interaction of the protein with the surrounding lipid matrix. However, the hypothesis pointing this amino acid as the most important for LacY-PE phospholipid has not been validated with our methodology.

- LacY reconstitutions in SLBs at low and high LPR analysed by topographic AFM mode showed that the protein inserts preferentially in L_α phases in POPE:POPG (3:1 mol/mol) and DPPE:POPG (3:1 mol/mol) systems. Hence, the affinity of LacY for L_α phases has been confirmed.

- Upon LacY insertion in a membrane, topographic changes were observed: the normally higher-stepped L_β phase became the lower observed phase because of the L_α phase increase in step-height. This increase was related to the presence of the protein in this phase and a possible reorganization of the phospholipids due to the hydrophobic matching with the protein. In addition to topographic changes, the nanomechanical parameters were modified for the LacY-enriched L_α phase: it displayed lower F_y and F_{adh} values than the pure-lipid system used as a control. Those effects were attributed to bulk lipid-LacY interaction.

- The reciprocal interaction between bulk lipids and LacY was evidenced by studying the differential unfolding of the protein depending on the lipid matrix where it was embedded: more force was required to unfold LacY from a DPPE:POPG (3:1, mol/mol) system than from a POPE:POPG (3:1, mol/mol) one. Thus, not only LacY modifies the characteristics of the matrices where it is embedded, but the lipid composition determines the forces governing the tight insertion of the protein into the lipid bilayer.

GENERAL CONCLUSION

In this thesis the relationship between LacY and its annular and bulk lipids in model systems has been unveiled. First, after validating LacY preference for phospholipid fluid (L_α) phases in the studied two-component model systems, a different composition between bulk and annular phospholipids was confirmed. Hence, bulk lipids, which were assimilated to the phospholipids in L_α phase, were mainly formed by PG, while PE was the main component of the annular region. This points to a direct phospholipid-LacY selectivity because it discards a random phospholipid distribution near the protein. Second, the LacY selectivity for precise phospholipid species at the annular region was found to be related to: (i) a neutral charged phospholipid (PE or PC, with preference for

the former), and (ii) phospholipids displaying a large negative spontaneous curvature (C_0) (DOPE > POPE). In addition, D68 was revealed as an important amino acid for the protein annular lipid selectivity. Third, the interaction between LacY and the bulk lipids was described as reciprocal. Accordingly, the presence of the protein largely modified the topography and the nanomechanics of the lipid system, especially for the L_α phase, whilst the nanomechanics of LacY itself were different depending on the surrounding lipid matrix: more force was needed to pull LacY form the DPPE:POPG (3:1, mol/mol) system than from the POPE:POPG (3:1, mol/mol) one. Therefore, the bilayer lipid composition seems to determine the forces governing the LacY tight interaction with the membrane and can be thus very important for the protein correct insertion and activity.

Chapter 7. References

[1] H. Lodish, D. Baltimore, A. Berk, S.L. Zipursky, P. Matsudaira, J. Darnell, Molecular cell biology, 2nd ed., Scientific American Books, 1995.

[2] D. Nicholls, S. Ferguson, Bioenergetics, 4th ed., Academic Press, 2013.

[3] R.B. Gennis, Biomembranes Molecular structure and function, Springer-Verlag, Harrisonburg, 1989.

[4] L.A. Bagatolli, J.H. Ipsen, A.C. Simonsen, O.G. Mouritsen, An outlook on organization of lipids in membranes: searching for a realistic connection with the organization of biological membranes, Progress in Lipid Research, 49 (2010) 378-89.

[5] N.S. Mueller, R. Wedlich-Söldner, F. Spira, From mosaic to patchwork: matching lipids and proteins in membrane organization, Molecular Membrane Biology, 29 (2012) 186-96.

[6] W. Dowhan, M. Bogdanov, Lipid-dependent membrane protein topogenesis, Annual Review of Biochemistry, 78 (2009) 515-40.

[7] C. Tanford, The hydrophobic effect: formation of micelles and biological membranes, 2nd ed., Wiley, 1980.

[8] E. Sackmann, Biological membranes architecture and function, in: R. Lipowsky, E. Sackmann (Ed.), Handbook of Biological Physics. Volume 1., Elsevier B.V., 1995: pp. 1-63.

[9] A. Kusumi, T.K. Fujiwara, R. Chadda, M. Xie, T.A. Tsunoyama, Z. Kalay, R.S. Kasai, K.G.N. Suzuki, Dynamic organizing principles of the plasma membrane that regulate signal transduction: commemorating the fortieth anniversary of Singer and Nicolson's fluid-mosaic model, Annual Review of Cell and Developmental Biology, 28 (2012) 215-50.

[10] S. Morein, A. Andersson, L. Rilfors, G. Lindblom, Wild-type *Escherichia coli* cells regulate the membrane lipid composition in a "window" between gel and non-lamellar structures, The Journal of Biological Chemistry, 271 (1996) 6801-9.

[11] S.J. Singer, G.L. Nicolson, The fluid mosaic model of the structure of cell membranes, Science, 175 (1972) 720-31.

[12] D.M. Engelman, Membranes are more mosaic than fluid, Nature, 438 (2005) 578-80.

[13] G. Vereb, J. Szöllosi, J. Matkó, P. Nagy, T. Farkas, L. Vigh, L. Mátyus, T.A. Waldmann, S. Damjanovich, Dynamic, yet structured: The cell membrane three decades after the Singer-Nicolson model, Proceedings of the National Academy of Sciences of the United States of America, 100 (2003) 8053-8.

[14] U. Coskun, K. Simons, Cell membranes: the lipid perspective, Structure, 19 (2011) 1543-8.

[15] O.G. Mouritsen, Model answers to lipid membrane questions, Cold Spring Harbor Perspectives in Biology, 3 (2011) a004622.

[16] A.G. Lee, Biological membranes: the importance of molecular detail, Trends in Biochemical Sciences, 36 (2011) 493-500.

[17] H.R. Horton, L.A. Moran, G. Scrimgeour, M.D. Perry, J.D. Rawn, Principles of biochemistry, 4th ed., Pearson International Edition, Upper Saddle River, 2006.

[18] S. Ollila, M.T. Hyvönen, I. Vattulainen, Polyunsaturation in lipid membranes: dynamic properties and lateral pressure profiles, The Journal of Physical Chemistry. B, 111 (2007) 3139-50.

[19] V.A. Frolov, J. Zimmerberg, Cooperative elastic stresses, the hydrophobic effect, and lipid tilt in membrane remodeling, FEBS Letters, 584 (2010) 1824-9.

[20] J.N. Israelachvili, D.J. Mitchell, B.W. Ninham, Theory of self-assembly of lipid bilayers and vesicles, Biochimica et Biophysica Acta, 470 (1977) 185-201.

[21] R. Koynova, M. Caffrey, An index of lipid phase diagrams, Chemistry and Physics of Lipids, 115 (2002) 107-219.

[22] M.F. Brown, Curvature forces in membrane lipid-protein interactions, Biochemistry, 51 (2012) 9782-95.

[23] T. Heimburg, Thermal biophysics of membranes, Willey-VCH, Weinheim, 2007.

[24] S.D. Connell, D.A. Smith, The atomic force microscope as a tool for studying phase separation in lipid membranes, Molecular Membrane Biology, 23 (2006) 17-28.

[25] S.J. Marrink, A.H. de Vries, D.P. Tieleman, Lipids on the move: simulations of membrane pores, domains, stalks and curves, Biochimica et Biophysica Acta, 1788 (2009) 149-68.

[26] J. Zimmerberg, M.M. Kozlov, How proteins produce cellular membrane curvature, Nature Reviews. Molecular Cell Biology, 7 (2006) 9-19.

[27] G. Lindblom, I. Brentel, M. Sjölund, G. Wikander, A. Wieslander, Phase equilibria of membrane lipids from *Acholeplasma laidlawii*: importance of a single lipid forming nonlamellar phases, Biochemistry, 25 (1986) 7502-10.

[28] A. Demchenko, Modern views on the structure and dynamics of biological membranes, Biopolymers and Cell, 28 (2012) 24-38.

[29] P.F. Devaux, A. Herrmann, N. Ohlwein, M.M. Kozlov, How lipid flippases can modulate membrane structure, Biochimica et Biophysica Acta, 1778 (2008) 1591-600.

[30] V.A. Frolov, A.V. Shnyrova, J. Zimmerberg, Lipid polymorphisms and membrane shape, Cold Spring Harbor Perspectives in Biology, 3 (2011) a004747.

[31] D. Lingwood, K. Simons, Lipid rafts as a membrane-organizing principle, Science, 327 (2010) 46-50.

[32] T.S. van Zanten, A. Cambi, M.F. Garcia-Parajo, A nanometer scale optical view on the compartmentalization of cell membranes, Biochimica et Biophysica Acta, 1798 (2010) 777-87.

[33] M.C. Giocondi, D. Yamamoto, E. Lesniewska, P.E. Milhiet, T. Ando, C. Le Grimellec, Surface topography of membrane domains, Biochimica et Biophysica Acta, 1798 (2010) 703-18.

[34] H.M. Seeger, C.A. Bortolotti, A. Alessandrini, P. Facci, Phase-transition-induced protein redistribution in lipid bilayers, The Journal of Physical Chemistry. B, 113 (2009) 16654-9.

[35] L.A. Bagatolli, P.B. Sunil Kumar, Phase behavior of multicomponent membranes: Experimental and computational techniques, Soft Matter, 5 (2009) 3234-48.

[36] L.A. Bagatolli, To see or not to see: lateral organization of biological membranes and fluorescence microscopy, Biochimica et Biophysica Acta, 1758 (2006) 1541-56.

[37] D. Alsteens, M.C. Garcia, P.N. Lipke, Y.F. Dufrêne, Force-induced formation and propagation of adhesion nanodomains in living fungal cells, Proceedings of the National Academy of Sciences of the United States of America, 107 (2010) 20744-9.

[38] L. Picas, F. Rico, M. Deforet, S. Scheuring, Structural and mechanical heterogeneity of the erythrocyte membrane reveals hallmarks of membrane stability, ACS Nano, 7 (2013) 1054-63.

[39] R. Lindner, H.Y. Naim, Domains in biological membranes, Experimental Cell Research, 315 (2009) 2871-8.

[40] A. Honigmann, C. Walter, F. Erdmann, C. Eggeling, R. Wagner, Characterization of horizontal lipid bilayers as a model system to study lipid phase separation, Biophysical Journal, 98 (2010) 2886-94.

[41] A. Cambi, D.S. Lidke, Nanoscale membrane organization: where biochemistry meets advanced microscopy, ACS Chemical Biology, 7 (2012) 139-49.

[42] W.H. Binder, V. Barragan, F.M. Menger, Domains and rafts in lipid membranes, Angewandte Chemie (International Ed. in English), 42 (2003) 5802-27.

[43] L.M.S. Loura, F. Fernandes, M. Prieto, Membrane microheterogeneity: Förster resonance energy transfer characterization of lateral membrane domains, European Biophysics Journal, 39 (2010) 589-607.

[44] P.A. Janmey, P.K.J. Kinnunen, Biophysical properties of lipids and dynamic membranes, Trends in Cell Biology, 16 (2006) 538-46.

[45] S.M. Gruner, Intrinsic curvature hypothesis for biomembrane lipid composition: a role for nonbilayer lipids, Proceedings of the National Academy of Sciences of the United States of America, 82 (1985) 3665-9.

[46] D. Marsh, Lateral pressure profile, spontaneous curvature frustration, and the incorporation and conformation of proteins in membranes, Biophysical Journal, 93 (2007) 3884-99.

[47] D. Marsh, Intrinsic curvature in normal and inverted lipid structures and in membranes, Biophysical Journal, 70 (1996) 2248-55.

[48] D. Marsh, Protein modulation of lipids, and *vice-versa*, in membranes, Biochimica et Biophysica Acta, 1778 (2008) 1545-75.

[49] R. Cantor, Lateral pressures in cell membranes: a mechanism for modulation of protein function, The Journal of Physical Chemistry B, 101 (1997) 1723-25.

[50] R.S. Cantor, The lateral pressure profile in membranes : a physical mechanism of general anesthesia, Biochemistry, 36 (1997) 2339-44.

[51] M.Ø. Jensen, O.G. Mouritsen, Lipids do influence protein function-the hydrophobic matching hypothesis revisited, Biochimica et Biophysica Acta, 1666 (2004) 205-26.

[52] D.L. Parton, J.W. Klingelhoefer, M.S.P. Sansom, Aggregation of model membrane proteins, modulated by hydrophobic mismatch, membrane curvature, and protein class, Biophysical Journal, 101 (2011) 691-9.

[53] A.J. García-Sáez, P. Schwille, Stability of lipid domains, FEBS Letters, 584 (2010) 1653-8.

[54] J. Fan, M. Sammalkorpi, M. Haataja, Formation and regulation of lipid microdomains in cell membranes: theory, modeling, and speculation, FEBS Letters, 584 (2010) 1678-84.

[55] L. Picas, P.E. Milhiet, J. Hernández-Borrell, Atomic force microscopy: a versatile tool to probe the physical and chemical properties of supported membranes at the nanoscale, Chemistry and Physics of Lipids, 165 (2012) 845-60.

[56] E.A. Disalvo, F. Lairion, F. Martini, E. Tymczyszyn, M. Frías, H. Almaleck, G.J. Gordillo, Structural and functional properties of hydration and confined water in membrane interfaces, Biochimica et Biophysica Acta, 1778 (2008) 2655-70.

[57] L.K. Tamm, H.M. McConnell, Supported phospholipid bilayers, Biophysical Journal, 47 (1985) 105-13.

[58] E. Castellana, P. Cremer, Solid supported lipid bilayers: From biophysical studies to sensor design, Surface Science Reports, 61 (2006) 429-44.

[59] A. Berquand, D. Lévy, F. Gubellini, C. Le Grimellec, P.E. Milhiet, Influence of calcium on direct incorporation of membrane proteins into in-plane lipid bilayer, Ultramicroscopy, 107 (2007) 928-33.

[60] E. Sackmann, Supported membranes: scientific and practical applications, Science, 271 (1996) 43-8.

[61] M. Loose, P. Schwille, Biomimetic membrane systems to study cellular organization, Journal of Structural Biology, 168 (2009) 143-51.

[62] S. Garcia-Manyes, F. Sanz, Nanomechanics of lipid bilayers by force spectroscopy with AFM: a perspective, Biochimica et Biophysica Acta, 1798 (2010) 741-9.

[63] M. Przybylo, J. Sýkora, J. Humpolíckova, A. Benda, A. Zan, M. Hof, Lipid diffusion in giant unilamellar vesicles is more than 2 times faster than in supported phospholipid bilayers under identical conditions, Langmuir, 22 (2006) 9096-9.

[64] R.P. Richter, R. Bérat, A.R. Brisson, Formation of solid-supported lipid bilayers: an integrated view, Langmuir, 22 (2006) 3497-505.

[65] L. Picas, C. Suárez-Germà, M. Teresa Montero, J. Hernández-Borrell, Force spectroscopy study of Langmuir-Blodgett asymmetric bilayers of

phosphatidylethanolamine and phosphatidylglycerol, The Journal of Physical Chemistry. B, 114 (2010) 3543-49.

[66] A.C. Simonsen, L.A. Bagatolli, Structure of spin-coated lipid films and domain formation in supported membranes formed by hydration, Langmuir, 20 (2004) 9720-8.

[67] I. Reviakine, A. Brisson, Formation of Supported Phospholipid Bilayers from Unilamellar Vesicles Investigated by Atomic Force Microscopy, Langmuir, 16 (2000) 1806-15.

[68] A.A. Brian, H.M. McConnell, Allogeneic stimulation of cytotoxic T cells by supported planar membranes, Proceedings of the National Academy of Sciences of the United States of America, 81 (1984) 6159-63.

[69] S. Ramadurai, A. Holt, V. Krasnikov, G. van den Bogaart, J.A. Killian, B. Poolman, Lateral diffusion of membrane proteins, Journal of the American Chemical Society, 131 (2009) 12650-6.

[70] A. Krogh, B. Larsson, G. von Heijne, E.L. Sonnhammer, Predicting transmembrane protein topology with a hidden Markov model: application to complete genomes, Journal of Molecular Biology, 305 (2001) 567-80.

[71] M.S. Almén, K.J.V. Nordström, R. Fredriksson, H.B. Schiöth, Mapping the human membrane proteome: a majority of the human membrane proteins can be classified according to function and evolutionary origin, BMC Biology, 7 (2009) 50.

[72] J. Zimmerberg, K. Gawrisch, The physical chemistry of biological membranes, Nature Chemical Biology, 2 (2006) 564-7.

[73] A. Engel, H. Gaub, Structure and mechanics of membrane proteins, Annual Review of Biochemistry, 77 (2008) 127-48.

[74] T.K.M. Nyholm, S. Özdirekcan, J. Killian, How protein transmembrane segments sense the lipid environment, Biochemistry, 46 (2007) 1457-65.

[75] O.S. Andersen, R.E. Koeppe, Bilayer thickness and membrane protein function: an energetic perspective, Annual Review of Biophysics and Biomolecular Structure, 36 (2007) 107-30.

[76] E.J. Denning, O. Beckstein, Influence of lipids on protein-mediated transmembrane transport, Chemistry and Physics of Lipids, 169 (2013) 57-71.

[77] A.G. Lee, How lipids affect the activities of integral membrane proteins, Biochimica et Biophysica Acta, 1666 (2004) 62-87.

[78] H. Palsdottir, C. Hunte, Lipids in membrane protein structures, Biochimica et Biophysica Acta, 1666 (2004) 2-18.

[79] A.M. Ernst, F.X. Contreras, B. Brügger, F. Wieland, Determinants of specificity at the protein-lipid interface in membranes, FEBS Letters, 584 (2010) 1713-20.

[80] D. Marsh, Lateral pressure in membranes, Biochimica et Biophysica Acta, 1286 (1996) 183-223.

[81] P.V. Escribá, J.M. González-Ros, F.M. Goñi, P.K.J. Kinnunen, L. Vigh, L. Sánchez-Magraner, A.M. Fernández, X. Busquets, I. Horváth, G. Barceló-Coblijn, Membranes: a meeting point for lipids, proteins and therapies, Journal of Cellular and Molecular Medicine, 12 (2008) 829-75.

[82] R. Phillips, T. Ursell, P. Wiggins, P. Sens, Emerging roles for lipids in shaping membrane-protein function, Nature, 459 (2009) 379-85.

[83] M. Andersson, A.N. Bondar, J.A. Freites, D.J. Tobias, H.R. Kaback, S.H. White, Proton-coupled dynamics in lactose permease, Structure, 20 (2012) 1893-904.

[84] K. Murzyn, T. Róg, M. Pasenkiewicz-Gierula, Phosphatidylethanolamine-phosphatidylglycerol bilayer as a model of the inner bacterial membrane, Biophysical Journal, 88 (2005) 1091-103.

[85] E.C. Mbamala, A. Ben-Shaul, S. May, Domain formation induced by the adsorption of charged proteins on mixed lipid membranes, Biophysical Journal, 88 (2005) 1702-14.

[86] A.G. Lee, Lipid–protein interactions in biological membranes: a structural perspective, Biochimica et Biophysica Acta, 1612 (2003) 1-40.

[87] D. Marsh, L.I. Horváth, Structure, dynamics and composition of the lipid-protein interface Perspectives from spin-labelling, Biochimica et Biophysica Acta, 1376 (1998) 267-96.

[88] M. Hayer-Hartl, H. Schägger, G. von Jagow, K. Beyer, Interactions of phospholipids with the mitochondrial cytochrome-c reductase studied by spin-label ESR and NMR spectroscopy, European Journal of Biochemistry, 209 (1992) 423-30.

[89] L. Qin, M.A. Sharpe, R.M. Garavito, S. Ferguson-Miller, Conserved lipid-binding sites in membrane proteins: a focus on cytochrome c oxidase, Current Opinion in Structural Biology, 17 (2007) 444-50.

[90] H. Belrhali, P. Nollert, A. Royant, C. Menzel, J.P. Rosenbusch, E.M. Landau, E. Pebay-Peyroula, Protein, lipid and water organization in bacteriorhodopsin crystals: a molecular view of the purple membrane at 19 Å resolution, Structure, 7 (1999) 909-17.

[91] F. Cymer, A. Veerappan, D. Schneider, Transmembrane helix-helix interactions are modulated by the sequence context and by lipid bilayer properties, Biochimica et Biophysica Acta, 1818 (2012) 963-73.

[92] F. Dumas, M.C. Lebrun, J.F. Tocanne, Is the protein/lipid hydrophobic matching principle relevant to membrane organization and functions?, FEBS Letters, 458 (1999) 271-7.

[93] A. Alessandrini, P. Facci, Unraveling lipid/protein interaction in model lipid bilayers by Atomic Force Microscopy, Journal of Molecular Recognition, 24 (2011) 387-96.

[94] M.D. Houslay, K.K. Stanley, Dynamics of biological membranes: influence on synthesis structure and function, Wiley & Sons, London, 1982.

[95] P.E. Milhiet, V. Vié, M.C. Giocondi, C. Le Grimellec, AFM characterization of model rafts in supported bilayers, Single Molecules, 2 (2001) 109–12.

[96] M. Sinensky, Homeoviscous adaptation--a homeostatic process that regulates the viscosity of membrane lipids in *Escherichia coli*, Proceedings of the National Academy of Sciences of the United States of America, 71 (1974) 522-5.

[97] A. Rietveld, T.J. van Kemenade, T. Hak, A.J. Verkleij, B. de Kruijff, The effect of cytochrome c oxidase on lipid polymorphism of model membranes containing cardiolipin, European Journal of Biochemistry, 164 (1987) 137-40.

[98] S.H. White, A.S. Ladokhin, S. Jayasinghe, K. Hristova, How membranes shape protein structure, The Journal of Biological Chemistry, 276 (2001) 32395-8.

[99] G. van den Bogaart, K. Meyenberg, H.J. Risselada, H. Amin, K.I. Willig, B.E. Hubrich, M. Dier, S.W. Hell, H. Grubmüller, U. Diederichsen, R. Jahn, Membrane protein sequestering by ionic protein-lipid interactions, Nature, 479 (2011) 552-5.

[100] C.R. Sanders, K.F. Mittendorf, Tolerance to changes in membrane lipid composition as a selected trait of membrane proteins, Biochemistry, 50 (2011) 7858-67.

[101] H.X. Zhou, T.A. Cross, Modeling the membrane environment has implications for membrane protein structure and function: influenza A M2 protein, Protein Science, 22 (2013) 381-94.

[102] W. Dowhan, Molecular basis for membrane phospholipid diversity: why are there so many lipids?, Annual Review of Biochemistry, 66 (1997) 199-232.

[103] G. van Meer, D.R. Voelker, G.W. Feigenson, Membrane lipids: where they are and how they behave, Nature Reviews. Molecular Cell Biology, 9 (2008) 112-24.

[104] H. Sprong, P.V.D. Sluijs, G.V. Meer, How proteins move lipids and lipids move proteins, Nature Reviews Molecular Cell Biology, 2 (2001) 504-13.

[105] A. Ortiz, J.A. Killian, A.J. Verkleij, J. Wilschut, Membrane fusion and the lamellar-to-inverted-hexagonal phase transition in cardiolipin vesicle systems induced by divalent cations, Biophysical Journal, 77 (1999) 2003-14.

[106] T.H. Haines, N.A. Dencher, Cardiolipin: a proton trap for oxidative phosphorylation, FEBS Letters, 528 (2002) 35-9.

[107] S.S. Pao, I.A.N.T. Paulsen, M.H. Saier, Major Facilitator Superfamily, Microbiology, 62 (1998) 1-34.

[108] L. Guan, H.R. Kaback, Lessons from lactose permease, Annual Review of Biophysics and Biomolecular Structure, 35 (2006) 67-91.

[109] M.G. Madej, S. Dang, N. Yan, H.R. Kaback, Evolutionary mix-and-match with MFS transporters, Proceedings of the National Academy of Sciences of the United States of America, 110 (2013) 5870-4.

[110] P. Mitchell, Chemiosmotic coupling in oxidative and photosynthetic phosphorylation 1966, Biochimica et Biophysica Acta, 1807 (2011) 1507-38.

[111] H.R. Kaback, M. Sahin-Tóth, A.B. Weinglass, The kamikaze approach to membrane transport, Nature Reviews. Molecular Cell Biology, 2 (2001) 610-20.

[112] J. Abramson, I. Smirnova, V. Kasho, G. Verner, H.R. Kaback, S. Iwata, Structure and mechanism of the lactose permease of *Escherichia coli*, Science, 301 (2003) 610-5.

[113] L. Guan, O. Mirza, G. Verner, S. Iwata, H.R. Kaback, Structural determination of wild-type lactose permease, Proceedings of the National Academy of Sciences of the United States of America, 104 (2007) 15294-8.

[114] Y. Nie, H.R. Kaback, Sugar binding induces the same global conformational change in purified LacY as in the native bacterial membrane, Proceedings of the National Academy of Sciences of the United States of America, 107 (2010) 9903-8.

[115] H.R. Kaback, I. Smirnova, V. Kasho, Y. Nie, Y. Zhou, The alternating access transport mechanism in LacY, The Journal of Membrane Biology, 239 (2011) 85-93.

[116] S. Frillingos, M. Sahin-Tóth, J. Wu, H.R. Kaback, Cys-scanning mutagenesis: a novel approach to structure function relationships in polytopic membrane proteins, FASEB Journal, 12 (1998) 1281-99.

[117] O. Mirza, L. Guan, G. Verner, S. Iwata, H.R. Kaback, Structural evidence for induced fit and a mechanism for sugar/H+ symport in LacY, The EMBO Journal, 25 (2006) 1177-83.

[118] Y. Zhou, X. Jiang, H.R. Kaback, Role of the irreplaceable residues in the LacY alternating access mechanism, Proceedings of the National Academy of Sciences of the United States of America, 109 (2012) 12438-42.

[119] I. Smirnova, V. Kasho, H.R. Kaback, Lactose permease and the alternating access mechanism, Biochemistry, 50 (2011) 9684-93.

[120] P.Y. Pendse, B.R. Brooks, J.B. Klauda, Probing the periplasmic-open state of lactose permease in response to sugar binding and proton translocation, Journal of Molecular Biology, 404 (2010) 506-21.

[121] S. Radestock, L.R. Forrest, The alternating-access mechanism of MFS transporters arises from inverted-topology repeats, Journal of Molecular Biology, 407 (2011) 698-715.

[122] W. Dowhan, M. Bogdanov, Molecular genetic and biochemical approaches for defining lipid-dependent membrane protein folding, Biochimica et Biophysica Acta, 1818 (2012) 1097-107.

[123] J. le Coutre, L.R. Narasimhan, C.K. Patel, H.R. Kaback, The lipid bilayer determines helical tilt angle and function in lactose permease of *Escherichia coli*, Proceedings of the National Academy of Sciences of the United States of America, 94 (1997) 10167-71.

[124] G. Enkavi, E. Tajkhorshid, Simulation of spontaneous substrate binding revealing the binding pathway and mechanism and initial conformational response of GlpT, Biochemistry, 49 (2010) 1105-14.

[125] J. Baker, S.H. Wright, F. Tama, Simulations of substrate transport in the multidrug transporter EmrD, Proteins, 80 (2012) 1620-32.

[126] C.D. Linden, K.L. Wright, H.M. McConnell, C.F. Fox, Lateral phase separations in membrane lipids and the mechanism of sugar transport in *Escherichia coli*, Proceedings of the National Academy of Sciences of the United States of America, 70 (1973) 2271-5.

[127] L. Thilo, H. Träuble, P. Overath, Mechanistic interpretation of the influence of lipid phase transitions on transport functions, Biochemistry, 16 (1977) 1283-90.

[128] L. Picas, A. Carretero-Genevrier, M.T. Montero, J.L. Vázquez-Ibar, B. Seantier, P.E. Milhiet, J. Hernández-Borrell, Preferential insertion of lactose permease in phospholipid domains: AFM observations, Biochimica et Biophysica Acta, 1798 (2010) 1014-9.

[129] J.Y. Lehtonen, P.K. Kinnunen, Evidence for phospholipid microdomain formation in liquid crystalline liposomes reconstituted with *Escherichia coli* lactose permease, Biophysical Journal, 72 (1997) 1247-57.

[130] X. Wang, M. Bogdanov, W. Dowhan, Topology of polytopic membrane protein subdomains is dictated by membrane phospholipid composition, The EMBO Journal, 21 (2002) 5673-81.

[131] L. Picas, S. Merino-Montero, A. Morros, J. Hernández-Borrell, M.T. Montero, Monitoring pyrene excimers in lactose permease liposomes: revealing the presence of phosphatidylglycerol in proximity to an integral membrane protein, Journal of Fluorescence, 17 (2007) 649-54.

[132] L. Picas, M.T. Montero, A. Morros, J.L. Vázquez-Ibar, J. Hernández-Borrell, Evidence of phosphatidylethanolamine and phosphatidylglycerol presence at the annular region of lactose permease of *Escherichia coli*, Biochimica et Biophysica Acta, 1798 (2009) 291-6.

[133] L. Picas, C. Suárez-Germà, M.T. Montero, J.L. Vázquez-Ibar, J. Hernández-Borrell, M. Prieto, L.M.S. Loura, Lactose permease lipid selectivity using Förster resonance energy transfer, Biochimica et Biophysica Acta, 1798 (2010) 1707-13.

[134] R.L. Dunten, M. Sahin-Tóth, H.R. Kaback, Role of the charge pair aspartic acid-237-lysine-358 in the lactose permease of *Escherichia coli*, Biochemistry, 32 (1993) 3139-45.

[135] S. Frillingos, M. Sahin-Tóth, J.W. Lengeler, H.R. Kaback, Helix packing in the sucrose permease of *Escherichia coli*: properties of engineered charge pairs between helices VII and XI, Biochemistry, 34 (1995) 9368-73.

[136] M.F. Lensink, C. Govaerts, J.M. Ruysschaert, Identification of specific lipid-binding sites in integral membrane proteins, The Journal of Biological Chemistry, 285 (2010) 10519-26.

[137] C.C. Chen, T.H. Wilson, The phospholipid requirement for activity of the lactose carrier of *Escherichia coli*, The Journal of Biological Chemistry, 259 (1984) 10150-8.

[138] M. Bogdanov, W. Dowhan, Phosphatidylethanolamine is required for in vivo function of the membrane-associated lactose permease of *Escherichia coli*, Journal of Biological Chemistry, 270 (1995) 732-39.

[139] M. Bogdanov, P.N. Heacock, W. Dowhan, A polytopic membrane protein displays a reversible topology dependent on membrane lipid composition, The EMBO Journal, 21 (2002) 2107-16.

[140] H. Vitrac, M. Bogdanov, W. Dowhan, Proper fatty acid composition rather than an ionizable lipid amine is required for full transport function of lactose permease from *Escherichia coli*, The Journal of Biological Chemistry, 288 (2013) 5873-85.

[141] M. Bogdanov, W. Dowhan, Phospholipid-assisted protein folding: phosphatidylethanolamine is required at a late step of the conformational maturation of the polytopic membrane protein lactose permease, The EMBO Journal, 17 (1998) 5255-64.

[142] M. Bogdanov, P. Heacock, Z. Guan, W. Dowhan, Plasticity of lipid-protein interactions in the function and topogenesis of the membrane protein lactose permease from *Escherichia coli*, Proceedings of the National Academy of Sciences of the United States of America, 107 (2010) 15057-62.

[143] J. Xie, M. Bogdanov, P. Heacock, W. Dowhan, Phosphatidylethanolamine and monoglucosyldiacylglycerol are interchangeable in supporting topogenesis and

function of the polytopic membrane protein lactose permease, The Journal of Biological Chemistry, 281 (2006) 19172-8.

[144] W. Dowhan, E. Mileykovskaya, M. Bogdanov, Diversity and versatility of lipid-protein interactions revealed by molecular genetic approaches, Biochimica et Biophysica Acta, 1666 (2004) 19-39.

[145] G. von Heijne, Membrane-protein topology, Nature Reviews. Molecular Cell Biology, 7 (2006) 909-18.

[146] H. Vitrac, M. Bogdanov, P. Heacock, W. Dowhan, Lipids and topological rules of membrane protein assembly: balance between long and short range lipid-protein interactions, The Journal of Biological Chemistry, 286 (2011) 15182-94.

[147] M. Bogdanov, J. Xie, P. Heacock, W. Dowhan, To flip or not to flip: lipid-protein charge interactions are a determinant of final membrane protein topology, The Journal of Cell Biology, 182 (2008) 925-35.

[148] D.C. Bay, R.J. Turner, Membrane composition influences the topology bias of bacterial integral membrane proteins, Biochimica et Biophysica Acta, 1828 (2013) 260-70.

[149] H. Vitrac, M. Bogdanov, W. Dowhan, In vitro reconstitution of lipid-dependent dual topology and postassembly topological switching of a membrane protein, Proceedings of the National Academy of Sciences of the United States of America, 110 (2013) 9338-43.

[150] M. Bogdanov, W. Dowhan, Lipid-dependent generation of dual topology for a membrane protein, The Journal of Biological Chemistry, 287 (2012) 37939-48.

[151] W. Zhao, T. Róg, A.A. Gurtovenko, I. Vattulainen, M. Karttunen, Role of phosphatidylglycerols in the stability of bacterial membranes, Biochimie, 90 (2008) 930-8.

[152] P. Viitanen, M.J. Newman, D.L. Foster, T.H. Wilson, H. Kaback, Purification, reconstitution, and characterization of the lac permease of *Escherichia coli*, Methods in Enzymology, 125 (1986) 429-52.

[153] H. Martinez-Seara, T. Róg, M. Karttunen, I. Vattulainen, R. Reigada, Why is the *sn*-2 chain of monounsaturated glycerophospholipids usually unsaturated whereas the *sn*-1 chain is saturated? Studies of 1-stearoyl-2-oleoyl-sn-glycero-3-phosphatidylcholine (SOPC) and 1-oleoyl-2-stearoyl-sn-glycero-3-phosphatidylcholine (OSPC). Membranes with and without Cholesterol, The Journal of Physical Chemistry. B, 113 (2009) 8347-56.

[154] O. Soubias, W.E. Teague, K.G. Hines, D.C. Mitchell, K. Gawrisch, Contribution of membrane elastic energy to rhodopsin function, Biophysical Journal, 99 (2010) 817-24.

[155] J. Seddon, R. Templer, Polymorphism of lipid-water systems, in: R. Lipowsky, E. Sackmann (Eds.), Handbook of Biological Physics. Volume 1., Elsevier Science B.V, 1995: pp. 97-160.

[156] J.M. Boggs, Lipid intermolecular hydrogen bonding: influence on structural organization and membrane function, Biochimica et Biophysica Acta, 906 (1987) 353-404.

[157] Ò. Domènech, F. Sanz, M.T. Montero, J. Hernández-Borrell, Thermodynamic and structural study of the main phospholipid components comprising the mitochondrial inner membrane, Biochimica et Biophysica Acta, 1758 (2006) 213-21.

[158] B. Pozo Navas, K. Lohner, G. Deutsch, E. Sevcsik, K.A. Riske, R. Dimova, P. Garidel, G. Pabst, Composition dependence of vesicle morphology and mixing properties in a bacterial model membrane system, Biochimica et Biophysica Acta, 1716 (2005) 40-8.

[159] A. Dicko, Study by infrared spectroscopy of the conformation of dipalmitoylphosphatidylglycerol monolayers at the air–water interface and transferred on solid substrates, Chemistry and Physics of Lipids, 96 (1998) 125-39.

[160] Y.P. Zhang, R.N. Lewis, R.N. McElhaney, Calorimetric and spectroscopic studies of the thermotropic phase behavior of the n-saturated 1,2-diacylphosphatidylglycerols, Biophysical Journal, 72 (1997) 779-93.

[161] H. Möhwald, Phospholipid monolayers, in: R. Lipowsky, E. Sackmann (Eds.), Handbook of Biological Physics. Volume 1, Elsevier Science B.V, 1995: pp. 161-211.

[162] J.R. Lakowicz, Principles of fluorescence spectroscopy, 2nd ed., Kluwer Academic/Plenum Publishers, New York, 1999.

[163] G. Weber, F.J. Farris, Synthesis and spectral properties of a hydrophobic fluorescent probe: 6-propionyl-2-(dimethylamino)naphthalene, Biochemistry, 18 (1979) 3075-8.

[164] T. Parasassi, G. De Stasio, A. D'Ubaldo, E. Gratton, Phase fluctuation in phospholipid membranes revealed by Laurdan fluorescence, Biophysical Journal, 57 (1990) 1179-86.

[165] T. Parasassi, G. De Stasio, G. Ravagnan, R.M. Rusch, E. Gratton, Quantitation of lipid phases in phospholipid vesicles by the generalized polarization of Laurdan fluorescence, Biophysical Journal, 60 (1991) 179-89.

[166] A.D. Lúcio, C.C. Vequi-Suplicy, R.M. Fernandez, M.T. Lamy, Laurdan spectrum decomposition as a tool for the analysis of surface bilayer structure and polarity: a study with DMPG, peptides and cholesterol, Journal of Fluorescence, 20 (2010) 473-82.

[167] S.S. Antollini, M.A. Soto, I. Bonini de Romanelli, C. Gutiérrez-Merino, P. Sotomayor, F.J. Barrantes, Physical state of bulk and protein-associated lipid in nicotinic acetylcholine receptor-rich membrane studied by laurdan generalized polarization and fluorescence energy transfer, Biophysical Journal, 70 (1996) 1275-84.

[168] F.M. Harris, K.B. Best, J.D. Bell, Use of laurdan fluorescence intensity and polarization to distinguish between changes in membrane fluidity and phospholipid order, Biochimica et Biophysica Acta, 1565 (2002) 123-8.

[169] Ò. Domènech, Y.F. Dufrêne, F. Van Bambeke, P.M. Tukens, M.-P. Mingeot-Leclercq, Interactions of oritavancin, a new semi-synthetic lipoglycopeptide, with lipids extracted from *Staphylococcus aureus*, Biochimica et Biophysica Acta, 1798 (2010) 1876-85.

[170] T. Parasassi, E.K. Krasnowska, L. Bagatolli, E. Gratton, Laurdan and Prodan as polarity-sensitive fluorescent membrane probes, Journal of Fluorescence, 8 (1998) 365–73.

[171] I.N. Levine, Physical chemistry, 6th ed., McGraw-Hill, 2008.

[172] G. Binnig, C. Quate, C. Gerber, Atomic force microscope, Physical Review Letters, 56 (1986) 930-934.

[173] G. Binnig, H. Rohrer, Scanning tunneling microscopy, Surface Science, 126 (1983) 236-44.

[174] C. Gerber, H.P. Lang, How the doors to the nanoworld were opened, Nature Nanotechnology, 1 (2006) 3-5.

[175] J. Ralston, I. Larson, M.W. Rutland, A.A. Feiler, M. Kleijn, Atomic force microscopy and direct surface force measurements (IUPAC Technical Report), Pure and Applied Chemistry, 77 (2005) 2149-70.

[176] A. Alessandrini, P. Facci, Nanoscale mechanical properties of lipid bilayers and their relevance in biomembrane organization and function, Micron, 43 (2012) 1212-23.

[177] M. Shibata, H. Yamashita, T. Uchihashi, H. Kandori, T. Ando, High-speed atomic force microscopy shows dynamic molecular processes in photoactivated bacteriorhodopsin, Nature Nanotechnology, 5 (2010) 208-12.

[178] D. Müller, Y. Dufrene, Atomic force microscopy as a multifunctional molecular toolbox in nanobiotechnology, Nature Nanotechnology, 3 (2008) 261-69.

[179] S. Moreno Flores, J.L. Toca-Herrera, The new future of scanning probe microscopy: Combining atomic force microscopy with other surface-sensitive techniques, optical microscopy and fluorescence techniques, Nanoscale, 1 (2009) 40-9.

[180] M. Stolz, U. Aebi, D. Stoffler, Developing scanning probe-based nanodevices--stepping out of the laboratory into the clinic, Nanomedicine, 3 (2007) 53-62.

[181] L. Picas, F. Rico, S. Scheuring, Direct measurement of the mechanical properties of lipid phases in supported bilayers, Biophysical Journal, 102 (2012) L01-3.

[182] T. Wang, H. Shogomori, M. Hara, T. Yamada, T. Kobayashi, Nanomechanical recognition of sphingomyelin-rich membrane domains by atomic force microscopy, Biochemistry, 51 (2012) 74-82.

[183] Y.F. Dufrêne, Towards nanomicrobiology using atomic force microscopy, Nature Reviews. Microbiology, 6 (2008) 674-80.

[184] J. Bernardino de la Serna, S. Hansen, Z. Berzina, A.C. Simonsen, H.K. Hannibal-Bach, J. Knudsen, C.S. Ejsing, L.A. Bagatolli, Compositional and structural characterization of monolayers and bilayers composed of native pulmonary surfactant from wild type mice, Biochimica et Biophysica Acta, 1828 (2013) 2450-59.

[185] L. Picas, M.T. Montero, A. Morros, M.E. Cabañas, B. Seantier, P.E. Milhiet, J. Hernández-Borrell, Calcium-induced formation of subdomains in phosphatidylethanolamine-phosphatidylglycerol bilayers: a combined DSC, ^{31}P NMR, and AFM study, The Journal of Physical Chemistry. B, 113 (2009) 4648-55.

[186] G. Oncins, L. Picas, J. Hernández-Borrell, S. Garcia-Manyes, F. Sanz, Thermal response of Langmuir-Blodgett films of dipalmitoylphosphatidylcholine studied by atomic force microscopy and force spectroscopy, Biophysical Journal, 93 (2007) 2713-25.

[187] L. Picas, M.T. Montero, A. Morros, G. Oncins, J. Hernández-Borrell, Phase changes in supported planar bilayers of 1-palmitoyl-2-oleoyl-*sn*-glycero-3-phosphoethanolamine, Ultrapure Water, 112 (2008) 10181-87.

[188] Z.V. Leonenko, E. Finot, H. Ma, T.E.S. Dahms, D.T. Cramb, Investigation of temperature-induced phase transitions in DOPC and DPPC phospholipid bilayers using temperature-controlled scanning force microscopy, Biophysical Journal, 86 (2004) 3783-93.

[189] D. Keller, N. Larsen, I. Møller, O. Mouritsen, Decoupled phase transitions and grain-boundary melting in supported phospholipid bilayers, Physical Review Letters, 94 (2005) 1-4.

[190] H. Butt, Measuring electrostatic, van der Waals, and hydration forces in electrolyte solutions with an atomic force microscope, Biophysical Journal, 60 (1991) 1438-44.

[191] B. Cappella, G. Dietler, Force-distance curves by atomic force microscopy, Surface Science Reports, 34 (1999) 1-104.

[192] V. Franz, S. Loi, H. Müller, E. Bamberg, H.J. Butt, Tip penetration through lipid bilayers in atomic force microscopy, Colloids and Surfaces B, 23 (2002) 191-200.

[193] S. Garcia-Manyes, L. Redondo-Morata, G. Oncins, F. Sanz, Nanomechanics of lipid bilayers: heads or tails?, Journal of the American Chemical Society, 132 (2010) 12874-86.

[194] L. Redondo-Morata, G. Oncins, F. Sanz, Force spectroscopy reveals the effect of different ions in the nanomechanical behavior of phospholipid model membranes: the case of potassium cation, Biophysical Journal, 102 (2012) 66-74.

[195] Y. Dufrêne, W. Barger, J. Green, G. Lee, Nanometer-scale surface properties of mixed phospholipid monolayers and bilayers, Langmuir, 7463 (1997) 4779-84.

[196] Y.F. Dufrêne, G.U. Lee, Advances in the characterization of supported lipid films with the atomic force microscope, Biochimica et Biophysica Acta, 1509 (2000) 14-41.

[197] S. Garcia-Manyes, G. Oncins, F. Sanz, Effect of ion-binding and chemical phospholipid structure on the nanomechanics of lipid bilayers studied by force spectroscopy, Biophysical Journal, 89 (2005) 1812-26.

[198] J.A. Poveda, A.M. Fernández, J.A. Encinar, J.M. González-Ros, Protein-promoted membrane domains, Biochimica et Biophysica Acta, 1778 (2008) 1583-90.

[199] M. Pasenkiewicz-Gierula, Y. Takaoka, H. Miyagawa, K. Kitamura, A. Kusumi, Charge pairing of headgroups in phosphatidylcholine membranes: A molecular dynamics simulation study, Biophysical Journal, 76 (1999) 1228-40.

[200] J.L. Vázquez-Ibar, L. Guan, M. Svrakic, H.R. Kaback, Exploiting luminescence spectroscopy to elucidate the interaction between sugar and a tryptophan residue in the lactose permease of *Escherichia coli*, Proceedings of the National Academy of Sciences, 100 (2003) 12706-11.

[201] J.L. Vázquez-Ibar, L. Guan, A.B. Weinglass, G. Verner, R. Gordillo, H.R. Kaback, Sugar recognition by the lactose permease of *Escherichia coli*, The Journal of Biological Chemistry, 279 (2004) 49214-21.

[202] I. Smirnova, V. Kasho, J. Sugihara, H.R. Kaback, Probing of the rates of alternating access in LacY with Trp fluorescence, Proceedings of the National Academy of Sciences of the United States of America, 106 (2009) 21561-6.

[203] I.N. Smirnova, H.R. Kaback, A mutation in the lactose permease of *Escherichia coli* that decreases conformational flexibility and increases protein stability, Biochemistry, 42 (2003) 3025-31.

[204] Y. Nie, F.E. Sabetfard, H.R. Kaback, The Cys154-->Gly mutation in LacY causes constitutive opening of the hydrophilic periplasmic pathway, Journal of Molecular Biology, 379 (2008) 695-703.

[205] J. Holyoake, M.S.P. Sansom, Conformational change in an MFS protein: MD simulations of LacY, Structure, 15 (2007) 873-84.

[206] A. Weinglass, J.P. Whitelegge, K.F. Faull, H.R. Kaback, Monitoring conformational rearrangements in the substrate-binding site of a membrane transport protein by mass spectrometry, The Journal of Biological Chemistry, 279 (2004) 41858-65.

[207] A.E. Jessen-Marshall, N.J. Paul, R.J. Brooker, The conserved motif, GXXX(D/E)(R/K)XG[X](R/K) (R/K), in hydrophilic loop 2/3 of the Lactose permease, The Journal of Biological Chemistry, 270 (1995) 16251-57.

[208] N. Pazdernik, E. Matzke, A.E. Jessen-Marshall, R.J. Brooker, Roles of charged residues in the conserved motif, G-X-X-X-D/E-R/K-X-G-[X]-R/K-R/K, of the lactose permease of *Escherichia coli*, The Journal of Membrane Biology, 174 (2000) 31-40.

[209] A.E. Jessen-Marshall, R.J. Brooker, Evidence that transmembrane segment 2 of the lactose permease is part of a conformationally sensitive interface between the two halves of the protein, The Journal of Biological Chemistry, 271 (1996) 1400-4.

[210] P. Hakizimana, M. Masureel, B. Gbaguidi, J.M. Ruysschaert, C. Govaerts, Interactions between phosphatidylethanolamine headgroup and LmrP, a multidrug transporter: a conserved mechanism for proton gradient sensing?, The Journal of Biological Chemistry, 283 (2008) 9369-76.

[211] Z. Liu, M.G. Madej, H.R. Kaback, Helix dynamics in LacY: helices II and IV, Journal of Molecular Biology, 396 (2010) 617-26.

[212] J.L. Rigaud, G. Mosser, J.J. Lacapere, A. Olofsson, D. Levy, J.L. Ranck, Bio-Beads: an efficient strategy for two-dimensional crystallization of membrane proteins, Journal of Structural Biology, 118 (1997) 226-35.

[213] J.L. Rigaud, D. Lévy, Reconstitution of membrane proteins into liposomes, Methods in Enzymology, 372 (2003) 65-86.

[214] J.L. Rigaud, D. Levy, G. Mosser, Detergent removal by non-polar polystyrene beads Applications to membrane protein reconstitution and two-dimensional crystallization, European Biophysics Journal, 27 (1998) 305-19.

[215] J. Zhuang, G.G. Privé, G.E. Werner, P. Ringler, H.R. Kaback, A. Engel, Two-dimensional crystallization of *Escherichia coli* lactose permease, Journal of Structural Biology, 125 (1999) 63-75.

[216] S. Merino-Montero, Ò. Domènech, M.T. Montero, J. Hernández-Borrell, Preliminary atomic force microscopy study of two-dimensional crystals of lactose permease from *Escherichia coli*, Biophysical Chemistry, 119 (2006) 78-83.

[217] B. Seantier, M. Dezi, F. Gubellini, A. Berquand, C. Godefroy, P. Dosset, D. Lévy, P.E. Milhiet, Transfer on hydrophobic substrates and AFM imaging of membrane proteins reconstituted in planar lipid bilayers, Journal of Molecular Recognition, 24 (2011) 461-6.

[218] P.-E. Milhiet, F. Gubellini, A. Berquand, P. Dosset, J.L. Rigaud, C. Le Grimellec, D. Lévy, High-resolution AFM of membrane proteins directly incorporated at high density in planar lipid bilayer, Biophysical Journal, 91 (2006) 3268-75.

[219] S. Scheuring, J.N. Sturgis, Chromatic adaptation of photosynthetic membranes, Science, 309 (2005) 484-7.

[220] R. Clegg, Förster resonance energy transfer—FRET what is it, why do it, and how it's done, in: T.W.J. Gadella (Ed.), Laboratory Techniques in Biochemistry and Molecular Biology, 1st ed., Elesvier B.V., 2009: pp. 1-57.

[221] B.W. Van der Meer, G. Cokker III, S.Y. Simon Chen, Resonance Energy Transfer Theory and data, VCH Publishers, Inc., Bowling Green, 1994.

[222] L.M.S. Loura, M. Prieto, F. Fernandes, Quantification of protein–lipid selectivity using FRET, European Biophysics Journal, 39 (2009) 565-78.

[223] E.J. Cabré, L.M.S. Loura, A. Fedorov, J. Perez-Gil, M. Prieto, Topology and lipid selectivity of pulmonary surfactant protein SP-B in membranes: Answers from fluorescence, Biochimica et Biophysica Acta, 1818 (2012) 1717-25.

[224] H. Wallrabe, M. Elangovan, A. Burchard, A. Periasamy, M. Barroso, Confocal FRET microscopy to measure clustering of ligand-receptor complexes in endocytic membranes, Biophysical Journal, 85 (2003) 559-71.

[225] L. Chen, L. Novicky, M. Merzlyakov, T. Hristov, K. Hristova, Measuring the energetics of membrane protein dimerization in mammalian membranes, Journal of the American Chemical Society, 132 (2010) 3628-35.

[226] D.S. Majumdar, I. Smirnova, V. Kasho, E. Nir, X. Kong, S. Weiss, H.R. Kaback, Single-molecule FRET reveals sugar-induced conformational dynamics in LacY, Proceedings of the National Academy of Sciences of the United States of America, 104 (2007) 12640-5.

[227] J. Zhao, J. Wu, F.A. Heberle, T.T. Mills, P. Klawitter, G. Huang, G. Costanza, G.W. Feigenson, Phase studies of model biomembranes: complex behavior of DSPC/DOPC/cholesterol, Biochimica et Biophysica Acta, 1768 (2007) 2764-76.

[228] M.J. Sarmento, M. Prieto, F. Fernandes, Reorganization of lipid domain distribution in giant unilamellar vesicles upon immobilization with different membrane tethers, Biochimica et Biophysica Acta, 1818 (2012) 2605-15.

[229] F. Fernandes, L.M.S. Loura, R. Koehorst, R.B. Spruijt, M.A. Hemminga, A. Fedorov, M. Prieto, Quantification of protein-lipid selectivity using FRET: application to the M13 major coat protein, Biophysical Journal, 87 (2004) 344-52.

[230] L.M.S. Loura, M. Prieto, Lateral membrane heterogeneity probed by FRET spectroscopy and microscopy, in: Y. Mély, G. Duportail (Eds.), Fluorescent Methods to Study Biological Membranes (Springer Series on Fluorescence Vol. 13), Springer Berlin Heidelberg, Berlin, 2013: pp. 71-113.

[231] P. Somerharju, Pyrene-labeled lipids as tools in membrane biophysics and cell biology, Chemistry and Physics of Lipids, 116 (2002) 57-74.

[232] J. Curdová, P. Capková, J. Plásek, J. Repáková, I. Vattulainen, Free pyrene probes in gel and fluid membranes: perspective through atomistic simulations, The Journal of Physical Chemistry. B, 111 (2007) 3640-50.

[233] J. Repáková, J.M. Holopainen, M. Karttunen, I. Vattulainen, Influence of pyrene-labeling on fluid lipid membranes, The Journal of Physical Chemistry. B, 110 (2006) 15403-10.

[234] M.J. Parry, M. Hagen, O.G. Mouritsen, P.K.J. Kinnunen, J.M.I. Alakoskela, Interlamellar coupling of phospholipid bilayers in liposomes: an emergent property of lipid rearrangement, Langmuir, 26 (2010) 4909-15.

[235] P.E. Milhiet, C. Le Grimellec, Observing the nanoscale organization of model biological membranes by atomic force microscopy, in: Y. Dufrêne (Ed.), Life at the Nanoscale, Pan Stanford publishing, Singapore, 2011: pp. 1-20.

[236] N.C. Santos, M.A.R.B. Castanho, An overview of the biophysical applications of atomic force microscopy, Biophysical Chemistry, 107 (2004) 133-49.

[237] T. Uchihashi, R. Iino, T. Ando, H. Noji, High-speed atomic force microscopy reveals rotary catalysis of rotorless F_1-ATPase, Science, 333 (2011) 755-8.

[238] D.J. Müller, A. Engel, U. Matthey, T. Meier, P. Dimroth, K. Suda, Observing membrane protein diffusion at subnanometer resolution, Journal of Molecular Biology, 327 (2003) 925-30.

[239] P. Eaton, J.R. Smith, P. Graham, J.D. Smart, T.G. Nevell, J. Tsibouklis, Adhesion force mapping of polymer surfaces : factors influencing force of adhesion, Langmuir, 18 (2002) 3387-89.

[240] A.N. Parbhu, W.G. Bryson, R. Lal, Disulfide bonds in the outer layer of keratin fibers confer higher mechanical rigidity: correlative nano-indentation and elasticity measurement with an AFM, Biochemistry, 38 (1999) 11755-61.

[241] S. Tan, R.L. Sherman, W.T. Ford, Nanoscale compression of polymer microspheres by atomic force microscopy, Langmuir, 20 (2004) 7015-20.

[242] A.P. Quist, S.K. Rhee, H. Lin, R. Lal, Physiological role of gap-junctional hemichannels Extracellular calcium-dependent isosmotic volume regulation, The Journal of Cell Biology, 148 (2000) 1063-74.

[243] M.R. Nussio, N.H. Voelcker, M.J. Sykes, S.J.P. McInnes, C.T. Gibson, R.D. Lowe, J.O. Miners, J.G. Shapter, Lateral heterogeneities in supported bilayers from pure and mixed phosphatidylethanolamine demonstrating hydrogen bonding capacity, Biointerphases, 3 (2008) 96-104.

[244] H. An, M.R. Nussio, M.G. Huson, N.H. Voelcker, J.G. Shapter, Material properties of lipid microdomains: Force-volume imaging study of the effect of cholesterol on lipid microdomain rigidity, Biophysical Journal, 99 (2010) 834-44.

[245] E. Dague, D. Alsteens, J.-P. Latgé, C. Verbelen, D. Raze, A.R. Baulard, Y.F. Dufrêne, Chemical force microscopy of single live cells, Nano Letters, 7 (2007) 3026-30.

[246] Y.F. Dufrêne, Using nanotechniques to explore microbial surfaces, Nature Reviews. Microbiology, 2 (2004) 451-60.

[247] C.V.G. Reddy, K. Malinowska, N. Menhart, R. Wang, Identification of TrkA on living PC12 cells by atomic force microscopy, Biochimica et Biophysica Acta, 1667 (2004) 15-25.

[248] F. Kienberger, A. Ebner, H.J. Gruber, P. Hinterdorfer, Molecular recognition imaging and force spectroscopy of single biomolecules, Accounts of Chemical Research, 39 (2006) 29-36.

[249] A. Galera-Prat, R. Hermans, R. Hervás, A. Gómez-Sicilia, M. Carrión-Vázquez, Single-molecule force spectroscopy, in: A.M. Baró, R.G. Reifenberger (Eds.), Atomic Force Microscopy in Liquid: Biological Applications, 1st ed., Willey-VCH, Weinheim, 2012: pp. 157-209.

[250] A. Marsico, D. Labudde, T. Sapra, D.J. Muller, M. Schroeder, A novel pattern recognition algorithm to classify membrane protein unfolding pathways with high-throughput single-molecule force spectroscopy, Bioinformatics, 23 (2007) e231-6.

[251] S.R.K. Ainavarapu, J. Brujic, H.H. Huang, A.P. Wiita, H. Lu, L. Li, K.A. Walther, M. Carrion-Vazquez, H. Li, J.M. Fernandez, Contour length and refolding rate of a small protein controlled by engineered disulfide bonds, Biophysical Journal, 92 (2007) 225-33.

[252] C. Bustamante, J. Marko, E. Siggia, S. Smith, Entropic elasticity of lambda-phage DNA, Science, 265 (1994) 1599-600.

[253] P. Eaton, P. West, Atomic force microscopy, Oxford university press, New York, 2010.

[254] D.J. Muller, AFM : A Nanotool in Membrane Biology, Biochemistry, 47 (2008) 7986-98.

[255] A. Kedrov, H. Janovjak, Deciphering molecular interactions of native membrane proteins by single-molecule force spectroscopy, Annual Review of Biophysics and Biomolecular Structure, 36 (2007) 233-60.

[256] S. Ishii, M.J. Sadowsky, *Escherichia coli* in the environment: implications for water quality and human health, microbes and environments, 23 (2008) 101-8.

[257] E.I. Goksu, M.L. Longo, Ternary lipid bilayers containing cholesterol in a high curvature silica xerogel environment, Langmuir, 26 (2010) 8614-24.

[258] E. London, How principles of domain formation in model membranes may explain ambiguities concerning lipid raft formation in cells, Biochimica et Biophysica Acta, 1746 (2005) 203-20.

[259] A. Cruz, L. Vázquez, M. Vélez, J. Pérez-Gil, Influence of a fluorescent probe on the nanostructure of phospholipid membranes: dipalmitoylphosphatidylcholine interfacial monolayers, Langmuir, 21 (2005) 5349-55.

Appendix A

Symbols and acronyms

A	FRET acceptor
A	Surface area
ABC	ATP-binding cassette
AFM	Atomic force microscopy
X	Mole fraction
C_0	Spontaneous intrinsic curvature
CL	Cardiolipin
C_s	Isothermal compressibility module
D	FRET donor
ΔH_{vH}	Van't Hoff molar enthalpy
$\Delta\tilde{\mu}_i$	Electrochemical potential of i
DMPC	1,2-dimyristoyl-*sn*-glycero-3-phosphocholine
$\Delta\mu_s$	Substrate concentration gradient
DOPC	1,2-dioleoyl-*sn*-glycero-3-phosphocholine
DOPE	1,2-dioleoyl-*sn*-glycero-3-phosphoethanolamine
DPPE	1,2-dipalmitoyl-*sn*-glycero-3-phosphoethanolamine
DSC	Differential scanning calorimetry
E	Pyrene excimer
E	FRET efficiency
E. coli	*Escherichia coli*
E/M	Excimer to monomer ratio
F	Force
F_{adh}	Adhesion force
FRET	Förster resonance energy transfer
FS	Force spectroscopy

FD	Force-distance
FV	Force volume
F_y	Breakthrough force
G	Gaseous
Γ	Line tension
γ	Surface tension
γ_0	Surface tension in absence of a surface agent
G^E	Excess Gibbs energy
GlcDAG	Monoglucosyl diacylglycerol
GlcGlcDAG	Diglucosyl diacylglycerol
GUV	Giant unilamellar vesicle
HPyr-PE	Pyrene head-labelled PE phospholipid
I_D	Fluorescence intensity of the donor
I_{DA}	Fluorescence intensity of the donor in the presence of acceptor
k_B	Boltzmann constant
k_s	Relative association constant between labelled and unlabelled phospholipids
λ	Wavelength
λ_{em}	Emission wavelength
λ_{ex}	Excitation wavelength
L_α	Lamellar liquid-crystalline phase or fluid phase
LacY	Lactose permease
L_β	Lamellar gel phase
L_c	Contour length
LC	Liquid condensed
LE	Liquid expanded
LPR	Lipid-to-protein ratio
LUV	Large unilamellar vesicle
M	Pyrene monomer
μ	Probability of a site in the annular ring being occupied by a pyrene-labelled phospholipid
MD	Molecular dynamic
MFS	Major facilitator superfamily
MLV	Multilamellar vesicle
p	Persistence length

π	Surface pressure
PC	Phosphatidylcholine
PE	Phosphatidylethanolamine
PG	Phosphatidylglycerol
PLS	Proteolipid sheet
POPC	1-palmitoyl-2-oleoyl-*sn*-glycero-3-phosphocholine
POPE	1-palmitoyl-2-oleoyl-*sn*-glycero-3-phosphoethanolamine
POPG	1-palmitoyl-2-oleoyl-*sn*-glycero-3-phospho-(1'-*rac*-glycerol) (sodium salt)
PS	Phosphatidylserine
Pyr	Pyrene
Pyr-PC	Pyrene acyl chain-labelled PC
Pyr-PE	Pyrene acyl chain-labelled PE
Pyr-PG	Pyrene acyl chain-labelled PG
S	Spreading pressure
S_0	Molecular ground state
S_1	Molecular singlet excited state
SDS	Sodium dodecyl sulfate
SLB	Supported lipid bilayer
S-N	Singer-Nicolson
SPM	Scanning probe microscopy
SPR	Surface plasmon resonance
STM	Scanning tunnelling microscopy
SUV	Small unilamellar vesicle
T	Temperature
TERS	Tip-enhanced Raman spectroscopy
TIRFF	Total internal reflection fluorescence
T_m	Transition or melting temperature
TM	Transmembrane segment
TMP	Transmembrane protein
T_{offset}	Temperature at which the melting of phospholipids finish
T_{onset}	Temperature at which the melting of phospholipids start
WLC	Worm-like chain model

Appendix B

List of publications and contributions to scientific events related to this thesis

B.1 Complete list of peer-reviewed publications

Suárez-Germà, C., Morros, A., Montero, M.T., Hernández-Borrell, J., Domènech, Ò.
Combined FS and AFM-based calorimetric studies to reveal the nanostructural organization of biomimetic membranes.
Submitted to *Soft Matter*

Suárez-Germà, C., Domènech, Ò., Montero, M.T., Hernández-Borrell, J.
Effect of lactose permease presence on the structure and nanomechanics of two-component supported lipid bilayers
Submitted to *Biochimica et Biophysica Acta - Biomembranes*

Suárez-Germà, C., Loura, L. M. S., Prieto, M., Domènech, Ò., Campanera, J. M., Montero, M. T., Hernández-Borrell, J. (**2013**).
Phospholipid-lactose permease interaction as reported by a head-labeled pyrene phosphatidylethanolamine: a FRET study.
The Journal of Physical Chemistry B, *117*,6741-8.

Suárez-Germà, C., Loura, L. M. S., Domènech, Ò., Montero, M. T., Vázquez-Ibar, J. L., Hernández-Borrell, J. (**2012**).
Phosphatidylethanolamine-lactose permease interaction: a comparative study based on FRET.
The Journal of Physical Chemistry B, 116(48), 14023-8.

Suárez-Germà, C., Loura, L. M. S., Prieto, M., Domènech, Ò., Montero, M. T., Rodríguez-Banqueri, A., Vázquez-Ibar, J. L., Hernández-Borrell, J. (**2012**).
Membrane protein-lipid selectivity: enhancing sensitivity for modeling FRET data.
The Journal of Physical Chemistry B, 116(8), 2438-45.

Suárez-Germà, C., Montero, M. T., Ignés-Mullol, J., Hernández-Borrell, J., Domènech, Ò. (**2011**).
Acyl chain differences in phosphatidylethanolamine determine domain formation and LacY distribution in biomimetic model membranes.
The Journal of Physical Chemistry B, 115(44), 12778-84.

Picas, L., **Suárez-Germà, C.**, Montero, M. T., Domènech, Ò., Hernández-Borrell, J. (**2011**).
Miscibility behavior and nanostructure of monolayers of the main phospholipids of *Escherichia coli* inner membrane.
Langmuir, 28(1),701-6.

Picas, L., **Suárez-Germà, C.**, Montero, M. T., Vázquez-Ibar, J. L., Hernández-Borrell, J., Prieto, M., Loura, L. M. S. (**2010**).
Lactose permease lipid selectivity using Förster resonance energy transfer.
Biochimica et Biophysica Acta, 1798(9), 1707-13.

Picas, L., **Suárez-Germà, C.**, Teresa Montero, M.T., Hernández-Borrell, J. (**2010**).
Force spectroscopy study of Langmuir-Blodgett asymmetric bilayers of phosphatidylethanolamine and phosphatidylglycerol.
The Journal of Physical Chemistry B, 114(10), 3543-3549.

B2. Contribution to scientific events

Suárez-Germà C.
"Probing phosphatidylethanolamine-lactose permease selectivity by using AFM and FRET tools"
Oral Communication
5ª Jornada del Institut de Nanociència i Nanotecnologia In2UB, Barcelona (Spain), 2012.

Suárez-Germà, C., Domènech, Ò., Campanera, M., Montero, M.T., Vázquez-Ibar, J.L., Hernández-Borrell, J.
"Probing phosphatidylethanolamine-lactose permease selectivity by using AFM and FRET tools"
Poster
17th European Bioenergetics Conference, Freiburg im Breisgau (Germany), 2012.

Suárez-Germà, C., Domènech, Ò., Montero, M.T., Hernández-Borrell, J.
"Combining FRET and AFM in the elucidation of the composition of the lactose permease-phospholipid interface"
Oral communication (Dr. Hernández-Borrell)

XII Congress SBE/International Congress of the Spanish BioPhysical Society, Barcelona (Spain), 2012.

Suárez-Germà, C., Loura, L.M.S., Prieto, M., Domènech, Ò., Campanera, J.M., Montero, M.T., Vázquez-Ibar, J.L., Borrell, J.
"Effect of acyl chain structure in phosphatidylethanolamine selectivity for lactose permease"
Oral communication
XV International Symposium on Luminescence Spectrometry, Barcelona (Spain), 2012.

Suárez-Germà, C., Domènech, Ò., Morros, A., Montero, M.T., Borrell, J.
"Influence of acyl chain composition on phosphatidylethanolamine-lactose permease interaction: a FRET study"
Plenary lecture (Dr. Borrell)
XV International Symposium on Luminescence Spectrometry, Barcelona (Spain), 2012.

Suárez-Germà, C., Montero, M.T., Hernández-Borrell, J., Domènech, Ò.
"Partitioning of lactose permease of *Escherichia coli* into biomimetic supported lipid bilayers"
Poster
AFM BioMed Conference (4th International Meeting on AFM in Life Sciences and Medicine), Paris (France) 2011.

Suárez-Germà, C., Domènech, Ò., Picas, L., Montero, M.T., Hernández-Borrell, J.
"Understanding lactose permease lipid selectivity from AFM observations of supported planar bilayers"
Poster
9th International Symposium on Scanning Probe Microscopy & Optical Tweezers in Life Sciences, Berlin (Germany) 2010.

Suárez-Germà, C., Thomas, A., Picas, L., Montero, M.T., Vázquez-Ibar, J.L., Hernández-Borrell, J.
"Lactose permease lipid selectivity using Förster resonance energy transfer"
Poster
51st International Conference on the Bioscience of Lipids, Bilbao (Spain) 2010.

Suárez-Germà, C., Domènech, Ò., Picas, L., Hernández-Borrell, J., Montero, M.T.
"Understanding lactose permease lipid selectivity from AFM observations of supported planar bilayers"
Poster
IV Spanish Portuguese BioPhysical Congress, Zaragoza (Spain) 2010.

Appendix C

Agraïments

En primer lloc voldria agrair als directors i tutora de tesi, Jordi Borrell Hernández, Òscar Domènech Cabrera i Maria Teresa Montero Barrientos per l'oportunitat que m'han ofert en permetre'm realitzar aquesta tesi doctoral en el seu grup, però sobretot per inculcar-me el seu entusiasme per la ciència. També voldria donar-los les gràcies per aquests 4 anys de molt bona convivència.

Voldria agrair especialment a totes aquelles persones que han col·laborat directa o indirectament en l'elaboració d'aquesta tesi: Laura Picas, Antoni Morros, José Luis Vázquez-Ibar, Arturo Rodríguez-Banqueri, Luís Loura, Manuel Prieto, Pierre-Emmanuel Milhiet, Bastien Seantier i Cédric Godefroy. (Thank you)

També donar les gràcies a tots els membres del Departament de Fisicoquímica per haver-me fet sentir com a casa aquests darrers quatre anys, així com als dels grups dels Drs. Palacín i Zorzano per la seva bona acollida i predisposició a ajudar. Un grand merci aussi aux gens du CBS pour son accueil chaleureux.

Gràcies a la Martha per totes les hores passades al laboratori, per contagiar tanta il·lusió i felicitat.

Gràcies a tots els meus actuals i antics companys de pis. Especialment al Marc, la Irena, la Laia i l'Aina per tots els bons moments compartits durant aquests darrers anys. Aquesta tesi en part també és vostra.

Voldria agrair també el gran recolzament rebut per part dels amics, perquè el temps passa, però vosaltres seguiu aquí: als amics de Castellar, del Vidal i als excompanys del departament de Fisiologia. Anomenar especialment a la Mireia i al Xavi, gràcies per ser-hi sempre. Moltes gràcies també a l'Anna i a la Mercè, per la seva amistat prop i lluny dels cavalls. I, evidentment, reconèixer allà on va començar tot: mercès a la Judit, la Catalina i la Laia. Deu anys d'aventura farmacèutica i per molts més...

Merci aussi à Hana et Zinou (et félicitations!), Loriana, Flore, Véro... bien que nos moments passés ensemble à Montpellier soient loin, on réussit à se tenir au courant de nos vies.

Finalment, voldria donar el meu profund agraïment a tota la meva petita gran família. A tots vosaltres, gràcies per ser tant a prop meu. I un record per aquells que ja són lluny: pare, avi, vosaltres m'heu fet qui sóc.

Pour finir, j'aimerai bien remercier Alexandre parce qu'il est la plus belle chose que cette thèse m'ait ramenée. Merci pour être le pilier de ma vie.

Carme, Setembre 2013